



UNIVERSITÀ DEGLI STUDI DI NAPOLI  
**FEDERICO II**

Scuola Politecnica e  
delle Scienze di Base



Università degli Studi di Napoli Federico II

Dottorato di Ricerca in

Ingegneria Strutturale, Geotecnica e Rischio Sismico

**THESIS FOR THE DEGREE OF DOCTOR OF PHILOSOPHY**

***Multi-risk assessment for  
disaster risk reduction:  
  
a framework for integrating  
physical, social and multi-hazard  
dimensions***

by  
Tocchi Gabriella

Advisor: Prof.ssa Maria Polese



Scuola Politecnica e delle Scienze di Base  
Dipartimento di Strutture per l'Ingegneria e l'Architettura



*To see the world, things  
dangerous to come to, to  
see behind walls, draw  
closer, to find each other,  
and to feel. That is the  
purpose of life.*

The Secret Life of Walter Mitty



***Multi-risk assessment for  
disaster risk reduction:  
a framework for integrating  
physical, social and multi-hazard  
dimensions***

Ph.D. Thesis presented  
for the fulfillment of the Degree of Doctor of Philosophy  
in Ingegneria Strutturale, Geotecnica e Rischio Sismico  
by  
Tocchi Gabriella

March 2023



Approved as to style and content by

---

Prof.ssa Maria Polese, Advisor

Università degli Studi di Napoli Federico II  
Ph.D. Program in Ingegneria Strutturale, Geotecnica e Rischio Sismico  
XXXV cycle - Chairman: Prof. Iunio Iervolino

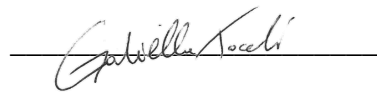


[www.dist.unina.it/dottorati-di-ricerca/dottorati](http://www.dist.unina.it/dottorati-di-ricerca/dottorati)

**Candidate's declaration**

I hereby declare that this thesis submitted to obtain the academic degree of Philosophiæ Doctor (Ph.D.) in Ingegneria Strutturale, Geotecnica e Rischio Sismico is my own unaided work, that I have not used other than the sources indicated, and that all direct and indirect sources are acknowledged as references.

Napoli, March 10, 2023

A handwritten signature in black ink, reading "Gabriella Tocchi", is written over a horizontal line.

Gabriella Tocchi



## Abstract

Prioritizing risks originating from different hazards in a region of interest is crucial to enable decisions on appropriate and cost-effective mitigation or preparedness measures. However, the performing of multi-risk assessment is a difficult task, mostly due to different methodologies and spatial/temporal resolutions adopted in the quantification of single risks. Moreover, evidence indicates that people in vulnerable situation may be disproportionately affected. Poverty and inequality have been officially recognized as risk drivers and the interest of governments and local stakeholders in understanding the influence of socio-economic factors on vulnerability to hazards notably increased during last years. However, conventional risk assessments typically fail to account for social vulnerability.

This study proposes a framework for integrating both socio-economic and physical factors in multi-risk analysis for overcoming the above limitations. A Risk Index (RI) was developed based on the combination of individual standardized indicators for hazard, physical and social vulnerability and exposure inputs. As a matter of fact, index-based approaches are the most suitable ones for measuring multidimensional concepts which cannot be captured by a single indicator. Indicators selected are combined defining suitable weights that may explicitly reflect stakeholder priorities in policymaking. This approach allows to rank regions exposed to multiple hazards and to identify multi-risk hotspots that more needs disaster risk reduction strategies, also accounting for socio-economic aspects. Hence, it may be a useful support for prioritizing area at risk in decision-making process, that is one the main challenges in Disaster Risk Reduction. The use of the proposed multi-risk index for earthquake and flood risk is demonstrated across the entire country of Italy, selecting the municipality as scale of analysis and residential buildings and population as assets at risk. This index-based approach allows to compare and rank those hazards in the country, leading to the identification of the regions where earthquakes/floods impacts are likely to be very high, due to high hazard level, poor performance of asset exposed to such hazard as well as weak capacity of people to adapt and respond to a natural



disaster. Exploiting the aforementioned index, a risk map of the Italian territory is obtained and the hotspots that should be prioritized in disaster risk reduction policies are identified. The application will also show that the involvement of social aspects in risk analysis may play a crucial role in the identification of such hotspots, underlying how ignoring social aspects in risk assessment may affect the effectiveness of disaster risk reduction plans. Sensitivity analyses are also performed in order to understand how multi-risk hotspots can change as a function of the relative importance given to a single RI component, i.e., how stakeholder priorities can affect the results.

For a proper quantification of expected economic losses, that are crucial for preparedness purposes, a quantitative risk assessment is also performed. The RI allows to identify the municipalities with highest risk score in a country. On the other hand, a detailed risk analysis is required to compare perils in terms of economic losses at municipal and sub-municipal scales. Through such analysis it is possible to identify the district with higher risk, both in terms of economic losses and social vulnerability, and to disaggregate losses on several social groups. For instance, low-income people may tend to experience the largest losses. Through detailed risk analysis the effectiveness of some mitigation strategies can also be estimated. The quantification of loss reduction associated to such strategies allows the definition of the most suitable mitigation options, also accounting for different social groups. Thus, for example, some mitigation policies may be particularly notable for the lowest income population class. To demonstrate the usefulness of such detailed assessment, among Italian municipality, the one with highest risk score is selected for performing a quantitative risk assessment at sub-municipal scale. The analysis show that low-income people tend to experience the largest expected annual losses per square meter both for earthquake and flood events. For the specific case study, risk assessment is repeated twice with some modelling modifications to evaluate the effectiveness of reducing expected losses through some disaster risk reduction strategies and related policies. The results show that the reduction of the expected losses thanks to the adoption such policies is particularly notable for the lowest income class. These types of analyses are likely to represent a helpful tool for

decision-makers, enabling them to select appropriate, cost-effective mitigation or preparedness measures that directly target those most in need.

**Keywords:** risk index, multi-risk, social vulnerability, disaster risk management, disaster risk reduction

## Sintesi in lingua italiana

L'analisi ed il confronto dei rischi derivanti da diversi pericoli naturali che possono interessare una medesima area è fondamentale per consentire la definizione di adeguate misure di mitigazione e di adattamento e per una efficace gestione delle emergenze. Tuttavia, l'analisi multirischio è solitamente complessa, soprattutto a causa delle diverse metodologie e risoluzioni spazio/temporali adottate nella quantificazione dei singoli rischi. Inoltre, gli eventi passati hanno mostrato che coloro che si trovano in situazioni di disagio e incertezza sociale ed economica tendono ad essere colpite in modo sproporzionato degli impatti di un disastro naturale. La povertà e la disuguaglianza sono state ufficialmente riconosciute come fattori di rischio e l'interesse dei governi e delle autorità locali nel comprendere come fattori socio-economici possano influenzare la vulnerabilità ai disastri naturali è notevolmente aumentato negli ultimi anni. Tuttavia, le analisi di rischio convenzionali generalmente non tengono conto di tali aspetti.

Questo studio propone un approccio basato su indicatori per integrare fattori di vulnerabilità socioeconomica e fisica nell'analisi multi-rischio, con l'obiettivo di superare i limiti sopra citati. È definito un indice di rischio (RI) sulla base della combinazione di singoli indicatori standardizzati rappresentativi della pericolosità di un territorio, in relazione ad uno o più hazard, e della vulnerabilità sia fisica che sociale dei beni e della popolazione esposta. Gli approcci basati su indici sono infatti i più adatti per misurare concetti multidimensionali che non possono essere catturati da un singolo indicatore. Gli indicatori selezionati vengono combinati definendo adeguatamente dei pesi che possono esplicitamente riflettere le priorità delle parti interessate nella definizione delle politiche di adattamento/mitigazione. Questo approccio consente di classificare le regioni esposte a molteplici pericoli e di identificare gli hotspots multirischio, ossia le aree che maggiormente necessitano di strategie di riduzione del rischio catastrofi, in quanto caratterizzate da un'elevata vulnerabilità non solo fisica ma anche sociale. Pertanto, lo strumento proposto può essere un utile supporto per prioritizzare le aree maggiormente esposte a rischio, che è una delle principali sfide nei processi decisionali di gestione dei disastri naturali. Viene mostrato l'utilizzo dell'indice multirischio proposto per il rischio sismico e alluvionale su

tutto il territorio italiano, selezionando il comune come scala di analisi e gli edifici residenziali e la popolazione come beni esposti a rischio. Questo approccio basato su indici consente di confrontare e classificare tali pericoli nel paese, portando all'identificazione delle regioni in cui la probabilità di avere impatti significativi a seguito di terremoti/alluvioni è particolarmente elevata, a causa dell'elevato livello di pericolo, delle scarse prestazioni dei beni esposti nonché la ridotta capacità degli abitanti di adattarsi e rispondere a un tale disastro naturale. Sfruttando il suddetto indice si ottiene una mappa del rischio del territorio italiano e si individuano gli hotspots a cui dare priorità nelle politiche di riduzione del rischio disastri. L'applicazione mostrerà che considerare gli aspetti socio-economici nelle analisi di rischio può modificare anche in maniera significativa l'identificazione di tali hotspot, sottolineando come ignorare gli aspetti sociali nella valutazione del rischio possa influenzare l'efficacia dei piani di riduzione del rischio di catastrofi. Vengono inoltre eseguite delle analisi di sensitività per comprendere come gli hotspot multi-rischio possono cambiare in funzione dell'importanza relativa data a un singolo componente RI, ovvero come le priorità degli stakeholder possono influenzare i risultati.

Per una corretta quantificazione delle perdite economiche attese, determinanti ai fini della definizione di strategie di adattamento e mitigazione, viene effettuata anche una valutazione quantitativa del rischio. Il RI consente di identificare i comuni con il punteggio di rischio più elevato in Italia. Per tali comuni, attraverso un'analisi dettagliata è possibile identificare il distretto che presenta il rischio più elevato, sia in termini di perdite economiche che di vulnerabilità sociale, nonché disaggregare le perdite economiche per i diversi gruppi sociali. Ad esempio, infatti, le persone a basso reddito tendono a subire le perdite maggiori. Attraverso tali analisi è inoltre possibile stimare l'efficacia di alcune strategie di mitigazione. La quantificazione della riduzione delle perdite associata a tali strategie consente di definire le opzioni di mitigazione più idonee, tenendo conto anche delle caratteristiche socio-economiche della popolazione. Così, ad esempio, è possibile selezionare delle politiche di mitigazione idonee per la classe di popolazione a reddito più basso. Per dimostrare l'utilità di tale valutazione dettagliata, tra i comuni italiani, viene selezionato quello con il punteggio di rischio più elevato per l'esecuzione di una valutazione quantitativa del rischio a scala sub-comunale.

L'analisi mostra che le persone a basso reddito tendono a subire le maggiori perdite annuali previste per metro quadrato sia per eventi sismici che alluvionali. Per il caso di studio specifico, la valutazione del rischio viene ripetuta due volte con alcune modifiche alla modellazione per valutare l'efficacia della riduzione delle perdite attese attraverso alcune strategie di riduzione del rischio di catastrofi e relative politiche. I risultati mostrano che la riduzione delle perdite attese grazie all'adozione di tali polizze è particolarmente rilevante per la classe di reddito più bassa. È probabile che questi tipi di analisi rappresentino uno strumento utile per i responsabili delle decisioni, consentendo loro di selezionare misure di mitigazione o di preparazione appropriate ed economiche che si rivolgono direttamente ai più bisognosi.

**Parole chiave:** indice di rischio, multirischio, vulnerabilità sociale, gestione rischio catastrofi, riduzione del rischio

## Acknowledgements

I would like to express my gratitude to my tutor Prof. Maria Polese for guiding me during these years. Her unwavering support and belief in me gave me the possibility to overcome my limits and achieve results beyond my expectations.

I would also like to thank Prof. Carmine Galasso and Asst. Prof. Gemma Cremen for their assistance during my internship at University College of London. Their true enthusiasm and passion motivated me to show my best and challenged me to improve for achieving even higher goals.

## List of Acronyms

ACRONYM	MEANING
AAL	Average Annual Losses
BAP	Budget Allocation Process
$CDR_{LS}$	Global Displacement-based ratio of Capacity to life-safety Demand
CT	Census Tract
CU	Unit Cost
DEM	Digital Elevation Model
DG	Del Gaudio et al. (2019)
DPM	Damage Probability Matrix
DRM	Disaster Risk Management
DRR	Disaster Risk Reduction
DSHA	Deterministic seismic hazard analysis
DTM	Digital Terrain Model
EAL	Expected Annual Losses
ECDF	Empirical Cumulative Distribution Function
EMS-98	European Macroseismic Scale (Grünthal, 1998)
FD	Flood Directive
FRP	Fiber Reinforced Polymer
FwDET	Floodwater Depth Estimation Tool
GED	Global Exposure Database
GEM	Global Earthquake Model
GIS	Geographic Information System
HFA	Hyogo Framework for Action
IDI	Infrastructure Density Index
IDNDR	International decade for Natural disaster reduction
INGV	Istituto Nazionale di Geofisica e Vulcanologia
IPCC	Intergovernmental Panel on Climate Change
ISPRA	Istituto Superiore per la Protezione e la Ricerca Ambientale
ISTAT	Istituto Nazionale di Statistica
LEC	Loss Exceedance Curve
NRA	National Risk Assessment
MAFE	Mean Annual Frequency of Exceedance
OECD	Organisation for Economic Co-operation and Development
OMI	Osservatorio del Mercato Immobiliare
PCA	Principal Component Analysis
PGA	Peak ground acceleration
PGD	Peak ground displacement
PGV	Peak ground velocity
PSHA	Probabilistic seismic hazard analysis
RC	Reinforced concrete
RI	Risk Index
SA	Spectral Acceleration
SoVI	Social Vulnerability Index
SSI	Social Susceptibility Index
TC	Town Compartments
UCPM	Union Civil Protection Mechanism
UNDP	United Nations Development Programme

UNDRO	United Nations Disaster Relief Office
UNDRR	United Nation Office for Disaster Risk Reduction
UNGA	General Assembly of the United Nations
UoM	Unit of Management
VI	Vulnerability Index



## List of Figures

Figure 1.1 – Number of deaths (a) and economic losses (b) recorded after natural disasters occurred since 1970. Decadal figures are measured as the annual average over the subsequent ten-year period. Source: <a href="https://ourworldindata.org/natural-disasters">https://ourworldindata.org/natural-disasters</a> . .....	19
Figure 1.2 – Risk management cycle. ....	21
Figure 1.3 – Timeline with major achievement in disaster risk reduction since 1945. ....	24
Figure 1.4 – Multi-scale framework for integrating physical and social dimension of risk. ....	29
Figure 2.1 – Peak ground acceleration (PGA) Shakemap of 2016 Centra Italy earthquake. Source: <a href="http://terremoti.ingv.it/">http://terremoti.ingv.it/</a> .....	33
Figure 2.2 – European seismic hazard map displaying the ground motion expected to be reached or exceeded with a 10% probability in 50 years (Woessner et al., 2013). ....	34
Figure 2.3 – Fragility curves for the most vulnerable class of buildings (Lagomarsino et al., 2021). ....	38
Figure 2.4 – Flood hazard maps for Isonzo river in Italy-Slovenia cross-border area. Adapted from BORIS (2022b). ....	45
Figure 2.5 - FIA flood damage functions for buildings adapted from FEMA (2022). ....	48
Figure 2.6 - An example of mixed-use curve definition adapted from Silvestro et al. (2016). ....	49
Figure 2.7 – Approaches for multi-risk assessment, from single hazard to multi-hazard. Adapted from Zschau (2017). ....	52
Figure 2.8 - Hazard matrix adapted from (Kunz & Hurni, 2008). ....	54
Figure 2.9 - Slovenian National Disaster risk matrix (GRS, 2018). ....	55
Figure 2.10 - Risk curves of the hazards due to windstorms, floods and earthquakes for the city of Cologne for losses concerning buildings and contents (Grünthal et al., 2006). ....	56
Figure 2.11 – Hazard interactions matrix. Adapted from De Pippo et al. (2008) .....	58
Figure 2.12 - Event Tree describing potential eruption scenarios for volcano Vesuvius and possible associated hazards that may develop. Adapted from Neri et al. (2008). ....	59
Figure 3.1 – Seismic hazard map of Italy with PGA values for a return period of 475 years. PGA values is expressed in units of g. ....	75
Figure 3.2 – Map of flood inundated areas expected to low probability or extreme events (P1), medium probability events (P2) and high probability or frequent events (P3). ....	80
Figure 3.3 – CAPRA depth-loss functions (Cardona et al., 2012). ....	82
Figure 3.4 – HAZUS depth-loss functions for single family home with no basement. ....	82
Figure 3.5 – Unemployment rate (a) and female employed rate (b) for Italian municipalities. ....	84
Figure 3.6 – Average annual income (euro) per family based on the number of components of the family. Source: ISTAT. ....	85
Figure 3.7 – SoVI map for Italy. ....	87
Figure 3.8 – ECDF for seismic hazard (a), flood hazard (b), social vulnerability (c) and residential population (d) indicators. ....	88
Figure 3.9 – Seismic hazard and physical vulnerability combination to get seismic risk score map. ....	89
Figure 3.10 – Multi-risk index map obtained using the geometric aggregation (a) and its comparison with the values obtained by linear aggregation (b). In the comparison map (b) red values indicate an increase in the multi-risk index got through the linear aggregation, while the blue ones a reduction in the index. ....	90
Figure 3.11 – Comparison between multi-risk scores obtained adopting the medium probability with (a) the high probability flood map and (b) the low probability flood map. Red values indicate an increase in the score values due to the selection of a different map (high probability or low probability). ....	92
Figure 3.12 – Comparison between multi-risk scores obtained adopting seismic hazard map for 475 years return period and (a) 100 years return period map and (b) 2500 years return period map. Red values indicate an increase in the score values due to the selection of a different map. ....	93
Figure 3.13 - Variation of multi-risk index when seismic risk (a), flood risk (b), social vulnerability (c) or population factor (d) is weighted more than the others. Red values indicate an increase in the index value. ....	94

Figure 4.1 – The main steps of the Cartis-based approach for regional exposure modelling...	101
Figure 4.2 – Diffusion of the vertical (irregular or regular layout) types on masonry building stock at regional scale, derived by Cartis-based inventory.....	103
Figure 4.3 – Occurrence percentages of masonry buildings built before 1919 in the vulnerability classes identified by DG model for different Italian regions.....	104
Figure 4.4 – Seismic physical vulnerability indicator obtained using the original DG exposure model (a) and the one derived through the Cartis-based approach for exposure modelling (b). .....	105
Figure 4.5 – Variation of RI index for municipalities in Tuscany region due to the adoption of Cartis-based approach, in case of equal weighting of indicators (a) and in case of seismic risk is weighted three times more than the others (b). .....	106
Figure 5.1 – Framework for detailed multi-risk assessment.....	108
Figure 5.2 – Municipality of Somma Vesuviana.....	111
Figure 5.3 – Delimitation of OMI zones in Somma Vesuviana. Each zone is identified by an alphanumeric code that categorises the zone as Central (B), Semi-central (C), Suburb (D) and rural (R). .....	112
Figure 5.4 – SoVI values (a) and normalized sub-indicator for population age (b), low educational index (c), number of families with more than 5 components (d) and earners of income (e) for each OMI zone. ....	114
Figure 5.5 – Town compartments identified in Somma Vesuviana by Cartis form. ....	115
Figure 5.6 – Procedure for compiling building inventory at OMI level integrating census and Cartis data.....	116
Figure 5.7 – Example of building inventory at census tract (CT) level.....	117
Figure 5.8 – Assignment of census tracts not included in original Cartis form.....	118
Figure 5.9 – Building inventory for masonry (a) and RC buildings (b) according to Rosti et al.(2021a) and Rosti et al.(2021b) models.....	120
Figure 5.10 – Vs30 map (a) proposed by Mori et al. (2020) and slope map (b) for the municipality of Somma Vesuviana (bounded with red poyline). ....	122
Figure 5.11 - Hydrogeographic network (a) and flood hazard maps provided by ISPRA (b) for Somma Vesuviana.....	123
Figure 5.12 – Representation of FwDET. The blue line represents “within banks” water level, and the brown line represents hypothetical floodwater level. Adapted from Cohen et al. (2018). .	124
Figure 5.13 – Flood hazard map with flood extension and expected water depth (m), obtained through FwDET-GEE.....	124
Figure 5.14 – Aerial view of Somma Vesuviana from Google Earth.....	125
Figure 5.15 – Flood hazard maps with flood extension, expected water depth (m) and expected flooded buildings with the corresponding inundation level (m). The depth-loss curves adopted for residential buildings are also reported. ....	126
Figure 5.16 – Risk curves for seismic and flood risk for the entire municipality.....	127
Figure 5.17 – Modified fragility curves for RC buildings classified in C2 vulnerability class, with medium height. The dashed curves are the original fragility curves of Rosti et al. (2021b). ...	133
Figure 5.18 – Expected losses expressed in euro(a) and euro/m <sup>2</sup> (b) calculated considering the implementation of hard policies (in yellow) and the difference with the corresponding losses calculated for the original scenario without any policies. ....	134
Figure 5.19 – Changing in flood damage curves due to mitigation actions for hazard reduction (HM) and mitigation actions for exposure/ vulnerability reduction (VEM).....	135
Figure 5.20 - Expected losses expressed in euro(a) and euro/m <sup>2</sup> (b) calculated considering the implementation of hard policies (in blue) and the difference with the corresponding losses calculated for the original scenario without any policies. ....	136
Figure 5.21 - Expected losses expressed in euro(a) and euro/m <sup>2</sup> (b) calculated considering the implementation of soft policies (in yellow) and the difference with the corresponding losses calculated for the original scenario without any policies. ....	138
Figure 5.22 - Expected losses expressed in euro(a) and euro/m <sup>2</sup> (b) calculated considering the implementation of soft policies (in blue) and the difference with the corresponding losses calculated for the original scenario without any policies. ....	139

Figure 5.23 - Expected losses expressed in euro(a) and euro/m2 (b) disaggregated across the three different income level classes. ....	140
Figure 5.24 - Expected losses expressed in euro(a) and euro/m2 (b) disaggregated across the three different income level classes. ....	141
Figure 6.1 - Map of the Risk Index values in the Campania region.....	144
Figure 6.2 – Delimitation of OMI zone for the city of Portici. Each zone is identified by an alphanumeric code that categorises the zone as Central (B), Semi-central (C) or Suburb (D). 146	146
Figure 6.3 - OMI homogeneous areas and their classification based on SoVI value. ....	147
Figure 6.4 – EAL/m2 for OMI zones.....	147
Figure 6.5 - Expected annual losses per square meter disaggregated across the three different income level classes.....	148
Figure 6.6 – Map of the 27 Italian municipalities involved in the pilot application of BORIS project. The map shows the values of EAL/m <sup>2</sup> at municipal level. An example of LEC for seismic and flood risk is also reported. ....	149
Figure 6.7 – Analysis of correlation between RI and expected losses per square meters. ....	151
Figure 6.8 – Flood hazard maps for the cities of Gradisca d'Isonzo (a) and Premariacco (b), considering a flood event with a return period of 100 years. Source: BORIS. ....	152
Figure 6.9 - Analysis of correlation between seismic risk score and expected losses per square meters.....	153

## List of Tables

Table 2-1 – Percentages of short term and long term unsafe buildings for each damage level of the EMS-98 scale, adopted in Dolce et al. (2021). .....	43
Table 2-2 - Main hazard types and their interactions. Source: Westen & Greiving 2017. ....	51
Table 3-1 – Indicators and variables derived from ISTAT and their impact on social vulnerability. ....	86
Table 3-2 – Italian municipalities with highest differences between risk index (RI) obtained through linear aggregation and geometric aggregation. The residential population (Pop), the PGA value for a return period of 475 years (ag), the seismic physical vulnerability indicator (Sv), the percentage of flooded area (F), the flood vulnerability index and the SoVI index for each municipality are also reported. ....	91
Table 4-1 - Occurrence percentages of vulnerability classes into 8 time intervals, defined by DG model. ....	100
Table 4-2 – DG exposure matrix derived by Cartis-based inventory, for Tuscany region. ....	104
Table 5-1 – List of the 10 of municipalities with highest risk index in Italy. The index is calculated in the hypothesis of equal weighting of indicators. ....	109
Table 5-2 – Municipalities included in the list of the first 100 Italian municipalities with highest score for three different weighting combination of indicators. Risk score refers to the case of equal weighting. ....	110
Table 5-3 – Municipality with highest risk score, assuming equal weights for indicators, included in Cartis database. ....	111
Table 5-4 – Real estate market value and lease value of residential buildings in each OMI zone. The values are referred to the municipality of Somma Vesuviana. ....	113
Table 5-5 - Definition of vulnerability classes based on type of vertical and horizontal structures and presence of connection devices, according to Rota et al. 2008. ....	119
Table 5-6 – Expected losses due to seismic and flood hazards. Ratio (F/S) refers to ratio between flood and seismic losses. The values of SoVI and residential population of each OMI zone are also reported. ....	128
Table 6-1 – List of the 10 municipalities with highest risk score in Campania region, adopting the equal weighting of indicators. ....	145
Table 6-2 – OMI zone identified in Portici. ....	146
Table 6-3 – Economic losses and RI values for the Italian municipalities involved in BORIS project. The ratio between EAL due to flood and EAL due to earthquake is also reported (Ratio). ....	150

# Contents

Abstract .....	1
Sintesi in lingua italiana .....	4
Acknowledgements .....	7
List of Acronyms .....	8
List of Figures .....	10
List of Tables .....	13
1. Introduction .....	17
1.1. Disaster Risk Management: where we are and where we need to be.....	17
1.2. Objectives of the study .....	27
1.3. Thesis outline .....	30
2. Understanding the risk.....	31
2.1. Earthquakes .....	31
2.1.1. Hazard model .....	31
2.1.2. Vulnerability modelling .....	35
2.1.3. Exposure modelling .....	38
2.1.4. Impact assessment.....	40
2.2. Floods.....	44
2.2.1. Hazard model .....	44
2.2.2. Exposure and vulnerability modelling for impact assessment .....	45
2.3. From single risk to multi-risk assessment.....	50
2.3.1. Multi-layer single risk assessment .....	52
2.3.2. Multi-hazard risk assessment: hazard interactions.....	57
2.3.3. Physical vulnerability for multiple hazards.....	60
2.3.4. Building taxonomy for multi-hazard risk assessment .....	61
2.4. Multi-dimensional nature of risk.....	62
2.4.1. Social Vulnerability .....	65
2.5. Current gaps and open issues .....	68
3. A framework for integrating social vulnerability in multi-risk assessment .....	71
3.1. Building a composite indicator .....	72
3.2. Indicators for physical and social dimensions.....	74
3.2.1. Seismic risk .....	74
3.2.2. Flood risk .....	78
3.2.3. Model for social vulnerability .....	83
3.3. Multi-risk index.....	88
3.4. Sensitivity analysis.....	91

4.	Regional based exposure models to account for local building typologies.....	96
4.1.	A Cartis-based approach for exposure modelling .....	99
4.2.	Application for Italian regions .....	101
4.3.	Effects on Risk Index .....	104
5.	Quantifying multi-risk: an application in Italy .....	107
5.1.	Case study selection .....	109
5.2.	Multi Risk assessment.....	111
5.2.1.	Seismic risk .....	114
5.2.2.	Flood risk .....	122
5.2.3.	Risk curves.....	126
5.3.	Mitigation policies for risk reduction.....	129
5.3.1.	Hard policies .....	131
5.3.1.1.	Seismic retrofitting.....	131
5.3.1.2.	Flood management measures .....	134
5.3.2.	Soft Policies .....	137
5.3.3.	Discussion .....	139
6.	Strengths, limits and future needs .....	142
6.1.	Risk Index for multi-dimensional single-risk assessment.....	143
6.2.	Evaluating the representativeness of risk index: comparison with detailed risk assessment.....	148
6.3.	The need of defining the relative importance of indicators .....	153
6.4.	Conclusion .....	155
7.	References .....	157



## Introduction

### 1.1. Disaster Risk Management: where we are and where we need to be

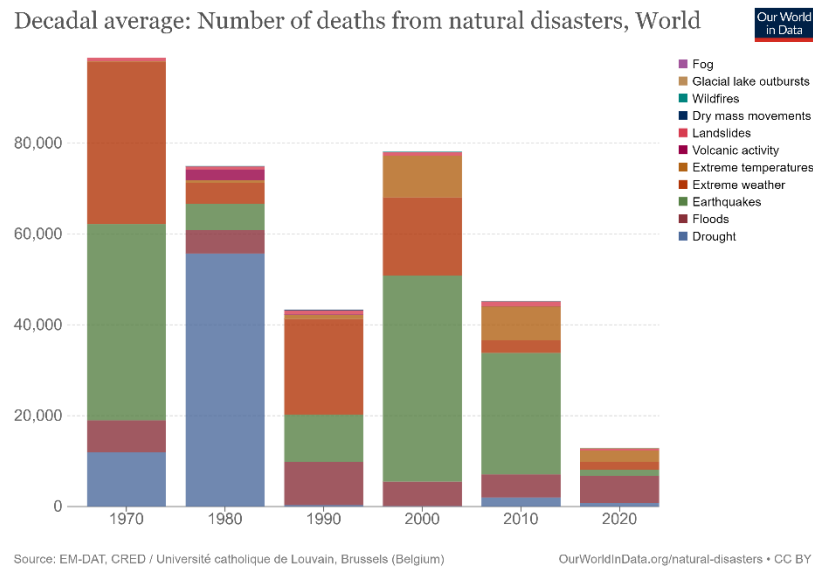
A natural hazard is defined as natural process or phenomenon that may cause loss of life, injury or other health impacts, property damage, loss of livelihoods and services, social and economic disruption, or environmental damage (UNISDR, 2009). They may be classified in different ways, for instance according to the main origin of the hazard in geophysical, meteorological, hydrological, climatological and biological (Guha-Sapir, et al., 2016). For example, we refer to geophysical or geological hazards as those hazards originating from solid earth, such as earthquakes or volcanic eruptions; hydrogeological hazards, such as floods, are caused by the occurrence of movement, and distribution of surface and subsurface freshwater and saltwater, while events like storms are considered meteorological hazards, caused by micro- to meso-scale extreme weather and atmospheric conditions.

During past decades, natural hazards have caused devastation to many communities throughout the world. One of the most notorious events is the 2004 Indian Ocean earthquake and tsunami, that involved 15 different countries and caused more 220,000 deaths. The 2010 Haiti earthquake was included in the list of ten deadliest natural disasters, estimating three million people affected and more than 300,000 fatalities. In March 2011 the Tōhoku earthquake was the most powerful earthquake ever recorded in Japan and the fourth most powerful earthquake in the world. The earthquake caused widespread damage on land and triggered a series of large tsunami waves that devastated many coastal areas of the country, counting 19,759 deaths, 6,242 injured, and 2,553 people missing (Fire and Disaster Management, 2022). Very heavy natural disasters have been also caused by hazards like flooding,

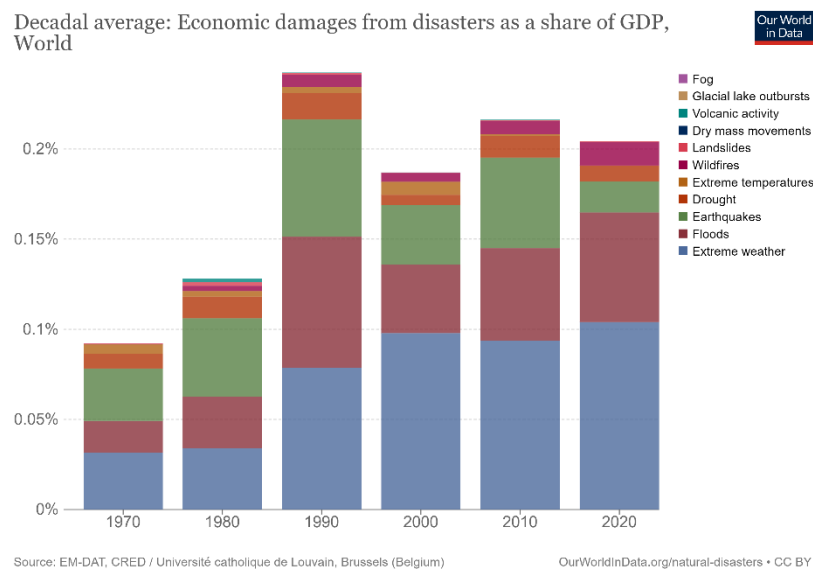


volcanic eruption, landslide, hurricanes. Just to name a few, the Cyclonic Storm Nargis (May 2008) was an extremely destructive and deadly tropical cyclone that hit the Southeast Asia with a death toll of about 138,000, while the 2005 hurricane Katrina, the 2012 hurricane Sandy and 2017 hurricane Maria are among the 10 worse hurricanes in the US history. In 2020 a series of floods have affected South Asia countries causing \$105 billion USD of damage and 6,511 fatalities, the highest impacts in a flood since Cyclone Sitr in 2007. In July 2021, severe floods also affected several European countries including Austria, Belgium, Croatia, Germany, Italy, Luxembourg, the Netherlands, and Switzerland, causing deaths and widespread damage. Among most recent natural disaster, also the 2019-2020 Australia wildfire and the 2022 European heat waves can be mentioned. Figure 1.1 shows the recorded number of deaths and the economic damages from natural disasters from 1970 (<https://ourworldindata.org/natural-disasters>). It can be noted that concerning deaths earthquakes were the main cause in the last two decades, while economic losses are significantly affected also by floods and extreme weather.

Disaster risk management (DRM) is the application of disaster risk reduction policies and strategies to prevent new disaster risk, reduce existing disaster risk and manage residual risk, contributing to the strengthening of resilience and reduction of disaster losses (UNDRR, 2009). Risk is defined as the potential for adverse consequences or impacts due to the interaction between one or more natural or human-induced hazards, exposure of humans, infrastructure and ecosystems, and systems' vulnerabilities (Casajus Valles, et al., 2020). Impacts of a hazardous events are usually expressed in terms of economic losses and people affected. Total economic impacts consist in direct and indirect economic losses: the former represents the monetary value of total or partial destruction of physical assets existing in the affected area, the latter the decline in economic value owing to business interruption. People affected are those who have suffered injury or illness, who were evacuated, displaced, relocated or have suffered direct damage to their livelihoods, economic, physical, social, cultural and environmental assets.



(a)



(b)

**Figure 1.1** – Number of deaths (a) and economic losses (b) recorded after natural disasters occurred since 1970. Decadal figures are measured as the annual average over the subsequent ten-year period.  
Source: <https://ourworldindata.org/natural-disasters>.

Risk is a combination of three components: hazard, vulnerability and exposure. Hazard is a process that has the potential to harm people or cause property damage, social and economic disruption. Hazards may be natural, if they are associated with natural processes and phenomena, or human-induced if they are induced predominantly by human activities and choices. Natural hazard events can be characterized by their magnitude or intensity, speed of onset, duration, and the area they cover. In defining the severity of a hazard, its intensity is correlated with its frequency. The latter is expressed in

probabilistic terms of recurrence intervals or return period and in general the longer the return period (i.e., the less frequent the hazard) the greater the intensity of the hazard. The extent of impact area is usually function of its severity as well. We can distinguish between intensive risk, referred to a risk associated with high-severity, mid to low-frequency disasters and with highly localized hazards (e.g., cyclones, earthquakes, tsunamis, severe floods and storms), and extensive risk, normally associated with weather-related hazards (e.g., fires and water-related drought) and with low-severity, high-frequency events that may affect large areas (UNDRR, 2015). Extensive risks are associated with persistent hazard conditions of low or moderate intensity, often of a highly localized nature, for instance the persistent impact of volcanic ash on the island of Montserrat since 1995. Exposure represents the assets exposed at risk, i.e. the presence of people, housing, infrastructure, production capacities, species or ecosystems, and other tangible human assets in places and settings that could be adversely affected by one or multiple hazards (IPCC, 2014; UNDRR, 2016). If hazard occurs in area with no exposure, then there is no risk (e.g., typhon hitting the Pacific Ocean, such as typhon Lekima in 2013). Exposure may vary in space and time: People and economic assets become concentrated in areas exposed to hazards through processes such as population growth, migration, urbanization and economic development. Vulnerability is the propensity or predisposition of an individual, a community, infrastructure, assets or systems to be adversely affected (UNDRR, 2016). As a matter of fact, disaster risk not only depends on the severity of hazard or the number of people or assets exposed, but also on the susceptibility of people and economic assets to suffer losses and damages. Thus, together with exposure, vulnerability can explain why some non-extreme hazards can lead to extreme impacts and disasters, while some extreme events do not.

Disaster risk reduction (DRR) strategies and policies define goals and objectives for preventing new and reducing existing disaster risk and managing residual risk. Disaster risk management (DRM) can be thought of as the implementation of DRR, since it describes the actions that aim to achieve the objective of reducing risk. Figure 1.2 shows the different steps of

risk management cycle, from risk identification to the implementation of risk management measures.



**Figure 1.2** – Risk management cycle.

Before the disaster strikes, the fundamental elements of risk (i.e., hazard, exposure and vulnerability) are integrated to quantify potential impacts resulting from a hazard event. According to ISO 31000 (ISO, 2009), risk assessment process is divided into three different stages: risk identification, risk analysis and risk evaluation. The first step is the identification of the asset exposed at risk that should be considered in the assessment (e.g., population, buildings, infrastructure, environment) and the identification of hazards which a country is exposed to. The latter can vary from country to country. For example, in Denmark assessing risk derived by floods and extreme weather phenomena like hurricanes and storms could be relevant, while earthquakes are usually not investigated as they are considered events unlikely to happen in or near Denmark (DEMA, 2013). Once the potential hazards are identified, human, economic, environmental as well as political and social impacts expected for a given scenario (i.e., future disaster event defined in terms of its magnitude and probability of occurrence) can be investigated through risk analysis. Based on the purpose of the assessment, the selected scale of analysis and the availability of data, several approaches can be used for the analysis. Qualitative and semi-quantitative risk analysis are used for rating or scoring risks based on expert knowledge and using

limited quantitative data. Risk matrix is an example of semi-quantitative approach: risk is represented by a diagram with classes of hazardous events on one axis and the consequences on the other axis. Risk matrices can be used for determining if the level of risk is acceptable and to visualize the effects of risk reduction measures. The limitation of this kind of approach is their subjectivity, as the ranking of risk classes as well as their corresponding limits require expert opinion. On the contrary, a quantitative risk assessment allows the spatial quantification of impacts for a single hypothetical scenario (determinist risk assessment) or considering several events with their own likelihood in terms of frequency and severity (probabilistic risk assessment). Finally, risk evaluation is the process of comparing the results of risk analysis in order to determine whether further action is required. To this aim, the outcomes of risk assessment need to be presented to stakeholders in DRM, who may not have a technical background. Therefore, preparing the risk outcomes in different and suitable ways (e.g., through bar charts, pie charts, maps) for an effective communication is a crucial step. The assessment of the risk enables decision makers to understand the nature and extent of disaster risk, to formulate prevention and mitigation policies and implement consequential preparedness or response acts. Disaster prevention indicates the set of activities and measures to avoid existing and future risks. As certain hazards cannot be eliminated, prevention aims at reducing vulnerability and exposure in such contexts in order to reduce the risk of disaster. Mitigation measures are actions put in place for lessening the severity and/or the extent of the adverse impacts of a hazardous event. They may include engineering techniques and hazard-resistant construction as well as improved environmental and social policies and public awareness. On the contrary, preparedness actions are carried out within the context of disaster risk management and aims to build the capacities needed to efficiently manage all types of emergencies and achieve orderly transitions from response to sustained recovery (UNDRR, 2009). Figure 1.2 shows the different steps of risk management cycle, from risk identification to the implementation of risk management measures.

The severity of the consequences of natural hazard events is largely dependent on the level of preparedness and resilience of society for such events. However, before 1970 measures adopted by the General Assembly of the United Nations (UNGA) regarding severe disasters were mostly focused on the emergency assistance in the aftermath of their occurrence, with the planning and application of responding and recovering actions. With the creation of the United Nations Disaster Relief Office (UNDRO) in 1971 the UNGA started to promote the study, prevention, control and prediction of natural disasters, highlighting how disaster prevention and pre-disaster planning are an integral part of the international development policy of governments and international organizations. Designing the 1990s as the international decade for Natural disaster reduction (IDNDR), more emphasis on disaster risk management as opposed to disaster management began to be placed: in 1994 the Guidelines for Natural Disaster Prevention, Preparedness and Mitigation and its Plan of Action were presented during the World Conference on Disaster Reduction held in Yokohama, Japan, and in 2000 the International strategy for disaster reduction (ISDR) was designed to foster this need to move from the previous emphasis of protection against hazards towards a process involving awareness, assessment and management of risk. To ensure the implementation of the ISDR, the United Nations Office for Disaster Risk Reduction (UNDRR) was specially created as well. The culmination of this process started in 1990 with the declaration of the IDNDR and the adoption of the Hyogo Framework for Action (HFA) 2005-2015: building the resilience of Nations and communities to disasters by the World Conference on Disaster Reduction. The expected outcome of the Framework was the substantial reduction of disaster losses in lives and in the social, economic and environmental assets of communities and countries, that should have been achieved through incorporation of risk reduction approaches into the design, monitoring disaster risks and enhancing early warning, reducing vulnerability of assets at risk and using knowledge and education to build a culture of safety and resilience at all levels.

Currently, the official global agreement on actions of DRR is the Sendai Framework for Disaster Risk Reduction 2015-2030, the successor instrument

of the HFA. To achieve the prefixed goal, i.e. prevent and reduce hazard exposure and vulnerability to disaster, increase preparedness for response and recovery, and thus strengthen resilience, the Sendai Framework outlines seven global targets to be achieved by 2030 that can be classified as substantial reductions (i.e., reduce global disaster mortality, reduce the number of affected people globally, reduce direct economic losses, reduce disaster damage to critical infrastructure and disruption of basic services) and substantial increases (i.e., increase the number of countries with national and local disaster risk reduction strategies, enhance international cooperation in developing countries, increase the availability of and access to multi-hazard early warning systems). Four priority action field have been identified:

- Understanding the risk
- Strengthening disaster risk governance to manage disaster risk
- Investing in disaster risk reduction for resilience
- Enhancing disaster preparedness for effective response, and to «Build Back Better» in recovery, rehabilitation and reconstruction

Figure 1.3 shows the timeline of the main achievements in disaster risk reduction in the last 50 years.

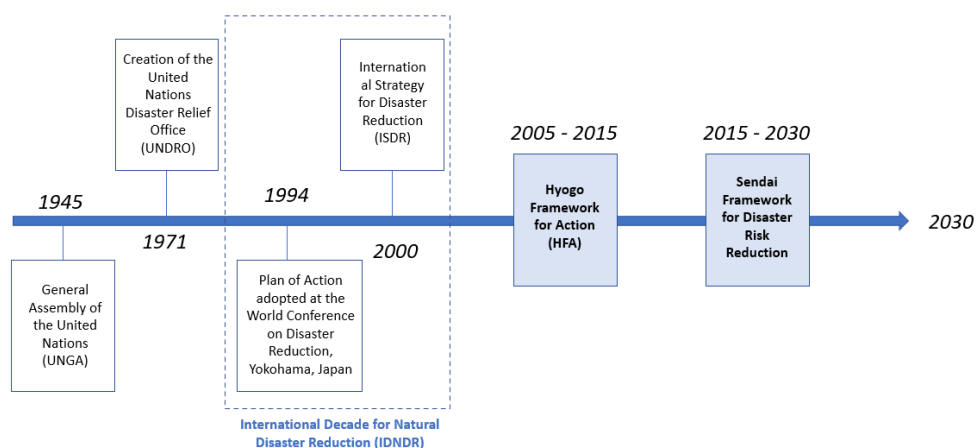


**Figure 1.3** – Timeline with major achievement in disaster risk reduction since 1945.

In prevention and reducing risk, a primary role is played by single States members. The UNDRR encourages the establishment of National Platforms for Disaster Risk Reduction, mechanisms for coordination and policy guidance on DRR strategies, plans and actions. The National Platform should

coordinate all stakeholder engagement at the national level and should also have an effective dialogue with Local Platforms in place in order to influence, encourage and coordinate local action. This platform may involve public actors such as the civil protection departments, national, regional and local governments as well as national scientific and academic community, insurance companies and volunteer's organizations active in the field of DRR and disaster risk management. As understanding the risk is a critical step to select suitable risk reduction strategies and implement response plans to address them, Decision No 1313/2013/EU of the European Parliament and of the Council calls participant States to periodically assess disaster risk. National Risk Assessment (NRA) became a well-known tool to identify the main risks that a country could face and to assess their likelihood and severity. A wide range of natural, anthropogenic and socio-natural risk can be identified and assessed in the NRA for a country, such as earthquakes, floods, droughts, wildfires, volcano eruption, biological disasters, and chemical and nuclear accidents. To facilitate countries on this task, the European Commission developed the Guidelines on risk assessment and mapping (Poljanšek, et al., 2019). The report describes different disaster risk assessment approaches that could be adopted by UCPM participant countries for developing their NRAs, also providing tools and methods for specific risk assessment related to certain hazard (e.g., earthquakes, floods and drought). An overview of NRAs in several countries can be found in OECD (2018).

Although some progress has been achieved in reducing disaster risk at local, national, regional and global levels by countries, the toll of people affected by disasters is still high. Moreover, evidence indicates that exposure of person and assets in countries increase faster than vulnerability and that people in vulnerable situation may be disproportionately affected. Poverty and inequality, unplanned and rapid urbanization, poor land management have been officially recognized as risk drivers in the Sendai Framework, highlighting the importance of capturing the multi-dimensional and dynamic nature of risk when assessing it. The need to reduce vulnerabilities and enhancing community resilience has increased the interest of governments and local stakeholders in understanding the influence of socio-economic



factors, such as age, education, employment status, on vulnerability to hazards and their contribution to community preparedness, disaster response and post-disaster recovery. The integration of socio-economic, cultural, political and physical factors in risk assessment process requires the definition of a more holistic risk concept (Marin Ferrer, et al., 2017).

On the other hand, the long-term evolutionary nature of risks should be considered instead of relying on past or static observations of society within current environmental conditions. Considering the dynamics of hazard, exposure, and vulnerabilities allows properly informed decisions on the spatial planning and risk-prevention measures/policies that will shape the coming decades (Cremen, et al., 2021). Moreover, the quantification of tomorrow's natural hazards commonly involves accounting for future climatic conditions, so climate change should also be taken into account (Cremen, et al., 2021; Dessler, 2021).

As many countries are exposed to multiple hazards, one of the main challenges of DRM is to prioritize the risks originating from these different hazards to enable decisions on appropriate and cost-effective mitigation or preparedness measures. A joint analysis of all risks that potentially can affect a territory is also crucial for a sustainable environment and land use planning. However, the performing of multi-risk assessment is a difficult task, mostly due to different methodologies and spatial/temporal resolutions adopted in the quantification of single risks (WMO 1999, Tyagunov et al., 2005, Marzocchi, et al., 2009, Kappes, et al., 2010). Different hazards may differ in their nature, return periods, intensity and impacts. Moreover, they often require different scale of analysis as extension of area impacted by diverse hazards can greatly vary. For instance, while seismic risk can be assessed at large scale (e.g., regional, municipal), the scale required for flood analysis is generally much smaller as flood hazard may varies spatially much more significantly than seismic hazard. Furthermore, floods are usually more frequent than earthquakes, that means that the former are characterized by very short return periods while the second by long or very long return periods. The consequence of such inherent differences is that also the metrics

commonly adopted to measure are very different and hardly directly comparable.

## 1.2. Objectives of the study

The main objective of this study is to investigate how to overcome the above-mentioned limitations. A framework for integrating both socio-economic and physical factors in multi-risk analysis is proposed. Analysing the state of art in multi-hazard and multi-risk modelling it has shown that index-based approaches are the most suitable ones for measuring multidimensional concepts which cannot be captured by a single indicator, and they are widely used for spatial multi-criteria evaluation (UNDP, 2010; De Groeve et al., 2015). First, a Risk Index (RI) based on the combination of individual standardized indicators for hazard, physical and social vulnerability and exposure inputs is developed. The major strengths of the proposed index-based approach are the following:

- It allows to compare and rank different hazard that potentially affects the same area, leading to the identification of the regions more exposed and more vulnerable to multiple risks;
- It may be a useful support for identifying hotspots to prioritise in decision-making process for risk reduction, that is one the main challenges in Disaster Risk Reduction;
- It is relatively simple and easily applicable approach for effective risk decision support across any other national or transnational context of interest;
- It appropriately accounts for uncertainties, relying on probabilistic distributions of hazard inputs, physical and social vulnerability indices, and population exposure for each individual risk of interest;
- It is a versatile approach, that fits the adoption of different hazard, vulnerability and exposure models; also, it fits both for integrating social aspects in single or multi-risk assessment and for use in multiple hazard risk assessment focused only on physical aspects (in a multi-layer single risk assessment framework);

- It can directly integrate relevant subjective perspectives and stakeholder priorities through assigning suitable weights for each indicator based on the defined aims.

In order to demonstrate the usefulness of the proposed approach, the RI is calculated for earthquake and flood risk across the entire country of Italy, selecting the municipality as scale of analysis and residential buildings and population as assets at risk. Exploiting the aforementioned index, a risk map of the Italian territory is proposed. Despite all prominent advantages described before, being a semi-quantitative approach the RI does not allow to quantify the expected social and economic losses due to future hazardous events, crucial for preparedness purposes. Moreover, if the effectiveness of some mitigation strategies would like to be estimated it would be impossible to quantify the loss reduction associated to them and to estimate the cost-benefit ratio. Therefore, an inclusive framework towards disaster risk reduction should be integrate two complementary steps: the former that allows to prioritise areas based on a multidimensional representation of risk; the second that consists in detailed analysis for risk quantification. Specifically, the goals of this detailed risk assessment are:

- Quantify seismic and flood risks in terms of social and economic losses at municipal and sub-municipal level;
- Compare the considered risks through risk curves and identify areas across the municipality more affected by negative consequences of such hazardous events;
- Disaggregate losses accounting for the income level of inhabitants and investigate if people belonging to different income classes tend to experience different grades of losses;
- Evaluate the effectiveness of risk reduction strategies and related policies performing risk analysis for different scenarios (i.e., original - no policies, with hard policy and soft policy);
- Investigate how the reduction of the expected losses thanks to the adoption of hard and soft policies impacts on different population income classes.

Thus, among Italian municipality, the one with highest RI is selected for performing such quantitative risk assessment at sub-municipal scale. Steps, tools and objectives of the proposed framework are reported in figure 1.4.

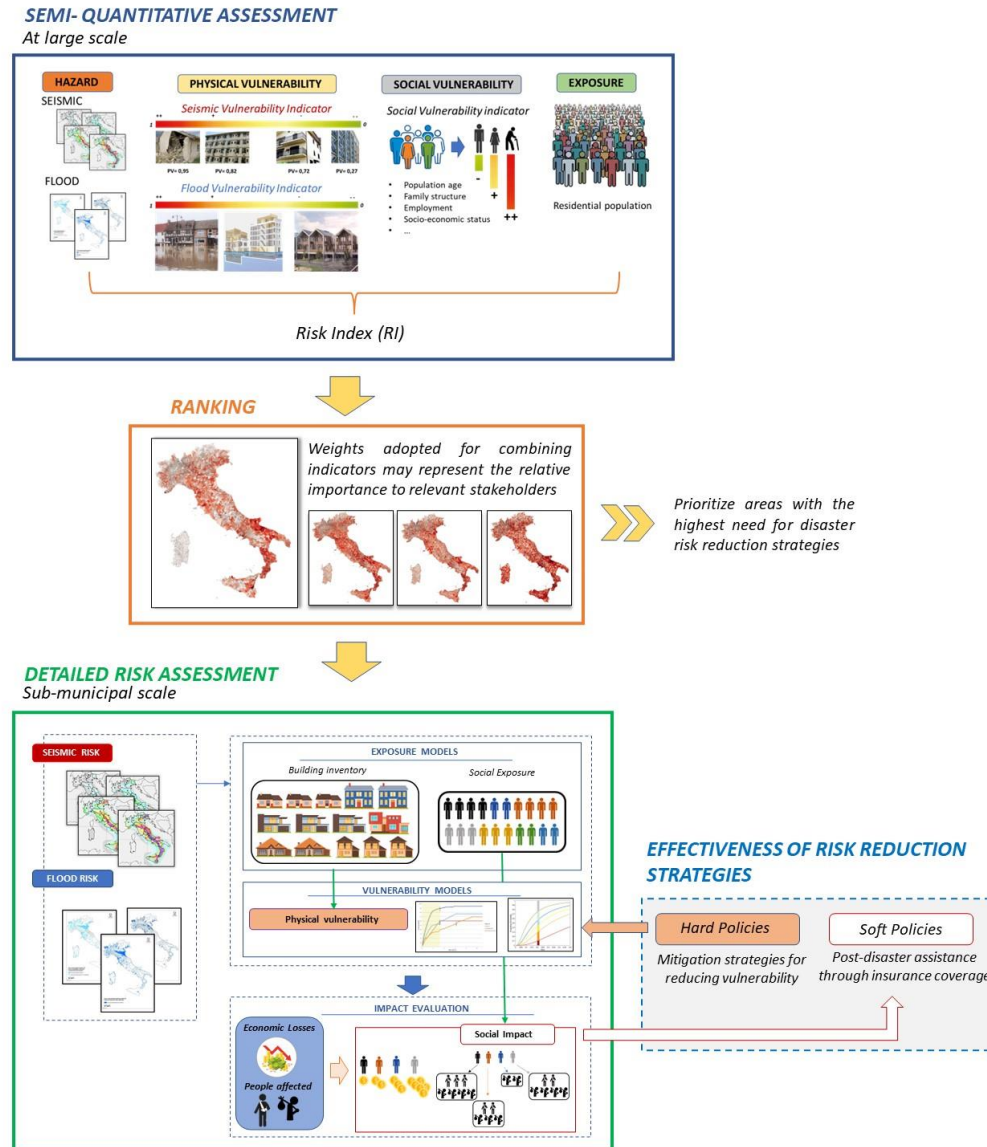


**Figure 1.4** – Multi-scale framework for integrating physical and social dimension of risk.

Finally, the approximation in risk estimation due to the use of a semi-quantitative approach are also evaluated by means of comparison with outcomes of quantitative analysis. To this aim, ranking obtained using the proposed risk-index approach is compared with some results of multi risk analysis available in Italy. The scope is to identify what are the limits of the approach and which aspects of it may be improved.

Risk assessment performed in this study can be defined as multi-dimensional and multi-scale. As a matter of fact, multiple dimensions are appropriately integrated through the index-based approach proposed; it also fits easily for adding more hazards and dimensions respect to the ones considered herein. The proposed framework is multi-scale as two different scale are adopted for semi-quantitative and quantitative risk assessment, considered as complementary steps: a large scale for the former (e.g., municipal level), a detailed scale for the second (e.g., town compartment level). Thus, it allows to prioritize areas (at national, regional, municipal or sub-municipal scale) potentially more affected by just one or several hazards as well as to identify the most suitable mitigation options in a given area. This study demonstrates how the types of analyses performed are likely to represent a helpful tool for decision-makers, enabling them to select appropriate, cost-effective mitigation or preparedness measures that directly target those most in need.

### 1.3. Thesis outline

The work is organized into six parts. After the introduction chapter, Chapter 2 presents a literature review of multi-hazard risk assessments. The evidence of the impacts of social and economic aspects on single and multi-risk assessment are also presented. Chapter 3 illustrates the implementation of the index-based approach proposed. Chapter 4 presents a methodology for improving building inventory and how a better exposure modelling can affect the RI calculation. In Chapter 5 the detailed risk assessment is performed. Seismic and flood risks at sub-municipal level are estimated in terms of economic losses and their disaggregation across different population income level classes is investigated. Chapter 6 draws the conclusions, showing the main findings and implications of the proposed framework, its limits and future improvements.

## Understanding the risk

Understanding the potential impacts of natural hazard is the foundation for effective DRM. Risk assessment consists in determining the nature and extent of disaster risk by analysing potential hazards and evaluating existing conditions of exposure and vulnerability (UNDRR, 2018). Risk presents the negative impacts of an event, in terms of loss of life, property damage, social and economic disruption or environmental degradation. The term “impact” indicates both the negative and positive consequences of hazardous event, while losses are only negative ones (De Groeve, et al., 2013). Thus, we can refer at risk assessment as the assessment of potential losses due to a future hazardous event. The quantification of disaster risk enables governments, communities and individuals to make informed decisions to manage their risk.

As mentioned before (see section 1.1), risk assessment process is divided into three stages: risk identification, risk analysis and risk evaluation. Risk analysis is the process of combining the risk components of hazard, exposure and vulnerability to determine the level of risk. For every risk, different risk analysis approaches can be used, from qualitative to quantitative ones, mostly based on the main purpose of the analysis, the time span of the assessment and the availability and reliability of information (Poljanšek, et al., 2019). In the following sections (section 2.1 and section 2.3) methodologies to carry out disaster risk assessment with reference to Floods and Earthquakes, the two major causes of losses in Europe in the last 60 years (Ritchie & Roser, 2014), will be described.

### 2.1. Earthquakes

#### 2.1.1. Hazard model

Seismic hazard is defined as strong ground motions produced by earthquakes that could affect engineered structures; thus, seismic hazard analysis refers to the

estimation of earthquake-induced ground motions. The results of seismic hazard analysis are obtained in terms of an intensity measure, such as peak ground acceleration, peak ground displacement, spectral acceleration and spectral displacement for the fundamental period of the structure. Deterministic seismic hazard analysis (DSHA) and Probabilistic seismic hazard analysis (PSHA) are the main methods for assessing the level of earthquake-induced ground motion at a given site. Deterministic analysis frequently refers to a Scenario as the maximum probable or maximum credible earthquake in the area, that is carrying out an analysis considering a worst-case scenario in terms of earthquake size and location (Wang, et al., 2012). More specifically, given the seismic sources surrounding the study area, in DSHA first are calculated a series of ground motions related to each source's maximum motion and shortest source-to-site distance, according to the adopted ground motion model. Then, the maximum motion among them is selected as Maximum Credible Earthquake, i.e., the selected scenario is basically governed by the seismic source that has the highest threat to the site with the largest ground motion estimated (Greensfelder, 1974; Kramer, 1996). Deterministic earthquake scenarios could also be based on the estimation of the worst historical event in a region, deriving its magnitude and its guessed location from known geological faults. To this aim, the ShakeMap® software (Wald, et al., 2006) is generally used. It was specifically designed to obtain maps of the peak ground motion parameters, and of the instrumentally-derived intensities. Exploiting available data of the observed ground motions and available seismological knowledge, this tool can generate maps of the spatial distribution of peak ground-motions (acceleration, velocity, and spectral response) as well as a map of instrumentally derived seismic intensities at local and regional scales. Figure 2.1 shows an example of ShakeMap derived by the Italian National Institute of Geophysics and Volcanology (Istituto Nazionale di Geofisica e Vulcanologia, INGV) for the August 24th, 2016 Central Italy earthquake (<http://terremoti.ingv.it/>).

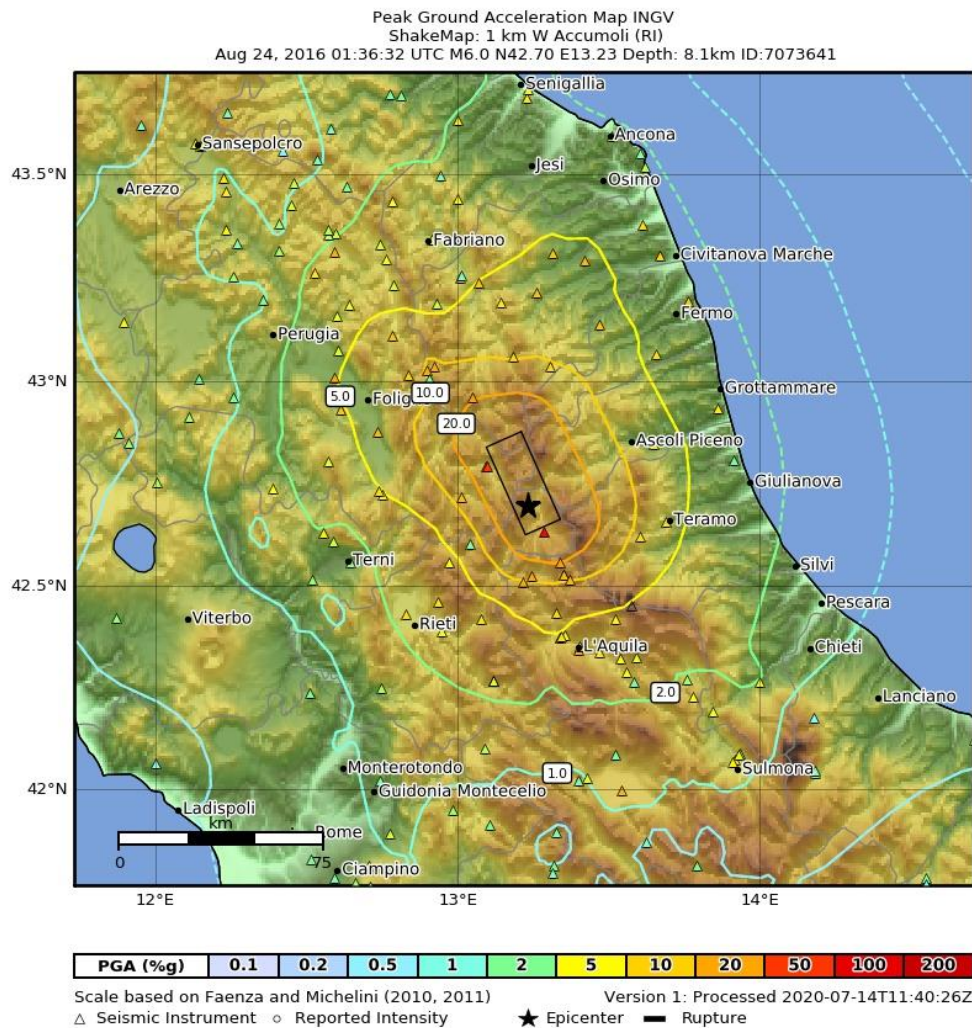


**Figure 2.1** –Peak ground acceleration (PGA) Shakemap of 2016 Centra Italy earthquake. Source: <http://terremoti.ingv.it/>

PSHA considers the contribution of all known potential sources of earthquake shaking. Uncertainties in source's characterization are threatened explicitly in PSHA, making this approach more suitable for use in engineering decision-making for risk reduction. All possible earthquake events and resulting ground motions are considered with their associated probability of occurrence. Once all earthquake sources are identified, the related distribution of magnitudes (i.e., the rates at which earthquakes of various magnitudes are expected to occur) are estimated based on a *recurrence law*, such as the Gutenberg-Richter law (Gutenberg & Richter, 1944), while the source-to-site distance distribution can be usually estimated using only the geometry of the source as locations are considered uniformly distributed, i.e., it is assumed that earthquakes will occur with equal probability at any location on the fault. The definition of ground motion prediction model (also called attenuation relation) allows to predict the



probability distribution of ground motion intensity for a given magnitude and distance. Next, with the seismic-hazard source model and attenuation relationships defined, the probabilistic-hazard calculation is performed combining this information using the total probability theorem (Baker, et al., 2021). The outcomes of a PSHA are a series of seismic hazard curves that show the annual rate or probability at which a specific ground motion level will be exceeded at the site of interest. Hazard curves typically have “annual probability of exceedance” or its reciprocal, “return period”, on the vertical axis on a logarithmic scale, and Peak ground acceleration (PGA, usually expressed in terms gravity, or “g”), or other relevant intensity measure such as Spectral Acceleration (SA), on the horizontal axis on an arithmetic scale. Another usual representation of PSHA products at territorial scale is through hazard maps, showing the spatial distribution of expected intensity at an assigned return period, or having a given probability of exceedance in an assigned interval of time. Figure 2.2 shows the European seismic hazard map proposed in (Woessner, et al., 2015).

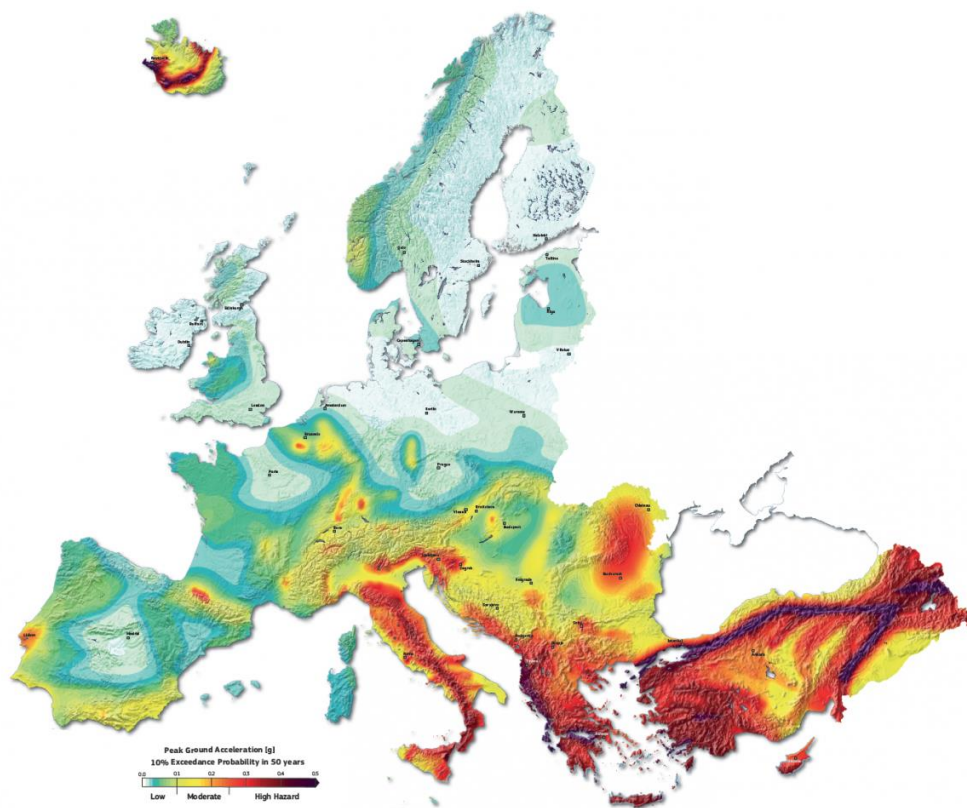


**Figure 2.2** – European seismic hazard map displaying the ground motion expected to be reached or exceeded with a 10% probability in 50 years (Woessner et al., 2013).

### 2.1.2. Vulnerability modelling

The seismic vulnerability of a structure expresses its susceptibility to sustain a certain damage level due to ground shaking of a given intensity. Thus, the aim of vulnerability assessment is to evaluate the probability of getting a damage level due to a scenario earthquake for a given structure. Level of vulnerability of a structure can be described through vulnerability or fragility functions. Given a level of ground shaking, former ones provide the probability of exceeding different limit states, represented by physical damages; the latter usually describe the probability of attained the mean damage, representing the weighted average of a discrete damage distribution (e.g., Lagomarsino & Giovinazzi, 2006) or the level of expected losses, such as social or economic losses, usually expressed as damage ratio, e.g., ratio of cost of repair to cost of replacement (Pitilakis, et al., 2014).

Conventionally, methods for derive fragility functions are classified into four categories: empirical, analytical, heuristic and hybrid. Empirical methods are based on post-earthquake surveys and observations of actual damage (Rossetto & Elnashai, 2003; Yamaguchi & Yamazaki, 2000; Karababa & Pomonis, 2010; Del Gaudio, et al., 2020; Rosti, et al., 2021a). These methods have the advantage of being based on real observed data, representing the most realistic source of damage statistics, and successfully account for various effects which govern the failure modes, as soil-structure interaction, site effects, and variability in the structural capacity of a group of buildings. However, empirical fragility assessment may also provide drawbacks, related to small sample size, the conversion of safety evaluations to equivalent damage state fragilities and the unavailability of data related to high-magnitude events. A wide presentation of empirical assessment's issues is described in Rossetto & Ioannou (2018). On the contrary, analytical methods rely on simulations of structural response subjected to seismic action (Singhal & Kiremidjian, 1996; NIBS, 2004; Rossetto & Elnashai, 2005; Borzi, et al., 2008; Polese, et al., 2008; Rota, et al., 2010; Donà, et al., 2021; Borzi, et al., 2021). Procedures for the analysis of structures and its loading can vary from traditional elastic analysis to non-linear time history analyses on 3D models of structures. One of the main disadvantages of these methods is that the procedure may be too computationally intensive and time

consuming, thus, a compromise must be made between the accuracy of the representation of the nonlinear behavior and cost-efficiency of the model. Heuristic approaches rely on experts' opinion on the structural response. The experts, who are guided by experience and expertise, are asked to provide an estimate of the mean loss or probability of damage of a given element at risk under different ground motion intensities. For instance, index-based approaches that estimate vulnerability of buildings based on visual diagnostic and expert judgement are an example of heuristic methods (Milutinovic & Trendafiloski, 2003; Lagomarsino & Giovinazzi, 2006). These techniques allow to define a vulnerability index (varying between 0 and 1) for a group of buildings as a function of their structural features (e.g., material, floor types, building height, presence of soft stories, quality of construction, irregularities, non-structural elements, age of building, etc.). The main advantage of such methods is that they are not affected by the lack of extensive damage data that usually affect empirical methods or the reliability of the structural model used in analytical ones. However, they have the drawback of being based solely on the individual experience of the experts consulted. Therefore, often results of heuristic approaches are also verified and/or calibrated using empirical data or the resulting fragility functions from the analytical methods (Lagomarsino et al., 2021). Hybrid methods result from the combination of the other approaches, using for instance both analytical and observational data, or integrated using expert judgment (Kappos, et al., 1995; 1998; Kappos et al., 2006). A detailed comparison among different approaches can be found in da Porto et al. (2021). The latter provides critical evaluation of the strengths and weaknesses of the different vulnerability models used in the NRA in Italy (Dolce et al., 2021), including empirical, analytical and heuristic approaches.

In order to correlate the ground motion with the damage to the structure, parameters representative of the seismic demand as well as the damage scale to adopt need to be defined. Traditionally, macroseismic intensity (I), peak ground acceleration (PGA) and spectral acceleration over a specific range of periods (SA) have been used as hazard parameters. Macroseismic intensity is a classification of the severity of ground shaking on the basis of observed effects in a limited area. This measure is usually adopted in defining empirical fragility

functions. On the contrary, intensity measure related to structural response (e.g., spectral acceleration  $S_a$  or spectral displacement  $S_d$ , for a given value of the period of vibration  $T$ ) are used for analytical fragility functions, whereas intensity parameters of the ground motion (PGA, PGV, PGD) are frequently used in both empirical and analytical methods. Damages are generally modelled through discrete damage scale. In empirical procedure the scales adopted for describing damage severity are usually defined based on the observed damage for both structural and non-structural components. Examples of such type of damage scales are the European Macroseismic Scale (EMS-98) (Grünthal, 1998) and the MSK (Medvedev, 1977). In analytical procedures the scale is related to limit state mechanical properties that are described by appropriate indices, such as for example displacement capacity in the case of buildings.

The vulnerability can be represented in terms of either Damage Probability Matrices (DPM) or Vulnerability/ Fragility Curves. While DPM describe the probability of damage occurrence at specified intensity measure level through a discrete relationship (Whitman, et al., 1973; Braga, et al., 1982; Di Pasquale, et al., 2005; Lagomarsino & Giovinazzi, 2006) fragility curves do it in a continuous way (Spence, et al., 1992; Lagomarsino, et al., 2021). Although alternative distributions could be adopted, such as the normal, or the exponential distributions (Rossetto & Elnashai, 2003; Karababa & Pomonis, 2010), fragility curves are usually described by the cumulative lognormal distribution. Hence, the probability of reaching or exceeding damage state  $DS$  can be expressed as follow:

$$P(ds \leq DS_i | PGA_j) = \Phi \left[ \frac{\log (PGA_j / \theta_i)}{\beta} \right] \quad (1)$$

where  $\Phi[\cdot]$  is the cumulative standard normal distribution,  $\theta_i$  is the median value of the fragility function corresponding to damage level  $DS_i$  and  $\beta$  is the logarithmic standard deviation. Figure 2.3 reports an example of empirical fragility curves proposed in (Lagomarsino, et al., 2021).

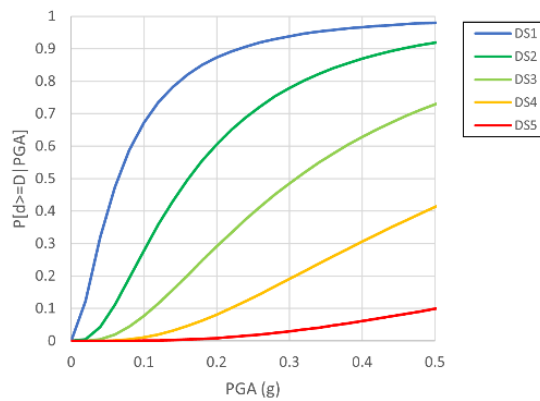


**Figure 2.3** – Fragility curves for the most vulnerable class of buildings (Lagomarsino et al., 2021).

### 2.1.3. Exposure modelling

Assets at risk that are usually considered are buildings and people, but for more comprehensive assessment of risk also other elements such as infrastructures, cultural heritage and the environment as well should be considered. In large scale vulnerability assessment, the buildings are clustered in relevant building classes or vulnerability classes based on the behavior that is expected during a seismic event, for which different vulnerability function are defined. For example, a common vulnerability classification is given by the European Macroseismic Scale EMS-98 (Grünthal, 1998) that categorizes buildings in 6 vulnerability classes (from A to F), based on the construction material of vertical structure and the code design level. Other vulnerability models identify vulnerability classes based on the construction material (masonry, reinforced concrete - RC, steel, wood) considering other structural and non-structural elements features, as well (Braga, et al., 1982; Rota, et al., 2008; Karababa & Pomonis, 2010; Del Gaudio, et al., 2020). In order to develop a uniform and comprehensive classification system for buildings, within the Global Earthquake Model (GEM) initiative a building taxonomy was proposed (Brzev et al., 2013). The taxonomy characterizes buildings according to those attributes that can influence their seismic performance (i.e., the seismic vulnerability). For instance, 13 buildings attributes were identified in the GEM building taxonomy, among which material of the lateral load-resisting system, lateral load-resisting system, building position within a block, date of construction or retrofit and the height.

Therefore, the exposure is generally expressed by building inventory, that provides the number of exposed buildings belonging to classes of structures identified by the vulnerability model and their distribution at territorial scale. Depending on the scale of the analysis, as well as on the data availability and resources, variable level building inventories databases can be developed. Building-by-building surveys may provide high quality vulnerability information and are generally the most complete source towards vulnerability classification. Due to the elevated costs and time required, these kinds of surveys are generally only available after post-earthquake usability and damage evaluation campaigns or for small scale vulnerability studies conducted for limited areas in a country, such as urban districts or small municipalities. To cover larger geographical areas at comparatively low costs, satellite remote sensing shows great potential for rapid vulnerability assessment capturing some buildings' features, that are visible from the outside, remotely by images. Several studies have explored techniques for extracting buildings footprints from high resolution optical satellite imagery (e.g. Taubenböck, et al., 2006; Saito, et al., 2004) and on the possibility of combining multiple imaging sources (Wieland, et al., 2012; Ploeger, et al., 2016). However, this technique based on image processing allow to gather only spatial type building features (building shape, position and height) while the features that are crucial for vulnerability assessment (e.g. building material or age of construction) cannot be easily derived. To overcome this issue, within GEM project (Pagani, et al., 2018) remote sensing is combined with local expertise and field observations to estimate the distribution of building types for urban areas (Bevington, et al., 2012). The resulting inventory can be input into the Global Exposure Database (GED), a global building inventory focused on people and residential buildings with global coverage at national and sub-national (province, municipality) level (Gamba, et al., 2012). Another global approach to inventory is presented in Jaiswal et al. 2010, within PAGER program. The global inventory presented is built combining available data sources (e.g. World Housing Encyclopaedia, Census of Housing) and published literature, such as research articles and reports, that provide country-specific building-stock data. Yepes-Estrada et al. (2017) proposed a residential building inventory for South America, relying only on public sources of information and adopting a judgment-based mapping of the available (census) data to the distribution of building classes. In

Europe, a similar effort was conducted within the NERA project by Spence et al. (2012), making a first attempt to harmonise the available data in each of the European countries (e.g. census data and data collected through building-by-building field surveys) to create the first single uniform database of the European building stock. A more recent European exposure model was developed within SERA project and presented in Crowley et al. (2020a). This model describes the distribution of the main residential, industrial and commercial building classes across all countries in Europe inferred from census data further informed by the local experts' judgment and a number of different public sources of data (e.g. World Housing Encyclopedia, PAGER building inventory, TABULA—Typology Approach for Building Stock Energy Assessment and NERA project).

When available, census data on buildings and population is the primary source for compiling building inventory. Although information on buildings provided by census is often limited to basic information on construction material, age of construction and number of storeys, this source is particularly suitable for large scale applications. As a matter of fact, usually census data are publicly accessible and cover the entire national territory. In general, in order to compile building inventory starting from census data, the association of building typology inferred by census to vulnerability classes through the definition of a suitable exposure model is required. The exposure model establishes the class assignment rules for associating each building typology to one or more vulnerability classes. This procedure may be calibrated on available survey data and/or expert judgment, analysing the correlation between the main vulnerability parameters for buildings and the census information (Lucantoni, et al., 2001; Di Pasquale, et al., 2005; Del Gaudio, et al., 2019; Rosti, et al., 2021a).

#### 2.1.4. Impact assessment

Seismic impact may be assessed using deterministic or probabilistic methods. As also referred in section 2.1, deterministic methods are based on DSHA, whereas probabilistic ones on PSHA. Thus, in a deterministic assessment earthquake hazard scenario could be the maximum probable or credible earthquake, i.e., the largest earthquake that is reasonable to expect in a region, or a Shakemap of an historical earthquake. In a probabilistic scenario, seismic hazard expresses the

probability of exceedance of levels of ground motion in a certain interval of time at a site, obtained by PSHA. Seismic hazard at a site can be represented through hazard curve, that relate the generic intensity measure IM to the mean annual frequency of exceedance of such intensity  $\lambda_{IM}$ , or through hazard maps that show the expected intensity at a site for selected return period, i.e., for selected points of the hazard curves. Hazard maps usually provide seismic intensity (PGA or spectral acceleration) for each point of a more or less dense grid. For example, ESHM20 (European seismic hazard model - Weatherill et al., 2020) adopt a grid of about 10 km per side, while the MPS04 (“Modello di pericolosità sismica” in Italian), the official hazard map developed for the Italian territory (Stucchi, et al., 2004; 2011), a 5 km x 5 km mesh.

Seismic risk is a convolution of hazard, vulnerability and exposure. In the following the procedure for seismic risk analysis is described with reference to building as asset at risk. The exposure provides the number of buildings and their distribution in the vulnerability classes defined by the selected vulnerability model; vulnerability is defined through fragility functions and allows the evaluation of expected damages on structures (see also section 2.1.3). Hence, damage assessment consists in estimating the number of buildings that are expected to reach different damage grades  $D_k$ , defined according to the selected scale (e.g., EMS-98). In a probabilistic framework, the mean annual rate  $\lambda_k$  of attaining damage state  $D_k$  is usually expressed as follow:

$$\lambda_k = \int_0^{\infty} P(D_k|im) \cdot |d\lambda_{IM}(im)| \quad (2)$$

where  $P(D_k|im)$  represents the fragility of the considered building class, i.e. the probability that the buildings in such class will attain damage state  $D_k$  when subjected to an earthquake with ground motion intensity level  $im$ , and  $\lambda_{IM}$  represents the mean annual frequency of exceedance of the ground motion intensity  $im$  (obtained through the hazard maps for the generic  $Tr$ ). The probability  $p_k$  of attaining damage state  $D_k$  in  $t$  years may be calculated assuming that the occurrence of earthquakes follows a Poisson process:

$$p_k = 1 - e^{-\lambda_k \cdot t} \quad (3)$$



Where  $p_k$  represents the unconditional seismic risk in  $t$  years referred to damage state  $D_k$ .

The estimation of expected damages is the starting point for the impact calculation. Commonly used indicators for seismic impacts are the expected number of collapsed and unusable buildings or dwellings, the expected numbers of those rendered homeless and casualties, and the extent of the direct and indirect economic losses (JRC, 2015; FEMA, 2013). For the quantification of economic and social losses suitable consequence functions (also called damage-to-loss models) are required. Generally, consequence functions are expressed as a function of buildings' damage, meaning that the above-mentioned indicators are determined as a function of the expected numbers of buildings (or dwellings) affected by the different damage levels, obtained according to the adopted damage model. According to HAZUS approach (FEMA, 2015), the number of collapsed buildings is defined as a portion of buildings reaching the heaviest damage state (DS4, according to the HAZUS damage scale). Collapse fractions are based on judgment and limited earthquake data and they are dependent on the material of the load-bearing structure and number of storeys of the building. For example, considering reinforced concrete moment resisting frame structures, the 13%, 10% or 5% of the total area of these type of buildings with 1-3 storeys, 4-7 storeys and more than 7 storeys respectively, that attained complete damage state DS4, is expected to be collapsed. The evaluation of the expected number of unusable buildings (i.e., buildings considered unsafe due to potential collapse, falling debris or unavailability of services) is crucial for the evaluation of the expected number of homeless and, in turn, of the indirect costs related to temporary shelters and other kinds of temporary arrangements for homeless. In Dolce et al. (2021) the consequence functions for estimating the quantity of unusable buildings express the percentage of unusable buildings as a function of the number of buildings that sustain damage levels on the EMS-98 scale, with a specification between the long and the short-term un-usability. The usability probability matrices matrix proposed are shown in table 2.1. Other examples of models for the evaluation of the unusable buildings can be found in Bertelli et al. (2018), Zucconi et al. (2017; 2022) and Rosti et al., (2018). Given the number of unusable buildings, the number of homeless can be defined as sum of number of

occupants in non-usable buildings, detracting the number of dead persons ( (Khazai, et al., 2012; Dolce, et al., 2021).

**Table 2-1** – Percentages of short term and long term unsafe buildings for each damage level of the EMS-98 scale, adopted in Dolce et al. (2021).

% Unsafe buildings	D1	D2	D3	D4	D5
$u_{stk}$	0	40	40	0	0
$u_{ltk}$	0	0	60	100	0

The number of injuries or deaths can be computed as a function of the damage level of the building, as well. As proposed in Coburn et al. (1992) casualties can be estimated as a percentage of the number of collapsed buildings, determined by factors that take into account several aspect concerning the occupancy of the buildings, such as the number of people effectively accommodated in buildings depending on the time of the event, the percentage of population trapped in collapsed buildings as well as the outright mortality when collapse occurs and the mortality of trapped victims after collapse. Several updates of the above-mentioned casualty model, that consider studies by various authors based on local context and observed data after significant earthquakes worldwide, are presented in Spence et al. (2011).

Economic losses due to earthquakes generally express the losses due to structural damages and they are computed as costs for the repair or replacement of damaged or collapsed buildings. A damage ratio (i.e., the percentage of the building replacement value) is assigned for each damage state as a function of the building typologies and/or the type of occupancy as well (FEMA, 2003; Chang, et al., 2008; Karaman, et al., 2008; Molina Palacios, et al., 2010); the expected losses for each damage state is calculated multiplying the built area of the considered building type/occupancy type and the relative probability to experience the considered damage state for the relative damage ratio and the building replacement cost. Indirect seismic economic losses are a systematic manifestation of losses in the chain of economic activities, that may be affected to by interruptions and general disruption in their normal operations (Boisvert, 1992; Chang, 2000; An, et al., 2004; FEMA, 2003; Enke, et al., 2008). Contrary to the direct losses, indirect economic losses could be affected by various disruptions, for example, transportation difficulty due to damaged highway and

transportation systems, water pipe damage, and electricity disruption, among others. Thus, this kind of losses are more difficult to evaluate as characterized with more ambiguous causes and the uncertain amount of losses. These reasons make the evaluation of indirect economic losses a complicated task and available studies are affected by high uncertainties.

## 2.2. Floods

### 2.2.1. Hazard model

Floods are natural phenomena that occur when an overflow of water submerges land that is usually dry. Flood events are classified according to the main drivers and the water bodies that cause the event itself (Poljanšek, et al., 2019): fluvial floods occur when river levels rise and burst or overflow their banks, inundating the surrounding land; flash floods can develop when heavy rainfall occurs suddenly; pluvial flooding, when heavy rainfall causes surface water flooding and the urban drainage systems become overwhelmed; coastal flooding, when land areas along the coast are inundated by seawater, due to high tide, storm surge and wave conditions.

Flood hazard is usually represented by maps, that should provide a spatial and temporal evaluation of the flood probability of occurrence, the flood extent, the water depth and the flow velocity (EU 2007). Figure 2.4 shows an example of flood hazard map for the Italy-Slovenia cross border area of Isonzo river (BORIS, 2022a). The probability of occurrence is usually expressed as return period, i.e., the estimated average time between events to occur. For instance, a 100-year flood event means that the event is expected to have 1% probability of occurring every year. Flood extent, water depth and flow velocity are characterized as spatial map, with reference to a given return period. For flood hazard mapping of an area of interest, the meteorological and the hydrogeological regime in such area are required. The definition of hydrogeological regime is usually carried out using physically based models, that simulates hydrological processes leading to flooding events using real data input (Bellos, 2012; Rofiat, et al., 2021). Modelling of physical process of flood generation for various flood scenarios requires topographic data provided by the digital terrain model (DTM) or digital elevation mode (DEM), hydrology data capable of providing information about

rainfall and river discharge, land use information, and bathymetry data (Anuar, 2018; Arseni, et al., 2020). These numerical models are based on complex flow equations, that require long time and intense processing efforts (Toombes & Chanson, 2011). In flood hazard assessment, empirical models that rely of historical data can be used as well. These data-driven approach retrieve useful flood information from observations, using different acquisition and processing techniques, such as remote sensing (Wang, et al., 2019; Marchesini, et al., 2021). They are usually adopted to delineate flood hazard/susceptibility regions, but they cannot predict flood parameters such as flow depth and velocity (Rofiat, et al., 2021).



**Figure 2.4** – Flood hazard maps for Isonzo river in Italy-Slovenia cross-border area. Adapted from BORIS (2022b).

### 2.2.2. Exposure and vulnerability modelling for impact assessment

Flood risk assessment is based on the combination of hazard, vulnerability and exposure. Flood hazard maps provide information on the extent of flood prone zones, the probability of occurrence of the corresponding event and its magnitude, in terms of water depth and flow velocity. Vulnerability is the susceptibility to damage of structures and their contents due to hazard's impact. Fragility and vulnerability functions express the likelihood that assets at risk will sustain varying degrees of loss, the former in terms of physical damage, the second in terms of direct economic consequences of physical damage. The use

of the fragility relationships, that relate the likelihood of attained different levels of damage for a given asset type and the range of hazard intensities, usually requires the definition of a damage-to-loss model for converting damage estimates to loss estimates. Although several studies investigated the influence of flood velocity on impacts (Kreibich, et al., 2009; Jonkman, et al., 2008), water depth is considered the strongest single predictor of building damage and therefore is the most widely used intensity measure in flood vulnerability modelling (NR&M, 2002; Seifert, et al., 2010; Schwarz & Maiwald, 2012; Scorzini & Frank, 2015; Huizinga, et al., 2017).

The development of vulnerability/fragility models can be based on empirical or analytical approaches. Empirical vulnerability functions are constructed using post-flood observations of damages and losses, collected over sites affected by different flood intensities, using statistical modelling to estimate a chosen functional form's parameters to fit the data (USACE, 1985; Smith, 1994; Nascimento, et al., 2006; Chang, et al., 2008). In analytical approaches numerical models are used for flood fragility derivation. The performance of the structure or the structural component of interest (e.g., a wall) while floodwater forces are applied is analysed. The main type of forces usually considered are the hydrostatic and the hydrodynamic forces and the force associated with floating debris dragged by water. Examples of analytically derived fragility functions can be found in Oliveri & Santoro (2000), Kelman and Spence (2003), De Risi et al. (2013) and Dong and Frangopol (2017). The synthetic approaches are also largely used for developing flood vulnerability functions (Galasso, et al., 2021). These approaches estimate the damage/loss expected under a flood scenario based on expert judgment, adopting the so-called *what-if* analysis (Merz, et al., 2004; Dottori, et al., 2016; Amadio, et al., 2019).

Generally, different fragility/vulnerability functions are developed for different asset classes, identified based on structure's features that play a critical role in damage resistance to flooding. As structural failure during flooding is rare and the major damage in flooding is to structural finishes, contents, and inventory, vulnerability models may identify classes not only based on the construction material (e.g., wood, masonry, RC, mud), but also accounting for the occupancy type (e.g., residential, school, office buildings), the number of storeys and the

presence or absence of basement. The European flood model developed by JRC (Joint Research Centre), presented in Huizinga (2007), proposes depth–loss functions (i.e., vulnerability functions) for five classes of assets at risk, i.e., residential, commercial, industrial, roads, and agriculture. These functions are derived from the analysis of existing studies in several European countries. Available damage functions are normalized scaling the maximum loss values in European countries to the gross domestic product (GDP) per capita and a mean value of all functions for each class of asset at risk is assumed as representative of the ‘average’ continental curve. These JRC curves relate water depth to damage ratio, i.e., a proportion of reconstruction cost, and can be used to evaluate both losses for structure and contents. Building contents are defined as furniture, equipment that is not integral with the structure, computers, and other supplies. Usually, non-structural components such as lighting, ceilings, and other fixtures are not considered as contents (FEMA, 2022). Contents damage is considered as a percentage of building damage and such percentage changes based on the occupancy class, e.g., contents damage is the 50% of building damage in case of residential buildings, the 100% in case of commercial buildings and 150% in case of industrial ones. In Huizinga et al. (2017) further continental-specific depth–damage functions are presented.

The HAZUS Flood Model (FEMA, 2009) uses the Federal Insurance Administration’s FIA depth-damage curves and selected curves developed by various districts of the U.S. Army Corps of Engineers USACE for estimating damage to the general building stock. Three inputs are required to estimate building damage: the building occupancy type, the number of storeys and the presence of basement. Moreover, for residential buildings a distinction between multiple storeys and split-level structures is also taken into account. Mobile homes are included as well. Figure 2.5 shows FIA damage functions for residential buildings (FEMA, 2022). It is worth noting that the water depths in the functions are measured relative to the top of the first finished floor, so it is possible for structural damage to occur at a depth of zero (Tate, et al., 2014). For the same classes of buildings, damage functions for estimation of contents damage are also proposed.

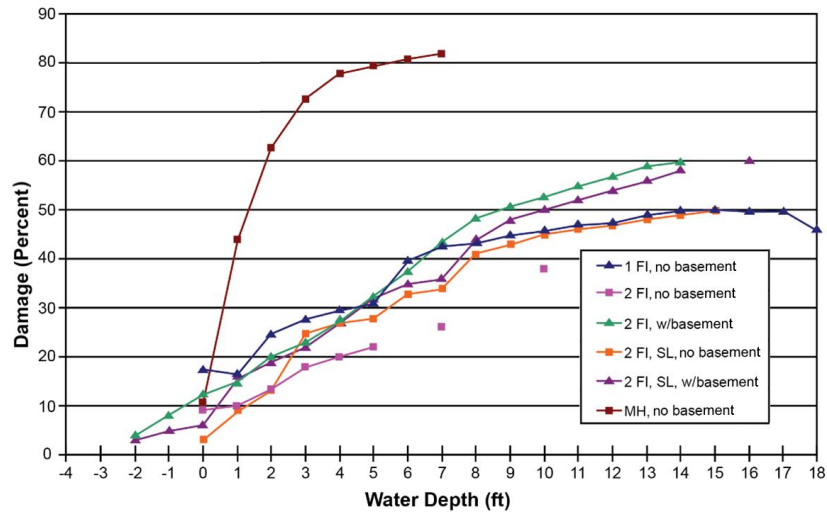


**Figure 2.5** - FIA flood damage functions for buildings adapted from FEMA (2022).

In Arrighi et al. (2018) and Silvestro et al. (2016) are proposed modified HAZUS building vulnerability functions tailored for the European context by combining the curves for specific uses. The original occupancy classes by HAZUS are extended considering “Mixed” residential and different commercial services on the ground floor. Figure 2.6 shows a comparison between depth-damage curves for different content: retail trade (COM1) building, generic one-floor residential (RES1) building, mixed retail trade on the first floor and residential on the second floor (COM1 + RES1) building, and mixed retail trade on the first floor and residential on the second and third floors (COM1 + RES1 + RES1) building. The mixed-use curves are derived by combining the single-use ones. For example, the light blue curve (COM1 + RES1), corresponding to the flood vulnerability function for a two-storey building with mixed commercial and residential use (i.e., retail trade on the ground floor and residential on the first floor). It is obtained combining RES1 curve (i.e., one-storey curve for generic residential building) with COM1 curve (i.e., one-storey curve for retail trade). The yellow section of the graph indicates the average height of the ground floor.

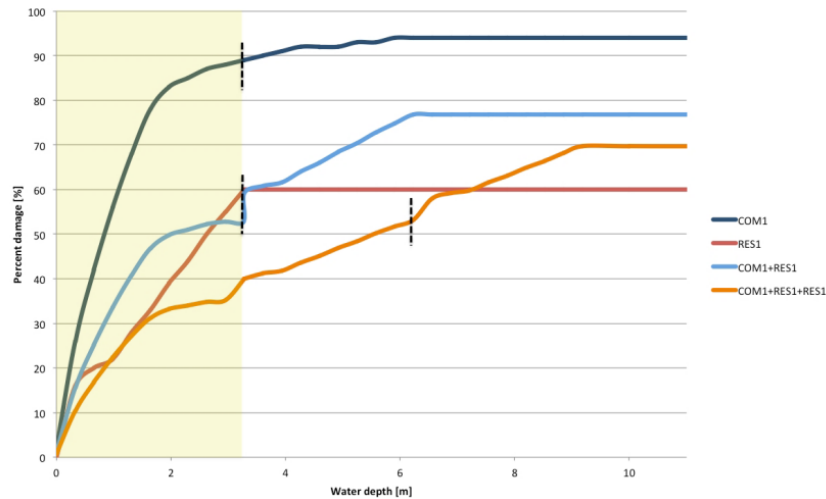


**Figure 2.6** - An example of mixed-use curve definition adapted from Silvestro et al. (2016).

In order to evaluate expected losses, it is necessary to characterize the spatial exposure of population and relevant assets. Among elements of the built environment at flood risk (homes, businesses, industry, and transportation infrastructure), residential buildings are the most frequently modelled element. To correctly identify the buildings which are most likely to be at risk from flooding a detailed buildings-level flood exposure is required. Typically, for representing the spatial distribution of the exposed asset G.I.S. (Geographical Information Systems) software is used. The latter allows to store spatial features through georeferenced vectors at which useful information for the following vulnerability assessment can be associated. For example, a shapefile containing the buildings geometry polygons and their spatial distribution with the associated information related to the material which they are built, the number of storeys or the type of occupancy.

Potential adverse consequences associated with flood scenario may involve not only the expected economic losses, both direct (due to damages to buildings and contents) and indirect (related to interruption of economic activities), but also the expected number of inhabitants potentially affected. The counting of the number of persons residing in flooded areas is typically adopted as indicator for affected population. Thus, the estimation of expected short-term shelter are not based on the degree of damage to structures but on the numbers of displaced people in inundated areas. Displaced individuals and household ds are also made up of those whose buildings have not been damaged but who were evacuated when a



warning was issued, or there is no physical access to the property because of flooded roadways. Moreover, according to HAZUS model, the corresponding number of individuals may be also modified by factors accounting for income and age. Despite the enormous impacts of floods is relatively limited insight into the factors that determine the loss of life caused by flood events (Silvestro et al., 2016). Methods aimed to assess the loss of lives due to flood events usually investigate the correlation between specific flood characteristics, such as flow velocity, and the mortality in the flooded area (DeKay & McClelland, 1993; Jonkman, et al., 2008).

### 2.3. From single risk to multi-risk assessment

As shown in the previous section, recognizing and assessing risk from natural hazards are the first steps toward reducing their adverse effects. As many regions of the world are not only subject to a single hazard but to multiple hazardous processes, all relevant threats related to a specific area should be identified and analyzed. Thus, the assessment of risk should enable stakeholders to understand the relative importance of a different risks for a given region and how underlying disaster risk drivers relate to components of risk to address a range of measures to reduce risk. The term “multi-hazard” in a risk reduction context is used to indicate assessment approaches that account for “more-than-one-hazard” (WMO, 1999; Kappes, et al., 2012). Traditionally, the evaluation of risks related to different sources is generally done through independent analyses and, in turn, disaster risk reduction measures are implemented to decrease the risk of a single hazard type despite their potential of having unwanted effects on other hazard typologies. These potentially negative effects between measures are defined by de Ruiter et al. (2021) as ‘asynnergies’.

Hazardous events may occur simultaneously or cumulatively over time and in this case the potential interrelated effects may amplify the overall risk. The case of landslides triggered by an earthquake (Chang, et al., 2007; Lee, et al., 2008) or a tsunami triggered by an earthquake (Mimura, et al., 2011) are the typical examples of one hazard that trigger another one. In other cases, one event may cause several different threats which are considered jointly, as in the case of a volcanic eruption with ash and lapilli fallout and lava flows (Zuccaro, et al., 2008;

Thierry, et al., 2008). We can refer to independent events when there are no interactions among events, and they could be analyzed separately. This would be for example the case for earthquake hazard and flood hazard. They have different triggering mechanisms, which do not directly interact. Even if, for instance, an earthquake may trigger landslides that may block a river leading to flooding, which makes that the earthquake and flood risk cannot be considered entirely independent (Westen & Greiving, 2017). If different hazard types are triggered by the same triggering event, we can refer to them as coupled events (Marzocchi, et al., 2009). Examples of such types of events are the effect of an earthquake on a snow-covered building (Lee & Rosowsky, 2006) and the triggering of landslides by earthquakes occurring simultaneously with ground shaking and liquefaction (Delmonaco, et al., 2006a; Marzocchi, et al., 2009).

**Table 2-2** - Main hazard types and their interactions. Source: Westen & Greiving 2017.

	Earthquake	Volcanic Eruption	Tsunami	Storm Surge	River Flooding	Landslides	Forest Fires
Earthquake	-	Independent	Chain	Independent	Independent	Chain	Independent
Volcanic eruption	Independent	-	Chain	Independent	Disposition	Disposition	Chain
Tsunami	Caused by	Caused by	-	Independent	Independent	Chain along coast	Independent
Storm surge	Independent	Independent	Independent	-	Chain	Chain	Independent
River flooding	Independent	Independent	Independent	Coupled	-	Coupled	Independent
Landslides	Caused by	Independent	Independent	Coupled	Coupled	-	Disposition
Forest Fires	Independent	Coupled	Independent	Independent	Disposition	Disposition	Independent

However, modelling these hazards is still very complicated as they occur in the same area simultaneously: the consequences of the modelled scenarios cannot be simply added up, as the intensity of combined hazards may be higher than the sum of both or the same areas might be affected by both hazard types, leading to overrepresentation of the losses, and double counting. Interactions defined as domino effects (Luino, 2005; Delmonaco, et al., 2006b; Perles Roselló & Cantarero Prados, 2010; Van Westen, et al., 2010; European Commission, 2011), cascades (Delmonaco, et al., 2006b; Carpignano, et al., 2009; Zuccaro & Leone, 2011) or concatenated/chains (Shi, et al., 2010) are refereed to events where one hazard may trigger the next, e.g., hazards may occur in sequence. Table 2.2 shows

the main hazard types and their interactions, according to Westen & Greiving (2017).

Ideally, for a complete multi risk assessment all risks derived from different perils potentially hitting the same area should be compared and ranked, taking into account possible interactions among the single hazards as well. In Zschau (2017) a definition of possible approaches for multi risk assessment is proposed (figure 2.7). In the following sections the different methodologies will be described.

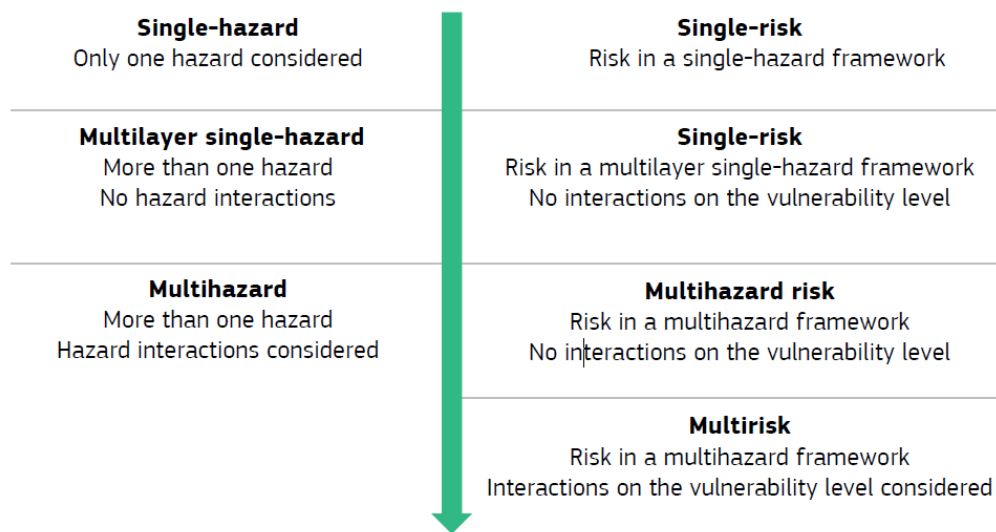


**Figure 2.7** – Approaches for multi-risk assessment, from single hazard to multi-hazard. Adapted from Zschau (2017).

### 2.3.1. Multi-layer single risk assessment

A first step towards a full multi risk assessment could be to analyse and compare two or more hazard potentially affecting a given region avoiding their possible interactions. This approach is known as multi-layer single risk assessment. Even if ignoring possible interaction among hazards may lead to underestimate the overall risk, in order to assist decision makers in the field of DRM also understanding the relative importance of different risks in a given area is still crucial. The main problem arising for the application of this approach is the comparability of the different risks. As a matter of fact, for different risks may be modelled adopting, for example, different intensity measure and different return period as well as different scale of analysis. Thus, a multi-layer single hazard approach is based on harmonization and standardization of the assessment procedures among risks. The main tool adopted for presenting risk results are

matrices, indices and curves (Poljanšek, et al., 2019). These tools perform well also for multi-risk comparison purposes and therefore they are the main standardization schemes used in this context (Zschau, 2017).

Standardization procedure could be applicable at different risk-levels (i.e., hazard, vulnerability and risk). At hazard analysis stage, the main problem concerns the intensity measures adopted: their magnitude may be measured using different reference units, for example the inundation depth for floods, ground motion or macro-seismic intensity for seismic (Carpignano et al. 2009). To overcome this issues, two major standardization approaches are usually adopted: the classification and the index-based scheme (Kappes et al. 2012). The former consists of classifying and ranking single hazard into hazards categories based on fixed intensity and frequency thresholds. In the Swiss guidelines for the analysis and the evaluation of natural hazards (Loat, 2010) these thresholds are defined by a combination of intensity and frequency based on the possible effects on buildings and humans. Thus, for example, a rock fall with a kinetic energy higher than 300 kJ and a flood higher than 2 m are considered equivalent with respect to the consequences in terms of damaged buildings and people affected. The intensity and frequency classes are represented by a matrix where a color code is used to define the different level of hazard (for instance ‘low’, ‘moderate’ and ‘high’) and the overall hazard level in a given area is derived overlying the classification results of all single hazards (figure 2.8). Similar approaches are used in Del Monaco et al. (2006b), Thierry et al. (2008) and Cariam (2006). A slightly different classification scheme is adopted in Chiesa et al. (2003), where the hazard level in the areas of interest is not determined by the maximum of overlapping classes, but by means of a matrix that correlates the hazard classes for the two different perils analyzed (i.e., earthquakes and tropical storms).

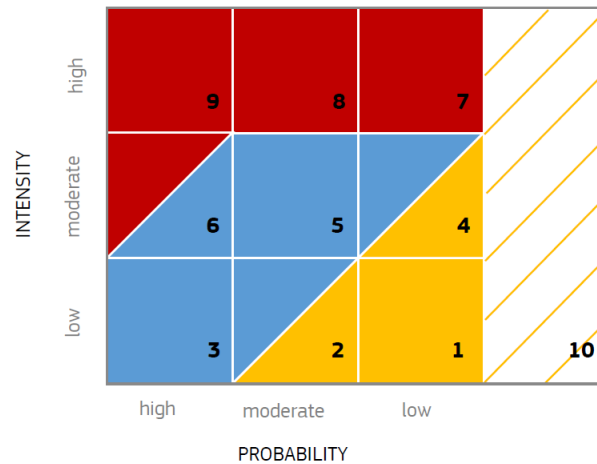


**Figure 2.8** - Hazard matrix adapted from (Kunz & Hurni, 2008).

Unlike matrices, that can be considered a qualitative approach for classifying and ranking hazards, indices are semi-quantitative approaches that allows the quantification of the differences between two hazards level. A first proposal of an index for comparing different hazards at community level can be found in Odeh Engineers, Inc (2001), where the *Hazard Score* is computed as a function of other three scores related to the hazard frequencies (i.e., events per year), the area potentially affected and its intensity level. Each parameter (i.e., frequency, intensity and impact area) is classified according to five levels and then they are multiplied to obtain the final score related to a given hazard. Thus, different hazards in a given community can be compared in a quantitative way. Other examples of indices for multi-hazard analysis can be found in Dilley et al. (2005), El Morjani et al. (2007) and Petitta et al. (2016).

Matrices, indices and curves are largely used for describing hazard-specific vulnerability (Braga et al., 1982; Lagomarsino & Giovinazzi, 2006; Zuccaro et al., 2020; Papathoma et al., 2003; Balica et al., 2009; Silva & Pereira, 2014; Petrone et al., 2016). However, as multi-hazard tool they are used more frequently for comparing risks resulting from different hazards in terms of social or economic losses. In this context, risk matrices usually relate likelihood (i.e., the probability that an event occur) and impacts. Thus, a highly likely event associated with catastrophic loss is ranked as having higher risk than an unlikely event associated with negligible loss. The color-code of the cells of the matrix allows an easier visualization and communication of the level of risk, ranging from green (small risk or tolerable) to red (great risk or intolerable risk) colors.

Fixing defined levels of risk, this tool allows to compare impacts due to different hazards. However, the ranking of impacts and the color code used in risk matrix strongly depend on experts' judgement, making such approaches highly subjective. In figure 2.9 is shown an example of risk matrix used in multi-risk field.

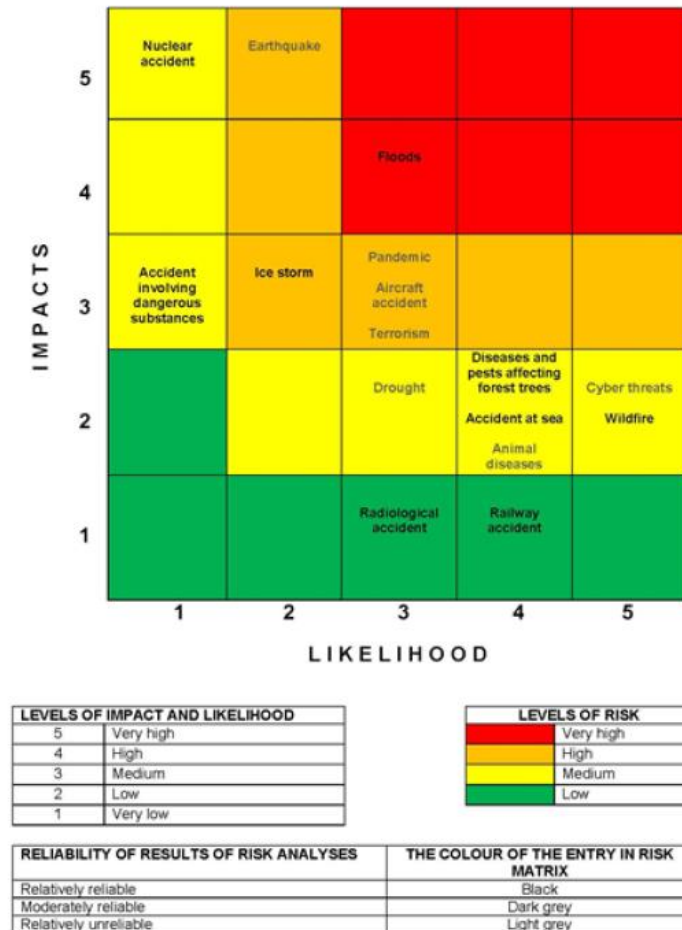


**Figure 2.9 - Slovenian National Disaster risk matrix (GRS, 2018).**

Risk curves represent a quantitative method for assessing natural hazards in a multi-layer single risk approach. The curve relates the mean annual frequency of exceedance of a given event to corresponding economic losses. The calculation of risk in a given period is a conditional relation of hazard and vulnerability with the exposed elements (UNDRO, 1980; Cardona, 1986). Considering all possible hazard events, defined by intensity and frequency, a fully probabilistic risk estimation can be performed using the following equation (Velásquez, et al., 2014):

$$v(p) = \sum_{i=1}^{Events} \Pr (P > p | Event_i) F_A(Event_i) \quad (3)$$

where  $v(p)$  is the exceedance rate of loss  $p$ ;  $F_A(Event_i)$  is the annual frequency of occurrence of the  $Event_i$ ;  $\Pr (P > p | Event_i)$  is the probability of the loss to be greater than or equal to  $p$ , conditioned by the occurrence of the  $Event_i$ . The graphical representation of  $v(p)$  is the risk curve, also called “Loss Exceedance Curve” (LEC). A commonly used risk metric is the “Average Annual Loss” (AAL), i.e., the weighted average of all plausible loss values calculated as area under the LEC (equation 4). This value is also called “Expected Annual Losses” (EAL).

$$AAL = \int_0^{\infty} v(p) dp \quad (4)$$

As exceedance probabilities are not expressed in a hazard-specific unit, losses among different hazards are directly comparable through risk curves. An example of risk curves that compare direct economic losses from earthquake, storm and flood, adapted from Grünthal et al. (2006), is reported in figure 2.10. Other approaches based on curves for comparing and ranking different risks can be found in Fleming et al. (2016) and BORIS (2022b).

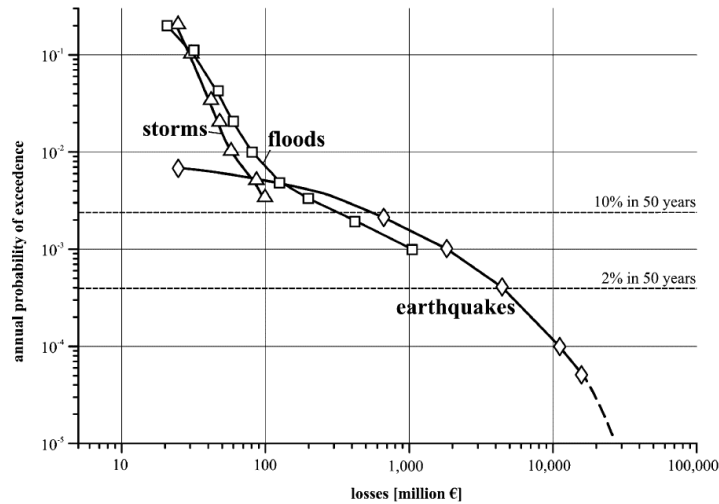


**Figure 2.10** - Risk curves of the hazards due to windstorms, floods and earthquakes for the city of Cologne for losses concerning buildings and contents (Grünthal et al., 2006).

Concerning risk index approaches, they are based on the combination of individual standardized indicators for hazard, vulnerability and exposure inputs to obtain a measure of risk scaled between 0 and 1. Risk index approaches are

widely used for spatial multi-dimension evaluation, accounting not only for the physical-dependent component of risk but also for socio-economic and environmental factors. An overview of these approaches will be presented in section 2.2.

### 2.3.2. Multi-hazard risk assessment: hazard interactions

Hazards interactions may be described using several terms: multiple hazard (Hewitt & Burton, 1971), domino effect (Zuccaro & Leone, 2011; Choine et al., 2015), triggering effect (Marzocchi et al., 2009), chains (Shi, 2002; Xu et al., 2014) or coinciding hazards (Tarveinen et al., 2006; European Commission, 2011). Although many of them are used to refer to one hazard that triggers another one, as follow-on events, the classification of interconnections between hazards can be more refined (Gill & Malamud, 2014; 2016).

The most used methods for accounting hazard interactions in risk assessment process are hazard-interaction matrices and event-tree approaches. As hazard and risk matrices adopted in single layer multi-risk assessment, the hazard-interaction matrices are semi-quantitative approaches that allow to examine and visualize interconnections among risks and to evaluate how strong these relations are. In De Pippo et al. (2008) a matrix-based multi-hazard analysis is carried out for the northern shoreline of the Campania region, in Italy. Five natural hazards potentially affect the study area are considered in the investigation, i.e., shoreline erosion, riverine flooding, storms, landslides, seismicity and volcanism. Cause-effect interactions among threats are analyzed in a descriptive matrix where the leading terms (i.e., the hazards) are posed in diagonal elements. The other elements of the matrix are filled according to a clockwise scheme: the element  $ij$ , where  $i$  is the generic row and  $k$  the generic column, represent the effect of the hazard  $ii$  on  $jj$  (figure 2.11). These effects indicate the influence of the morphological parameters on the system (the cause of the phenomena) or the influence of the system on phenomena's parameters (the effect of the phenomena). Thus, for example, a large fetch affected to strong wind and high waves (element 3.1) determines a high rate of erosion (influence on the effect), whereas it is well known that seismic shakes can induce landslides (element 5.4, influence on the cause). A semiquantitative code from 0 to 4 (from none to



critical) is assigned to each cause/effect interactions, based on recurrence times of the event (the lower is the recurrence time, the higher the code). The overall costal hazard is finally obtained as weighted sum of the product of each hazard parameter's code and the relative importance coefficient, defined as the percentage of influence of one parameter over the other in the considered location.

SHORELINE EROSION 1.1	NO INTERACTION 1.2	A narrow steep beach without berms is open to wave attack 1.3	Coastal retreat contributes to the decrease in strength 1.4	NO INTERACTION 1.5
Flooding can cause extensive coastline retreat close to the river mouth or inlet 2.1	RIVERINE FLOODING 2.2	The concurrence of large waves breaking and flooding along the same coast increases destabilization 2.3	Breaches or overwash related to flooding induce landslides 2.4	NO INTERACTION 2.5
A large fetch and/or a wide coastal sector exposure to the prevailing wind determines the highest rate of erosion 3.1	The contemporary occurrence of flooding and large waves breaking on the same coast increase destabilization along it. 3.2	SURGES 3.3	Surges can affect a high cliff, both eroding the base (wave-cut notch) and scattering the marine spray along the slope 3.4	NO INTERACTION 3.5
The occurrence of landslides, associated to the quick removal of the talus, can accelerate the rate of cliff recession 4.1	Landslides and related phenomena can contribute to cut off or divert a flow in a water course 4.2	NO INTERACTION 4.3	LANDSLIDES 4.4	NO INTERACTION 4.5
NO INTERACTION 5.1	NO INTERACTION 5.2	Earthquakes and rapid falls into the sea of debris from volcanic eruptions can induce anomalous wave heights (tsunami) 5.3	Seismic shakes can induce landslides 5.4	SEISMICITY AND VOLCANISM 5.5

**Figure 2.11** – Hazard interactions matrix. Adapted from De Pippo et al. (2008)

Other examples of the use of matrices for analysing multi-hazard interactions are presented in Tarvainen et al. (2006), Kappes et al. (2010), Mignan et al. (2014) and Liu et al. (2015).

Event-tree approaches are quantitative methods for analysing hazard chains in a multi-hazard risk assessment. The tree-based scheme allows the identification of all consequences of a system that have a given probability of occurring after an initiating event. All the considered events are linked to each other through nodes that express all possible states of the system; the branches of the event tree that connect nodes define the probability of occurrence of each state. The event-tree shown in figure 2.12 was used in Neri et al. (2008) to investigate future scenarios at the volcano Vesuvius. The initial pre-eruption stages (i.e., precursor, initiation and progression stages) represent the specific Vesuvius situations that may lead to an eruption. If an eruption does ensue, all the main possible eruption styles and the secondary hazards associated with them are specified in the next set of branches on the event-tree. For each different eruptive style (i.e., explosive and

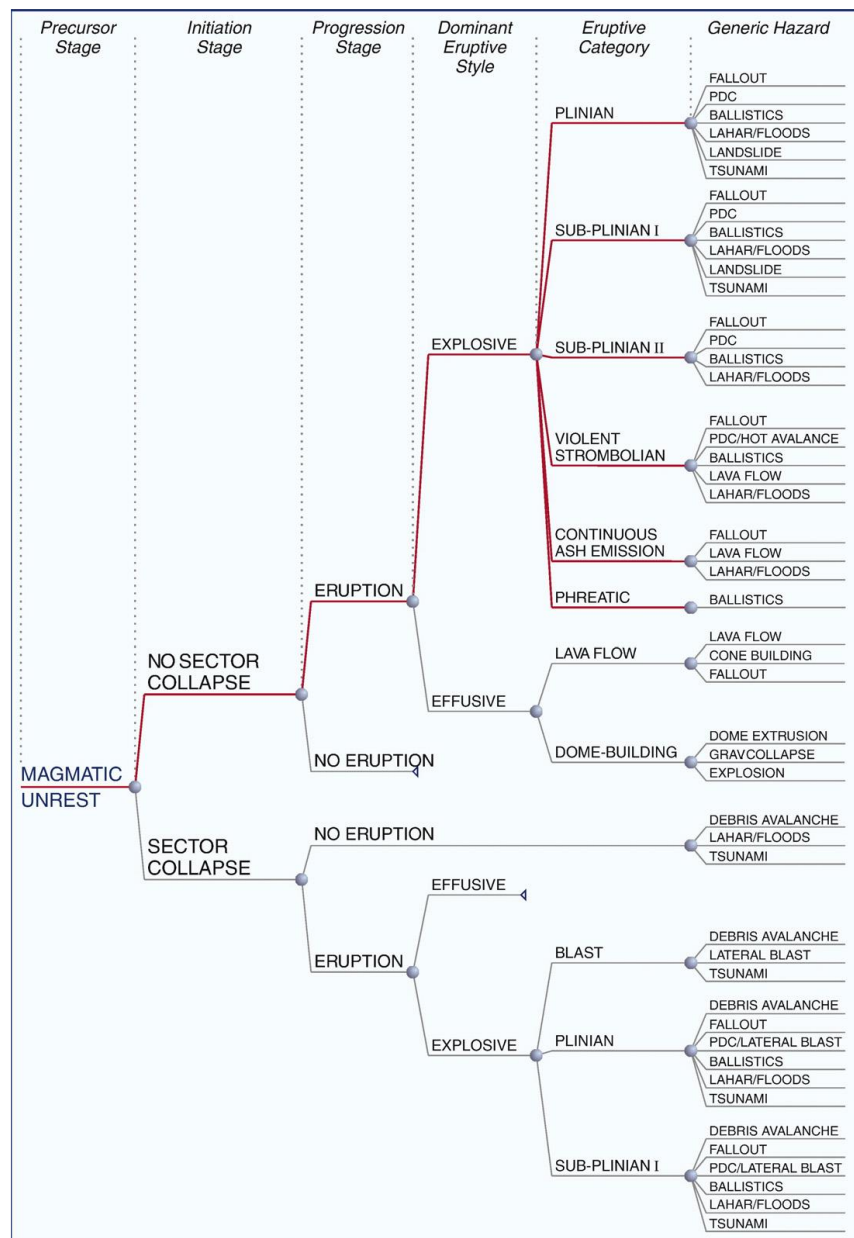


**Figure 2.12** - Event Tree describing potential eruption scenarios for volcano Vesuvius and possible associated hazards that may develop. Adapted from Neri et al. (2008).

effusive) the main types of eruption activities, such as the so-called Plinian or Sub-Plinian for the explosive event and the lava flow type for the effusive class of eruption, are described with further branching. All those categories if event differ in magnitude and intensity. Moreover, a frequency of occurrence was also associated to such events, based on a combination of statistical treatment of Vesuvian eruptive records and expert judgment. The relevant Generic Hazards that might arise during and after each eruptive event were also identified. For example, seven eruptive phenomena associated with explosive events are identified: ash and lapilli fallout; pyroclastic density currents; ballistics showers;

lahars and floods; landslides, lava flows, and tsunamis. In this study, the possible physical processes that might influence the arising of the consequence hazards were also analysed and specified as additional branches. Event tree structure for describing hazard interactions were also presented in Newhall and Hoblitt (2002), Marzocchi et al. (2004; 2008; 2010), Lacasse et al. (2008) and Selva et al. (2012).

### 2.3.3. Physical vulnerability for multiple hazards

Usually, natural-hazard risk assessment focuses on static vulnerability and exposure models, associated with current conditions. However, not only the exposed population to natural hazard may increase, driven by factors such as urbanization, socioeconomic growth and the resulting movement of people from rural to urban areas, but also the vulnerability may increase in time. In Zschau (2017) a distinction between the time-dependent and the state-dependent fragility is proposed. The former refers to a gradual change of vulnerability with time, due to degradation processes, lack of maintenance, unplanned or informal modifications of the structure. An example is the gradual deterioration of buildings and bridges performance against earthquakes due to corrosion (Ghosh & Padgett, 2010; Iervolino, et al., 2015a; Zamanian, et al., 2020; Soltani, et al., 2021). The second refers to the changes in vulnerability caused by the interaction between two different hazards that occur close in time. As a matter of fact, when two hazards interact, vulnerability of the exposed elements may be altered by the first one and, in turn, their capacity to response to the second hazard may dramatically change. For instance, the presence of a load on a system such as the snow on a roof could determine an increment of the vulnerability during a seismic event. An example of load-dependent modified vulnerability due to ash loads is presented in Garcia-Aristizabal et al. (2013). Through an application in the district of Arenella, in the city of Naples, the authors demonstrated that the expected loss from earthquakes are remarkably sensitive to the thickness of the ash layer from volcanic activity assumed as additional load on buildings' roofs. Vulnerability may be also modified due to the presence of a pre-damage state, as in the case of the accumulation of damage in structures pre-damaged by a seismic main shock and threatened by aftershocks. Pre-damage-dependent seismic vulnerability/fragility for earthquake aftershock risk assessment were analysed in Bazurro et al. (2004), Sanchez-Silva et al. (2011), Polese et al. (2012; 2015),

Iervolino et al. (2015a; 2015b), Aljawhari et al. (2020), Gentile and Galasso (2020), and Papadopoulos et al. (2020). In Selva (2013) the effect of hazard interactions on people exposed was also analysed; this is for example the case of a strong local earthquake that leads people to escape from their damaged houses and go towards the seaside areas, which are the areas exposed to tsunami risk.

#### 2.3.4. Building taxonomy for multi-hazard risk assessment

As already mentioned, building taxonomy describes how to characterize buildings according to those attributes that can affect their performance during a hazardous event. Building taxonomies were mostly developed to describe and classify building structures according to their seismic performance. HAZUS (FEMA 2003) is the most popular taxonomy developed in the United States, which identifies 36 structural categories based on structural parameters affecting structural capacity and response, such as basic structural system (e.g., steel moment frame, steel brace frame, concrete moment frame, concrete shear walls, unreinforced masonry bearing walls), building height (i.e., low-rise, mid-rise, high-rise) and occupancy type (e.g., residential, commercial, industrial). In Europe, the EMS-98 scale (Grunthal, 1998) is the most widely used taxonomy, that classifies buildings into 15 classes based on the construction material (masonry, reinforced concrete, steel, wood) and the structural system type (e.g., rubble stone, unreinforced masonry with RC floors, RC frame with or without earthquake-resistant design). Based on the expected seismic vulnerability, each building class is also assigned to a vulnerability class, from A (most vulnerable) to F (least vulnerable), as already described in section 2.1.3 as well. Within RISK-UE project (Mouroux et al. 2004) a building taxonomy defining 23 building classes based on the combination of structural type, construction material, height class and building design code level was also proposed for seven European cities. Examples of building taxonomies focusing on seismic performance can be also found in Crowley et al. (2011), EERI (2000), Jaiswal and Wald (2008) and Brzev et al. (2013).

Despite the usefulness of these existing taxonomies, one of their main limitations is related to their use in multi-hazard risk modelling applications. As a matter of fact, in such cases the assets should be grouped into categories based on attributes

relevant to characterize their vulnerability to all hazards of interest. Thus, for example, while the construction material and the lateral load-resisting system are suitable indicators of the expected seismic vulnerability, the type and material of the roof is crucial for the characterization of building performance against cyclones as well as building height and the presence of basement are crucial for characterizing performance against floods. In Silva et al., 2018 the GEM taxonomy (Brzev et al., 2013) was expanded into a classification system suitable for multi-hazard assessment, also called GEM4ALL. The GED4ALL taxonomy identifies 14 building's attributes relevant to structural response under multi-hazard actions. Together with the attributes relevant against earthquakes (already mentioned before), other specific ones associated with flood hazard, wind hazard and fire hazard were added (i.e., ground floor hydrodynamics, fire protection, openings in exterior walls). A detailed description of this taxonomy and its comparison with the GEM one can be also found in Silva et al., (2022). Examples of exposure model for European and Middle East countries based on GEM4ALL building taxonomy can be found in Rodrigues, et al. (2019), Crowley et al. (2020a,b) and Dabbeek and Silva (2019).

## 2.4. Multi-dimensional nature of risk

Figures from recent disasters highlighted the influence that socioeconomic and cultural factors have on impacts of hazardous event. Almost the 50% of people who died in Louisiana because of Hurricane Katrina in 2008 were people older than 75 years (Brunkard et al., 2008) and the average age of deaths recorded after the wildfires in 2017 and 2018 in California was over 70 (Hamideh et al., 2022; Los Angeles Times, 2017, 2018 - [www.latimes.com](http://www.latimes.com)). Hence, older age, which is related to issues of mobility, healthy and communication, may increase the susceptibility of people to disasters. The study conducted by Ritchie et al. (2022) underlines that populations in low-income countries are more vulnerable to effects of natural disasters. As a matter of fact, when low-frequency, high-impact events occur in countries with low SDI (socio-demographic index), an index representing health, social conditions and economic development for a country, a dramatic high number of deaths is recorded, whereas highly developed countries seem to be much more resilient to disaster events and therefore the number of deaths results consistently low. According to past experiences, also

cultural factors may influence the consequences of a natural hazard, as they affect people perception of risk and how they prepare for it (Alexander, 2012; Wachinger, et al., 2013). Therefore, characteristics of the asset exposed play a crucial role in understanding the risk, explaining why some social groups could be more effected than others.

Understanding the importance of such social factors and their contribution to community preparedness, disaster response and post-disaster recovery, is critical not only for reducing existing disaster risk but also for enhancing community resilience (UNDRR, The TEN Essentials for Making Cities Resilient). Resilience is defined as the ability of a community exposed to hazards to resist, absorb, accommodate, adapt to, transform and recover from the effects of a hazard in a timely and efficient manner (UNISDR, 2009). In other words, the more resilient is a system, the greater is its ability to reduce failure probability, reduce consequences from failures and reduce time to recovery (Bruneau, et al., 2003). While the former two features of the system depend on its vulnerability (both physical and social), time to recovery refer to the restoration time required to get the normal level of performance, i.e., the pre-event level, and it depends on the redundancy of the system and its capacity to react in an efficient timely manner. Hence, community resilience depends on multiple components. Although a large amount of studies have been conducted for modelling resilience, the selection of an appropriate number of resilience components is still a significant challenge (Nguyen & Akerkar, 2020).

According to Bruneau et al. (2003), resilience can be conceptualized through four interrelated dimensions: the technical dimension, that refers to the ability of the physical system to keep an acceptable level of performance; the organizational dimension, that refers to the capacity of managing critical facilities, establishing priorities and mobilizing resources in order to bring the system to its normal condition; social and economic dimensions involve the community capacity to withstand and recover quickly from the disaster, such as the capacity to provide emergency shelter and short-term housing for people affected, the ability to restore services to residential dwellings or the availability of government programs and insurance payouts that facilitate housing reconstruction. In PEOPLE Resilience Framework (Renschler, et al., 2010) the previous proposal

of Bruneau et al. (2003) was expanded, identifying seven component-dimensions in assessing community resilience: population and demographic, that includes population's indicators of age, gender, education attainment and income level; environmental/ecosystem, referring to quality of natural resources; organized governmental services, related to executive and administrative capacity of local authorities; physical infrastructure, that measures the accessibility to residential/commercial/cultural facilities as well as lifelines services (e.g., internet, postal, tv, phones) and health care; lifestyle and community competence, that reflects the quality of life and community self-organization; economic development, that reflects the level of financial and employment services, transportation and utilities; social/cultural capital, that concerns all services specifically designed for population needs (e.g., child and elderly services).

According to Barkham et al. (2014) all resilience components could be grouped into two main dimensions: vulnerability and adaptive capacity. Thus, resilience increases when communities have more adaptive capacity and decreases when they are more vulnerable. The vulnerability dimension refers to the capacity of a country to guarantee an adequate standard of living to its inhabitants reducing the physical vulnerability to natural hazards and environmental threats and social vulnerabilities due to poverty and inequality, efficiency of transport infrastructure and basic utilities. The adaptive capacity refers to institutions capacities to communicate within government bodies at all levels and associated groups such as non-governmental and community organisations as well as the capacity to put in place disaster management plans and emergency procedures.

In Ferrer et al. (2017), all components of resilience are incorporated into a single multi-dimensional risk index. The INFORM (INdex FOr Risk Management) is a tool aimed at supporting decision-makers on prioritisation of emergency preparedness and resilience activities. The conceptual framework is based on a holistic perspective of disaster risk for a community, identifying risk as the interaction of hazard, exposure, vulnerability and capacity measures. As already underlined in previous studies (Wisner, et al., 2004; Cardona & Carreño, 2011), disaster can be interpreted as the interaction between socio-economic pressures and physical exposure to the hazardous event. INFORM risk concept identifies three dimensions of risk: hazard and exposure, vulnerability and lack of resilience

to cope and recover. The hazard and exposure dimensions are merged into a single one to reflect the probability of physical exposure associated with specific hazards. Indeed, there is no risk if there is no physical exposure, no matter how severe the hazardous event is. The physical vulnerability, that is a hazard dependent characteristic, is incorporated into the hazard and exposure dimension. On the contrary, the vulnerability dimension refers to the fragility of the socio-economic systems. The lack of coping capacity, instead, measures the ability of a country to face up with disasters in terms of DRR activities and governance as well access to communication services, physical infrastructures and health system, which contribute to the reduction of disaster risk.

Socio-economic and demographic factors that affect the resilience of communities usually characterize the vulnerability dimensions. This means that they could increase the susceptibility of a community to the impacts of hazards. In general, we refer to this dimension of the vulnerability as social vulnerability. An overview of the methodologies adopted for the estimation of social vulnerability for a community and the parameters that may affect it are presented in the following section.

#### 2.4.1. Social Vulnerability

As crucial component of community resilience, social vulnerability has been examined by researchers across a multitude of academic disciplines. The concept of social vulnerability within the disaster management context was introduced in the 1970s when researchers recognized that vulnerability to hazards may be influenced by many socio-economic factors, such as age or income (Morrow, 1999; Juntunen, 2005). Social vulnerability refers to the increased likelihood of some social groups to suffer negative consequences of natural hazards, due to their lack of capacity to react and manage the effect of hazard related processes (Oliver-Smith, 1999; McCarthy, et al., 2001; Cutter, et al., 2003; Wisner, et al., 2004; Adger, 2006; Barros, et al., 2014).

In research literature, different socio-economic and demographic factors have been identified as social vulnerability components. The main parameters adopted to assess social vulnerability are gender, age, education, socioeconomic status, public health condition, employment status, and access to resources (Frigerio, et



al., 2018). For example, discriminatory atmosphere to women, especially in developing countries, causes a limited access to resources and information for female population, limitations that may affect their physical and mental health during and after disasters (Sohrabizadeh, et al., 2014). Several studies highlight that females are usually linked to a higher rate of mortality and poverty in disaster contexts compared to males (Wisner, et al., 1994; Fatemi, et al., 2017). Children and elderly people living alone are the age groups that mostly affect social vulnerability, as they are dependent on others and require protection, financial support, transportation, medical care and assistance with ordinary daily activities (Schmidtlein & King, 1995; Rosenkoetter, et al., 2007; Ardalan & Mazaheri, 2010). Hence, children less than 5 and people 65 years and older might have many problems in emergency and recovery phases and require special treatment by disaster response planners and operational officers. Minority groups such as disabled, migrant or social or ethnic community, might be characterized by high social vulnerability if they live in more risky areas or has experienced language and communication problems (Peacock, et al., 1997; Carnelli & Frigerio, 2016). To give an example, real-time evacuation information during emergencies is not generally provided to people with limited dominant language proficiency, the hearing and visually impaired, and other special needs groups (U.S., 2006). Employment and socioeconomic status may influence both exposure to natural hazards and the ability to recover from a disaster, as well (Cutter, et al., 2000; Wisner, et al., 2004; Carnelli & Frigerio, 2016). For instance, many low-income people in New Orleans were stranded in the wake of Hurricane Katrina because they had no personal transportation and public authorities did not provide emergency mass transit (Flanagan, et al., 2011). Still, population density may increase social vulnerability not only due to evacuation difficulties but also because of urban sprawl issues that can easily lead to disasters (Kelman, 2017).

Quantifying and mapping social vulnerability allow the identification of the most vulnerable areas for the implementation of prevision and prevention measures for risk reduction. To measure social vulnerability, indicator-based approach are the most used methods (Yoon, 2012). As a matter of fact, indicators allow to aggregate and compare different metrics. Additionally, these indicators are relatively easy to interpret also for non-experts, that makes composite indicators

particularly suitable for policymaking and public risk communication. Some examples are the Human Development Index (United Nations Development Programme, 2020) the Prevalent Vulnerability Index (Inter American Development Bank, 2010), and the Social Vulnerability index (Cutter, 2003). The latter, also referred to as SoVI, is still the leading conceptual framework to assess social vulnerability. This method was formulated to measure the social vulnerability of U.S. counties to natural hazards. Besides age, gender, race, and socioeconomic status, other characteristics that identified specific population needs or lack of the normal social safety nets necessary in disaster recovery phase are also taken into account (e.g., physically or mentally challenged, non-English speaking immigrants, rural population, etc.). To examine the social vulnerability, originally 42 independent variables were collected, subsequently reduced to 11 components applying principal component analysis (PCA). The latter is a statistical technique for reducing the dimensionality of a dataset, i.e., PCA transforms high-dimensions data into lower-dimensions while retaining as much information as possible. Through PCA, the observations in the dataset are geometrically converted in new variables that are linear functions of the original ones. The new set of variables, called principal components (PCs), are such that they are uncorrelated with each other and successively maximize variance, i.e., the first PCs is the one that minimize the variance. The importance of each component decreases when going to 1 to n, it means the 1 PC has the most importance, and n PC will have the least importance.

Personal health, age, density of the built environment, race and ethnicity are some of the considered components.

A limitation in using SoVI proposed in Cutter (2003) is that such index should be specific for the context of analysis, i.e., to assess social vulnerability in different places, it needs to be modified to account for context-specific local dimensions. Thus, for example, in Frigerio et al. (2018) SoVI index was suitably fitted in order to apply the same methodology to the Italian context. The number of components turn from 11 to 16 and more emphasis was given to the educational level, the employment and the socio-economic status. In Mesta et al. (2022) an application of SoVI for Nepal was presented. Eleven variables contain demographic and socio-economic attributes of Kathmandu Valley's population

that may affect their social vulnerability to natural hazards were considered. All variables are associated with one of five indicators (i.e., Population, Education, Economy, Habitat, Infrastructure). As developing country, not surprising that, for example, the percentage of households with no toilet facility or the percentage of households with no mobile phone or telephone service is considered as a variable for SoVI calculation. Other applications of SoVI for specific local context can be found in Chen et al. (2013), Guillard-Goncalves et al. (2014), Solangarachchi et al. (2012) and Wood et al. (2010).

## 2.5. Current gaps and open issues

In the previous sections it has been shown that multi-hazard risk analysis is not the simple sum of single hazard risk estimation. Despite the large availability of consolidated approaches for single hazard evaluation, only few studies analyzed multiple hazards and standard approaches for multi-risk assessment are not still available (Kappes et al., 2012).

The rigorous implementation of multi-hazard analysis that account for hazard coincidence and interactions are still scant. Historical catalogues that take properly into account the simultaneous occurrence of different hazards are rarely available, as well. Moreover, multi-hazard processes are often specifically developed for a given context and therefore they can be applied only in specific cases. Exposure modelling to multiple hazards should account for hazard-specific vulnerability of structures but only few studies on multi-hazard taxonomies are available. Also ignoring hazard interactions, the comparability of risks derived from multiple hazards requires to use at least the same output metrics and scale of analysis. Still, the temporal resolution of analysis needs to be comparable and suitable for the purpose of the analysis, for instance, several days for planning emergency activities, years, decades or centuries for land-use planning activities (Marzocchi et al., 2012). For instance, potential impacts of an earthquake are often estimated to plan mitigation and adaptation strategies, while assessment of volcanic or landslides risk are primarily aimed at evacuation and prevention (Foerster et al. 2009).

Another open issue on multi-risk analysis concerns the integration of socio-economic aspects in the analysis. Although consolidated approaches for

evaluation and measure of social vulnerability to natural hazards are available (see section 2.4.1), such socioeconomic and demographic risk drivers are usually ignored in conventional risk assessment procedures. Some studies investigated the spatial interactions between natural hazards and social vulnerability. In Fekete (2010) a Social and Infrastructure Flood Vulnerability Index for Germany is proposed. Demographic statistics of Federal Statistical Office are used to evaluate a Social Susceptibility Index (SSI) for German counties. As indicator, the SSI is demonstrated to be integrable with hazard information, derived from inundation maps of rivers. The exposure is calculated using a Geographic Information System (GIS) software, considering the percentage of settlement area inundated for the considered event scenario. Additional information on the location of critical infrastructures, such as power plants, electricity facilities, heating and water supply, and their ratio per country (i.e., the number of all critical infrastructure items per county) is used for calculating an Infrastructure Density Index (IDI). Then, the flood vulnerability index for each country is calculated as the product of the SSI, the IDI and the exposure area. In 2016 Frigerio et al. proposed a GIS based methodology for integrating social vulnerability into the seismic risk analysis in Italy. The approach proposed in Cutter et al. (2003) for assessing the SoVI was adopted. A multivariate statistical analysis was conducted in order to identify suitable socio-economic indicator to use. The map of the seismic classification of the Italian territory proposed in the Ordinance of President of the Council of Ministers of 28 April 2006 (OPCM 3519/06) is considered representative of the seismic hazard. Thus, using a GIS, the spatial variability of social vulnerability to seismic hazard was identified. Through the use of a risk matrix, the classes of a social vulnerability index map were combined with those of a seismic hazard map. A qualitative social vulnerability exposure map to earthquakes was produced, highlighting areas with high seismic and social vulnerability levels. Interaction between flood hazard, urban growth and social vulnerability in Kathmandu Valley, Nepal, was investigated in Mesta et al. (2022). The flood hazard model used is the one proposed by Sampson et al. (2015), while the cellular automata SLEUTH model (Chaudhuri & Clarke, 2013) is applied to simulate Kathmandu Valley's urban growth in 2050. The SoVI index was adapted to account for Nepal's specific context and used to quantify social vulnerability. The spatially overlapping of

those factors (hazards, urban growth, social vulnerability) allows the identification of critical location where disaster risk is likely to increase drastically in the future.

However, all cited studies focus on single risk, e.g., flood or seismic, without any consideration of possible combination of several hazards. One of the best examples of tools that allow a holistic assessment of risk is the INFORM index, as also shown in section 2.4.1. The latter is a global index-based multi-hazard approach that allows to combine three different dimensions of risk at country level: hazard and exposure, that involves several hazards such as earthquakes, tsunamis, floods, tropical cyclones and drought and the exposure/vulnerability of the built environment to such perils; vulnerability, that represents economic, political and social characteristics of the community; lack of coping capacity, that measures the ability of a country to cope with disasters in terms of organised activities of the country's government as well as the efficiency of the existing infrastructure, which contribute to the reduction of disaster risk. The INFORM index assign a score between 0.0 and 10.0 to each country. The low values of the index represent a positive performance, and the high values of the index represent a negative performance in terms of managing risk. Thus, the index allows the ranking of countries, i.e., the identification of countries with higher or lower than the others. The countries may be also grouped in classes based on the level of risk of humanitarian crises (e.g., very low, low, medium, high and very high risk). Another possible use of the index is to follow trends in time series. However, the main limitation of this approach is that requires many inputs information, that may lead data collection phase time consuming. Also, some data may be not available in all countries and hypothesis made on missing data may distort the real value of the composite indicator in such countries (Marin Ferrer et al., 2017).

## A framework for integrating social vulnerability in multi-risk assessment

Modelling and quantifying natural-hazard risk enables decision-makers to understand the potential types and the extent of future disaster impacts. For facilitating development and implementation of appropriate preparedness and mitigation strategies, risk quantification approaches should capture the effects of multiple hazards. The simple listing of all hazards potentially affecting an area gives no indication about their relevance. Thus, comparing and ranking different hazards as well as accounting for their possible interactions is crucial for supporting authorities in defining risk reduction measures. However, performing multi-risk assessments can be challenging, particularly at large geographic scales, because of the requirements in terms of input data and computational resources involved. Furthermore, past disasters underlined that impacts of hazards are not equally distributed within society (UNDRR, 2015). Socio-economic factors such as age, gender, health, origin, educational level, employment and income level, may affect susceptibility of various social groups to harm and their response capacities to hazards. Given its complex multidimensional nature, risk assessment for effective disaster-risk management and decision-making should consider both physical and social vulnerability factors.

This study addresses the challenge of integrating crucial physical and social vulnerability factors in multi-risk analysis, aiming to overcome the aforementioned limitations. As also shown previously, index-based approaches are particularly suitable for measuring multidimensional realities too complex to be summarized by a single indicator. For this reason, a straightforward multi-risk index that combines multiple hazards and both physical and social exposure and vulnerability is proposed herein. More specifically, a multi risk index for the entire country of Italy, using municipality-level scale of analysis, is obtained combining earthquake and flood risk with social vulnerability. The procedure

adopted for constructing the index, the single indicators selected for each dimension (i.e., hazard, social and physical vulnerability and exposure) as well as the variables used for their calculation are described in the following sections. The proposed metric is used to identify hotspots across the Italian territory that should be prioritised for actions that promote disaster risk reduction. Moreover, sensitivity analyses of methodologies and metric weights used to combine single indicators is also performed in order to evaluate how these hotspots can change as a function of stakeholder priorities and single risk considerations.

### 3.1. Building a composite indicator

A composite indicator is a mathematical combination of a set of individual sub-indicators that represent different dimensions of a concept and have no common unit of measurement (Nardo, et al., 2005). The main stages involved in the construction of a composite indicator are the selection of the sub-indicators, their normalization, the choice of aggregation model and the weights of the sub-indicators. The starting point in constructing composite indicators is the definition of a theoretical framework, i.e., the definition of the phenomenon to be measured through the composite indicator. As a matter of fact, the choice of which sub-indicators to use, which weighting method has to be used and as well as how aggregate information, are subjective choices that can be used to manipulate the results. Thus, the theoretical framework provides the criteria for the selection and combination of variables based on the defined purposes.

First, the factors that significantly affect the phenomenon are chosen. Multi-dimensional concepts are divided into several sub-groups (i.e., sets of sub-indicators), guiding by the theoretical framework. Such a nested structure improves the user's understanding of the driving forces behind the composite indicator. Indicators should be selected based on their relevance to the phenomenon being measured and relationship to each other as well as their accessibility and their country coverage. The selection of a group of individual indicators can be based on expert opinion or using analytical approaches, such as principal component analysis, that allows to investigate the relationship among potential indicators in order to retain and use only the most representative ones.

Individual indicators selected are then normalized to make them comparable. Normalization of data is a required step prior to any data aggregation as the indicators often have different measurement units. After normalization, indicators are transformed into pure, dimensionless, numbers. Several normalization techniques can be used. One of the simplest and most common normalization procedure is the maximum-minimum method. It consists in a linear rescaling of each indicator value by subtracting the minimum value and dividing by the range of the indicator values, so that the minimum value of that factor among all units of analysis is mapped to 0, while the maximum value to 1. Distance to a reference measure is a method that provides the relative position of a given indicator with respect a reference point. The latter could be a target to be reached in a given time frame (e.g., the reduction target for CO<sub>2</sub> emissions) or a value assumes in a benchmark country. An extensive overview of normalization methods can be found in Nardo et al. (2008).

The definition of the weights to assign and the aggregation procedure to use for combining different dimensions is central in the construction of a composite indicator. The different weights assigned to single indicators should reflect their importance in expressing the considered phenomenon. Thus, for example, if the factors are considered of the same importance, equal weights can be assigned. If a high degree of correlation exists between two or more variables, statistical models such as principal component analysis or factor analysis should be used to overcome the double counting problem of indicators that partially measure the same behaviour (Nardo et al., 2005). Alternatively, participatory methods that incorporate various stakeholders' opinions can be used to assign weights. Subjective weights may be set by a group of experts such as technicians and policy makers or even by citizens through social surveys that allow to get how important are individual indicators for people. In the budget allocation approach, for example, weights are quantified by providing experts a "budget" of N points to distribute over a number of individual indicators; the expert "pays" more for those indicators whose importance they want to place more emphasis on.

Aggregation rules to combine all the components to get the final composite indicator can vary as well. The composite indicator can be obtained by the weighted sum of the sub-indicators (e.g., linear aggregation), their product (e.g.,



geometric aggregation) or aggregating them using non-linear techniques such as multi-criteria analysis. There is no obvious way of aggregating sub-indicators. The suitable aggregation method should be selected based on the aim of the work and the characteristics of the sub-indicators adopted. Linear aggregation is a compensatory approach that allows full compensability among dimensions, i.e., poor performance in one dimension can be compensated by sufficiently high performance of another (Greco et al., 2018). The geometric aggregation also implies a certain degree of compensability between individual dimensions. However, while in a linear aggregation the compensability is full and constant, in the geometric aggregation compensability is lower for sub-indicators with lower value (Nardo et al., 2008). Hence, it could be considered as a less compensatory approach. In case of compensability among dimensions is not allowed, non-compensatory method such as the multi-criteria analysis should be used. Some general guidelines for the selection of the most suitable methods for the construction of a composite indicator can be found in Mazziotta & Pareto (2013).

In the next sections, the indicators selected for describing physical and social dimensions involved in the calculation of the proposed multi-risk index are presented. The normalizing, weighting and aggregation methods adopted are briefly described following as well (section 3.3).

## 3.2. Indicators for physical and social dimensions

### 3.2.1. Seismic risk

The assessment of seismic risk implies the combination of seismic hazard, vulnerability and exposure. Thus, sub-indicators for each of these components have to be defined.

The seismic hazard indicator is derived from a measure of earthquake-induced ground shaking at the municipal centroid, which is quantified according to a selected hazard map. In Italy the official reference is the MPS04 model proposed by Stucchi et al. (2004; 2011). Seismic hazard is obtained by the PSHA. The results of the PSHA were elaborated by INGV (Istituto Nazionale di Geofisica e Vulcanologia) and presented in terms of maps showing the value of peak ground acceleration (PGA) and spectral acceleration at reference elastic periods ( $S_a(T)$ )

corresponding to an exceedance probability in a given period of time or, equally, to an assigned return period. Nine different hazard maps of Italy were realized by INGV for nine different return periods (2500, 1000, 475, 200, 140, 100, 72, 50 and 30 years) or probabilities of exceedance in 50 years (2%, 5%, 10%, 22%, 30%, 39%, 50%, 63% and 81%). The PGA value for 475-year return period (or 10% probability of exceedance in 50 years) is selected as measure of ground shaking in this application as it is the most common standard used in the industry for assessing seismic risk, and it is also the basis for most building codes for seismic design. The model provides the seismic actions for each point of a 5x5 km mesh covering all the Italian territory. The PGA value at municipal centroid is obtained as weighted average on distance, considering the closer grid points. Figure 3.1 shows the hazard map of Italy representing hazard input value at municipal level.

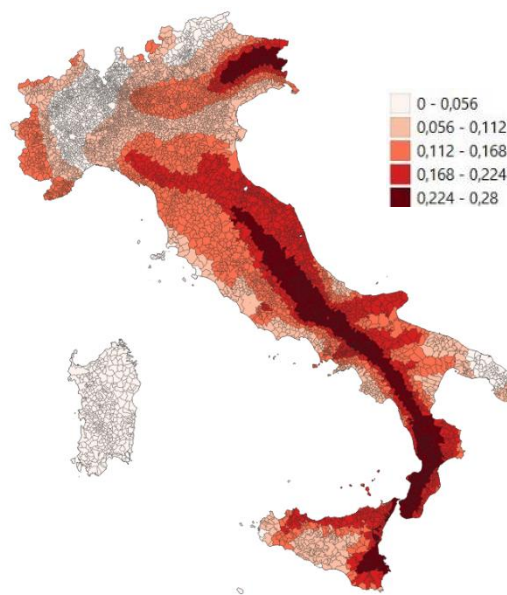


**Figure 3.1** – Seismic hazard map of Italy with PGA values for a return period of 475 years. PGA values is expressed in units of g.

The physical vulnerability indicator expresses the susceptibility of buildings to be damaged by an earthquake of a given intensity. As also shown in section 2.1.2, in performing vulnerability assessment buildings are usually clustered in relevant classes representing their expected performance during a seismic event and for each class different vulnerability functions (i.e., a function relating seismic intensity with the expected level of damage for the structure) are defined. Herein, we adopt the Risk-UE index-based approach (Lagomarsino & Giovinazzi, 2006)

to derive seismic vulnerability indicator. This model clusters buildings into vulnerability classes based on values of a Vulnerability Index (VI) and for each class a different DPM, expressing the expected damages as a function of the macroseismic intensity level, is defined. The six vulnerability classes of the EMS-98 (Grunthal, 1998) approach are considered (i.e., A, B, C, D, E, F). The VI for buildings is derived from basic information on construction material (e.g., masonry, RC), structural system (e.g., simple stone, massive stone, adobe, for masonry structures; frame or walls for RC) and additional information on vulnerability factors, such as the height of the structure, the type of horizontal structures for masonry buildings and the level of earthquake resistant design in the case of RC. An initial value of the VI is defined as a function of the sole construction material/structural system, which can then be modified based on further information, if available. For example, a value of 0.87 is assigned to masonry buildings with irregular layout, and this value could increase if vaults (+0.08) or flexible slabs (+0.02) characterise the lateral structural system. Specifically, the VI ranges between 0 and 1, with values close to 1 indicating the most vulnerable buildings and close to 0 indicating buildings with superior seismic performance. Intervals of VI values for the vulnerability classes are defined so that, given the VI value for a building or a building typology, the vulnerability class of belonging can be assigned.

For the purpose of this application, seismic vulnerability indicators can be simply expressed by the VI calculated at municipal level. The information on buildings can be derived by the latest census database (ISTAT, 2011). In Italy, ISTAT (Italian national institute of statistics) provides the number of buildings and information on building characteristics such as the construction material (masonry, reinforced concrete, other), the number of storeys (1,2,3, 4 or more storeys) and construction age (< 1919, 1919-1945, 1946-1961, 1962-1971, 1972-1981, 1982-1991, 1991-2001, 2001-2005, > 2005) at census tract level. However, for privacy reason, such data are available in aggregated form, e.g., it is not possible to know how many masonry buildings with two storeys are built before 1919. On the contrary, disaggregated data are available at the municipality level or larger scales. For RC buildings three information are taken into account for the calculation of the VI: the structural system type, the design level and the

number of stories. For the former one, moment resistant frame structure type is assumed, considering their huge diffusion on the Italian territory. The second one is defined comparing the age of construction of the building (given by census) and the year of entry in force of the main seismic code (i.e., the seismic classification year of the considered municipality). This means that to all buildings having the same age of construction is assigned the same VI. Then, the VI value could be modified based on the class of height of belonging.

As census data provides only typological information on buildings, the other information on masonry buildings required for VI calculation are derived by adopting a suitable exposure/vulnerability model that defines rules to assign census building typologies (e.g., defined based on construction material and age of construction) to building classes (see also section 2.1.1). More specifically, the exposure model proposed by Del Gaudio et al. (2019) is adopted. The authors identified four vertical structural types (i.e., regular layout or good quality, irregular layout or poor-quality structure with or without tie rods/beams), and five horizontal structural types (i.e., vaults with or without tie rods, beams with flexible, semi-rigid or rigid slabs). Based on the combination of vertical and horizontal structure types (e.g., irregular layout structure without tie rods or tie beams and flexible slabs), 14 building classes are defined. Using data derived from a sample of 22,618 residential masonry buildings surveyed after L'Aquila earthquake, the authors inferred the percentage of occurrence of each of the 14 classes within 8 times intervals ( $< 1919$ , 1919-1945, 1946-1961, 1962-1971, 1972-1981, 1982-1991, 1991-2001,  $> 2001$ ) defined by ISTAT (2001). Thus, given the number of masonry buildings in each period (information provided by ISTAT at municipal level), adopting such percentages it is possible to derive the number of buildings belonging to different classes. As the building classes identified in the model do not account for the height of buildings, those percentage are considered as constant across all height classes, i.e., for buildings with 1, 2, 3, 4 or more stories belonging to the same age of construction period the same percentages of occurrence in each of the 14 classes are adopted. The corresponding VI value for each class is assigned as a function of the relative features (e.g., vertical and horizontal structure type, class of height). Thus, the physical vulnerability indicator is first evaluated at the building class level, i.e.,

for each class of buildings with the same structural features. Then, the final municipal-level indicator is obtained as a weighted average based on building class presence in the municipality. In this way, also physical exposure is accounted for in the definition of the physical vulnerability indicator. It is worth noting that buildings categorized as “other” material are not included, as in Italy these kinds of structures are not very widespread. A confirmation of such statement is that no vulnerability model for this typology is officially included in NRA for Italy (Dolce et al., 2021).

This approach has been selected to be consistent with the structure of the other terms of the risk indicator, in particular with the social vulnerability term (see section 3.2.3). As a matter of fact, the use of score-based approaches for measuring both physical and social vulnerabilities make them easily aggregable and comparable. Moreover, Risk-UE approach allows to automatically rank municipalities based on their physical exposure and vulnerability by VI values, without the need for defining an arbitrary score to each vulnerability/building class or other criteria necessary to define physical vulnerability scores of municipalities.

### 3.2.2. Flood risk

Directive No 2007/60/EC, also known as the Flood Directive (FD), is the reference for the assessment and management of flood risks in Europe. The FD requires Member States to assess their territory for significant risk from flooding, to map the flood extent, identify the potential adverse consequences of future floods for human health, the environment, cultural heritage and economic activity in these areas, and to take adequate and coordinated measures to reduce this flood risk. The procedure to reduce the risk of floods comprises three stages: a preliminary flood risk assessments for the identification of river basins and coastal areas at risk of flooding; the preparation of flood hazard maps, describing the flood extent and the water level (i.e., water depth), and flood risk maps, showing the potential adverse consequences associated, for three different scenarios corresponding to events with low, medium and high probability of occurrence; establishment of flood risk management plans defining appropriate objectives for the reduction of potential adverse consequences of flooding for human health, the environment, and economic activity, and, if considered

appropriate, on non-structural flood prevention initiatives. In Italy, the FD was implemented with the with Legislative Decree 49/2010. The implementation of FD requires the preliminary identification of the management units (Unit of Management - UoM) and the related competent authorities (Competent Authority - CA). The FD defines a management cycle, which is renewed through an iterative process with a periodicity of 6 years. During each management cycle, the three stages to assess and manage flood risk (i.e., preliminary flood risk assessment, flood hazard and risk maps, flood risk management plans) should be implemented in succession at the river basin district or UoM level. The entire Italian territory is divided into 8 Districts, having jurisdiction over the 47 UoM identified. Legislative decree 49/2010 establishing that the District Basin Authorities must provide for the fulfilments of the FD, transmitting the information to ISPRA (Istituto Superiore per la Protezione e la Ricerca Ambientale), an institute acting under the vigilance and policy guidance of the Italian Ministry for the Environment and the Protection of Land and Sea.

According to FD, flood hazard maps should be developed considering three probability scenarios: low (extreme events), medium (events with return period of 100 years or greater) and high (frequent events). In Italy, the Legislative Decree 49/2010 characterizes events corresponding to medium probability as infrequent events with a return period between 100 and 200 years and events corresponding to a high probability as frequent events with a return period between 20 and 50 years. Extreme events correspond to events with a return period of 300 years or greater. ISPRA carried out maps for containing the perimeter of the geographical areas that could be affected by floods, bounded by the District Basin Authorities, according to three aforementioned scenarios ([www.isprambiente.gov.it](http://www.isprambiente.gov.it)). Such maps are shown in figure 3.2. However, further information required to characterize flood hazard, i.e., water depth, are not reported in the above maps, as such data is not included in all District hazard maps.

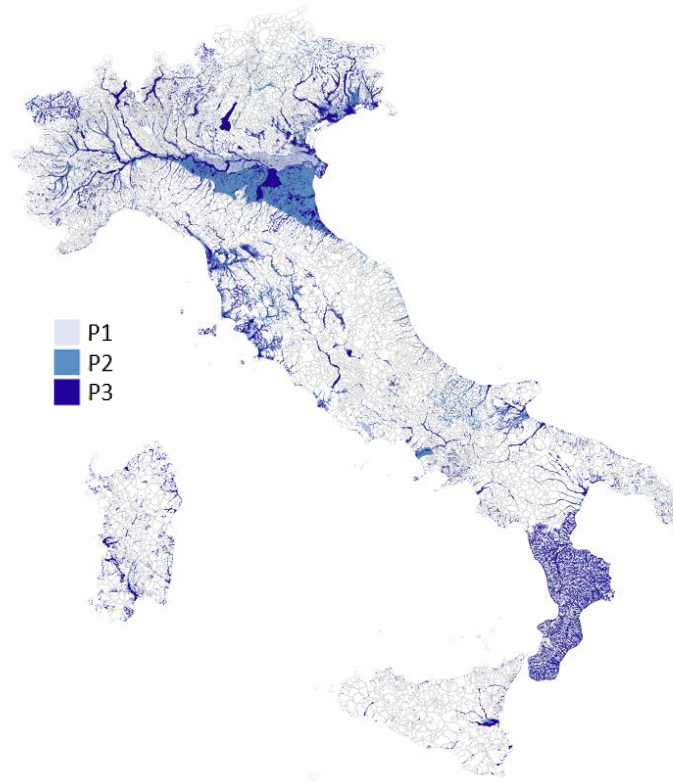


**Figure 3.2** – Map of flood inundated areas expected to low probability or extreme events (P1), medium probability events (P2) and high probability or frequent events (P3).

Although approaches for calculating water depth by flood extension maps are available (Cohen, et al., 2018; Peter, et al., 2022), their application for the entire country may be time consuming. Moreover, a detailed flood assessment is beyond the scope of this study. Flood hazard indicator should measure the greater or lower probability for assets at risk in the considered unit of analysis (municipality) to be affected by a flood event. Therefore, the sole information of the area potentially inundated can be considered an acceptable and satisfactory information. Similarly, a detailed exposure assessment would require the use of a GIS software for detecting exposure at building level as building footprint. Therefore, to combine the need to estimate the flood hazard at municipality scale for the whole national territory with the one to have a rapid exposure assessment the hazard indicator at municipal level is estimated as the percentage of municipal area potentially inundated by a flood event. The inundated area is considered representative of the exposure as well. That means that, as potentially flooded buildings cannot be exactly estimated, the spatial distribution of buildings within a municipality is assumed uniform; therefore, the percentage of inundated area in the municipality is considered proportional to percentage of exposed buildings.

In other words, greater the inundated surface, greater the number of buildings potentially flooded. Specifically, the map of inundated areas by an event with medium probability of occurrence i.e., with a return period between 100 and 200 years, is considered for calculating hazard indicator. As a matter of fact, too frequent events with a return period between 20 and 50 years are not suitable for the comparison with the seismic term. Events with a return period greater than 300 years are excluded as well, as flood events too rare and unlikely.

Flood vulnerability for buildings is often expressed as a function of the occupancy type, the construction material and building's height. As this study focuses on residential buildings, only fragility model referred to such occupancy type are analysed. Several studies propose different fragility functions based on the main construction material of the building. The European depth-loss functions for residential buildings proposed in Huizinga (2007) do not account for different construction materials but only for different type of use. Maximum damage values are calculated for buildings made of generally resistant material such as concrete or masonry. Correspondingly, this relates to western countries or urban areas in more rural countries. However, if less resilient building materials are assumed to be used, for instance mud dwelling with straw roof mostly used in rural areas of developing countries (Maiti, 2007), total loss damage (i.e., damage ratio = 1) is reached much sooner than compared to concrete or masonry buildings. Therefore, the authors suggest defining a suitable "undamageable" part (reducing the maximum damage value) for buildings based on their resistant material. It is suggested to set the "undamageable" part to zero for materials with worse performance (e.g., mud), while the "undamageable" part is round 40% for RC and masonry buildings. These values are in line with the damage function from the CAPRA database (Central American Probabilistic Risk Assessment), reported in figure 3.3 (Cardona, et al., 2012).



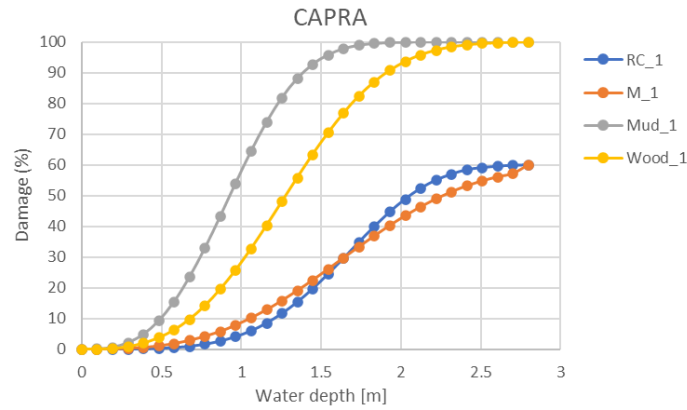


**Figure 3.3** – CAPRA depth-loss functions (Cardona et al., 2012).

As this application is proposed for the Italian territory, where almost all residential buildings are in RC or masonry, there are not significant differences between those typologies in terms of vulnerability. Thus, the only buildings feature expected to significantly affect their flood performance is the height. Analysing HAZUS depth-loss curves (figure 3.4) it can be noted that the buildings with 1 story tend to be more vulnerable with respect to the ones with 2 or 3 storeys. Therefore, the fraction of residential buildings with 1 story within the municipality is considered as flood vulnerability indicator. The greater the number of low buildings with 1 story in the municipality, the greater its susceptibility to be affected by negative consequences by a flood event. Although it is a simplifying approach, the adopted criteria allow to represent the physical flood vulnerability through a simple indicator, calculated using only public accessible data (i.e., census). It is worth mentioning that despite the presence of basement is a crucial information in flood vulnerability assessment, this data is not available by census, therefore it is not considered herein.

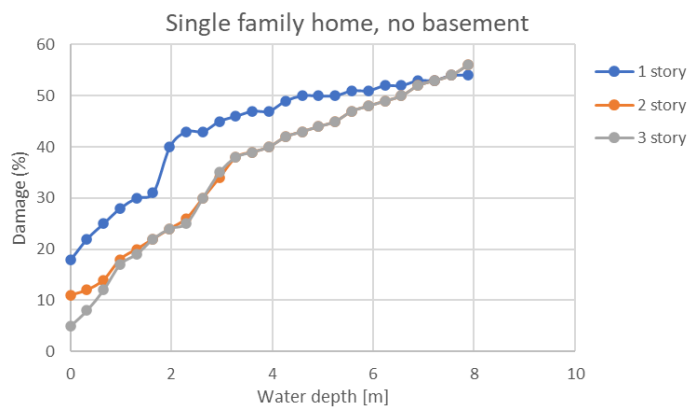


**Figure 3.4** – HAZUS depth-loss functions for single family home with no basement.

### 3.2.3. Model for social vulnerability

For the evaluation of social vulnerability, the modified SoVI index proposed by Frigerio et al. (2018) is adopted, as specifically developed for the Italian territory. Based on a literature review and taking into account also the data availability, the authors selected 16 variables for quantifying social vulnerability in Italy. These variables are representative of 7 demographic and socio-economic indicators relevant to the specific context, that can increase or decrease social vulnerability, i.e., family structure, education, socioeconomic status, employment, age, population growth, race/ethnicity, as also shown in table 3.1.

Age indicator involves variable such as rate of children (i.e., population under 14), rate of elderly (i.e., population over 65), aging index and dependency ratio. The aging index refers to the number of elders compared to persons younger than 15 years old in a specific population (Preedy & Watson, 2010). The dependency ratio is the ratio of persons of nonworking age to persons of working age, usually the 20–65-year-olds (Simon, et al., 2012). Information on population is provided by latest census (i.e., ISTAT 2011) at census tract level. In ISTAT database population is classified by age (<5, 5-9, 10-14, 15-19, 20-24, 25-29, 30-34, 35-39, 40-44, 45-49, 50-54, 55-59, 60-64, 65-69, 70-74, >74) and gender (male, female). Therefore, the above-mentioned variables at municipal level (that is the scale of analysis of this study) can be calculated considering all census tract data belonging to the same municipality.

Education indicator is expressed through two variables: low educational index and high educational index. About education, ISTAT provides the following information: number of people with a degree, number of people with high school diploma, number of people with secondary school diploma, number of people with primary school diploma, illiterate people. Moreover, in the BES (“benessere equo e sostenibile”) report by ISTAT (ISTAT, 2016) people with at least high school diploma, people with a degree and people early exit from the education system are considered the main educational indicators. People with at least high school diploma indicator is expressed by the percentage of 25-64 aged persons with a high school diploma, people with a degree indicator by the percentage of 30-34 aged persons with a degree and people early exit from the education system

indicator is described as the percentage of 18-24 aged persons who only obtained a secondary school license and are not included in a program of education or training. Therefore, in this study high educational index is calculated comparing the total number of people with a degree (estimated by ISTAT 2011 database) to over 30 aged population. Low educational index is calculated comparing the number of people who only obtained a secondary school diploma to over 15 aged population. The latter (over 15 aged) is selected as threshold because of the population age ranges considering in census database, described above.

As representative of socio-economic status, the commuting rate and the quality of buildings are the variables taken into account. The commuting rate is calculated as ratio of commuters and people in working age, defined as over 15 aged (ISTAT, 2011). In census databased the quality of buildings is expressed classifying buildings by their state of preservation: very good, good, bad or very bad. In this application the number of buildings with a bad or very bad state of preservation at municipal level is considered as variable representative of the quality of buildings. The unemployment rate, employed and female employed are calculated as ratio of unemployed, employed, female employed and people in working age respectively. Figure 3.5 shows the maps of Italian municipalities ranked by unemployment rate and the rate of female employed.

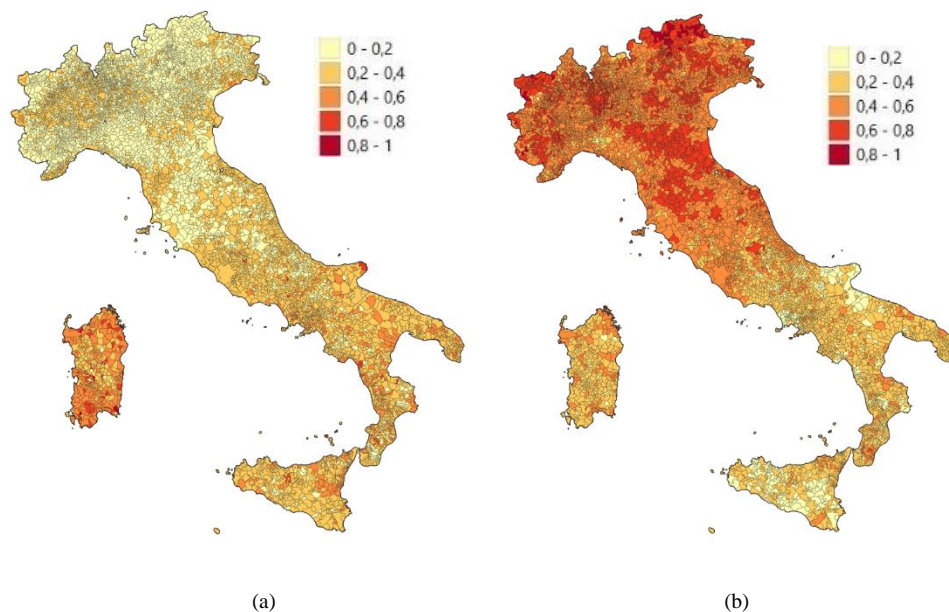


**Figure 3.5** – Unemployment rate (a) and female employed rate (b) for Italian municipalities.

Concerning family structure, in Frigerio et al. (2018) the number of family with more than 6 members is considered as variable. However, families with more than 6 members represent only the 0.05% of families in Italy, so it may be not relevant data for SoVI calculation. Also, ISTAT provides the value of the average annual income of family in Italy, classifying families based on their number of components as families with 1, 2, 3, 4, 5 or more components ([www.istat.it/it/dati-analisi-e-prodotti/banche-dati/statbase](http://www.istat.it/it/dati-analisi-e-prodotti/banche-dati/statbase)). Figure 3.6 shows that the income is not proportional to the number of components per family, but the larger the family the lower the income. Therefore, families with more than 5 components are considered as indicator for social vulnerability.

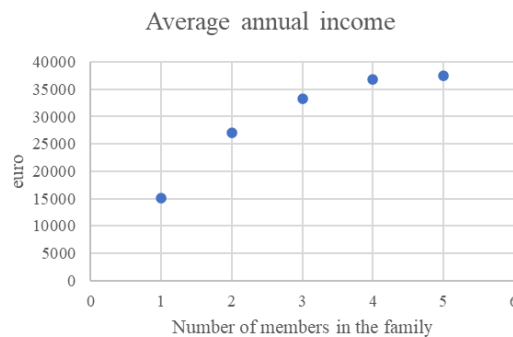


**Figure 3.6** – Average annual income (euro) per family based on the number of components of the family.  
Source: ISTAT.

As indicator of race/ethnicity, the percentage of foreign resident in the considered municipality is selected. The population density is calculated using a GIS software and relating the residential population with the surface area (km<sup>2</sup>) of the municipality. Together with the population density, also the crowding index is considered as variable for population growth indicator. This index usually indicates the number of co-residents per room. As such detailed information is not available, the number of co-residents per flat is considered, calculated as number of dwellings compared to residential population.

It is worth noting that Built-up area, variable included in the study of Frigerio et al. (2018), is not considered herein as it is an information not detectable only on census data but would require the covered area of buildings determined by building footprints. Furthermore, such variable could be considered representative of population density, factor already included in the SoVI calculation.

**Table 3-1** – Indicators and variables derived from ISTAT and their impact on social vulnerability.

Variables	Indicators	Impact on social vulnerability
Under 14 aged	Age	+
Over 65 aged		+
Aging index		+
Dependency ratio		+
Families with more than 6 components	Family structure	+
High educational index	Education	-
Low educational index		+
Buildings with very bad or bad state of preservation	Socio-economic status	+
Commuting rate		+
Unemployed	Employment	+
Employed		-
Female employed		-
Population density	Population growth	+
Crowding index		+
Foreign resident	Race/Ethnicity	+

Normalization process is required in order to make variables comparable and aggregable. In Frigerio et al. (2018) a spatiotemporal analysis of SoVI, evaluating its value across three periods is performed (1991, 2001 and 2011, corresponding to years of ISTAT census campaigns). Thus, the Mazziotta–Pareto index method (Mazziotta & Pareto, 2015) is adopted in normalizing variables, that accounts for their absolute change over time. This temporal evaluation is beyond the aim of this study. Therefore, the min-max transformation is adopted as normalization method. Each variable value is converted to a normalized value by subtracting the minimum value and dividing by the range of the indicator values, according to following equation:

$$NV_m = \frac{V_m - \min_m}{\max_m - \min_m} \quad (5)$$

Where  $V_m$  is the value of the variable for the municipality  $m$ ,  $\min_m$  and  $\max_m$  are the correspondent minimum and maximum values over all Italian municipality, respectively and  $NV_m$  the normalized value of the variable. In this way, each variable is expressed in a standard scale, where 0 indicates the lowest value within the whole sample and 1 the highest one.

Finally, SoVI value at municipal level is calculated using the follow mathematical expression:

$$SVI = \sum_i^n \pm NI_i \quad (6)$$

Where NI is the normalized value of the considered variable  $i$ , and the  $\pm$  symbol shows the direction of each NI. The latter is determined according to the influence of the variable  $i$  on social vulnerability: positive (+) direction is assigned to variables that increase vulnerability and negative (-) direction to variables that decrease it. Therefore, SoVI indicator assumes values less than 0 (for low social vulnerability) and greater than 1 (for high social vulnerability), as it is obtained as the sum of normalised variables, each one with either a positive (increasing) or negative (decreasing) effect on social vulnerability. Figure 3.7 shows the map of the social vulnerability, calculated at municipal level, for the Italian territory. It can be noted that the regions in the south of Italy together with Sardinia are the most affected by social vulnerability. In the north part of the country SoVI tends to be higher in small towns.

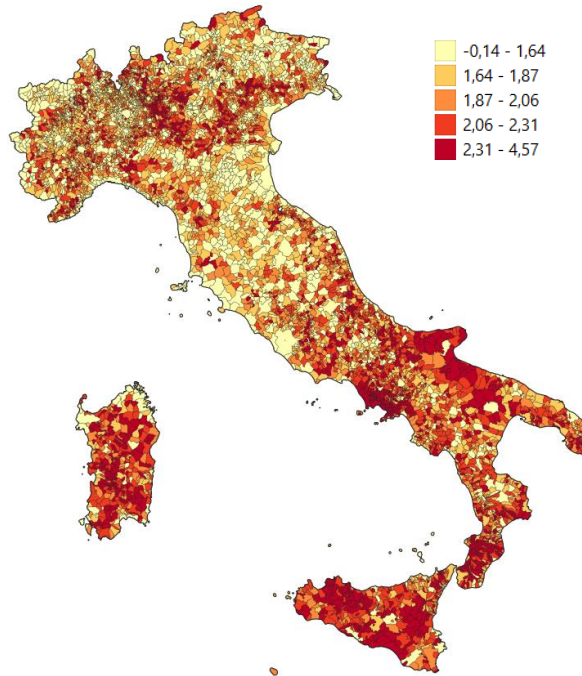


**Figure 3.7** – SoVI map for Italy.

### 3.3. Multi-risk index

In previous sections five individual indicators involved in the calculation of the multi risk index are presented: seismic hazard (s) and seismic physical vulnerability indicators (sv); flood hazard (f) and flood physical vulnerability indicators (fv); social vulnerability indicator (SoVI). Seismic and flood physical exposure are included in the vulnerability indicator and in the hazard one, respectively. The exposed population is considered as part of the risk index, as well. This indicator quantifies the residential population at the municipal level derived from the most recent census.

The selected indicators have to be normalized before aggregating them, in line with the procedure presented in Nardo et al. (2008). Normalization is performed through their empirical cumulative distribution functions (ECDFs). ECDF expresses the probability that a random variable  $X$  will take a value less than or equal to a given value  $x$ , i.e.,  $P(X \leq x)$ , based on sample observations. For example, considering hazard indicator,  $X$  is the value of PGA for the selected return period at the municipal centroid for all Italian municipalities. In this way, all indicators assume a value between 0 and 1. Figure 3.8 shows the ECDF for seismic and flood hazard, social vulnerability and exposure population.

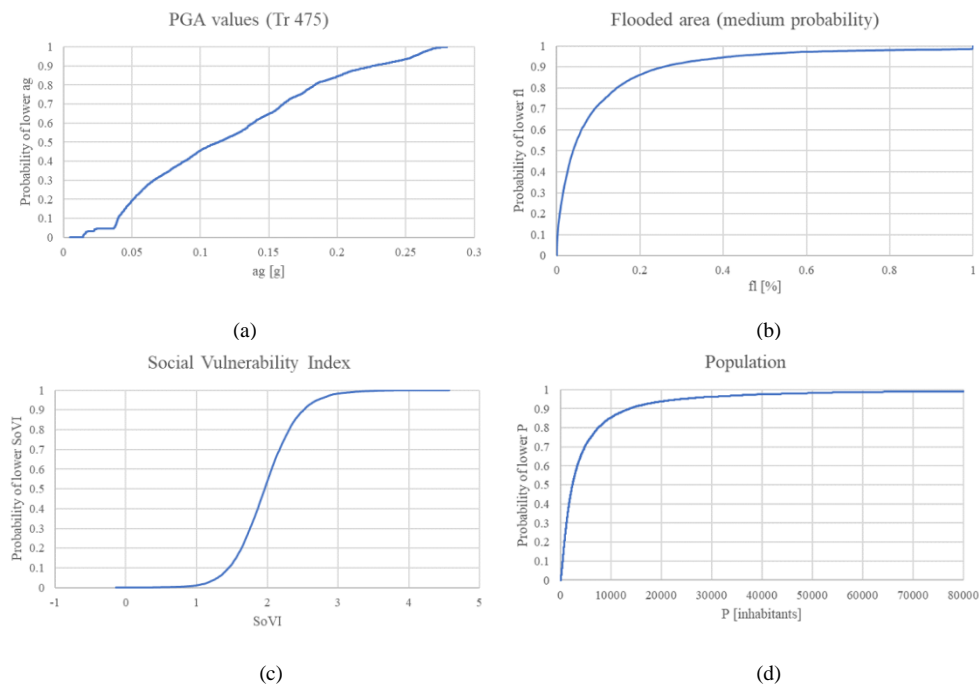


**Figure 3.8** – ECDF for seismic hazard (a), flood hazard (b), social vulnerability (c) and residential population (d) indicators.

The multi-risk index is finally obtained combining the normalized indicators according to the following equation:

$$RI = [F_h^s(h_j) \cdot F_{Pv}^s(v_j)]^{w_s} \cdot [F_h^f(h_j) \cdot F_{Pv}^f(v_j)]^{w_f} \cdot F_{sv}(sv_j)^{w_{sv}} \cdot F_p(p_j)^{w_p} \quad (7)$$

where  $F_h^s(h_j)$ ,  $F_{Pv}^s(v_j)$ ,  $F_h^f(h_j)$ ,  $F_{Pv}^f(v_j)$ ,  $F_{sv}(sv_j)$  and  $F_p(p_j)$  are the ECDF values of the seismic hazard, seismic physical vulnerability, flood hazard, flood physical vulnerability, social vulnerability and residential population indicators, respectively, evaluated at municipality  $j$ .  $w_s$ ,  $w_f$ ,  $w_{sv}$ , and  $w_p$  are the weights adopted for each indicator, representing the relative importance of individual indicators to relevant stakeholders.

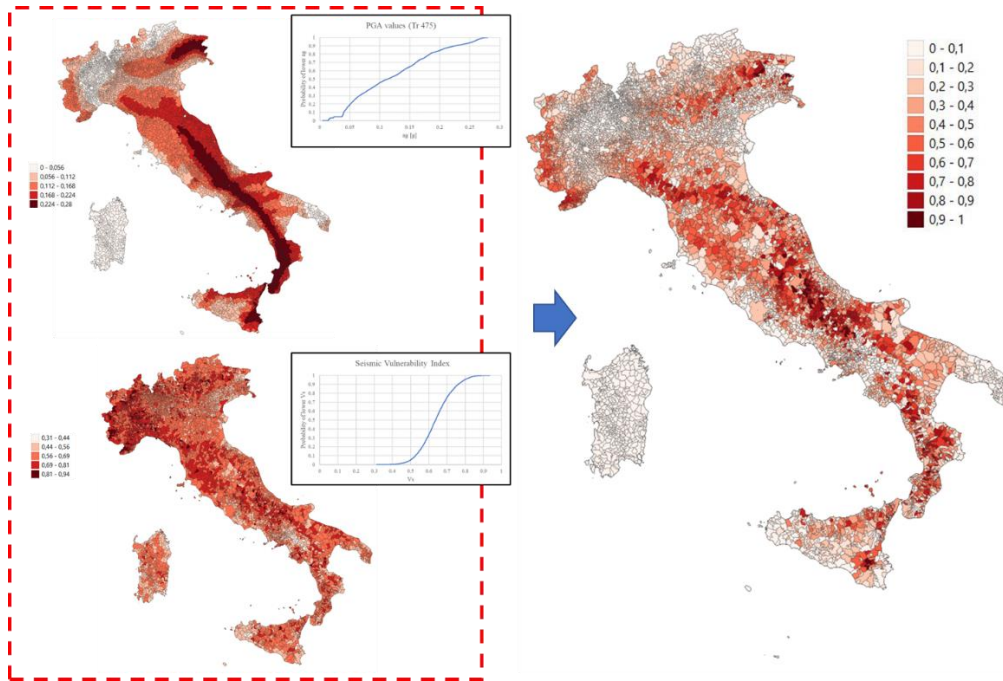


**Figure 3.9** – Seismic hazard and physical vulnerability combination to get seismic risk score map.

It is worth noting that hazard and physical vulnerability indicators, both for seismic and flood hazards, are first combined to get a unique indicator representative of the hazard related risk, i.e., the expected level of negative consequences due to specific hazard of a given intensity (e.g., figure 3.9 represents a risk score map). Next, the resulting risk score (still assuming value between 0 and 1) is weighted and aggregated with the other terms.

The weights can be defined using various techniques. For example, a weighting method that allows to involve stakeholders and decision-makers is the BAP (Budget Allocation Process), also described in section 3.1. This method



quantifies weights by providing users with a “budget” of  $N$  points to distribute over a number of individual indicators; the user “pays” more for those indicators whose importance they want to place more emphasis on. The weights take values between 0 and 1 and sum to 1. A first attempt of multi-risk index calculation is performed considering equal weights ( $w_s = w_f = w_{sv} = w_p = 0.25$ ). A sensitivity analysis assuming that one variable (e.g., social vulnerability) is weighted three times more than the other two (e.g.,  $w_{sv} = 0.5$ ,  $w_s = w_f = w_p = 0.166$ ) is also performed and described in the next section.

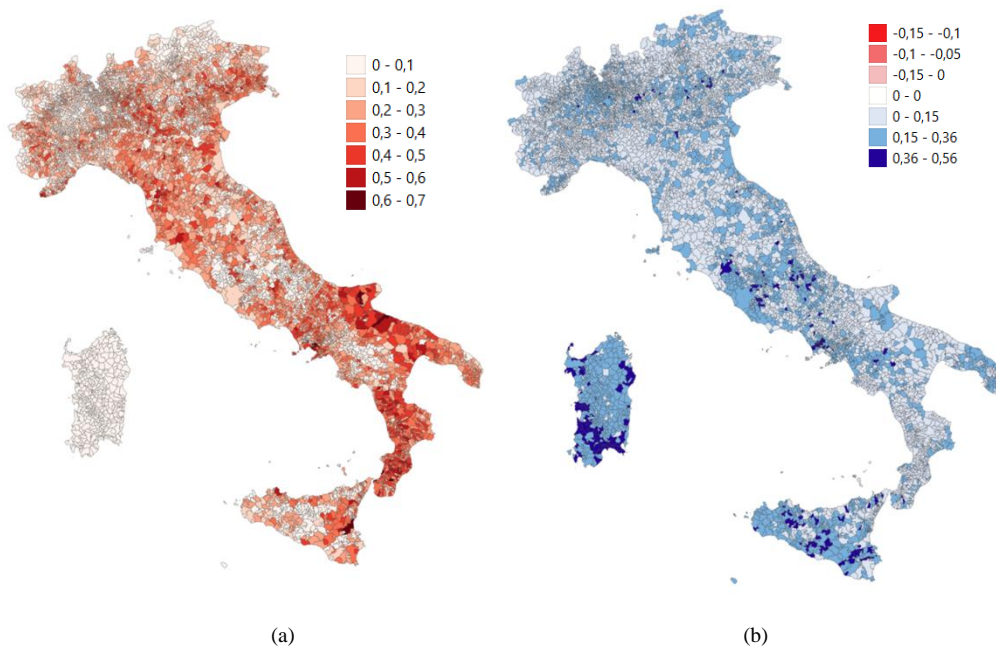


**Figure 3.10** – Multi-risk index map obtained using the geometric aggregation (a) and its comparison with the values obtained by linear aggregation (b). In the comparison map (b) red values indicate an increase in the multi-risk index got through the linear aggregation, while the blue ones a reduction in the index.

The aggregation is geometric, where, compared to a linear aggregation, a high value of the ECDF for one indicator does not compensate as much as for a low value of the ECDF for another type of indicator (Nardo et al., 2008). Figure 3.10 shows the risk scores for Italy adopting the geometric aggregation and the differences of index values estimated using the linear aggregation and the geometric one (i.e., the difference at municipal level between value of risk index obtained through linear aggregation and through geometric one). It can be noted that mostly in every municipality multi-risk index calculated through equation (7) is lower than the correspondent index calculated using a linear combination of the indicators (blue values in the figure 3.10b), except for those municipality where all indicators assume low and similar values (e.g., Valverde in Lombardy

region). This means that the geometric aggregation significantly de-empathize areas where only one hazard dominates. Therefore, it is more suitable for expressing multi hazard risk.

Table 3.2 gives an example of how a compensatory approach (i.e., linear aggregation) works. Using the linear aggregation, the absence of seismic hazard (ag) in some municipalities (i.e., all municipalities in Sardinia) is totally compensated by a high value of flood hazard, flood vulnerability or social vulnerability. This means that the risk index (RI) will be still high regardless of the seismic hazard component. Similarly, the absence of flood hazard (F) in the city of Francofonte, in Sicily region, is compensated with a high value of the seismic hazard and the social vulnerability. On the contrary, adopting the geometric aggregation, a null or very low value of a component requires a much higher value of the other components for compensating.

**Table 3-2** – Italian municipalities with highest differences between risk index (RI) obtained through linear aggregation and geometric aggregation. The residential population (Pop), the PGA value for a return period of 475 years (ag), the seismic physical vulnerability indicator (Sv), the percentage of flooded area (F), the flood vulnerability index and the SoVI index for each municipality are also reported.

Municipality	Region	Pop	ag [g]	Sv	F [%]	Fv	SoVI	RI linear	RI geom	Delta
Terralba	Sardinia	10328	0.00	0.61	0.59	0.29	1.35	0.63	0.06	0.56
Uta	Sardinia	7696	0.00	0.59	0.12	0.44	1.49	0.59	0.05	0.54
Cabras	Sardinia	8950	0.00	0.63	0.28	0.43	1.25	0.61	0.07	0.54
Monsezzato	Sardinia	20335	0.00	0.56	0.18	0.38	0.99	0.57	0.04	0.52
San Giovanni Suergiu	Sardinia	5983	0.00	0.60	0.13	0.47	1.46	0.57	0.05	0.52
Decimoputzu	Sardinia	4256	0.00	0.60	0.21	0.38	1.39	0.56	0.05	0.50
Sorso	Sardinia	14163	0.00	0.60	0.06	0.36	1.26	0.55	0.05	0.50
Francofonte	Sicily	12791	0.27	0.65	0.00	0.14	1.91	0.57	0.08	0.49
Serramanna	Sardinia	9128	0.00	0.63	0.13	0.20	1.32	0.55	0.06	0.49
Villasor	Sardinia	6767	0.00	0.59	0.18	0.28	1.16	0.54	0.05	0.49

### 3.4. Sensitivity analysis

One of the limitations of the proposed approach may be that the risk score is calculated with reference to a specific level of the hazard. Specifically, PGA values corresponding to 10% probability of exceedance in 50 years, or equally to a return period of 475 years, were used as seismic hazard inputs at municipal level, while the map with flooded areas characterizing an event with medium probability of occurrence (return period between 100 and 200 years) was used as flood hazard input. Therefore, further analysis considering also other hazard level

are performed, in order to evaluate how the choice of the hazard input can affect the results.

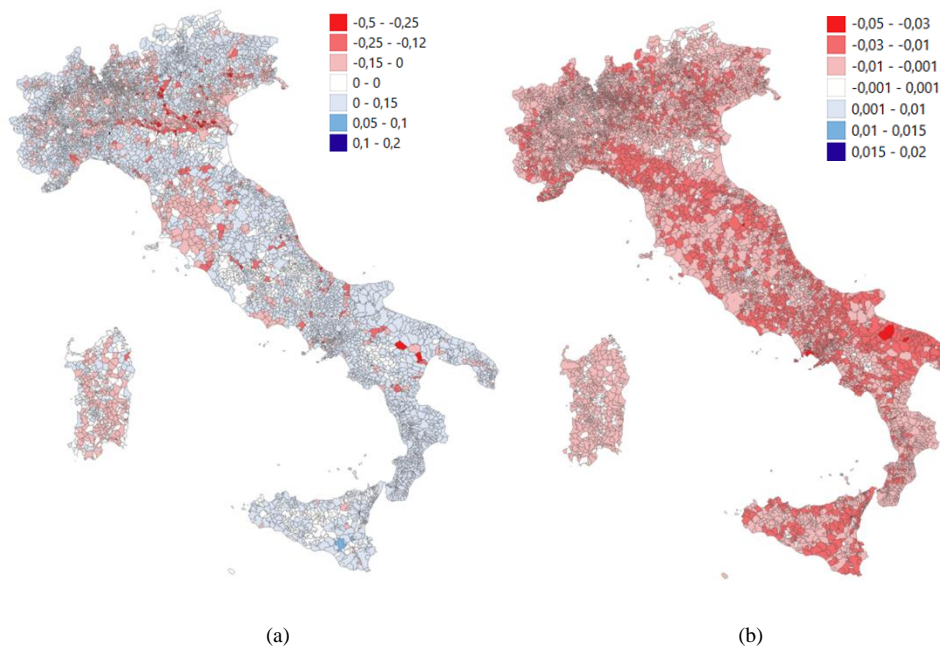


**Figure 3.11** – Comparison between multi-risk scores obtained adopting the medium probability with (a) the high probability flood map and (b) the low probability flood map. Red values indicate an increase in the score values due to the selection of a different map (high probability or low probability).

Figure 3.11 shows the differences in risk indices obtained using the medium probability flood hazard map, the high probability (return period between 20-50 years) and low probability (return period greater than 300 years) maps. The comparisons are carried out adopting the seismic hazard map for a return period of 475 years and equal weighting of the variables. It can be noted that using the low probability map (highest hazard) only for few municipalities the risk index value significantly increases, due to the notable increase of the inundated area at municipal level. Although this scenario would represent a more severe event, a reduction of the index in several municipalities can be observed as well. This variation can be explained by the ECDF changing. For example, in the town of Cagliari, in Sardinia, the inundated area represents the 40% of the municipal surface area according to the medium probability scenario, with a ECDF value equal to 0.94 (i.e., the 94% of the municipalities show a lower percentage of area inundated). Despite the inundated area increases considering the low probability scenario (49%), the probability got through the ECDF is 0.90, that means that such increment is less significant than the increment observed in other municipalities. Hence, the flood risk scores for medium probability scenario

results greater than the score for low probability scenario. Adopting high probability scenario (lowest hazard), almost constant increment of risk index is observed across all municipalities, between 0.01 and 0.05. This increment can be explained through ECDF values as well.

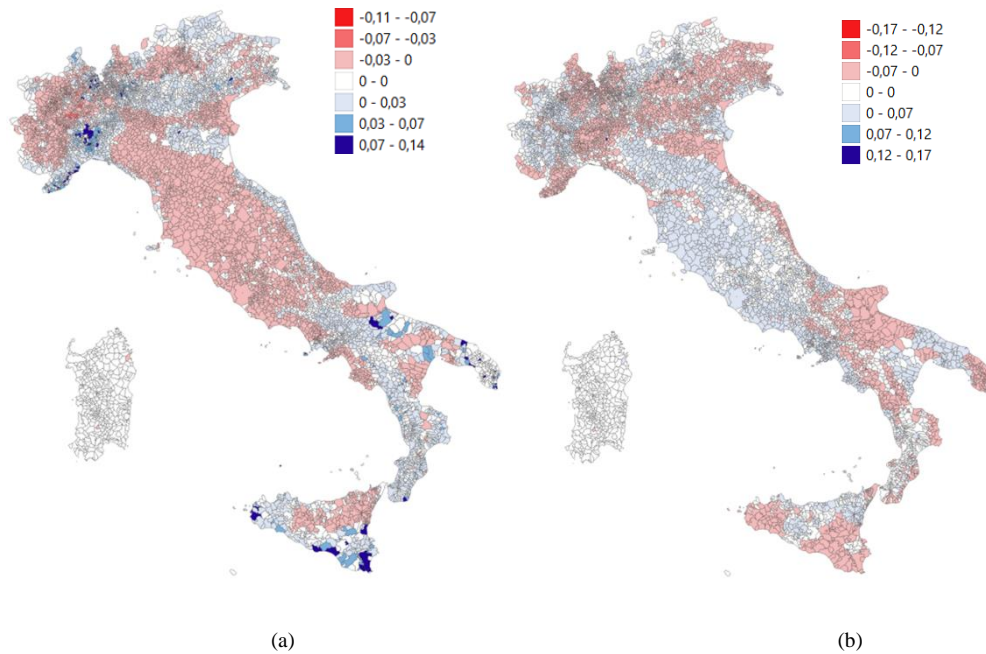


**Figure 3.12** -- Comparison between multi-risk scores obtained adopting seismic hazard map for 475 years return period and (a) 100 years return period map and (b) 2500 years return period map. Red values indicate an increase in the score values due to the selection of a different map.

Figure 3.12 shows the comparison of the index calculated using the seismic hazard map for a return period of 475 years and the index obtained using two different seismic scenarios: seismic input values corresponding to a probability of occurrence of 39% in 50 years (i.e., return period of 100 years) and of 2% in 50 years (i.e., return period of 2500 years). Flood hazard map used is the one representing medium probability floods. In both cases the variation of the index is between the -0.17 and +0.17, with a mean value over all municipalities equal to -0.03 using the 100 years return period map and to +0.05 for the 2500 years one. As observed for flood, also in this case the increase of hazard values may not lead to an increase of the final risk index, because the variables normalization allows to account for the relative changes of the hazard variables and not the absolute ones.

Sensitivity analysis changing the weights assigned to each indicator is performed as well. Three different scenarios are analysed. In each scenario is assumed that

one variable (i.e., seismic risk, flood risk, social vulnerability, population) is weighted three times more than the others (e.g.,  $w_{sv} = 0.5$ ,  $w_s = w_f = w_p = 0.166$ ). As not significant variations were observed changing the hazard inputs, in this analysis the medium probability flood hazard map and the seismic hazard map for 475 years return period are used.

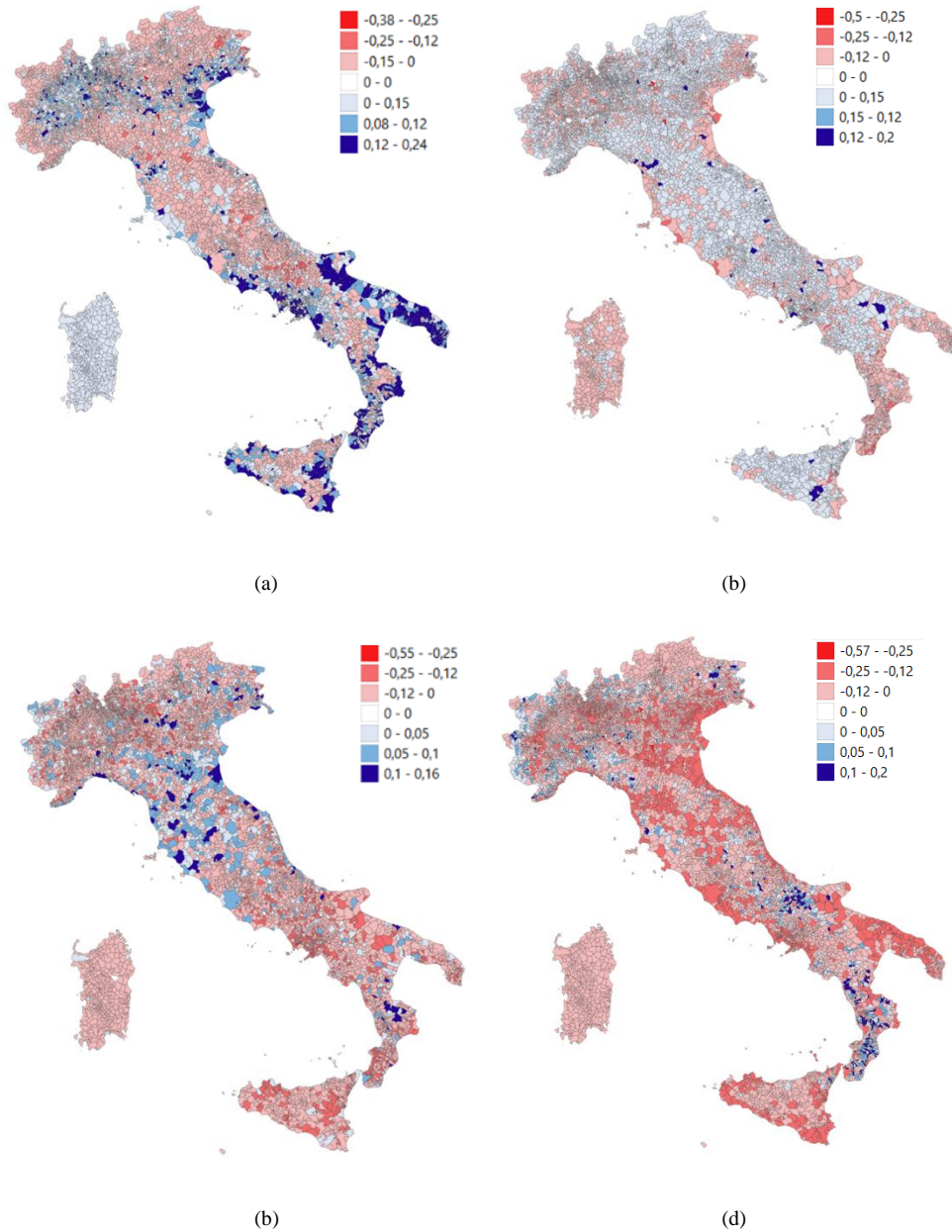


**Figure 3.13** - Variation of multi-risk index when seismic risk (a), flood risk (b), social vulnerability (c) or population factor (d) is weighted more than the others. Red values indicate an increase in the index value.

Figure 3.13 shows the variation in the risk index due to the different weights' combinations. Generally, a higher value of the index is obtained where the variable to which the greatest weight is assigned is predominant. For example, it

can be noted that if higher weight is assigned to seismic risk indicator, the increment of overall risk index basically follows the seismic hazard map trend (figure 3.1), varying accounting for the different physical vulnerability as well. If social vulnerability indicator is weighted more than others, greater values of the risk index can be observed mostly in the south of Italy and in small cities in the north part, consistently with map shown in figure 3.7. On the contrary, if the highest weight is assigned to population indicator, big cities (more densely populated) tend to get a higher overall risk score.



## Regional based exposure models to account for local building typologies

The development of building inventory at the territorial scale is a fundamental step in the framework of earthquake risk analysis. Indeed, the knowledge of the geographical distribution of building vulnerability classes, that is building inventory, is a pre-requisite to perform realistic risk estimations in a region of interest. For compiling building inventory, the key structural characteristics of exposed buildings are required. As shown before (section 3.2.1), when this information is not available throughout the territory, exposure model should define how to account vulnerability classes' distribution at urban, regional or national scale.

Census database is often the primary employed source, thanks to their easy availability and diffusion on whole national territory. However, information provided on buildings by Census are often limited to the construction age, building material and number of storeys (Crowley, et al., 2014). Thus, a tool to associate building typology inferred by ISTAT to vulnerability classes defined by the model is required. The exposure model establishes the class assignment rules for associating each building typology to one or more vulnerability classes. For instance, the exposure model proposed by Del Gaudio et al. (2019) for masonry buildings is the one used previously for the RI calculation (section 3.2.1). The model proposes an exposure matrix that reports the percentages of occurrence of each of the vulnerability classes identified within times intervals defined by Italian census (ISTAT, 2001). Such percentages were inferred on the data from the sample of 22,618 residential masonry buildings surveyed after L'Aquila earthquake. Other examples of exposure models can be found in Lucantoni et al. (2001), Di Pasquale et al. (2005), Bernardini et al. (2010) and Cacace et al. (2018). Acknowledging its usefulness to compile building

inventory, in the methodology adopted in the last NRA for Italy, the role of the exposure modelling is formally recognized as well (Dolce et al., 2021).

Generally, exposure models are calibrated on available survey data and/or expert judgment, analysing the correlation between the main vulnerability parameters for buildings and the census information. This approach has the advantage of allowing an implicitly validated association of typology to vulnerability classes. However, it has the drawback of being based on data from specific geographic areas, namely the ones that have been hit by damaging earthquakes, despite the buildings' characteristics can vary greatly for different areas of a country. For example, Del Gaudio et al. (2019) and in several other vulnerability models for unreinforced masonry buildings (Braga et al. 1982, Di Pasquale et al. 2005, Rota et al. 2008, Rosti et al. 2020), the type of vertical structure (e.g. regular, irregular, round stone, regular stone etc.) or of horizontal structure (flexible, rigid, semirigid and vaults) has a clear influence on seismic vulnerability. However, the distribution of building typologies in a country may vary significantly depending on the availability of construction material in the area, the evolution of construction techniques, the seismic history and the codes in force at the time of construction, also depending on the seismic classification. The type of available stones to be employed in the construction of masonry buildings is influenced by the geography of the territory, by the presence of quarries, waterways and volcanic areas. Construction techniques are closely related to the type of stone, as well: for example, tuff and travertine, commonly used in Italy, can be cut into square blocks, while limestone is used for irregular blocks. Similarly, the presence of cobblestones, that can be found in historical centre built near rivers, can determine the presence of irregular masonry structures. In Italy, limestone can be found mainly in the internal Apennine areas, tuff is typical of volcanic areas and bricks are typical of the Adriatic coast and many northern towns, due to the large presence of alluvial deposits (Salmoiraghi, 1982; Rodolico, 1965; Zuccaro, et al., 1999). Thus, for example, the city of L'Aquila, in Abruzzi region, in which limestone is widespread, is characterized by the presence of irregular masonry buildings; in Naples, Campania region, masonry buildings are mostly regular masonry, due to the large diffusion of tuff, but in Benevento, an inland city of the same region, cobblestones are widespread instead, due to the nearness



to rivers (Sabato and Calore), that lead the presence of irregular masonry buildings.

Acknowledging the variability of building typological distribution at the territorial scale, recently the Italian Civil Protection Department financed the “Territorial Themes” ReLUIS project, where a specific survey form “Cartis” was developed. The interview-based Cartis form (Zuccaro, et al., 2015) aims at the survey of ordinary building typologies in sub-areas of the town denominated Town Compartments TC, characterized by homogeneity of the building stock in terms of construction age and construction techniques and/or structural types. Thanks to the speediness of the form compilation for relatively large areas, the Cartis approach represents an alternative source towards the assemblage of large-scale inventories, allowing to rapidly collect information on relevant buildings features at urban level. Nowadays, more than 380 Italian municipalities were investigated with Cartis (<http://cartis.plinivs.it/>). The Italian regions with the highest completeness rate (number of surveyed municipalities versus the total number of municipalities in the region) are Tuscany (20%), Basilicata (16%) and Campania (13%). At the current state, the whole database covers about the 5% of national territory.

The study presented herein investigates the effects of an improved exposure modelling, adopting a building inventory based on Cartis data, on the vulnerability characterization at the territorial scale. Based on the Cartis survey available for several municipalities in three regions in Italy, an improved building inventory for such areas is built, allowing to take into account local typological features that are variable in different parts of the country. Such inventories can be used for updating the exposure/vulnerability models. The methodology is described herein using the vulnerability/exposure models for masonry buildings proposed by Del Gaudio et al. (2019), referred as to DG below. It will be shown that the variation in vulnerability can vary depending on the analysed region. Then, the effects of such region-specific exposure/vulnerability models on previous presented risk index are estimated.

The methodology adopted herein is also used in Polese et al. (2021) and Tocchi et al. (2022a), where the influence of a better knowledge level of the building

environment on detailed seismic risk assessment at regional scale is evaluated, showing that an improved characterization of regional vulnerability may strongly influence the impacts.

#### 4.1. A Cartis-based approach for exposure modelling

As briefly mentioned in section 3.2.1, the vulnerability classes for masonry buildings adopted in DG model are identified by the combination of bearing structure types (irregular layout structure with or without tie rods/beams – classes B and C, regular layout structure with or without tie rods/beams – classes D and E) and horizontal structure ones (vaults, flexible, semi-rigid or rigid slabs, classes 23, 4, 5 and 6 respectively). Therefore, each class is identified by alphanumeric code, e.g., Class 23BC represents irregular layout masonry buildings with/without tie roads/beams with vaults, and class 5D regular layout masonry buildings with tie rods/beams and semi-rigid slabs (table 4.1). For these building classes, lognormal fragility curves were developed based on the statistical treatment of typological and damage data of masonry buildings damaged after the 2009 L'Aquila earthquake. To allow building classification based on poor level data, the authors also proposed to build fragility curves directly referred to construction age intervals, the same as identified by census returns. To this end, based on the data derived from the sample of 22,618 residential masonry buildings surveyed after L'Aquila earthquake, the authors inferred the percentage of occurrence of each of the 14 classes within the 8 times intervals (< 1919, 1919-1945, 1946-1961, 1962-1971, 1972-1981, 1982-1991, 1991-2001, > 2001), defined by ISTAT (2001), as reported in table 4.1. Looking at the distribution of buildings belonging to different age ranges, it can be noted that the older buildings (<1919) are mainly poor quality masonry buildings with vaults (Class 23BC) or beams with flexible (4B or 4C) or semi-rigid slabs (5B or 5C). This percentage gradually decreases over the years in favour of good quality masonry buildings with rigid slabs (6D or 6E). The percentages of occurrence of table 4.1 were used to build age-dependent fragility curves, i.e. fragility defined for census-compatible age intervals. Such curves were derived as weighted averages of the 14 sets of typological fragility curves with the percentage of occurrence of each class, as reported in table 4.1.

**Table 4-1** - Occurrence percentages of vulnerability classes into 8 time intervals, defined by DG model.

	Vaults with or w/o tie rods		Beams with Flexible slab				Beams with Semi-rigid slab				Beams with Rigid slab			
	Irregular layout or poor quality	Regular layout or good quality	Irregular layout or poor quality	Regular layout or good quality	Irregular layout or poor quality	Regular layout or good quality	Irregular layout or poor quality	Regular layout or good quality	Irregular layout or poor quality	Regular layout or good quality	Irregular layout or poor quality	Regular layout or good quality	Irregular layout or poor quality	Regular layout or good quality
			W/o tie rods or tie beams	With tie rods or tie beams	W/o tie rods or tie beams	With tie rods or tie beams	W/o tie rods or tie beams	With tie rods or tie beams	W/o tie rods or tie beams	With tie rods or tie beams	W/o tie rods or tie beams	With tie rods or tie beams	W/o tie rods or tie beams	With tie rods or tie beams
	23BC	23DE	4B	4C	4D	4E	5B	5C	5D	5E	6B	6C	6D	6E
<19	22%	3%	25%	5%	2%	1%	21%	6%	4%	2%	3%	2%	1%	2%
19-45	8%	2%	23%	3%	4%	1%	23%	6%	9%	4%	4%	3%	3%	7%
46-61	2%	1%	9%	1%	4%	1%	17%	6%	13%	8%	5%	7%	7%	20%
62-71	1%	0%	3%	1%	6%	1%	4%	3%	9%	9%	3%	5%	12%	43%
72-81	0%	0%	2%	0%	4%	1%	2%	1%	6%	8%	1%	2%	11%	62%
82-91	0%	0%	2%	0%	6%	2%	2%	1%	5%	6%	2%	2%	11%	62%
92-2001	2%	1%	4%	1%	7%	4%	3%	2%	5%	5%	2%	2%	10%	53%
>2001	3%	0%	3%	1%	5%	5%	4%	3%	3%	9%	3%	2%	6%	52%

In this study, the information collected through the Cartis form are used to re-calibrate the exposure model in different Italian regions. The Cartis approach allows to detect many of the distinctive masonry buildings elements that have significant influence on seismic behaviour and are strongly incisive for vulnerability classification for buildings. For example, the type of masonry (e.g. irregular layout masonry or regular layout with square stones or bricks), horizontal slab type (e.g. flexible, rigid or semi-rigid slabs), type of vaults (if present) and the presence of tie rods or tie beams are some of the vulnerability factors considered. Figure 4.1 synthetizes some of the main steps for application of the methodology proposed for the calibration of the Cartis-based exposure model in combination with census data in large scale risk analysis. The first step (step 1) consists in the extrapolation of Cartis relevant data for each TC of a town and the compiling of building inventory at urban scale in terms of building typologies and/or vulnerability classes, according to classification of the selected vulnerability model. Next, as the percentage distribution of each building typology within a TC is also provided, given the total number of buildings in each TC, the number of buildings characterized by certain vulnerability features

(i.e., the type of vertical and horizontal structures, the age of construction and the number of storeys) can be estimated (step 2); thus, considering the vulnerability classes used in the adopted vulnerability model, the building inventory at municipal level can be obtained. Finally, considering all municipalities belonging to the same region and for which the Cartis was compiled, the analysis of statistical distribution of vulnerability classes into ISTAT building typologies allows the calibration of the Cartis-based exposure model (step 3). An example of procedure for compiling building inventory starting from Cartis database is reported in Tocchi et al. (2022).

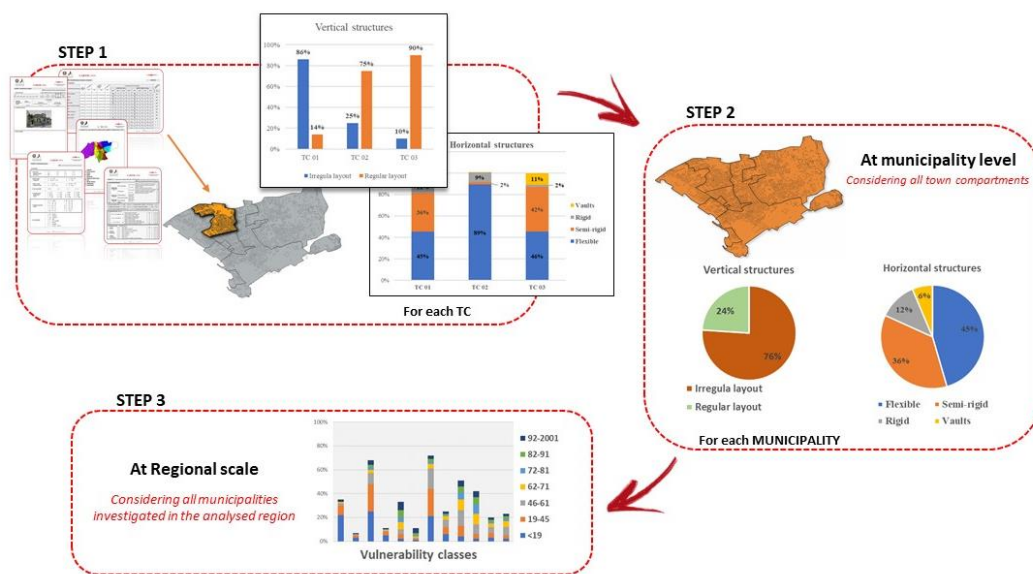


**Figure 4.1** – The main steps of the Cartis-based approach for regional exposure modelling.

## 4.2. Application for Italian regions

The procedure introduced above is applied to evaluate the Cartis-based inventory at municipality scale, for the towns where Cartis form is available. Starting from the inventory in these towns, new statistics concerning the occurrence percentage of building typologies at regional scale are derived and employed to re-calibrate regional based exposure models. The application is proposed for six Italian regions: Abruzzi, Campania, Emilia-Romagna, Tuscany, Veneto and Marche. The percentage of towns surveyed by Cartis varies regions by regions, from the 20% of municipalities surveyed in Tuscany and only the 6% in Veneto. For all the towns where Cartis information is available, the Cartis-based inventory is compiled, according to the procedure previously described. These inventories are used to derive the statistical distribution of building typologies at regional level.

Although the database does not cover the whole regional territory, the municipalities surveyed by Cartis are considered as representative of the entire region. This simplifying hypothesis that may lead to inaccurate estimations at the regional scale. However, the main scope of this study is to evaluate how much the vulnerability characterization at regional level may change using more refined database, being aware that the results should be updated as more data become available. Considering ISTAT 2001 age ranges, the occurrence percentages of the building typologies, derived based on Cartis data, into seven time-intervals (< 1919, 1919-1945, 1946-1961, 1962-1971, 1972-1981, 1982-1991, 1991-2001) are used to re-calibrate the DG exposure model.

The analysis of the regional inventories shows very different distribution of masonry building typologies. For instance, in Abruzzi region irregular layout structures are widespread, while in Campania only the 12% of masonry buildings have irregular layout vertical structure, mostly typical of the inland towns, and in Emilia-Romagna this typology is almost absent (figure 4.4). In Tuscany it can be noted that a large diffusion of irregular layout vertical structures, that representing about 76% of masonry buildings. In Veneto this typology (i.e., irregular layout) characterizes just the 16% of the total, and in Marche region only the 9%. The incidence percentages of the horizontal structures for the two types of vertical structure, regular and irregular layout, in each region are also analysed. Specifically, flexible and semi-rigid slab types are widespread in Tuscany and Abruzzi region, semi-rigid and rigid slab types in Campania and Marche while the Veneto and Emilia-Romagna rigid slabs are predominant. Vaults represent a significant percentage of slab types only in Abruzzo (20%) and Campania (13%). Considering Cartis inventories at regional scale, the statistical analysis of the data allows the derivation of an alternative exposure matrix, more suitable for grasping the specific vulnerability characterization of different regions of Italian territory. Table 4.2 shows the percentage distribution of typologies into relevant ISTAT age ranges for Tuscany region. The matrices with the percentage distribution derived for the other regions can be found in Polese et al. (2021) and Tocchi et al. (2022).

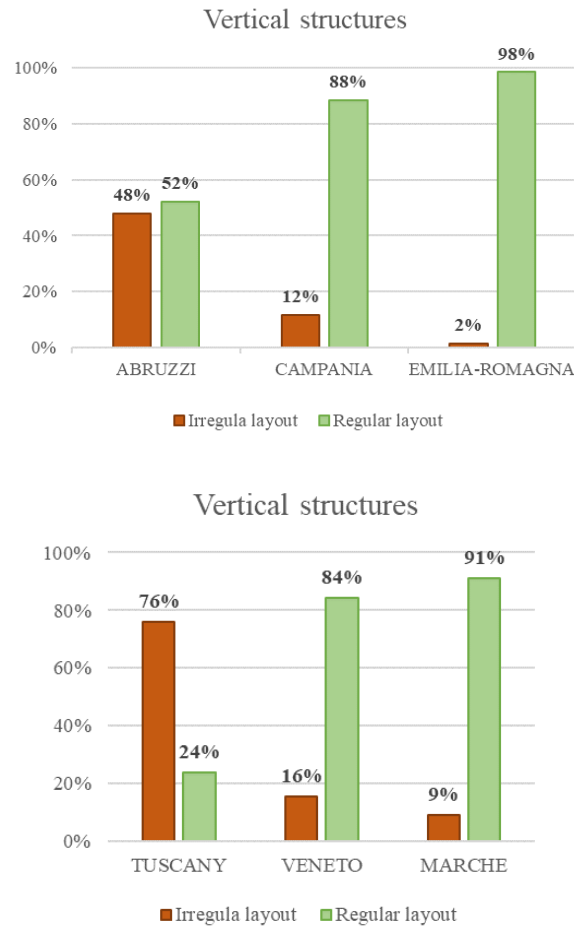


**Figure 4.2** – Diffusion of the vertical (irregular or regular layout) types on masonry building stock at regional scale, derived by Cartis-based inventory.

Figure 4.5 shows the occurrence percentages of the most ancient buildings (<1919) within the vulnerability classes of the DG model identified thanks to the Cartis data available for different Italian regions; the percentage evaluated with the original DG model is also shown for comparison. In Campania and Marche the regular structures are the most frequent ones (classes D and E); on the contrary, a high percentage of irregular layout masonry structures can be observed for Tuscany (classes 4B and 5B). It is worth noting that in Marche region older buildings (<1919) are mostly with regular layout and rigid floors (6D and 6E); the high concentration of this particular typology is probably due to the massive structural intervention carried out in this region after past earthquakes (Saretta, et al., 2021).

**Table 4-2** – DG exposure matrix derived by Cartis-based inventory, for Tuscany region.

	Vaults with or w/o tie rods		Beams with Flexible slab				Beams with Semi-rigid slab				Beams with Rigid slab			
	Irregular layout or poor quality	Regular layout or good quality	Irregular layout or poor quality	Regular layout or good quality	Irregular layout or poor quality	Regular layout or good quality	Irregular layout or poor quality	Regular layout or good quality	Irregular layout or poor quality	Regular layout or good quality	Irregular layout or poor quality	Regular layout or good quality	Irregular layout or poor quality	Regular layout or good quality
			W/o tie rods or tie beams	With tie rods or tie beams	W/o tie rods or tie beams	With tie rods or tie beams	W/o tie rods or tie beams	With tie rods or tie beams	W/o tie rods or tie beams	With tie rods or tie beams	W/o tie rods or tie beams	With tie rods or tie beams	W/o tie rods or tie beams	With tie rods or tie beams
	23BC	23DE	4B	4C	4D	4E	5B	5C	5D	5E	6B	6C	6D	6E
<19	8%	1%	43%	11%	5%	0%	23%	6%	0%	0%	1%	0%	1%	0%
19-45	3%	1%	21%	5%	7%	1%	41%	9%	1%	0%	7%	2%	3%	0%
46-61	0%	1%	12%	5%	8%	3%	31%	13%	7%	3%	7%	3%	5%	2%
62-71	0%	0%	1%	1%	1%	1%	1%	2%	1%	2%	12%	16%	22%	40%
72-81	0%	0%	1%	1%	1%	2%	1%	1%	1%	3%	10%	18%	16%	46%
82-91	0%	0%	0%	0%	1%	3%	0%	0%	1%	2%	12%	6%	14%	61%
92-2001	0%	0%	0%	0%	68%	1%	0%	0%	1%	0%	23%	0%	7%	0%
>2001	0%	0%	0%	0%	0%	0%	0%	0%	0%	0%	9%	0%	77%	15%

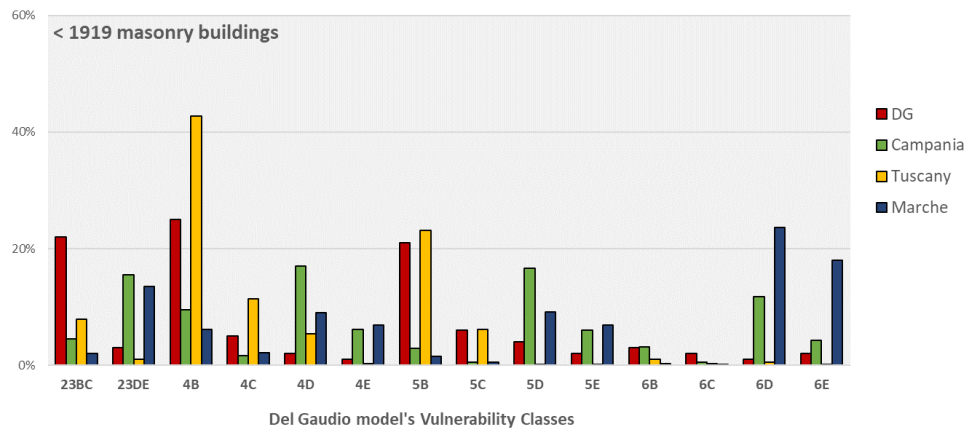


**Figure 4.3** – Occurrence percentages of masonry buildings built before 1919 in the vulnerability classes identified by DG model for different Italian regions.

### 4.3. Effects on Risk Index

The effects of the use of Cartis-based exposure model on the RI are estimated. This study is carried out for Tuscany region, one of the Italian municipalities most investigated by Cartis. To this aim, the exposure matrix obtained applying the procedure described before and reported in table 4.2 is used. It can be noted that the main differences with the original DG model (table 4.1) concern the strong presence of irregular masonry structures in Tuscany. In the first time interval (< 1919) the percentage of poor quality masonry structures without tie rods or tie beams and with flexible slabs (4B) are considerable higher in Tuscany than in Abruzzi (according to DG model), with a percental variation of +71%. In

the second time interval (1919-1945), irregular masonry structures without tie rods and semi-rigid slabs (5B) are more widespread than in DG model (+77%). Still, this type of structures represents a not negligible percentage of more recent built buildings (6B and 6C). The large diffusion of irregular structures also in last decades is probably because buildings built in such periods (although few) are mostly built in suburban or rural areas, as it can be observed for the municipality of Piazza al Serchio.

The matrix obtained through Cartis database is used to get the vulnerability indicator needed for the RI calculation. As described before (section 3.2.2), given the number of masonry buildings in each time interval, the number of buildings belonging to each of the 14 building classes is derived and the corresponding VI value is assigned as a function of the relative features (e.g., vertical and horizontal structure type, class of height). The final municipal-level indicator is obtained as a weighted average based on building class presence in the municipality. It is worth pointing out that, as the VI value assigned to each building class does not change, the only element updated in the calculation of the physical vulnerability indicator is the number of buildings that belong to each class. Figure 4.9 shows the comparison between vulnerability indicator at municipal level obtained using the original DG exposure model and the one calibrated using Cartis-based approach. It can be noted that almost in all municipalities the indicator value increase, with an increment between 0.1 and 0.2.

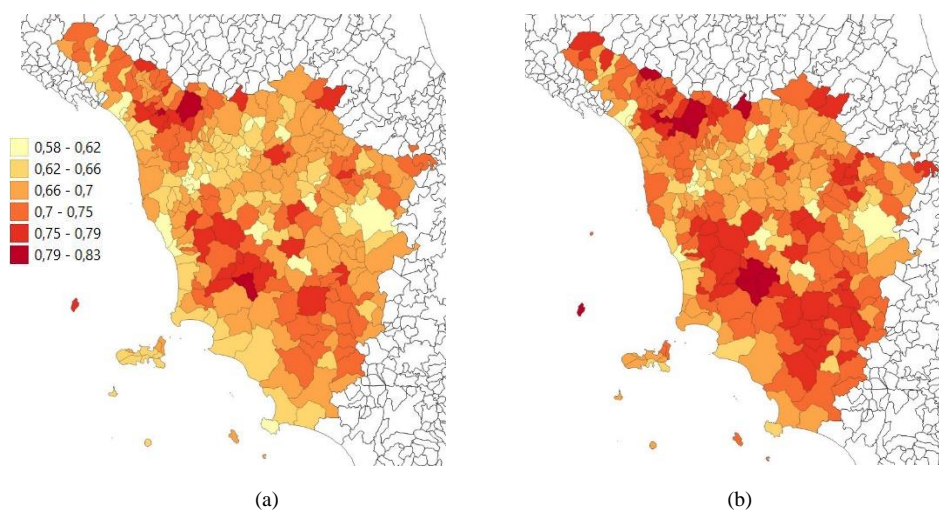


**Figure 4.4** – Seismic physical vulnerability indicator obtained using the original DG exposure model (a) and the one derived through the Cartis-based approach for exposure modelling (b).



The vulnerability indicator obtained is first normalized, through ECDF, and then aggregated with the other terms of equation (1), which remain unchanged. Figure 4.10 shows the variation of multi-risk index in Tuscany region when the Cartis-based approach is used to estimate seismic physical vulnerability. It also appears clear that such variation is even higher if seismic risk is weighted more than other indicators, with an increment between 0.07 and 0.2 in 12% of municipalities in the region. It is worth mentioning that, although this application demonstrated that the Cartis-based approach may be a useful tool for improving building inventory at regional scale, the RI maps shown in previous chapter are not updated using the procedure proposed herein. As a matter of fact, the calculation of RI has been performed for the whole Italian territory, but the exposure model calibrated on Cartis were built only in few regions, the ones most investigated by the form.

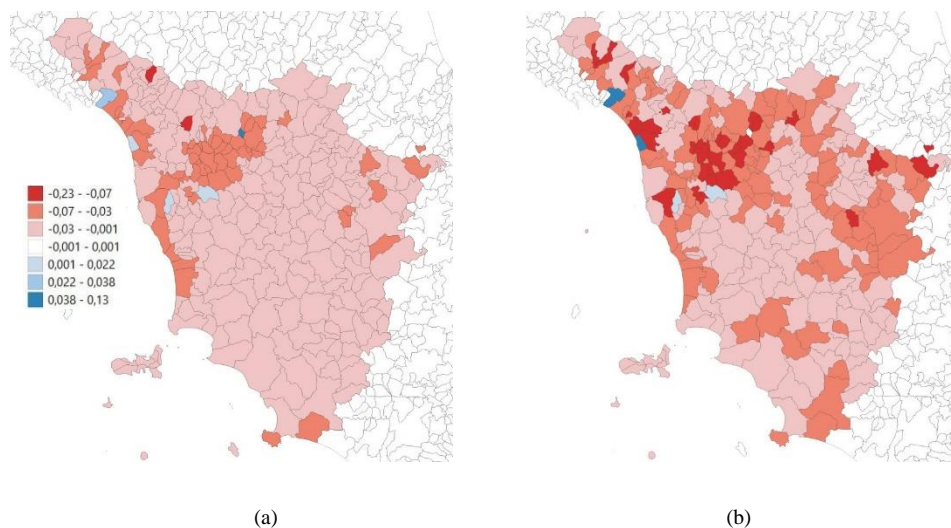


**Figure 4.5** – Variation of RI index for municipalities in Tuscany region due to the adoption of Cartis-based approach, in case of equal weighting of indicators (a) and in case of seismic risk is weighted three times more than the others (b).

## Quantifying multi-risk: an application in Italy

Index-based approach presented in Chapter 3 is a useful tool for prioritizing areas at risk. It allows to compare and aggregate multi-hazard, physical and social dimensions at municipal level and to rank all municipalities in Italy based on resulting risk scores. Although the application was proposed for Italian territory, the approach is suitable also for application in other countries. Despite all the above-mentioned advantages, this approach is a semi-quantitative tool for multi-risk estimation. Thus, once identified municipalities more exposed at multiple risks, a more detailed and quantitative analysis should be performed for supporting decision-makers in selecting suitable preparedness and mitigation actions for risk reduction.

A detailed multi-risk analysis considering both seismic and flood risk is presented in this chapter. Exploiting multi-risk index at municipal level obtained previously, the case study municipality for this application is selected. For the selection also the availability of Cartis information is taken into account. Available Cartis data for municipalities is assumed as filter in selection phase because further information provided by such database may allow a better estimation of seismic vulnerability and therefore of seismic risk (Polese et al., 2021; Tocchi et al., 2022). To account for socio-economic aspects as well, sub-municipal areas homogeneous in socio-economic conditions of residential population are chosen as unit of analysis. For each area of analysis, seismic and flood risk assessments are performed and SoVI is calculated as well. In this way, it is possible to evaluate expected losses (due to future earthquakes and floods) for specific social groups, e.g., low-income people or high socially vulnerable population.

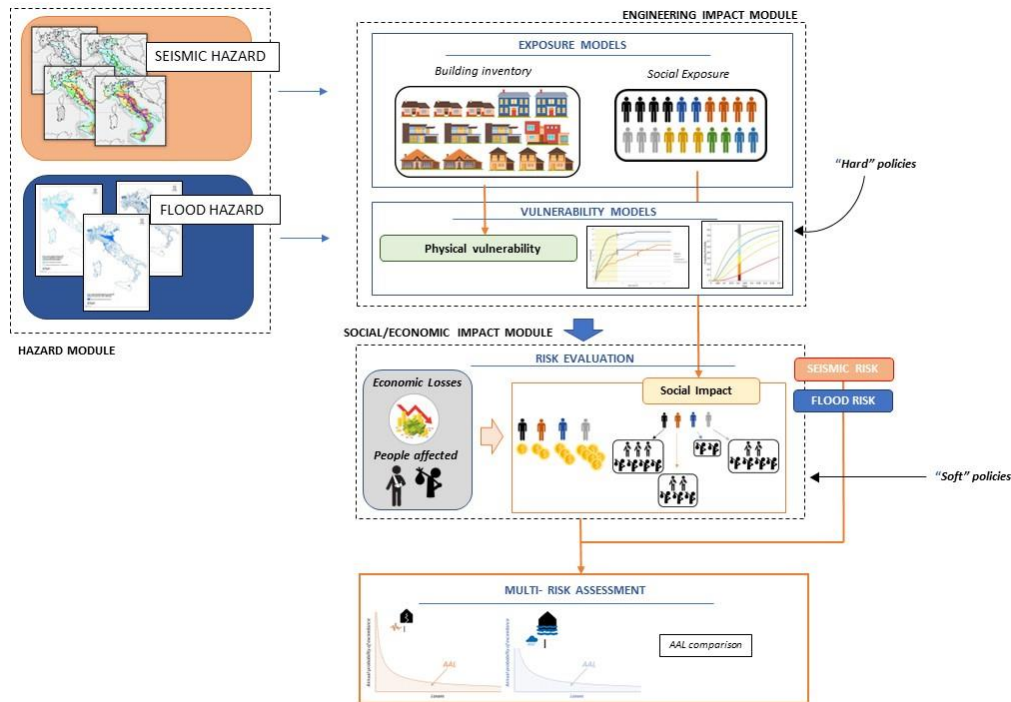


**Figure 5.1** – Framework for detailed multi-risk assessment.

Risk assessment associated with the implementation of some mitigation measures is also performed. More specifically, different scenarios for different sets of so-called hard and soft policies are defined. Hard policies are directly referred to physical aspects of building environment and they may include retrofitting actions or urban planning. Soft policies are represented by social safety nets and post-disaster financing or insurance. General scheme of the proposed procedure is shown in figure 5.1. In detailed risk assessment, it is possible to identify three different modules of analysis (Cremen, et al., 2022 ): the hazard module, involving the calculation of hazard inputs both for seismic and flood risk; engineering impact module, that consists in defining exposure and physical vulnerability modelling for buildings and population; social and economic impact module, through which the expected physical (i.e., damages), economic and social losses are estimated. The social and economic impact module also allows to get the distribution of expected losses across different social groups. The final step is the comparison and ranking of considered risks through risk curves. This process can be repeated adopting different input hypotheses to account for mitigation policies. Specifically, hard policies affect the engineering impact module, as they involve modifications of buildings behavior against hazards or modification of exposure through spatial planning;

soft policies mostly vary how such losses impact on population and different social groups, namely the social and economic impact module.

### 5.1. Case study selection

The application of the proposed index-based methodology allows to rank all Italian municipalities based on multi-risk score. The map with scores is shown in figure 3.10 of chapter 3. Table 5-1 reports the 10 municipalities with highest risk index, adopting equal weighting of indicators (i.e., seismic risk, flood risk, social vulnerability and population).

**Table 5-1** – List of the 10 of municipalities with highest risk index in Italy. The index is calculated in the hypothesis of equal weighting of indicators.

Position	Municipality	Italian Region	Risk Index
1	Barletta	Puglia	0.736
2	Canosa di Puglia	Puglia	0.732
3	Platì	Calabria	0.723
4	Lentini	Sicilia	0.708
5	Villa San Giovanni	Calabria	0.701
6	Palmi	Calabria	0.687
7	Catania	Sicilia	0.680
8	San Marco in Lamis	Puglia	0.651
9	Somma Vesuviana	Campania	0.646
10	Grotteria	Calabria	0.644

This list may vary changing the weighs used to combine individual indicators. Thus, for example, city of Barletta, the one with highest score using equal weights combination, still has the highest score in Italy if SoVI factor is weighted more than the other indicators, while become the 13<sup>th</sup> highest if seismic risk is weighted more the others. Similarly, Somma Vesuviana, move from the 9<sup>th</sup> position according to table 5-1, to 16<sup>th</sup> if flood risk assumes the highest weight and to the 7<sup>th</sup> if SoVI is assumed to be weighted more than the other indicators. Table 5-2 lists the municipalities included in the top 100 with highest risk scores for to at least 3 different weighting combinations, e.g., equal weights (1° combination), seismic risk weighted more than others (2° combination) and SoVI weighted more than others (3° combination).

**Table 5-2** – Municipalities included in the list of the first 100 Italian municipalities with highest score for three different weighting combination of indicators. Risk score refers to the case of equal weighting.

<b>Municipality</b>	<b>Italian Region</b>	<b>Risk score</b>
<b>Somma Vesuviana</b>	Campania	0.677
<b>San Marco in Lamis</b>	Puglia	0.676
<b>Trinitapoli</b>	Puglia	0.668
<b>Ercolano</b>	Campania	0.654
<b>Salgareda</b>	Veneto	0.645
<b>Cinquefrondi</b>	Calabria	0.645
<b>Polistena</b>	Calabria	0.645
<b>Vicopisano</b>	Toscana	0.643
<b>Sant'Anastasia</b>	Campania	0.635
<b>Ginosa</b>	Puglia	0.634
<b>Fossalta di Portogruaro</b>	Veneto	0.632
<b>Boscotrecase</b>	Campania	0.631
<b>San Giorgio Morgeto</b>	Calabria	0.629
<b>Morano Calabro</b>	Calabria	0.629
<b>Trani</b>	Puglia	0.624
<b>Torre Annunziata</b>	Campania	0.623
<b>Trecase</b>	Campania	0.621
<b>Palagonia</b>	Sicilia	0.618
<b>Paladina</b>	Lombardia	0.618
<b>Guardavalle</b>	Calabria	0.612
<b>San Paolo di Civitate</b>	Puglia	0.611
<b>Massafra</b>	Puglia	0.611
<b>Tiriolo</b>	Calabria	0.610
<b>Gussola</b>	Lombardia	0.610
<b>Verbicaro</b>	Calabria	0.609
<b>Montebello Jonico</b>	Calabria	0.608
<b>Luzzi</b>	Calabria	0.607
<b>Mileto</b>	Calabria	0.606
<b>Laureana di Borrello</b>	Calabria	0.604
<b>Calcinato</b>	Lombardia	0.604
<b>Bisceglie</b>	Puglia	0.602
<b>Orta Nova</b>	Puglia	0.602
<b>Tufino</b>	Campania	0.598
<b>Luco dei Marsi</b>	Abruzzo	0.595
<b>Carpino</b>	Puglia	0.593
<b>San Giorgio a Cremano</b>	Campania	0.593
<b>Ponte Buggianese</b>	Toscana	0.592
<b>Fossato di Vico</b>	Umbria	0.592
<b>Stilo</b>	Calabria	0.590
<b>Laino Borgo</b>	Calabria	0.586
<b>Rocca di Neto</b>	Calabria	0.584
<b>San Ferdinando di Puglia</b>	Puglia	0.583
<b>Anoia</b>	Calabria	0.576
<b>Firmo</b>	Calabria	0.571
<b>Candela</b>	Puglia	0.540

As mentioned before, in selecting case study for this application also availability of Cartis data is used as filter. In table 5-3 the list of the municipalities with highest scores (equal weighting of indicators) and for which Cartis form is compiled is reported. Although the equal weight combination was chosen to build

such list, it can be noted that Somma Vesuviana, Sant’Anastasia, Polistena and San Giorgio Morgeto are also in the list of the first 30 municipalities with highest score for different combination of indicators (table 5-2). Based on the results above described, Somma Vesuviana is selected as case study. Somma Vesuviana is a municipality in the province of Naples, in the south of Italy. It is located on the slope of the Vesuvius volcano (figure 5.2). Therefore, it is potentially exposed to volcanic risk as well, even if such risk is not considered herein.

**Table 5-3** – Municipality with highest risk score, assuming equal weights for indicators, included in Cartis database.

Municipality	Region	Risk score	Cartis	Inundated area	ag [g]	SoVI	Population
<b>Somma Vesuviana</b>	Campania	0.646	YES	0.1349	0.1730	1.5709	34502
<b>Serra San Bruno</b>	Calabria	0.626	YES	0.1374	0.2294	1.3040	6766
<b>Polistena</b>	Calabria	0.603	YES	0.1808	0.2662	1.3182	10597
<b>Sant’Anastasia</b>	Campania	0.592	YES	0.1003	0.1722	1.6281	27065
<b>Andria</b>	Puglia	0.580	YES	0.0284	0.1873	1.5848	99722
<b>Minervino Murge</b>	Puglia	0.571	YES	0.0284	0.1913	1.1474	9266
<b>San Giorgio Morgeto</b>	Calabria	0.568	YES	0.1426	0.2535	2.0875	3077

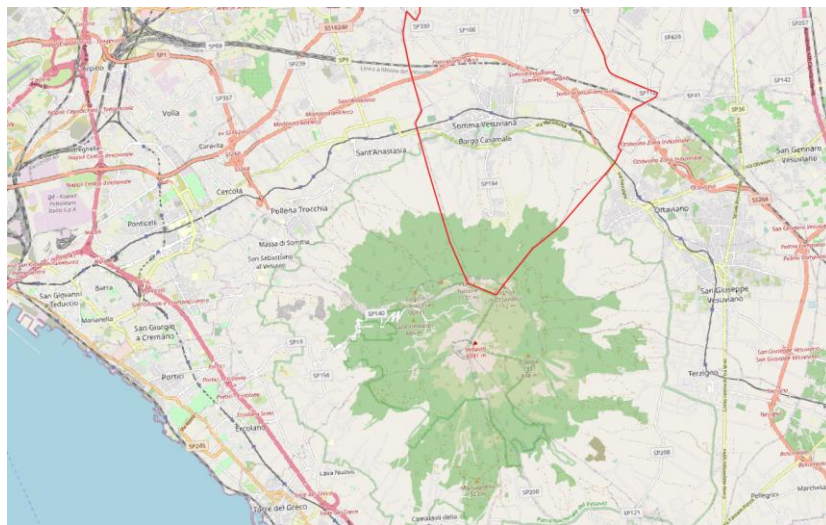


**Figure 5.2** – Municipality of Somma Vesuviana.

## 5.2. Multi Risk assessment

For multi-risk analysis, a multi-layer single risk assessment is performed herein. This approach consists in evaluating risks through independent analysis, ignoring any possible hazard and vulnerability interactions (see also chapter 2). However, to ensure the comparability of risks, it is necessary to standardize risk assessment procedures, harmonizing the type of analysis (deterministic or probabilistic), risk metric adopted as well as the territorial scale of analysis. Probabilistic time-based risk assessment is performed for both seismic and flood hazards. Thus, hazard

maps for the study area covering all possible intensities (i.e., available maps for all possible return periods) are used as hazard inputs for losses evaluation, that are performed separately for each hazard. Buildings and population are considered as asset at risk, and direct economic losses caused by buildings structural damage are selected as indicators of negative impacts. The risks (seismic and flood) are finally compared through risk curves (i.e., LEC), which points relate the value of expected losses of an event with its mean annual frequency of exceedance (i.e., the reverse of its return period). Hence, for building the LEC, first losses have to be calculated for different levels of hazard intensity (i.e., return periods), separately for each risk. Then, the EAL, representing the selected impact indicator, is calculated as area under the hazard-specific risk curve.

The municipal territory is divided into sub-areas representing broad socioeconomic statuses of the residential population. The real estate observatory (Osservatorio del Mercato Immobiliare – OMI – in Italian) identifies homogeneous municipal areas based on maximum/minimum market and lease real estate values, expressed in euro per surface unit (square meters), type of property and state of conservation. Those areas are selected as the unit of analysis for this application. Figure 5.3 shows the OMI zones for Somma Vesuviana and the corresponding market and lease real estate values are reported in table 5.4.

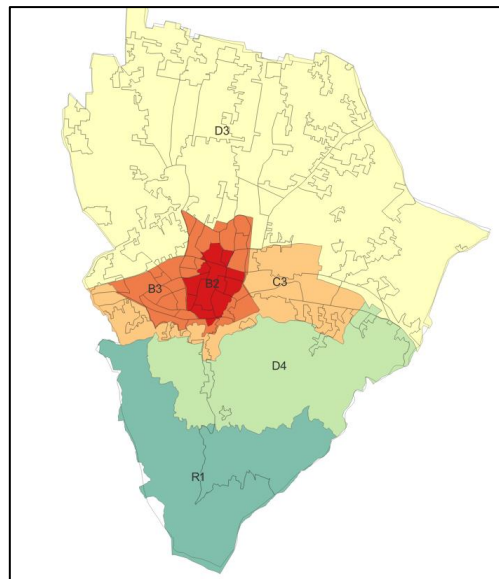


**Figure 5.3** – Delimitation of OMI zones in Somma Vesuviana. Each zone is identified by an alphanumeric code that categorises the zone as Central (B), Semi-central (C), Suburb (D) and rural (R).



**Table 5-4** – Real estate market value and lease value of residential buildings in each OMI zone. The values are referred to the municipality of Somma Vesuviana.

OMI zone - denomination	Market value (euro/mq)		Lease value (euro/mq per month)	
	min	max	min	max
B2 – Central (Historical centre)	1050	1600	3.2	4.9
B3 – Central (First belt of historical centre)	1050	1600	3.2	4.9
C3 – Semi central (RIONE TRIESTE - VIA POMINTELLA)	900	1350	2.8	4.2
D3 – North Suburban (STRADA STATALE DEL VESUVIO / SS. 268)	840	1300	2.6	4
D4 – Suburban, slope of mountain Somma (VIA S. MARIA DELLE GRAZIE)	760	1150	2.3	3.5
R1 – Suburban (mountain Somma)	-	-	-	-

For each OMI zone, SoVI is also calculated. As already mentioned, socio-economic and demographic data on population are provided by ISTAT at census tract level. ISTAT data are associate to OMI zones based on geographically belonging of census tract to each zone, determined through a GIS software. Thus, for example, residential population in an OMI zone is derived summing residential population in all census tracts belong to such zone. The most populous zone is the D3 with 14322 inhabitants, about the 42% of the total population of the municipality. Zone B3 includes the 28% of the population, zones B2 and C3 the 14% each while zone D4 is sparsely inhabited with only the 2% of the population. Indicators and variable used for SoVI calculation are the ones reported in table 3.1 of chapter 3. Figure 5.4 reports the SoVI values obtained. It can be noted that for all zones the index assumes values greater than 0, underling a high social vulnerability for the considered municipality. D3 zone shows the highest value (5.61), while D4 the lower (2.26). In both zones, the high number of people under 14 in the area against the low number of people over 65 leads to very small values both for the aging index and the dependency ratio. However, in D3 zones the high percentage of families with more than 5 components, the high value of the low educational index as well as the low value of high educational index, contribute to increase the SoVI value. On the contrary, the moderate value of the low educational index, the low population density as well as the very low percentage of foreigner inhabitants in D4 area lead to a small SoVI. It is also worth mentioning that such area (D4) includes only the 2% of the residential population and all variables that determine low SoVI value may be affected by demographic size.



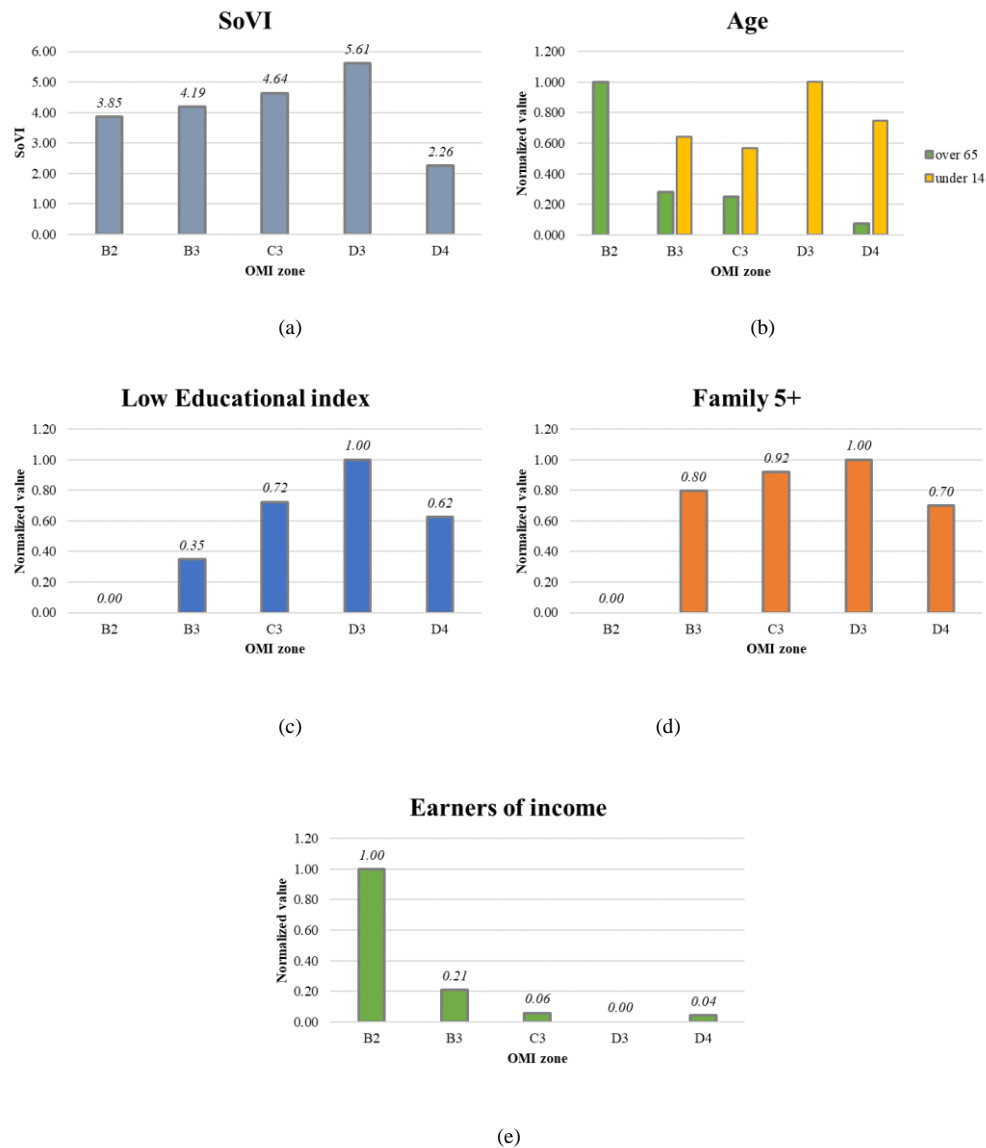


**Figure 5.4** – SoVI values (a) and normalized sub-indicator for population age (b), low educational index (c), number of families with more than 5 components (d) and earners of income (e) for each OMI zone.

In figure 5.4 standardized value of earners of income is also reported. Although this variable is not included in SoVI calculation, it may be representative of the economic status and the income level of inhabitants within each zone. The highest percentage of people earner of income is observed in B2 zone and B3 zones, that are also the areas with the highest real estate market and lease value.

### 5.2.1. Seismic risk

At OMI zones, selected as unit of analysis, are associated only information related to market and lease values of residential buildings. Thus, census data are integrated with Cartis information for compiling building inventory for seismic

risk assessment. The latest census (ISTAT, 2011) only provides information on the number of masonry buildings, RC buildings and buildings classified as other construction material (e.g., steel) at census tract (CT) level. Disaggregated information of buildings features (i.e., age of construction, number of storeys) are not available at such scale. Thus, they can be detected from Cartis database. According to Cartis form, eight different Town Compartments (TC) are identified in Somma Vesuviana (figure 5.5).

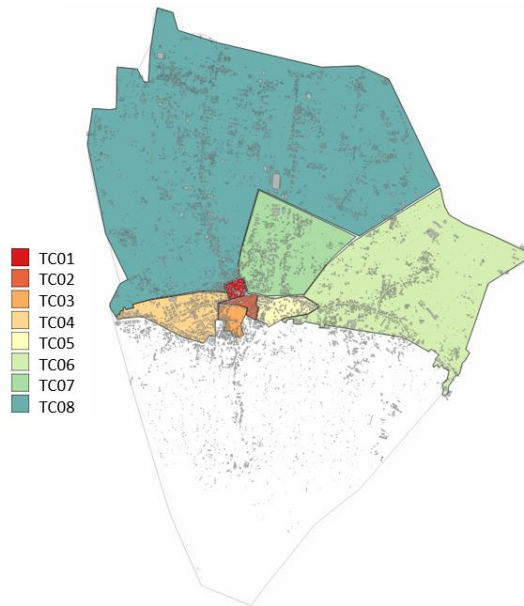


**Figure 5.5** – Town compartments identified in Somma Vesuviana by Cartis form.

The first three TCs (TC01, TC02, TC03) include the historical center of the town, where masonry buildings with flexible slabs and oldest RC buildings are widespread. TC04 and TC05 represents semi central and first expansion areas, while TC06 and TC07 more recent expansion areas and TC08 suburban area.

The procedure adopted for compiling building inventory integrating census with Cartis data is shown in figure 5.6. First, percentages occurrence of prevailing building typologies (e.g., masonry structures without tie rods and flexible slabs) derived through Cartis are used to build inventory at CT level. Specifically, Cartis buildings' features are assigned to all buildings included in a CT based on the TC which it belongs to. For example, according to Cartis database, in TC07 masonry buildings are mostly built between 1946 and 1971, they are 1 or 2 storeys high, have regular layout vertical structure, tie rods (100%) and flexible slabs (100%). RC buildings in the same TC are predominantly built between 1972 and 1991

and are 3 or 4 storeys high. Census tract n°39 contains 24 masonry buildings and 108 RC ones. As the latter belongs to TC07 (figure 5.7), corresponding Cartis features are associated, i.e., the 22 masonry buildings are supposed to be with regular layout, tie rods and flexible slabs, half with 1 storey (11 buildings) and half with 2 storeys (11 buildings), of which 6 built between 1946-1961 and 6 between 1962-1971 (according to ISTAT period of construction ranges) for each height class (1 or 2 storeys). Similarly, 54 RC buildings are supposed built between 1972 and 1981 and the other 54 between 1982 and 1991, of which 50% with 3 storeys and 50% with 4 storeys (i.e., 27 buildings in every age class). Buildings of other construction materials represent only a negligible percentage of residential buildings, so they are not included in the analysis.

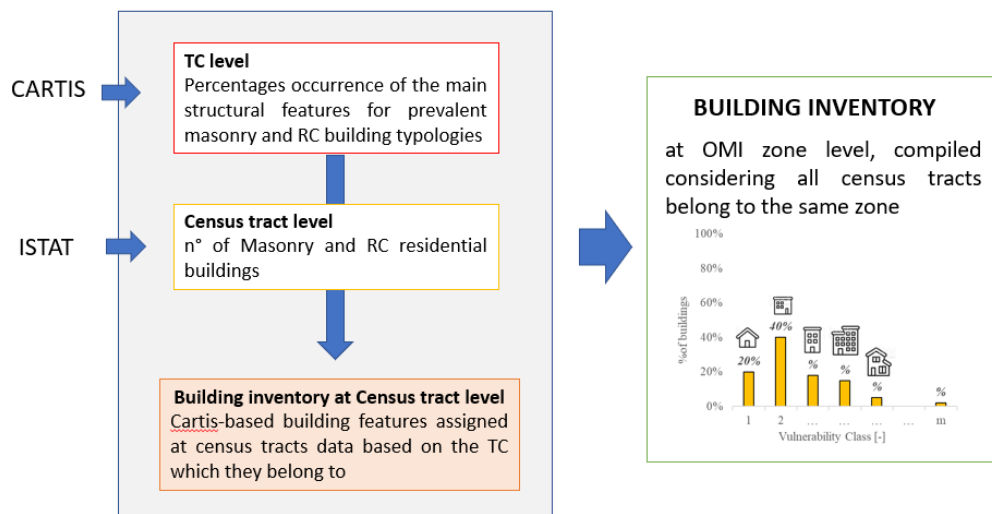


**Figure 5.6** – Procedure for compiling building inventory at OMI level integrating census and Cartis data.

If a CT is divided by two different TCs, fraction of area belongs to each TC is considered representative of the percentage of buildings belong to one or the other TC, as already proposed in Polese et al. (2019). Finally, building inventory at OMI level is compiled grouping all CTs that geographically belong to the same zone.

From figure 5.5 it can be noted that not all built areas are included in Cartis form. As a matter of fact, lack of information for a part of the municipality may be due to the lack of knowledge of the interviewed technicians on the area or the assumption that such area is not expected to be for residential use. However, residential population in this area amounts to 8373 inhabitants, the 24% of the

entire population of the municipality, and residential buildings to 1426 (the 23% of the total). For this reason, also the municipal area missing Cartis data is considered in this study.

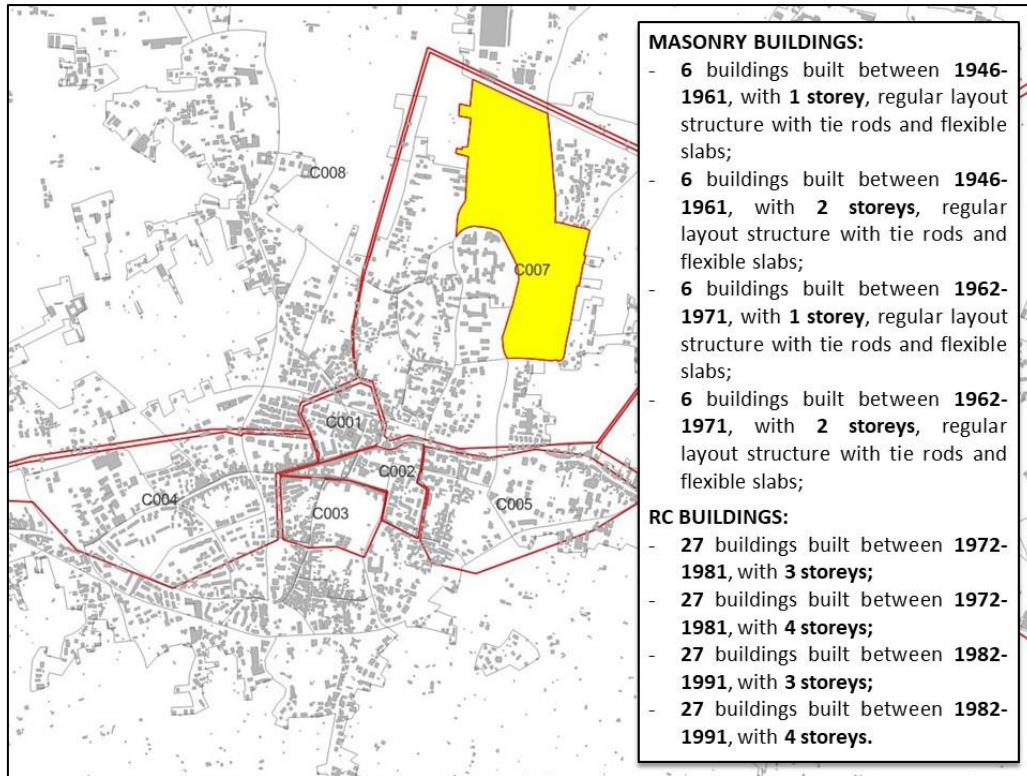


**Figure 5.7** – Example of building inventory at census tract (CT) level.

In order to compile building inventory for this area, Cartis information are assigned on CTs based on the prevailing age of construction of their buildings and the associated population density. In Tocchi et al. (2022b), a study aimed to find a trend between available census data at CT level and the TCs identified withing Cartis form is presented. Exploits available Cartis data, a machine-learning based approach that correlates CTs' features to the TC of belonging is proposed. For example, it was found that CTs with high population density have high probability to belong to the historical center of the town, while lower the population density of the CT, greater the percentage of oldest buildings (built before 1945) required so that such CT belongs to the center. The procedure adopted herein is based on the outcomes of this study and can be described through the following steps: first, trends in terms of population density and period of construction of buildings in each not-assigned CT are identified; then, they are grouped in the TC that shows similar trends in terms of population density and prevailing period of construction of its buildings. Finally, building inventory at

CT level is compiled assuming that building features are the same of the TC which it is associated to. For instance, CTs with a percentage of buildings built before 1945 greater than 51% are associated with TC03; if this percentage is lower than 51% but greater than 27%, the CT is associated to TC05; else if such percentage is lower than 27% but the percentage of buildings built before 1980 is very high (more than 80%), the CT is associated with TC04. For TC06, TC07 and TC08 this association is based on population density values. Figure 5.8 shows the CTs not included in Cartis and the TC associated according to the above mentioned procedure. Once building inventory at CT level is built, the inventory for OMI zones is compiled considering all CTs belonging to the same zone with the aid of a GIS software (figure 5.8).

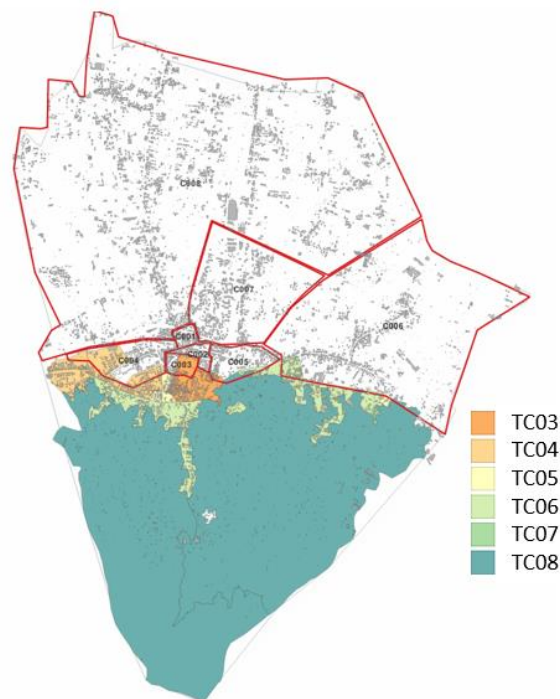


**Figure 5.8** – Assignment of census tracts not included in original Cartis form.

Building inventory provides the spatial distribution of buildings in the vulnerability classes identified by the vulnerability model. The Risk-UE model was leveraged as part of the multi risk index calculation. This model proposes Damage Probability Matrices for each vulnerability class and adopts macroseismic intensity as the ground-shaking intensity measure. As hazard maps are expressed in terms of PGA and for a more refined quantification of expected damages and losses, for this application the vulnerability models proposed by

Rosti et al. (2021a) and Rosti et al. (2021b) for masonry and RC buildings, respectively. Moreover, these models are also officially adopted for the NRA in Italy (Dolce et al., 2021).

In Rosti et al. (2021a) empirical based fragility curves for masonry buildings were derived from post-earthquake data relative to 1980 Irpinia and the 2009 L'Aquila events. Eight building typologies representative of the Italian built environment were identified, according to the typological classification proposed by Rota et al. (2008). The attribute considered for the classification are quality of the masonry fabric (i.e., irregular layout or poor-quality masonry, regular layout and good-quality masonry), in-plane flexibility of diaphragms (i.e. flexible, rigid), presence (or absence) of connecting devices, such as tie-rods and tie-beams. These buildings typologies were merged into three vulnerability classes of decreasing vulnerability (i.e. A: high vulnerability, B: medium vulnerability, C1: low vulnerability), based on the similarity of the observed seismic fragility, using a hierarchical agglomerative clustering technique. Table 5.5 reports the classification rules proposed by Rota et al. (2008) to assign the vulnerability classes based on combination of vertical (poor or good quality masonry) and horizontal structures (rigid or flexible) and presence of connection device. These vulnerability classes are further specified based on the building height, Low L: 1–2 storeys and Medium High MH: > 2 storeys. Six vulnerability classes are finally defined (A-L, A-MH, B-L, B-MH, C1-L, C1-MH) to which a specific set of fragility curves for the 5 damage grades of the EMS-98 scale is assigned.

**Table 5-5** - Definition of vulnerability classes based on type of vertical and horizontal structures and presence of connection devices, according to Rota et al. 2008.

Horizontal structure	Irregular texture or poor quality masonry		Regular texture and good quality masonry	
	w/o connecting device	with connecting device	w/o connecting device	with connecting device
Flexible	A	A	B	C1
Semi-rigid	A	A	B	C1
Rigid	A	B	C1	C1
Vaults	A	B	C1	C1

The same post-earthquake databases were used in Rosti et al. (2021b) for deriving fragility curves for RC buildings. As for masonry buildings, the five damage grades of the EMS-98 scale are adopted for developing fragility curves. Two vulnerability classes of decreasing vulnerability (i.e., C2 and D) were defined

considering the main seismic codes issued in Italy. Thus, vulnerability class C2 includes RC buildings built before 1981, designed for both gravity and seismic loads, while D2 class refers to RC constructions with seismic design post-1981. Vulnerability classification is further specified based on the building height, distinguishing between low (L), medium (M) and high (H) buildings, corresponding respectively to 1-2 storeys, 3-4 storeys, more than 4 storeys building (C2 -L, C2-MH, D-L, D-MH). Figure 5.9 shows building inventory obtained by the described procedure at OMI zone level. As may be noted, the highest percentage of most vulnerable buildings (class B) is associate with D3 zone, which highest SoVI is associated as well.

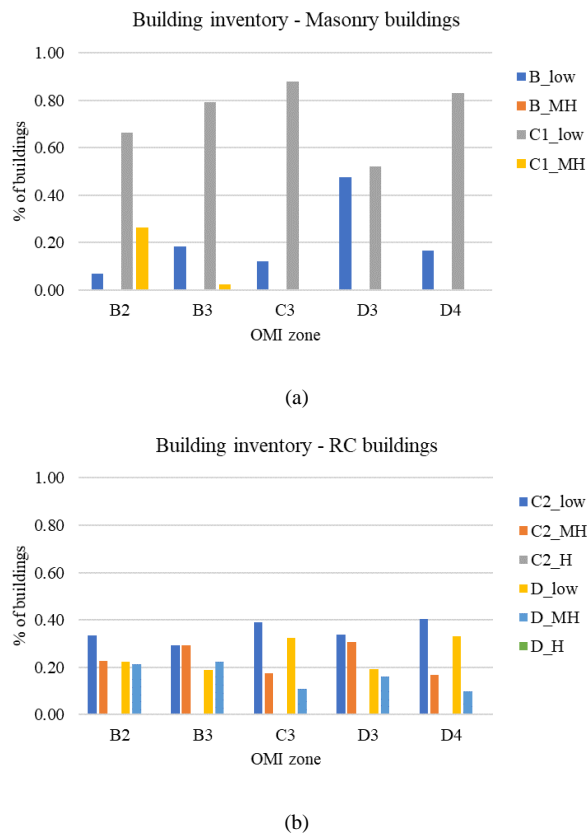


**Figure 5.9** – Building inventory for masonry (a) and RC buildings (b) according to Rosti et al.(2021a) and Rosti et al.(2021b) models.

At census tract level also disaggregated information about buildings' living area and residential population, required for losses estimation, are missing. Thus, the values of living surface per building and residential population per building are derived from statistics available at municipal level.

As hazard input, INGV hazard maps providing PGA values for nine different return periods (2500, 1000, 475, 200, 140, 100, 72, 50 and 30 years) or

probabilities of exceedance in 50 years (2%, 5%, 10%, 22%, 30%, 39%, 50%, 63% and 81%) are used. Seismic action is provided for each point of a 5x5 km mesh covering all the Italian territory. This grid is not so tight to allow the definition of a ground shaking measure at OMI zone level, set as unit of analysis. Hence, PGA value at municipal centroid (obtained as weighted average on distance of the closer grid points, as reported in section 3.2.1) is assumed as input of risk analysis for all zones. On the contrary, some micro zonation studies are available in Italy and are used here to refine seismic input for accounting soil effects. An amplification map containing  $V_{s30}$  values with a spatial resolution of  $50 \times 50$  m is proposed in Mori et al. (2020) and adopted herein. Criteria for soil category identification adopted are the ones reported in the new Italian building code (NTC18). Five soil categories are identified (A, B, C, D, E), based on topographic characterization and corresponding  $V_{s30}$  values and for each category soil amplification factors of the spectral acceleration are defined. For each area of analysis (i.e., OMI zone) the percentage occurrence of soil types can be obtained as weighted average of all grid points ( $V_{s30}$  map) included in the area. Then, the soil factor to apply can be defined as weighted average of soil type factors based on the percentage of soil types in the area. In figure 5.10 is shown the map with  $V_{s30}$  values for Somma Vesuviana. Based on this map, the soil type B represents the entire municipality. Thus, the soil factors corresponding to such type is applied to amplify the hazard input (PGA) in each zone.

In figure 5.10 the slope map is also shown. The latter is used to define topographic amplification factors. The code (NTC18) defines four topographic categories based on the slope (expressed in degrees). A specific topographic amplification factor should be applied if the slope exceeds the  $15^\circ$ . It can be noted that only in few areas of the town the slope is greater than  $15^\circ$ . In such areas amplification factors are considered in the definition of hazard input. Specifically, amplification values to adopt are obtained considering the weighted average of all points that have a given slope and the associated factors, as also describe before for soil factors.



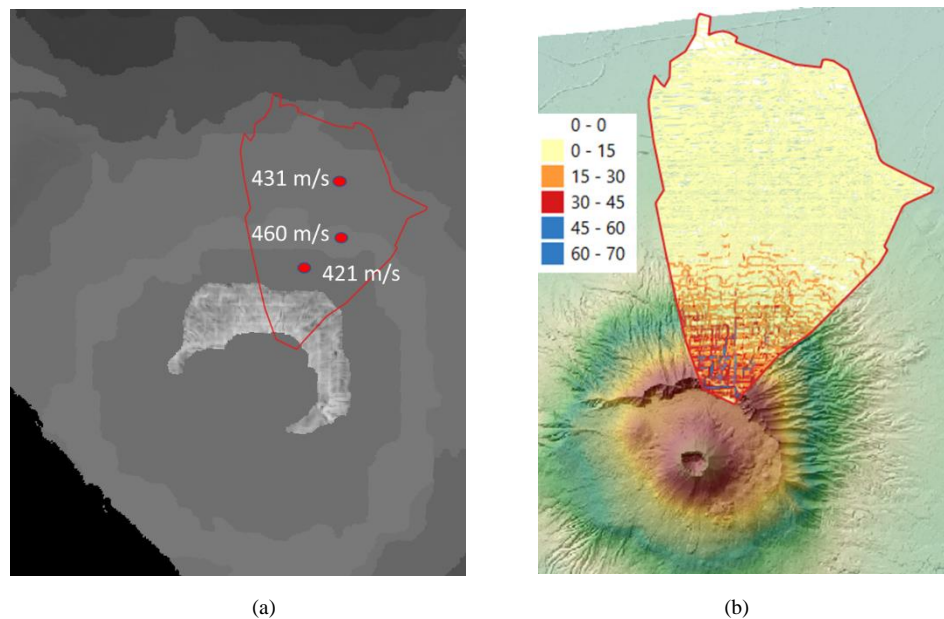


**Figure 5.10** – Vs30 map (a) proposed by Mori et al. (2020) and slope map (b) for the municipality of Somma Vesuviana (bounded with red poyline).

### 5.2.2. Flood risk

The hydrogeographic network for the town of Somma Veuviana is shown in figure 5.11. The area is part of the Lagni Vesuviani basin. The Regi Lagni are a network of rectilinear canals, mostly artificial, whose basin extends over an area of 1095 km<sup>2</sup> in 99 municipalities of the metropolitan city of Naples and the provinces of Caserta, Avellino and Benevento. The Regi Lagni are the result of a work of canalization and hydraulic reclamation carried out during the Spanish domination in Italy between 1610 and 1616, under the direction of the architect Domenico Fontana. These canals were created to overcome the frequent flooding of the Clanio river, a river that flows between the provinces of Naples, Caserta and Avellino. The canals are called “lagni” as this is an ancient name with which the watercourse that crossed the Nolan to get to the Campania plain, and “Regi” because their history is linked to the Bourbon administration, that completed and perfected the layout of the network sketched out in the 1600s. The canals have the peculiarity that the width of the riverbed decreases continuing from upstream towards valley, due to the permeability of the land which progressively reduces its flow. Moreover, they are in bad state of repair, in particular they are filled with filling materials with a high percentage of waste, and they are inadequate for dimensions and anthropic works that decrease the flow rate. Indeed, such areas have historically been affected by the problem of flooding in the downstream

portion in conjunction with particularly intense rainfall events. In figure 5.11 the ISPRA map with the extension of inundated areas is also reported. It is worth noting that area expected to be inundated by low probability (P1) and medium probability events (P2) is the same, whereas it is only lightly different considering frequent events (P3).

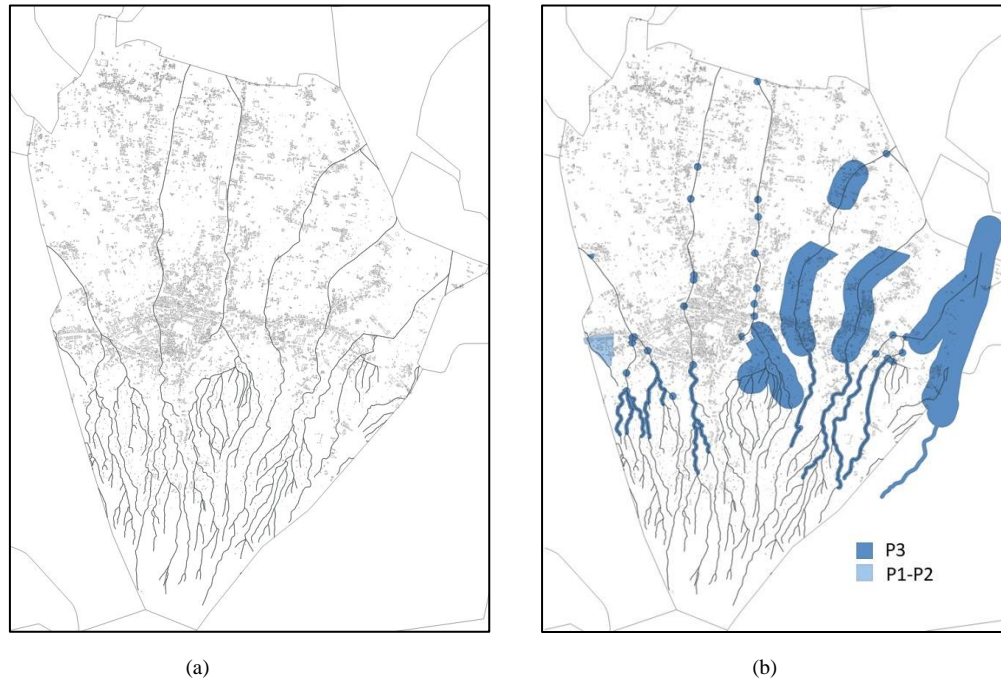


**Figure 5.11** - Hydrogeographic network (a) and flood hazard maps provided by ISPRA (b) for Somma Vesuviana.

As mentioned in section 3.2.2, flood maps provided by ISPRA do not contain any information about flood water depth. Hence, Floodwater Depth Estimation Tool (FwDET) proposed by Cohen et al. (2018) is adopted herein. This tool allows to estimate floodwater depth based solely on an inundation map and a digital elevation model (DEM). Figure 5.12 shows a theoretical illustration of the FwDET for the case of flooding in an alluvial plain. Given the local elevation of hypothetical floodwater level (brown line in the figure), the water depth can be estimated at any point as the difference between flood water elevation and inundated land elevation. Using a GIS software, first DEM values are associated with the flooded domain boundary cells (i.e., cells of the polyline representing the flood extension boundaries). Then, local water elevation values are calculated for each point within the flooded domain from its closest boundary grid cell (Focal Statistic Tool - ESRI, 2017). Finally, calculation of the floodwater depth

is obtained subtracting the topographical elevation from the local water elevation in point.

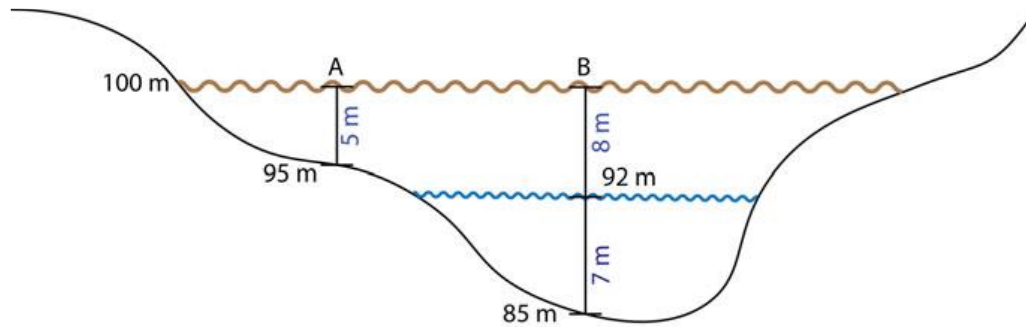


**Figure 5.12** – Representation of FwDET. The blue line represents “within banks” water level, and the brown line represents hypothetical floodwater level. Adapted from Cohen et al. (2018).

In 2022, Peter et al. presented a FwDET implementation in Google Earth Engine (FwDET-GEE). It is an open access and easy to use tool that allows to mapping flood depths across large areas. The use of cloud-sourced geospatial data and analysis functionalities of Google Earth Engine (GEE) greatly reduces FwDET’s most time-consuming pre-processing step. The only input information required are a shapefile with the flooded extent boundaries, water body data and DEM in raster format that cover the area under study. Floodwater depth map in figure 5.13 is obtained through FwDET-GEE using the low probability flood extent map.

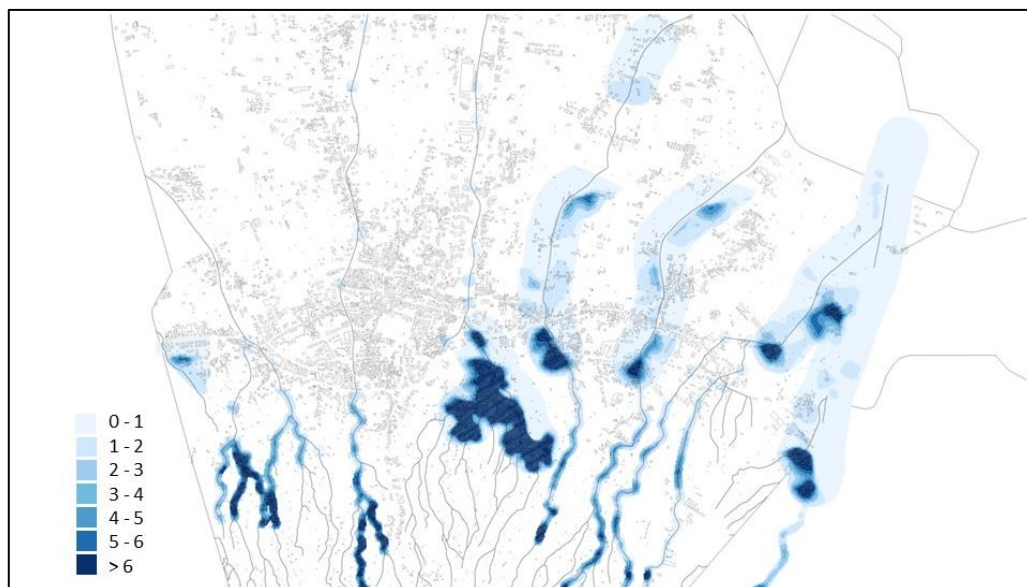


**Figure 5.13** – Flood hazard map with flood extension and expected water depth (m), obtained through FwDET-GEE.



It is worth mentioning that the high value of water depth ( $> 6$  m) in several areas is due to the specific terrain morphology in such areas, with large portions of land lowered even by 30 m compared to the surrounding areas (figure 5.14).



**Figure 5.14** – Aerial view of Somma Vesuviana from Google Earth.

The maximum value of water depth in the figure (6 m) is defined as the flood vulnerability curves adopted in this study, the JRC depth-loss curves for European residential buildings (Huizinga, 2007), associate such depth value with the maximum possible losses. The curves are reported in figure 5.15. Overlapping building footprints to floodwater depth map, the water level in meter associated with each building can be defined. The corresponding damage factor can be obtained by the curves. Figure 5.15 also reports buildings included in the inundated area and the related water depth reached. According to Huizinga et al. (2017), the maximum structural damage for Italian buildings corresponds to a loss of 473 euro/m<sup>2</sup>. Buildings' surface could be derived from footprint layer. However, as it is not possible to get the type of use for the buildings (residential, offices, industrial) just from building footprint, according to statistics based on ISTAT data it is assumed that the 90% of buildings within the municipality is residential. Accordingly, an average living surface per buildings is assumed (100 m<sup>2</sup> per building). More specifically, average living surface area is assigned to each building in the inundated area. Such surface is multiplied by the damage

factor calculated based on the water depth reached by building and the structural damage loss (473 euro/m<sup>2</sup>). The value of losses obtained from all damaged buildings is then multiplied by the fraction representative of residential buildings (90%).

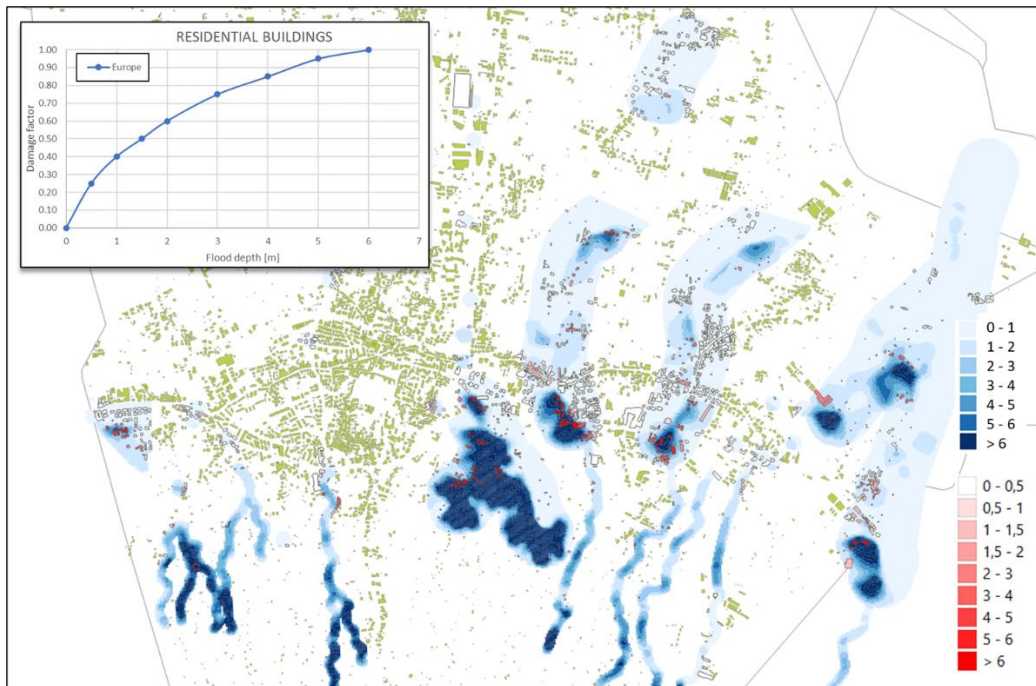


**Figure 5.15** – Flood hazard maps with flood extension, expected water depth (m) and expected flooded buildings with the corresponding inundation level (m). The depth-loss curves adopted for residential buildings are also reported.

### 5.2.3. Risk curves

Seismic risk is assessed using hazard maps related to the 9 different return periods, i.e., considering as inputs different PGA values corresponding to 9 different probabilities of exceedance in 50 years. Given intensity measure, fragility curves of Rosti et al. (2021a, b) are used together with building inventory to estimate the number of buildings reaching each damage level (i.e., the five damage grades of the EMS-98 scale). To estimate economic losses damage-to-loss functions are required. As mentioned before (see section 2.1.3), those functions estimate the amount of losses as function of the number of buildings that sustain damage levels on the selected damage scale. Direct economic losses, associated to physical damages of structures, are usually calculated defining a cost ratio, i.e., a ratio of the reconstruction cost, for each damage grade. Specifically, the consequence functions proposed in Dolce et al. (2021) are adopted herein and direct economic losses are calculated as follows:

$$L = CU \left( \sum_{j=1}^{n_t} \sum_{k=1}^5 A_j \cdot p_{j,k} \cdot c_k \right) \quad (8)$$

Where  $n_t$  is the number of building classes considered by the vulnerability model, CU is the Unit cost (Euro/m<sup>2</sup>) of a building (i.e. the reconstruction cost, estimated taking into account the demolition and the reconstruction cost, including technical expenses and VAT),  $A_j$  is the built area of the  $j$ th building class;  $p_{j,k}$  is the probability for the  $j$ th building class to experience structural damage state  $D_k$  (EMS-98 scale)  $c_k$  is the percentage cost of repair or replacement (with respect to CU) for each structural damage state  $D_k$ , assumed equal to 0.02, 0.1, 0.3, 0.6 and 1 from damage level from D1 to D5. The reconstruction cost (i.e., CU) is assumed equal to 1350 euro/m<sup>2</sup>.

For flood the procedure describe in section 5.2.2 is used to calculate expected economic losses for the three flood maps available (low, medium, high probability). High probability map is associated with events having a return period of 20 years, the medium probability with events with a return period of 100 years and the high probability one with 300 years return period events. Flood risk is assessed using each of those maps as input.

The results in terms of economic losses of both seismic and flood assessment are then reported on a graphic where the MAFE (mean annual frequency of exceedance) of the considered event are shown in ordinate and the corresponding economic losses in abscissa. Risk curves comparing seismic and flood risks in terms of economic losses are shown in figure 5.16. Those curves are obtained for the entire municipality, i.e., sum the losses obtained in each OMI zone.

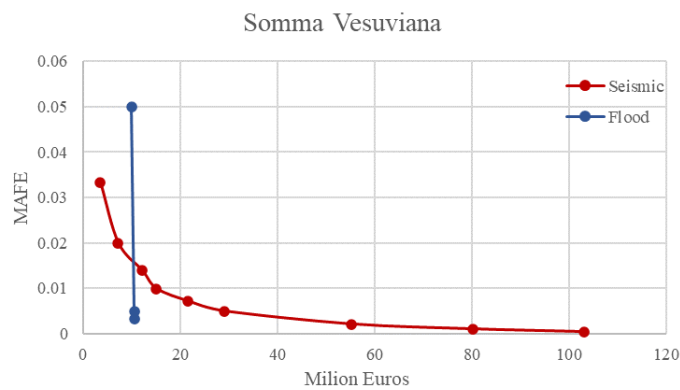


**Figure 5.16** – Risk curves for seismic and flood risk for the entire municipality.

It can be noted that curve for flood is almost linear because of inundated area remains nearly constant in all flood scenarios (low, medium, high probability). The area under the loss curve represents the EAL (expected annual losses). Seismic EAL for the entire municipality amount to about 465.000 euros, while EAL due to floods to about 492.000 euros, with a ratio between the two risks about 1. In table 5.6 EAL values obtained from seismic and flood risk analysis for each OMI zone are reported. From values of losses per square meter (EAL/m<sup>2</sup>) it can be noted that expected losses for earthquakes are quite high in every zone (> 0.40 euro/m<sup>2</sup>) but they are particularly high for D3 zone (0.59 euro/m<sup>2</sup>). On the contrary, economic losses due to floods assume high values only in the area directly affected, that are C3 and D4 zone. The extremely high value of EAL/m<sup>2</sup> observed in D4 is due to the population distribution within such area. As a matter of fact, despite only the 2% of total population resides in the area, residential buildings are mostly located in inundated area, explaining a such high value of losses per m<sup>2</sup>. In table 5.6 also SoVI values associated with each OMI zone are reported. It is noteworthy that the two zones with highest value of losses (EAL/ m<sup>2</sup>) are also the ones for which the SoVI is higher (C3 and D4), excluding zone D4 which residential population is negligible.

**Table 5-6** – Expected losses due to seismic and flood hazards. Ratio (F/S) refers to ratio between flood and seismic losses. The values of SoVI and residential population of each OMI zone are also reported.

OMI Zone	EAL seismic	EAL/m <sup>2</sup>	EAL flood	EAL/m <sup>2</sup>	RATIO (F/S)	SoVI	POP
B2	56466.103	<b>0.42</b>	4896.2295	<b>0.04</b>	<b>0.09</b>	<b>3.85</b>	0.14
B3	78920.7121	<b>0.52</b>	37321.826	<b>0.25</b>	<b>0.47</b>	<b>4.19</b>	0.28
C3	55601.0816	<b>0.46</b>	250670.48	<b>2.06</b>	<b>4.51</b>	<b>4.64</b>	0.14
D3	265506.232	<b>0.59</b>	107766.97	<b>0.24</b>	<b>0.41</b>	<b>5.61</b>	0.41
D4	9166.19719	<b>0.47</b>	91545.293	<b>4.67</b>	<b>9.99</b>	<b>2.26</b>	0.02

Consequence functions for the estimation of people affected by earthquakes are also available. Functions proposed in Dolce et al. (2021) allows the calculation of the expected number of deaths, injured people and homeless. Injured people and deaths can be estimated as a percentage of occupants in buildings experiencing damage grade D4 and D5 (of the EMS-98 scale): the 1% and 10% of occupants in buildings reaching respectively grade D4 and D5 are considered as deaths, the 5% and 30% as injures. The number of homeless can be estimated as the number of inhabitants in unusable buildings, in the short and long term, subtracting the estimated number of deaths. Unusable buildings are buildings that

may be unsafe for occupancy or entry due to potential collapse, falling debris, the unavailability of services or unsanitary conditions. More specifically, it is possible to distinguish between long term unusable and short term unusable buildings. This classification is directly derived from the AeDES usability form, the official form used for post-earthquake damage and usability assessments in Italy (Baggio, et al., 2007), that defines different building usability classes. Buildings are considered as long term unusable if the building cannot be used in any of its parts, even after short-term counter-measures, while they are short-term unusable if the dangerous state may be reduced to an acceptable level for inhabitants applying short-term counter-measures. In Dolce et al. (2021) a model for estimating the number of unusable buildings based on damage attained is also proposed. People affected by flood risk are usually estimated counting of the number of persons residing in flooded areas. As a matter of fact, despite the enormous impacts of floods, there is relatively limited insight into the factors that determine the loss of life caused by flood events, as also underlined in Silvestro et al. (2016). Therefore, the loss function for population adopted is just a binary function that indicates affected or not affected populations, without distinction among deaths, major injuries or displaced. For this reason, the number of expected people affected by earthquakes and floods is not directly comparable.

### 5.3. Mitigation policies for risk reduction

Information provided by risk assessment facilitates the understanding of potential damages and losses arising from future disasters, enabling decision makers to implement risk reduction policies and preparedness activities aimed to anticipate and mitigate risk and manage residual risk. Disaster preparedness consists of a set of measures undertaken in advance by governments, organisations, communities, or individuals to better respond and cope with the immediate aftermath of a disaster. Providing a measure of the impact of different hazard events makes it possible to establish detailed and realistic plans for better response to disasters. For instance, installing early warning systems, identifying evacuation routes and preparing emergency supplies. On the contrary, prevention activities and measures aimed at avoiding existing and new disaster risks, for example, relocating exposed people and assets away from a hazard area. Mitigation measures focus specifically on actions that eliminate or reduce



damages and/or casualties in future disaster events. They consist in physical interventions aimed at reducing facilities vulnerability through construction and reconstruction projects or retrofitting actions. For instance, structural measures for improving performance of building elements to resist lateral forces from winds and earthquakes. Non-structural mitigation measures to improve the seismic resistance of non-structural building components such as parapets, chimneys, or to anchor building contents, especially tall and/or heavy items that pose life safety risks if they fall, such as bookcases, file cabinets, storage shelves, computers, monitors, televisions and others. Elevation of existing buildings or construction of flood barriers such as flood walls or berms are very common flood mitigation measure for buildings. Anyhow, replacement of an existing building with a new building well outside of the flood hazard area remains the only flood mitigation measure which is 100% effective in avoiding future damages. National and local governments can also take steps to reduce the negative financial effects of disasters in a way that protects both people and assets. Financial protection strategies help to address residual risk, which is either not feasible or not cost effective to mitigate. The main beneficiary groups of financial protection include not only national and local governments but also homeowners and small and medium-sized enterprise.

To evaluate the effectiveness of some mitigation actions, further risk scenarios accounting for the implementation of such measures are also considered herein. A set of hard and soft policies, for reducing both seismic and flood risk, are defined and their effects on expected damages and losses are evaluated. Hard policies refer to physical interventions on structures, such as local strengthening and retrofitting, while soft policies indicate financial strategies for insurance coverage of a certain level of post-event damage. The comparison between EAL associated to original scenario (without policies) and the EAL obtained considering the adoption of such mitigation actions (hard and soft policies) allows to quantify the effectiveness of such strategies. Each unit of analysis (i.e., OMI zone) is investigated separately, in order to identify those locations where mitigation actions might lead to a greater risk reduction and if a strategy is more adequate than another for reducing risk in a given area.

### 5.3.1. Hard policies

#### 5.3.1.1. Seismic retrofitting

Earthquake resistant design of buildings provides them adequate strength, stiffness and inelastic deformation capacity to withstand a given level of earthquake-generated force. This is generally accomplished through the selection of an appropriate structural configuration and the careful detailing of structural members. However, many existing buildings in earthquake prone regions are not conform to modern seismic design codes. This has led to significant economic and life losses during past earthquakes (Mazzoni, et al., 2018; Stewart, et al., 2018; Di Ludovico, et al., 2021). Seismic retrofitting is then an essential tool for mitigating the consequences of earthquakes on such buildings and improve their seismic performance. Last seismic events occurred in Italy have highlighted the main structural deficiencies of residential buildings, such as the lack of connection between walls and/or slabs and walls in masonry buildings and the non-ductile local failure mechanism, (e.g., joint failure) in RC buildings (Reluis, 2011). The most used retrofit strategies in the post-earthquake reconstruction process were RC jacketing or FRP (fiber reinforced polymer) jacketing, adding RC shear walls or bracing in RC buildings; reinforced plaster and tie rods and tie beams insertions were mostly used in masonry buildings to prevent in plane and out of plane failure mechanism (Reluis, 2015,2022).

For considering the above-mentioned retrofit actions in seismic risk analysis it is necessary to modify the vulnerability of buildings, in terms of exposure or fragility. The first approach consists in changing the belonging vulnerability class of building based on building's features modified by retrofitting. This strategy is adopted herein for masonry buildings. According to the vulnerability model adopted, the insertion of tie rods in buildings with regular layout vertical structure leads to a change of the vulnerability class of the buildings (table 5.5), specifically from class B (more vulnerable) to class C1 (less vulnerable). Supposing to retrofit all buildings belong to class B, such buildings move in C1 class. This means that, for representing their vulnerability, fragility functions developed for vulnerability class C1 are used in risk analysis (instead of fragility for class B).

For RC buildings only two vulnerability classes are defined by the model: class C2 representing not seismically design buildings or buildings seismically designed using old codes (pre-1981); class D that represents buildings designed according to the actual seismic regulations. Changing building class from C2 to D would require to totally adequate the buildings belong to the former class (C2) according to new seismic design codes. Retrofitting techniques required to this aim (changing of vulnerability class) may be too wasteful in terms of time and money for being applicable at large scale. Thus, only local strengthening techniques are considered herein as retrofit measures. These retrofit actions do not allow a complete adjustment of buildings to more recent design codes (and therefore the total changing of vulnerability class), but still lead to an improvement of the seismic performance of buildings. This improvement can be taken into account through fragility functions modification, namely the fragility curves of vulnerability class C2 are modified for considering the better seismic behavior (or lower vulnerability) obtained after retrofit interventions. To this aim, the study proposed by Aljawhari et al. (2022) is taken as reference. The study proposes an approach for mapping the increase of  $CDR_{LS}$  (the global displacement-based ratio of capacity to life-safety demand) due to retrofitting to the building-level fragility reduction. An archetype of RC structure, not conformed to modern seismic design requirements, is considered retrofitted using three different techniques: FRP wrapping of columns and joint, RC jacketing and steel jacketing. For each technique several retrofit configurations were defined, based on number and location of retrofitted elements. Push over analysis was performed to find the  $CDR_{LS}$  correspondent to different retrofitting solutions, including as built (i.e., without retrofit) configuration. Nonlinear models both for as-built and retrofitted case studies were developed and nonlinear time-history analyses for a large set of ground-motion records were performed for deriving fragility relationships for structure-specific damage states. Assuming that the relationship between  $CDR_{LS}$  and the median of the fragility relationship for a given damage state ( $\mu_{DS}$ ) is pseudo-linear (Aljawhari, et al., 2021), the variation of  $\mu_{DS}$  with respect to the original configuration due to retrofit intervention is then defined.

The  $\mu_{DS}$  variation estimated in Aljawhari et al. (2022) are applied to fragility curves adopted in this study (Rosti et al., 2021b) to account for the reduction in fragility due to seismic retrofitting. To this aim, it is assumed that the same retrofit solution is adopted for all buildings belong to vulnerability class C2 (i.e., not seismically design). More specifically, the configuration adopted is the so-defined “basic performance” one, which basically corresponds to retrofitting of external joints and columns of first floors of the archetype structure. Assuming such configuration would correspond to assume that the percentage of retrofitted elements is constant for every height class of buildings (e.g., the 2/3 of columns are retrofitted both in 1 storeys and in 4 storeys buildings).

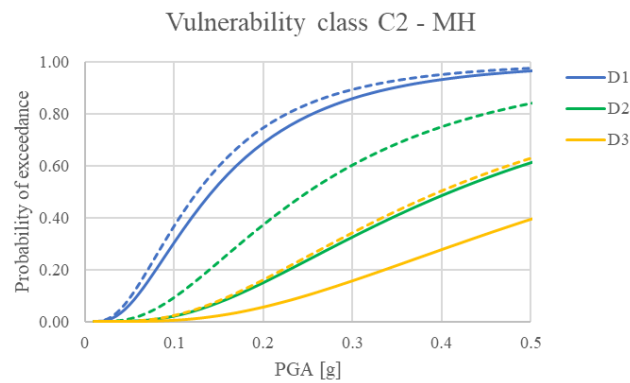
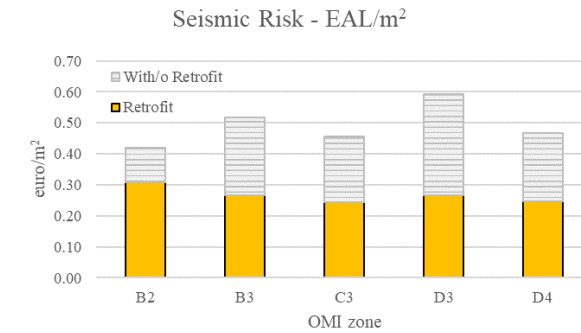
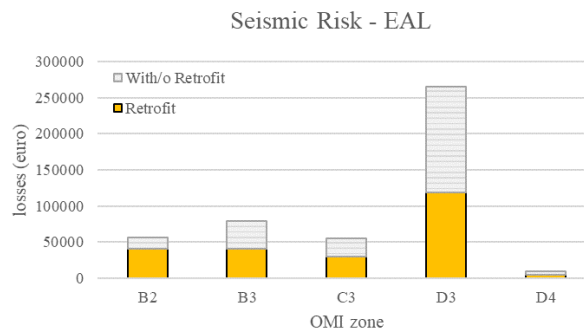


**Figure 5.17** – Modified fragility curves for RC buildings classified in C2 vulnerability class, with medium height. The dashed curves are the original fragility curves of Rosti et al. (2021b).

The  $\mu_{DS}$  variation is also dependent on the damage state considered. Therefore, it is necessary to establish a correspondence between the structure-specific damage state adopted in Aljawhari et al. (2022) and the EMS-98 damage grades adopted herein. As criteria adopted for mapping of damage state (Aljawhari, et al., 2020) can be considered similar to the ones adopted in HAZUS (FEMA, 2015), the conversion rules proposed in Lagomarsino and Giovinazzi (2006) to convert the HAZUS damage levels into the EMS-98 grades are adopted. Thus, considering the average variation among the three solutions proposed (FRP, RC and steel jacketing), the median of C2 class fragility curves increases of the 13%, 64% and 52% for damage grade D1, D2 and D3 respectively (figure 5.17). Figure 5.18 shows the reduction in losses due to retrofit actions in each unit of analysis. It can be noted that the absolute reduction is particularly high in compartment D3. Also, the decrease in losses/m<sup>2</sup> in this zone is higher than other zones (-0.55%).



(a)



(b)

**Figure 5.18** – Expected losses expressed in euro(a) and euro/m<sup>2</sup> (b) calculated considering the implementation of hard policies (in yellow) and the difference with the corresponding losses calculated for the original scenario without any policies.

### 5.3.1.2. Flood management measures

Mitigation measures for reducing flood damages can be aimed to reduce the intensity of the hazard or to reduce structure vulnerability and exposure. The rising of levees, bridge gates or temporary dikes are examples of mitigation actions for hazard reduction, usually carried out by civil protection. On the contrary, measures of flood proofing constructions are an example of measures aimed to minimize damages limiting the exposure and reducing the vulnerability. As a large percentage of total damages caused by floods usually concern furniture and supply facilities (e.g., heating, electrical equipment), appropriate use and equipment of buildings allows to limit damages by refraining from vulnerable uses of rooms located below flood depth. Sealing measures are an example of dry flood proofing that consist in making waterproof the shell of the buildings and the cellar. However, in existing construction the permanent sealing of buildings and cellar may require considerable expenditure and effort. Another possible dry flood proofing solution is the shielding, aimed to keep water away from the

building. For instance, the construction of an embankment or a wall is a permanent shielding measure. Still, mobile flood walls may also be raised during flooding events. Land use control and zoning ordinance are measures for limit the exposure. They are specifically used for reducing the increase of damage potential in built areas, without any reduction of potential damages for existing constructions. As a matter of fact, on the long term, building codes and zoning ordinances entail a reduction of damage compared to unaffected growth.

Mitigation actions on hazard reduction lead to a decrease in water depth in the flooded areas, that can be estimated through hydraulic analysis. On the contrary, mitigating exposure/vulnerability leads to a reduction of expected damages for a certain water depth. This means that the effects of flood mitigation measures can be represented by a changing in the curves describing damage, as reported in figure 5.19 (Molinari, et al., 2013 ).

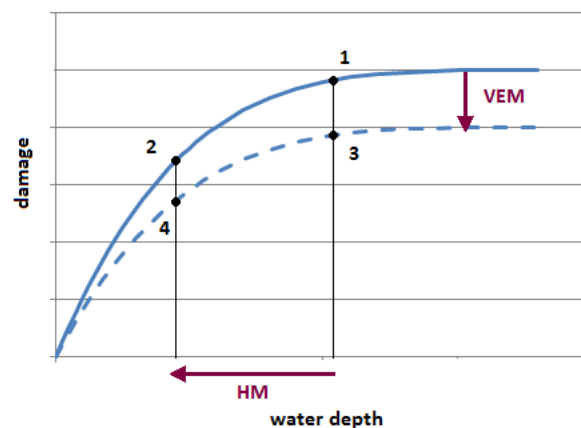


**Figure 5.19** – Changing in flood damage curves due to mitigation actions for hazard reduction (HM) and mitigation actions for exposure/ vulnerability reduction (VEM).

As this study focuses on residential buildings and only structural damages/losses are considered, shielding and sealing are taken into account as flood mitigation measures. The effects of such measures are considered through a fixed drift in the depth-loss curves so that reduction in losses can be considered as a fixed percentage of potential losses, for every water depth value. Reference values for damage reduction corresponding to several mitigation actions proposed in the International Commission of the Protection of the Rhine (ICPR, 2002) are adopted herein. It is assumed that to a given percentage of damage reduction corresponds the same percentage of loss reduction. Expected reduction of

potential damage (and losses) between 50% and 100% are estimated in case of sealing and shielding flood measures. It is also mentioned that the suggested effects of preventive construction measures are related to moderate water surface elevation ( $< 2$  m). Therefore, a reduction in losses of 75% is considered only for buildings located in flooded areas with a predicted water depth lower than 2 m. Thus, in other cases (buildings in flooded area with water depth  $> 2$  m) those measures are considered ineffective.

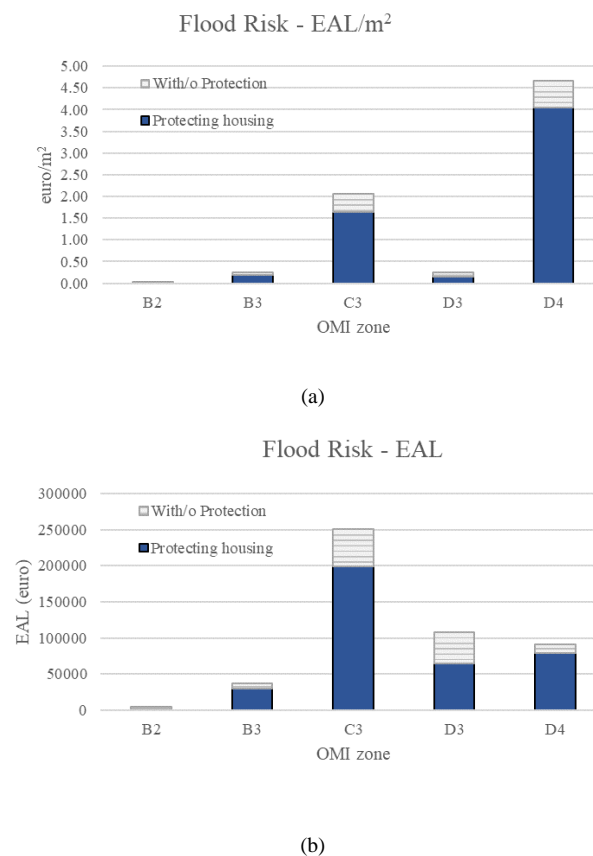


**Figure 5.20** - Expected losses expressed in euro(a) and euro/m<sup>2</sup> (b) calculated considering the implementation of hard policies (in blue) and the difference with the corresponding losses calculated for the original scenario without any policies.

From figure 5.20 it can be noted that mitigation measures against flood risk are less effective than the ones adopted for seismic risk reduction, with a reduction in losses/m<sup>2</sup> of 21% and 13% for C3 and D4 zones respectively. This is mostly due to the assumption that the selected measures allow to protect only buildings situated in a low-depth flooded area. It represents a limitation of the low intrusive flood management measures. Although the 60% of buildings in flooded areas are expected to be inundated with a low-depth flood ( $< 2$ m) and therefore affected by the considered protection measures, the 15% of the remaining buildings reach

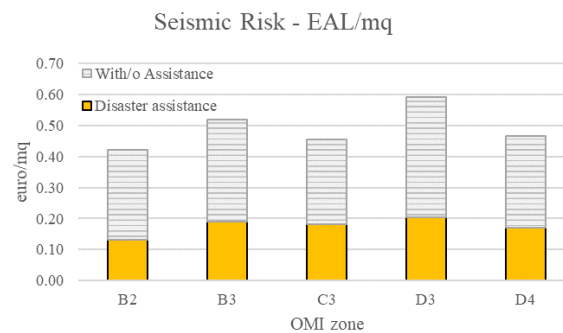
the maximum possible structural damage. In such cases the most effective actions for risk reduction remain planning and land use control.

### 5.3.2. Soft Policies

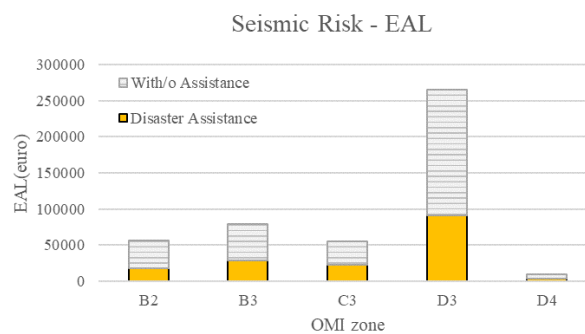
Insurance indemnity payments after a hazardous event can provide quick compensation to households to repair or reconstruct damaged buildings and replace possessions. In case of business activities, insurance coverage may also compensate for losses due to disrupted production - thereby reducing the economic disruption caused by the event. The level of insurance coverage for natural catastrophe perils provided by private and public insurers varies across countries, with various levels of deductibles and limits offered to policyholders. Earthquake insurance carries a deductible, generally in the form of a percentage rather than a dollar amount. In Canada and the United States deductibles can range anywhere from 2 % to 20 % of the replacement value of the structure. This means that if it cost \$100,000 to rebuild a home and there was 2 percent deductible, the consumer would be responsible for the first \$2,000 dollars. Considering the cost parameters used for earthquake losses calculation (see section 5.2.3), a deductible percentage between 2% and 10% of reconstruction cost (or unit cost) would correspond to losses caused by D1 and D2 level damages. Therefore, in order to account for the application of such policies, the contribution of only these two damage grades is considered in EAL calculation, while losses related to heaviest damages (D3, D4 and D5 grades) are considered covered by insurance. Similarly, flood insurance is supposed to cover damages with a deductible up to 20% of unit cost. According to the adopted vulnerability model (Huizinga, 2007), the maximum structural damage for Italian buildings due to flooding is 473 euro/m<sup>2</sup>. The authors defined an “undamageable” part for buildings based on their construction material, that leads to a reduction in maximum damage value (see also section 3.2.2). Such “undamageable” part is set equal to 40% for masonry and RC buildings. In other words, for Italian masonry and RC buildings, the maximum damage value of 473 euro/m<sup>2</sup> does not correspond to losses caused by destruction, as can also be observed in CAPRA model, where the maximum percentage of damage corresponding to those typologies is the 60% (figure 3.3 in Chapter 3). Therefore, a deductible between 10% and 20% of the reconstruction cost (set at the value of 1350 euro/m<sup>2</sup>) would



correspond to a value between 30% and 60% of the maximum possible structural damage for buildings (set at the value of 473 euro/m<sup>2</sup>). Hence, in this application losses exceeding the 40% of maximum structural damage are considered covered by insurance, while under this threshold the losses should be suffered by households. Figures 5.21 and 5.22 show the expected losses obtained considering the implementation of soft policies, both for seismic and flood risk, and their differences between losses resulting from the original scenario without policies application.

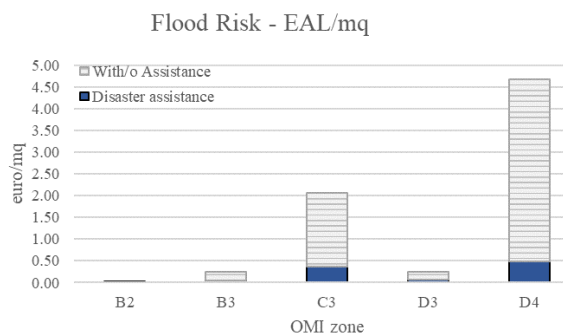


(a)



(b)

**Figure 5.21** - Expected losses expressed in euro(a) and euro/m2 (b) calculated considering the implementation of soft policies (in yellow) and the difference with the corresponding losses calculated for the original scenario without any policies.



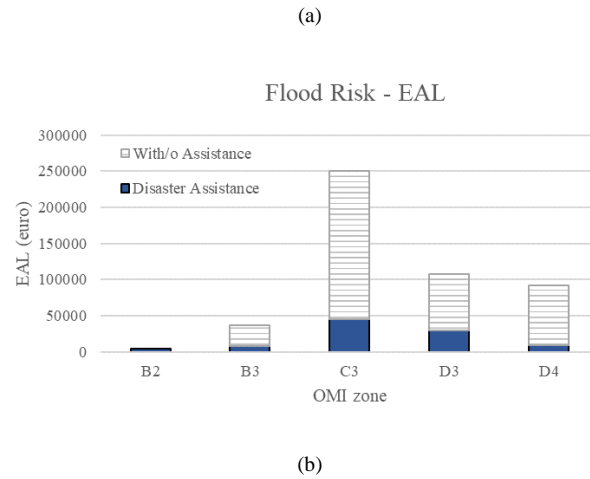


**Figure 5.22** - Expected losses expressed in euro(a) and euro/m<sup>2</sup> (b) calculated considering the implementation of soft policies (in blue) and the difference with the corresponding losses calculated for the original scenario without any policies.

### 5.3.3. Discussion

Losses values obtained for all scenarios considered (i.e., original with no policies, hard policy and soft policy) and for each risk analysed are disaggregated across three different income groups. The proportion of people in different income levels is obtained from OMI zone market values (table 5.4). High-income zones are designated as those where the minimum market value is greater than 1,000 euro per square meter (euro/ m<sup>2</sup>), middle-income zones are designated as those where the market value is greater than 900 euro/m<sup>2</sup>, and low-income zones are those where the market value is lower than 900 euro/ m<sup>2</sup>. This criterion leads to considered OMI zone B2 and B2 (that have the same market values) as high-income level zones, C3 as medium level and to group D3 and D4 zones into low-income level zone. Figures 5.23 and 5.24 show the comparison of expected losses (EAL and EAL/m<sup>2</sup>) with and without policies implementation for the three income groups. The reduction in seismic EAL and EAL/m<sup>2</sup> from adopting the hard policy quite high for all three income classes but it is particularly notable for those of the lowest income. Indeed, EAL/m<sup>2</sup> reduction ranges from -40% for high income group to -55% for low-income group. Such result highlights that for in areas populated by low-income people not only social vulnerability is high but also physical vulnerability tends to be higher than other zones (also considering that hazard input does not change much within municipal areas). The different income classes also benefit from adopting the proposed soft policy, that leads to an average reduction in losses of -63%. The slightly difference in the

effectiveness of the policies may be because hard policies directly affect buildings' physical vulnerability, reducing probability of attaining damages mostly from light to moderate. In contrast, the considered soft policy allows to cover not only losses due to moderate damages but also losses associated with heaviest.

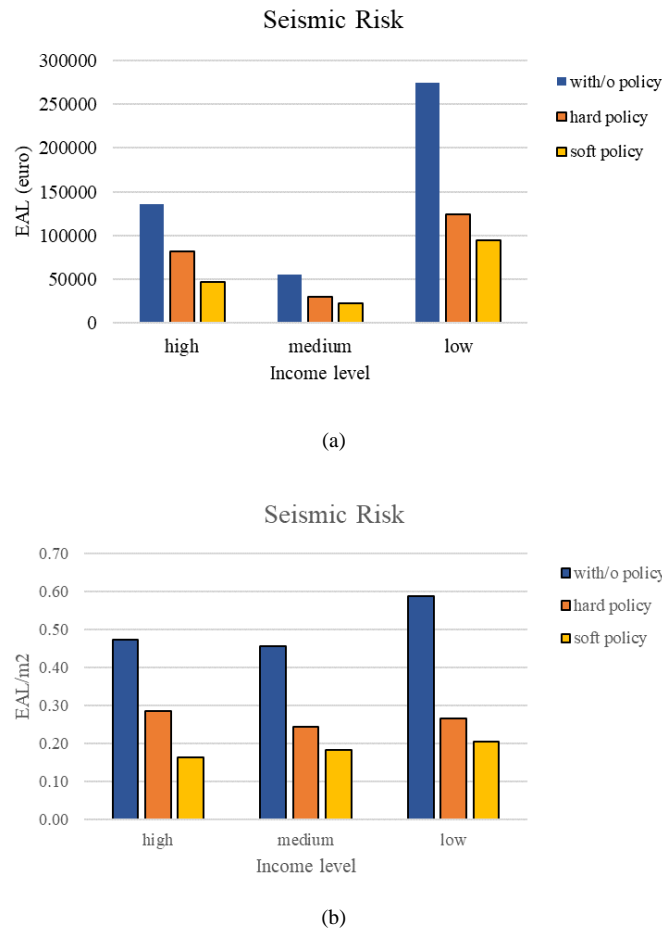


**Figure 5.23** - Expected losses expressed in euro(a) and euro/m<sup>2</sup> (b) disaggregated across the three different income level classes.

From figure 5.24 it can be noted that absolute losses due to floods are quite high for both medium and low-income groups. However, EAL/m<sup>2</sup> are tremendously high for medium-income group. As a matter of fact, it is known that flood events, for their nature, usually affect specific areas, that may be small with respect to the administrative boundaries. Hard policy does not affect expected losses much, due to the above-mentioned limit of protection measures adopted (i.e., they are considered effective only if inundated depth is less than 2 m). Thus, the most effective hard policy against floods remains the urban planning, reducing or fully eliminating buildings exposed to such events. On the contrary, soft policies could

be a very useful tool for supporting population towards existing flood risk that cannot be eliminated. Soft policies lead to a reduction of expected losses of the 81%, as they can cover heavy damages that cannot be avoided using the hard policies considered.

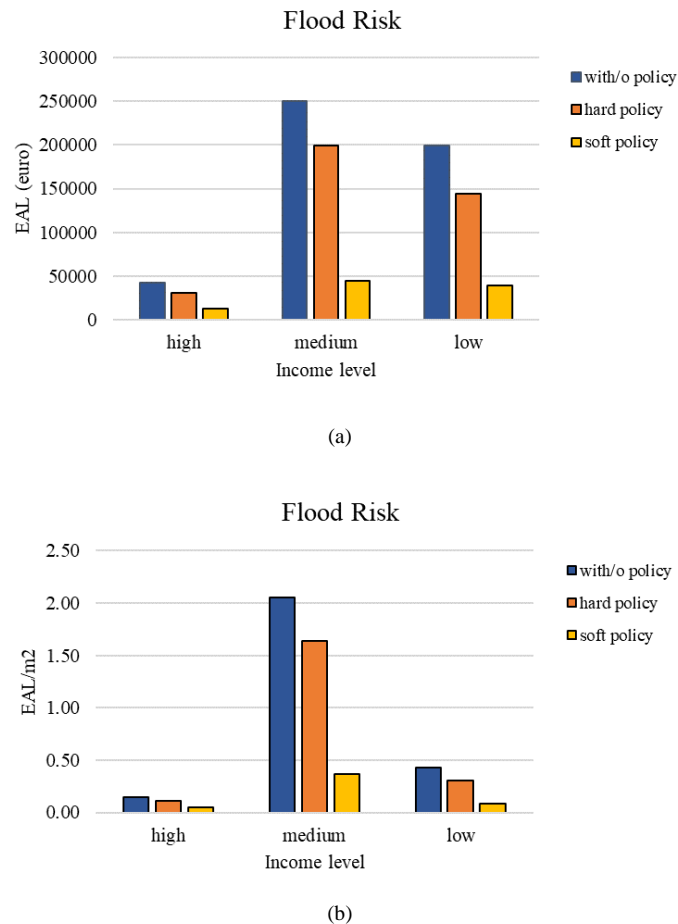


**Figure 5.24** - Expected losses expressed in euro(a) and euro/m<sup>2</sup> (b) disaggregated across the three different income level classes.

It is worth mentioning that results obtained through this application also depends on the assumptions made. First, simplified approach used to develop flood water depth may lead to inaccurate results as it is based only on flood extension map and a ground topographic model (i.e., DTM). That means that a more accurate flood depth estimation may also lead hard policies more effective. Furthermore, deductible considered in soft policies may vary. For instance, a higher deductible may lead seismic hard policies more convenient than seismic soft policies. Moreover, the lower the deductible the higher the insurance premium. For this reason, a cost-benefit analysis would be also needed to establish which is the most beneficial option.

## Strengths, limits and future needs

Index-based approach shown in Chapter 3 is a versatile tool that can be easily modified to account for more hazards and dimensions. Similarly, it could be adopted for measuring risk considering fewer dimensions. For instance, for estimating the influence of socio-economic aspects on one hazard. Still, it could be use as tool for multi-layer single risk assessment, harmonizing different hazards and allowing their comparison and ranking. Despite all those prominent advantages, it is a semi-quantitative approach; in other words, it is useful for ranking areas of interest based on defined risk score, but it does not allow a proper estimation of expected social and economic losses due to a given scenario. For this reason, detailed analysis is also required for quantifying losses and estimate the effectiveness of any mitigation actions (chapter 5).

In this chapter both strengths and weaknesses of the proposed framework are pointed out. First, an application aiming to demonstrate further possible uses of RI is performed. A RI integrating seismic risk with social vulnerability is defined. The application is proposed for Campania region, in the south of Italy. All the municipalities in this region are classified based on such RI value. The municipality with highest score is then selected for a detailed risk assessment. The implementation of some risk mitigation policies is considered in risk assessment and the outcomes, in terms of economic losses, are disaggregated classifying population based on income level. The procedure adopted is the one shown in chapter 5. Besides demonstrate the adaptability of the RI for different purposes, this application also allows to make comparisons with results obtained for Somma Vesuviana, highlighting how more appropriate mitigation actions may vary from town to town.

Later, a comparison between results obtained through the proposed semi-quantitative approach, in term of risk score, and the outcomes of a detailed risk assessment, in terms of EAL, is performed. To this aim, risk results obtained

within BORIS project are used. The BORIS project (Cross BOrder RISk assessment for increased prevention and preparedness in Europe) is a European project focused on the assessment of seismic risk and flood risk in transboundary areas among Italy, Austria and Slovenia. Within the project, a shared methodology to perform harmonized cross-border single risk (seismic risk and flood risk) as well as multi-risk analyses is proposed and applied in two pilot transboundary regions at the Italy-Slovenia and Slovenia-Austria borders. Risk curve comparing seismic and flood risk are developed for each municipality in the pilot areas and the correspondent EAL is calculated. Specifically, EAL values related to municipalities in Italian side of the pilot are used herein. The latter are compared with results in terms of risk score, derived by the application of the procedure presented in chapter 3. As in BORIS social vulnerability aspects are not accounted, for allowing the comparison the RI is slightly modified in order to involve only the two hazards (i.e., seismic and flood). Thank to such application, it is possible to verify whether RI is able to adequately express a measure of expected losses in a given area. Moreover, location where a high risk in terms of losses does not correspond to a high RI are analysed in order to define which issues may arise in the utilization of the proposed index. In this way, the limits and the future needs of the tool are also defined.

## 6.1. Risk Index for multi-dimensional single-risk assessment

In this application, RI integrates individual indicators for seismic hazard and both physical and social exposure and vulnerability. According to the proposed procedure, the RI is calculated by normalising, weighting and aggregating such individual indicators. The considered indicators are defined analogously to previous application. Thus, seismic hazard indicator is the PGA value with a 10% probability of exceedance in 50 years (i.e., corresponding to a mean return period of 475 years), defined at the municipal centroid and derived from the official hazard model in the country (Stucchi et al., 2004; 2011). As social vulnerability indicator SoVI is adopted, calculated according to approach proposed by Frigerio et al. (2018) and presented in section 3.2.3. The indicators and variables used to estimate the SoVI are reported in table 3.1 and derived from ISTAT database (ISTAT, 2011). Physical vulnerability indicator is derived using the Risk-UE index-based approach (Lagomarsino & Giovinazzi, 2006). The procedure to

estimate the Risk-UE indicator at municipal level is reported in section 3.2.1. Indicator representing exposed population quantifies the residential population at the municipal level, and it is derived from the most recent census (ISTAT, 2011).

Each indicator is first normalized through their empirical cumulative distribution functions (ECDFs) and then aggregated. The RI is computed by aggregating each indicator as follows:

$$RI = [F_h^s(h_j) \cdot F_{pv}^s(v_j)]^{w_s} \cdot F_{sv}(sv_j)^{w_{sv}} \cdot F_p(p_j)^{w_p} \quad (9)$$

where  $F_h^s(h_j)$ ,  $F_{pv}^s(v_j)$ ,  $F_{sv}(sv_j)$  and  $F_p(p_j)$  are the ECDF values of the seismic hazard, physical vulnerability, social vulnerability and residential population indicators, respectively, evaluated at municipality  $j$ . Note that physical exposure is accounted for in the definition of the physical vulnerability indicator, in line with the approach presented in chapter 3). The weights adopted for each indicator ( $w_s$ ,  $w_{sv}$ , and  $w_p$ ) represent their relative importance to relevant stakeholders.

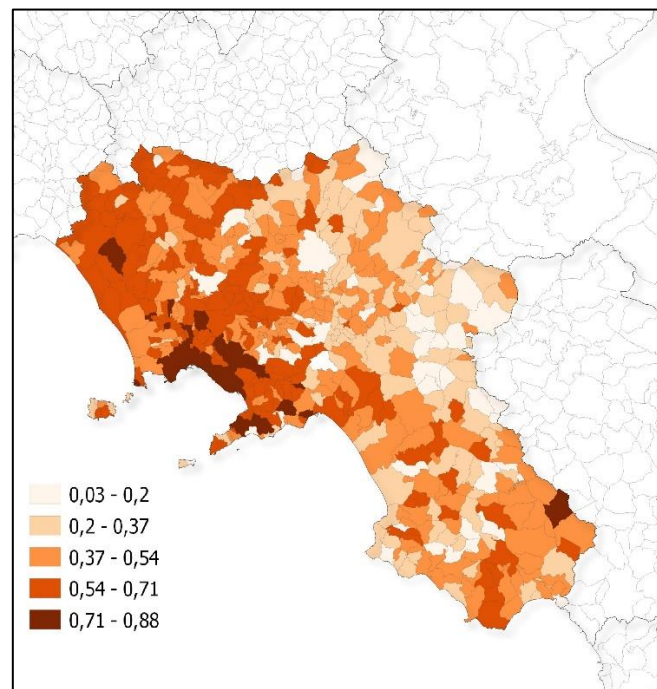


**Figure 6.1** - Map of the Risk Index values in the Campania region.

The RI presented in Eq (9) is demonstrated for the Campania region of Italy using a municipality-level scale of analysis. Its calculation is carried out for the case of equal weights ( $w_s = w_{sv} = w_p = 0.333$ ). The values obtained for each municipality in the Campania region are shown in figure 6.1. In table 6-1 the list of the 10 municipalities with highest scores is reported. It can be noted that also Somma

Vesuviana is included in such list. However, whereas it is the one with highest score in Campania if also flood risk is involved, considering only seismic risk and social vulnerability this municipality still has very high risk score but not the highest one. Moreover, comparing these results with the ones reported in table 5.1 of chapter 5, it may be point out that risk indices tend to be lower than the scores obtained considering multiple hazards. For instance, Somma Vesuviana has a score equal to 0.795. Despite the latter is not the highest value, it is still higher than the one reported in table 5.1, obtained integrating seismic, flood risk and social vulnerability. In other words, the more indicators, the lower the final risk index. This is due to normalization process.

**Table 6-1** – List of the 10 municipalities with highest risk score in Campania region, adopting the equal weighting of indicators.

<b>MUNICIPALITY</b>	<b>RISK INDEX</b>
Portici	0.876
San Giorgio a Cremano	0.868
Ercolano	0.838
Frattamaggiore	0.836
San Giuseppe Vesuviano	0.828
Ottaviano	0.823
Napoli	0.814
Poggiomarino	0.812
Boscotrecase	0.797
Somma Vesuviana	0.795

The town of Portici produces the highest RI score in Campania. For a deeper investigation of spatial interactions between overall seismic risk and social vulnerability, detail risk assessment for Portici is performed.

According to the latest census information, Portici has a residential population of about 55,400. It belongs to a medium-to-high seismicity class according to the Italian code classification of seismic zones (OPCM 3274, 2003), with a PGA value equal to 0,167 g for a mean return period of 475 years. The municipal territory is divided into sub-areas representing broad socioeconomic statuses of the residential population. To this aim, data provided by real estate observatory (i.e., OMI) are used. The OMI zone identified for the town of Portici, the alphanumeric code associated, and the related market and lease real estate values are reported in table 6-2 and figure 6-2.



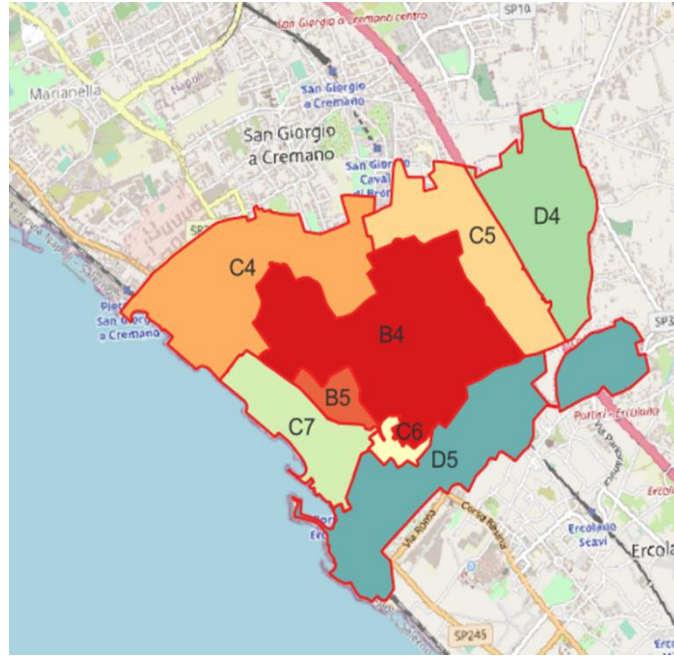


**Figure 6.2** – Delimitation of OMI zone for the city of Portici. Each zone is identified by an alphanumeric code that categorises the zone as Central (B), Semi-central (C) or Suburb (D).

**Table 6-2** – OMI zone identified in Portici.

OMI zone	Market value (euro/m <sup>2</sup> )		Lease values (euro/m <sup>2</sup> per month)	
	min	max	min	max
B4 - Centra/ VIA DIAZ, VIA LIBERTA', VIA L. DA VINCI	1900	2900	5.9	8.9
B5 - Central/Historical centre	1650	2500	5.1	7.7
C4 - Semi-central/VIA PICENNA, VIA MARTIRI DI VIA FANI, CORSO GARIBALDI DA SAN GIORGIO A INCROCIO VIA DIAZ	1600	2450	4.9	7.6
C5 -Semi-central/BELLAVISTA	1800	2700	5.6	8.30
C6 - Semi-central/CENTRO STORICO DEGRADATO	1350	2050	4.2	6.30
C7 -Semi-central/PARCHI RESIDENZIALI LITORANEI	1950	3000	6	9.30
D4 -Suburban	1500	2250	4.6	6.90
D5 - Suburban/GRANATELLO - REGGIA E PARCO - SVINCOLO AUTOSTRADA PORTICI / ERCOLANO	1450	2200	4.5	6.80

The SoVI is calculated for each subdivided unit (i.e., OMI zone) of the municipality, adopting the same approach used in application for Somma Vesuviana, presented in chapter 5 (figure 6.3). The necessary information for the SoVI estimation is derived from the most recent census data at the census tract level. All census tracts belonging to the same OMI zone are grouped through GIS software. Vulnerability models proposed by Rosti et al. (2021a) and Rosti et al. (2021b) for masonry and RC buildings, respectively, are adopted. The building inventory is compiled integrating census data with Cartis data, as also explained in section 5.2.1. The consequence model proposed by Dolce et al. (2021) to estimate economic losses are used. A probabilistic seismic risk assessment is performed and the EAL are calculated (figure 6.4). The resulting losses are quite

high for all OMI areas, with a value greater than 0.20 EAL/m<sup>2</sup> everywhere. The area with the highest value is B5 (0.73 EAL/ m<sup>2</sup>), followed by the C6 zone (0.40 EAL/ m<sup>2</sup>) and C4 zone (0.36 EAL/ m<sup>2</sup>); for all these areas, the SoVI is very high as well (see figure 6.3).

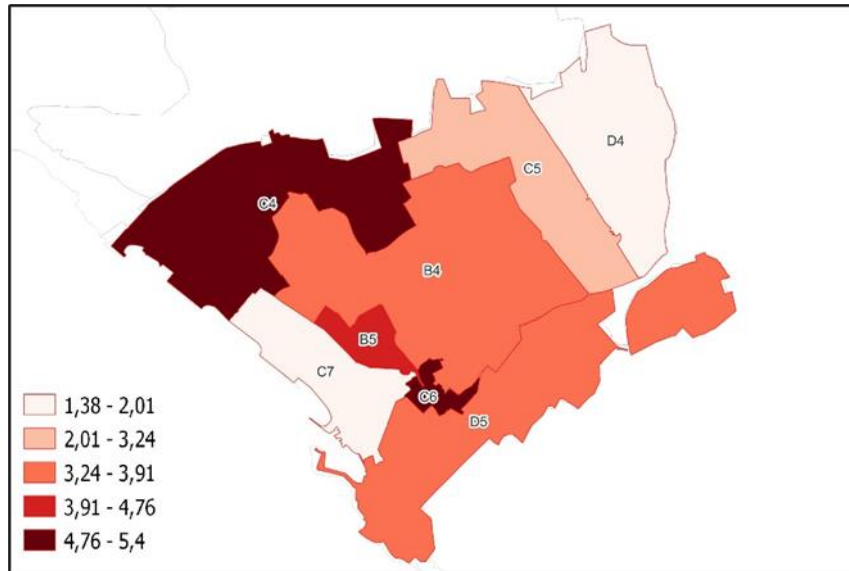


**Figure 6.3** - OMI homogeneous areas and their classification based on SoVI value.

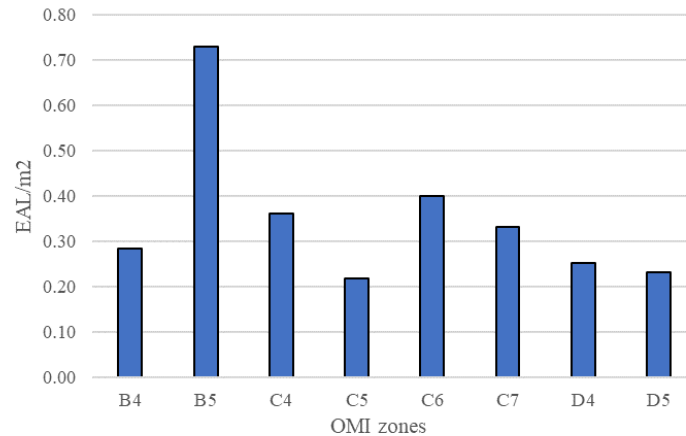


**Figure 6.4** – EAL/m<sup>2</sup> for OMI zones.

The assessment is repeated twice for evaluating the effectiveness of loss reduction through the implementation of some mitigation strategies, i.e., building retrofit (a hard policy) and post-disaster assistance through insurance coverage (a soft policy). Such strategies are accounted in the calculation using the assumptions already adopted in section 5.3.1.1 (hard policies) and in section 5.3.2 (soft policies). Figure 6.5 compares the EAL/m<sup>2</sup> values obtained for all scenarios considered (i.e., original - no policies, hard policy and soft policy) across three

defined income groups. The proportion of people in different income levels is obtained from OMI zone market values. High-income zones are designated as those where the minimum market value is greater than 1,900 euro per square meter (euro/ m<sup>2</sup>), middle-income zones are designated as those where the market value lies between 1,650 euro/m<sup>2</sup> and 1,900 euro/ m<sup>2</sup>, and low-income zones are those where the market value is lower than 1,650 euro/m<sup>2</sup>. EAL/m<sup>2</sup> is consistently highest for the most vulnerable population class (i.e., low-income). The reduction in EAL/m<sup>2</sup> from adopting the hard policy is highest for all three income classes (approximately 73% on average) and is particularly notable for those of the lowest income. The different income classes benefit to a lesser extent from adopting the proposed soft policy, which again leads to the largest reduction in EAL/m<sup>2</sup> for the low-income class (of 65%).

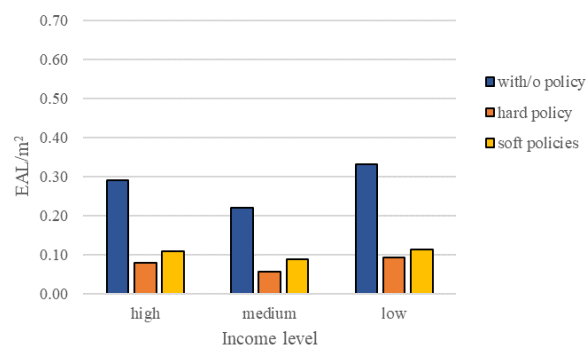


**Figure 6.5** - Expected annual losses per square meter disaggregated across the three different income level classes.

Unlike Somma Vesuviana, in this case hard policy seems to be more effective than soft one. This is probably due to the higher number of buildings achieving minor and moderate damages with respect to the heavily damaged ones. The considered retrofitted actions are mostly effective for such type of damages (minor/moderate), leading to a significant reduction of EAL as well. In contrast, the considered soft policy only covers losses associated with heaviest damages.

## 6.2. Evaluating the representativeness of risk index: comparison with detailed risk assessment

Within BORIS project multi-layer single assessment was performed to compare and rank seismic and flood hazard. As the project is focused on harmonizing cross-border risk assessments, risk analysis involved only few Italian

municipalities in the cross-border area between Italy and Slovenia. The map of the 27 Italian municipalities involved in the pilot application of the BORIS project with the correspondent EAL values (as sum of seismic and flood EAL) is reported in figure 6.1. In the figure, also an example of risk both for seismic and flood risk for the city of Gorizia is shown.

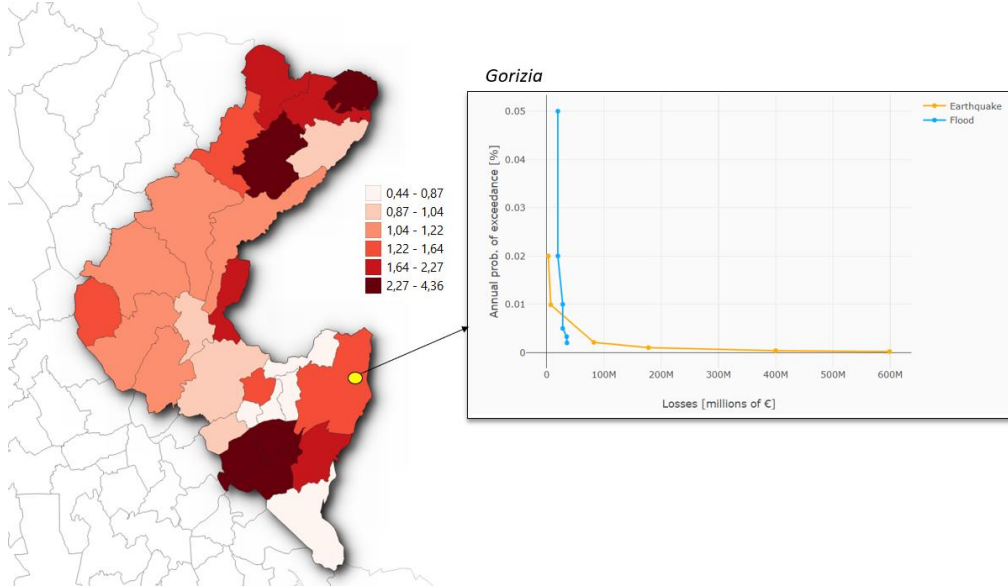


**Figure 6.6** – Map of the 27 Italian municipalities involved in the pilot application of BORIS project. The map shows the values of EAL/m<sup>2</sup> at municipal level. An example of LEC for seismic and flood risk is also reported.

Using the approach described in chapter 3, RI for all those municipalities is estimated as well. However, to be coherent with analysis performed in BORIS, RI should be slightly modified. More specifically, as in BORIS socio-economic aspects are not considered at all, the RI should not include such indicator. Moreover, as in EAL calculation physical exposure is accounted only in terms of buildings and not in terms of population, also the corresponding indicator (i.e., population) has not to be considered in evaluating RI. Therefore, Eq (7) is modified as follows:

$$RI = [F_h^s(h_j) \cdot F_{Pv}^s(v_j)]^{w_s} \cdot [F_h^f(h_j) \cdot F_{Pv}^f(v_j)]^{w_f} \quad (10)$$

where  $F_h^s(h_j)$ ,  $F_{Pv}^s(v_j)$ ,  $F_h^f(h_j)$  and  $F_{Pv}^f(v_j)$  are the ECDF values of the seismic hazard, physical vulnerability, flood hazard and flood (physical) vulnerability indicators, respectively, at municipality  $j$ ;  $w_s$  and  $w_f$  are the weights associated with seismic and flood risk, assumed to be equals. Models used for hazards and vulnerabilities are the same adopted in chapter 3.

Table 6.3 shows the values of EAL obtained in BORIS and RI values calculated using Eq (10) for each municipality. It can be noted that for several municipalities high value of EAL/m<sup>2</sup> corresponds to high value of RI (e.g., Farra d'Isonzo, Gradisca d'Isonzo, San Leonardo).

**Table 6-3** – Economic losses and RI values for the Italian municipalities involved in BORIS project. The ratio between EAL due to flood and EAL due to earthquake is also reported (Ratio).

Municipality	EAL (euro)	EAL/m <sup>2</sup>	Normalized EAL/m <sup>2</sup>	Ratio (F/S)	RI
Buttrio	307685	1.58	0.290	0.82	0.18
Capriva del Friuli	134831	1.61	0.299	1.87	0.38
Cividale del Friuli	637062	1.17	0.186	0.50	0.32
Cormons	306874	0.88	0.112	0.24	0.43
Corno di Rosazzo	157250	0.95	0.130	0.69	0.30
Doberdò del Lago	29620	0.44	0.000	0.00	0.03
Dolegna del Collio	35859	1.71	0.324	0.95	0.11
Drenchia	17104	2.32	0.480	1.95	0.05
Farra d'Isonzo	238524	2.66	0.567	3.81	0.57
Gorizia	1982808	1.27	0.213	1.35	0.30
Gradisca d'Isonzo	1351157	4.36	1.000	6.18	0.42
Grimacco	37132	2.11	0.427	1.03	0.07
Manzano	343023	1.06	0.159	0.43	0.38
Mariano del Friuli	78933	0.99	0.142	0.45	0.32
Moraro	32911	0.85	0.104	0.61	0.25
Mossa	66706	0.87	0.110	0.80	0.17
Premariacco	222243	1.07	0.160	0.27	0.24
Prepotto	50016	1.22	0.199	0.51	0.24
Sagrado	253021	2.47	0.518	5.73	0.24
San Floriano del Collio	26330	0.70	0.068	0.05	0.21
San Giovanni al Natisone	310758	1.07	0.161	0.63	0.30
San Leonardo	143749	2.41	0.504	2.34	0.32
San Lorenzo Isontino	55004	0.73	0.075	0.22	0.17
San Pietro al Natisone	140472	1.30	0.220	1.41	0.16
Savogna	50533	1.99	0.397	0.80	0.09
Savogna d'Isonzo	192003	2.18	0.443	4.74	0.31
Stregna	19187	0.92	0.124	0.66	0.11

Values of EAL/m<sup>2</sup> are standardized with maximum-minimum technique (see section 3.1), in order to obtain values between 0 and 1, compatible with RI ones. In figure 6.7 normalized values of EAL/ m<sup>2</sup> are related to RI values. The trendline in the figure shows a positive correlation between data. Despite such correlation is not strongly significant, generally larger the losses, higher the RI. As a matter of fact, municipalities with greatest value of EAL/ m<sup>2</sup> also have highest risk score (e.g., Gradisca di Isonzo). However, some municipalities do not show the same trend. For instance, in Drenchia expected losses are very high (2.3 euro/m<sup>2</sup> or

0.48 as normalized value) but estimated RI is very low (0.05). Similarly, for the city of Grimacco a value of losses of 2.11 euro/ m<sup>2</sup> corresponds to a RI of 0.07.

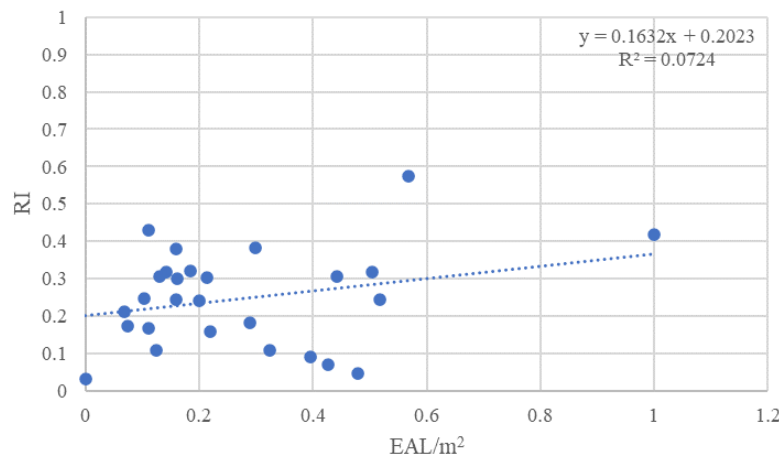
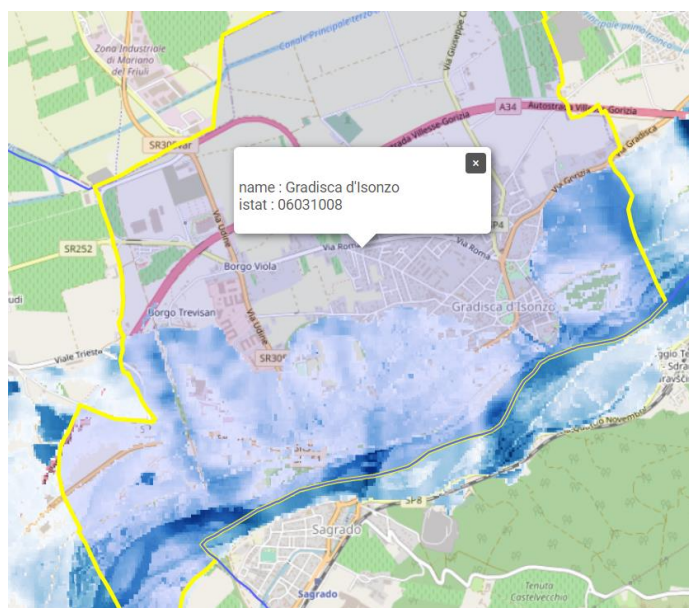


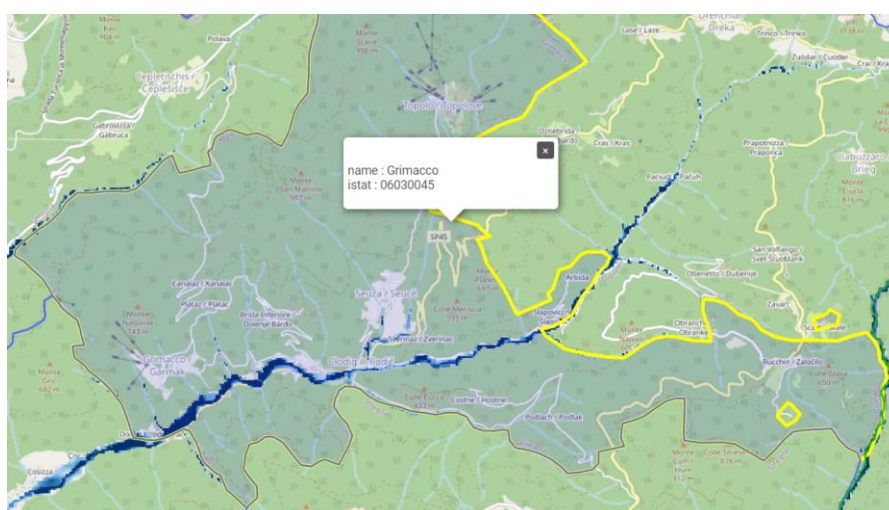
**Figure 6.7** – Analysis of correlation between RI and expected losses per square meters.

More detailed analysis of the dataset highlights that a possible cause of such discrepancy may be the value of the flood risk indicator adopted in RI calculation. Indeed, for the above-mentioned municipalities (i.e., Grimacco and Drenchia) value assumed for this indicator is very low. In Grimacco, flood hazard indicator assumes a value of 0.04. As the latter is representative of the inundated area within the municipality, this means that only the 4% of municipal surface is expected to be inundated by an event with a return period of 100 years (according to the model adopted for flood hazard). This indicator is considered representative of the exposure as well. Results obtained point out the main issue of such assumption, namely that the real distribution of buildings within the municipality is not taken into account in the definition of flood risk indicator. In fact, whether most of residential buildings are located nearby the river, they are supposed to be all inundated (leading to very high value of losses) even if the flood extent is relatively small with respect to the whole municipal surface. Figure 6.8 shows an example for two towns in the dataset: Gradisca d’Isonzo, where very high extent of flooded area (40%) leads to a high RI as well, and Grimacco where very low inundated surface (about 1%) causes a low RI.





(a)



(b)

**Figure 6.8** – Flood hazard maps for the cities of Gradisca d'Isonzo (a) and Premariacco (b), considering a flood event with a return period of 100 years. Source: BORIS.

To check the causes of observed discrepancies, the correlation between EAL caused only by earthquakes and the seismic risk score is analysed. It is reported in figure 6.9. A positive and significant correlation is observed between the seismic risk indicator and quantitative estimation of such risk (i.e., EAL) at municipal level. This result confirms that the lack of accuracy in some municipalities is probably due to simplified assumptions made for flood risk evaluation.

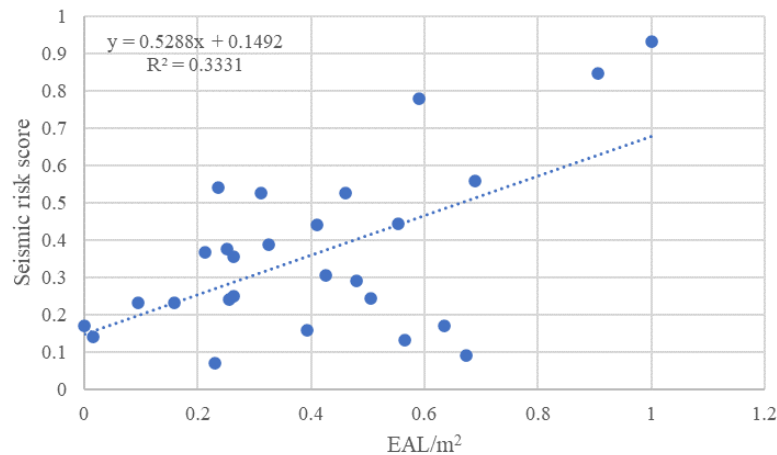


**Figure 6.9** - Analysis of correlation between seismic risk score and expected losses per square meters.

### 6.3. The need of defining the relative importance of indicators

The definition of the weighting methods to use to define the relative importance of individual indicators of the proposed approach is still an open issue. As already mentioned, several weighting techniques can be used, including both statistical models and participatory methods. Factor analysis and data envelopment analysis are examples of statistical approaches that could be used. Like principal component analysis, in factor analysis each factor reveals the set of indicators having the highest association with it (see also section 2.4.1). However, through such approach's weights cannot be estimated if no correlation exists between indicators (Nardo et al., 2008). Data Envelopment Analysis is a non-parametric methodology usually employed for frontier estimations in assessments of productivity and efficiency applied to all fields of economic activities. An ideal efficiency frontier is used as benchmark to measure the performance of a given set of countries. Countries are ranked according to the score of single indicators and the measurement of the distance of each country with respect to the benchmark is a measure of its performance: the countries nearest to the frontier are classified as the best performing, while more distant countries have lower performance. The set of weights derives from this comparison. Through an optimization process, the best combination of weights for a given country is obtained as the one that allows to get the best performance.

On the contrary, participatory approaches involve public or expert judgement. As already mentioned, in the BAP experts are given a budget of N points, to be



distributed over a number of indicators, paying more for those indicators whose importance they want to stress. An alternative are public opinion polls, consisting in asking people to express “much” or “little concern” about certain problems measured by the indicators. It is preferred to use in public polls instead of BAP, as it could be more difficult to ask the public to allocate a hundred points to several indicators than to express a degree of concern about the problems that the indicators represent. The Analytic Hierarchy Process is a multi-criteria decision-making tool. It consists in decomposing a problem into a hierarchy of more easily comprehended sub-problems, each of which can be analysed independently. The different levels of the problems are constituted by goal, criteria, sub-criteria and alternatives. Once the hierarchy is built, stakeholders compare the importance of various elements by comparing them to each other two at a time, with respect to their impact on an element above them in the hierarchy. For instance, by firstly posing the question “which of the two element is more important?” and secondly “by how much?”. These evaluations are then converted into numerical values, namely the numerical weight or priority derived for each element of the hierarchy.

As already highlighted in the Hyogo Framework for Action 2005-2015 and further underlined in the Sendai Framework for Disaster Risk Reduction 2015-2030, community-based and people-centred approaches are strongly recommended in DRM as they allow to incorporate local and indigenous knowledge into management plans. Public participation may act as a useful tool towards empowering individuals and communities threatened by hazards to act in a timely and appropriate manner. They enable people to explain their vulnerabilities and priorities, allowing local authorities to correctly define problems in order to design and implement suitable responsive measures. Several authors demonstrated the usefulness of such approaches in different context (Bustillos Ardaya et al., 2019; Stec & Jendrośka, 2019; Marchenzini et al. 2017; Ashu & Van Niekerk, 2019; Roopnarine et al., 2021). Therefore, one of the participatory approaches above presented should be adopted to assigne suitable weighs in the proposed index-based approach as well.

## 6.4. Conclusion

The applications shown in chapter 4, 5 and 6 highlighted the prominent advantages of the framework proposed herein. The calculation of RI at municipal level allows to rank all municipalities in a given region based on their propension to suffer losses due to earthquakes and floods and the potential capacity of inhabitants to react to such losses. Hence, it may be a useful support for identifying hotspots in decision-making process, without the need of complex and time-consuming analysis. Data collection and preparation is very easy as well, as only publicly available data and models are adopted. Such characteristics make the index-based approach particularly suitable for large scale (national or regional) investigations. In this chapter was also underlined as this tool can be easily used and modified based on stakeholders' needs. Further hazards can be included in the estimation simply adding a parameter to the RI equation. On the other hand, the RI can be also used to assess the interaction of a specific hazard with social vulnerability. Application proposed in chapter 4 also shown the versatility of this approach, that it is able to account for more refined regional exposure and vulnerability models.

Municipalities can be classified based on RI value and detailed multi-risk assessment is suggested for those with highest score. As a matter of fact, one of the limit of index is being a semi-quantitative approach. In other words, it does not allow a quantitative estimation of expected losses, crucial for preparedness and response actions planning. A simplified methodology for modelling the implementation of hard and soft mitigation actions in multi-risk assessment was proposed. The results of the analysis shown that a significant reduction in losses may be obtained adopting the proposed risk reduction strategies, although the convenience of one policy with respect to another one may vary from town to town as well as for different areas of a same municipality.

A measure of representativeness of the RI proposed is also evaluated through the comparison with outcomes of detailed risk assessment in terms of EAL. To this aim, results of multi-layer single risk assessment performed in BORIS project is considered. The  $EAL/m^2$  obtained for 27 Italian municipalities, calculated accounted both seismic and flood risk, is compared with a suitable modified RI.

A positive correlation is observed, i.e., larger the EAL higher the RI. However, discrepancies observed for some municipalities pointed out the main limitation of the approach. The latter concerns the assessment of buildings potentially exposed to flood. A large-scale analysis like the one proposed herein does not allow a proper estimation of the flooding exposure, that should require information at building level (i.e., building footprint). This inaccurate evaluation may significantly change results in terms of RI. Therefore, further analysis and modifications would be needed to get to a refined and more reliable version of the multi-dimensional risk index proposed.

Despite the mentioned limits, it was demonstrated that the proposed framework is likely to represent a helpful tool for decision-makers, enabling them to select appropriate, cost-effective mitigation or preparedness measures that directly target those most in need. Last but not the least, the framework can directly integrate relevant subjective perspectives, through the weights used as part of the RI calculation, e.g., adopting participatory methods as the Budget Allocation Process to account for expert and decision-makers' opinions and assign suitable weights for each indicator based on the defined aims. Similarly, decision makers' and other stakeholders' priorities can be taken into account in the detailed analysis stage, through the selection and the choice of mitigation strategies.

## References

- Adger, W. 2006. Vulnerability. *Global Environmental Change*. 16(3): 268–281.
- Alexander, D. 2012. Models of Social Vulnerability to Disasters. *RCCS Annual Review*. 10.4000/rccsar.412.
- Aljawhari, K., Gentile, R., Freddi, F. & Galasso, C. 2020. Effects of ground-motion sequences on fragility and vulnerability of case-study reinforced concrete frames. *Bulletin of Earthquake Engineering* 19: 6329–6359.
- Aljawhari, K., Gentile, R. & Galasso, C. 2021. Mapping performance-targeted retrofitting to seismic fragility reduction. *Proceedings of the 8th international conference on computational methods in structural dynamics and earthquake engineering methods in structural dynamics and earthquake engineering (COMPDYN'2021)*. Athens, 28–30 June, pp. 1301–1321. National Technical University of Athens.
- Aljawhari, K., Gentile, R., Galasso, C. & M.EERI. 2022. A fragility-oriented approach for seismic retrofit design. *Earthquake Spectra* 2022, Vol. 38(3) 1813–1843.
- Amadio, M., Scorzini, A.R., Carisi, F., Essensfelder, H.A., Domeneghetti, A., Mysiak, J., Castellarin, A. 2019. Testing empirical and synthetic flood damage models: the case of Italy. *Nat. Hazards Earth Syst. Sci.* 19. 661–678, <https://doi.org/10.5194/nhess-19-661-2019>.
- An, D., Gordon, P., Moore, J. I. & Richardson, H. 2004. “Regional Economic Models for Performance Based Earthquake Engineering,” *Natural Hazards Review*, 5(4), 188-94.
- Anuar, B. 2018. Flood Inundation Modeling and Hazard Mapping under Uncertainty in the Sungai Johor Basin. *Delft University of Technology, Malaysia*.
- Ardalan, A. & Mazaheri, M. 2010. Elders’ needs following the disasters: older people's needs following major disasters: a qualitative study of Iranian elders’ experiences of the Bam earthquake. *Ageing Soc.* 30 (2010) 11–23.
- Arrighi, C., Rossi, L., Trasforini, E., Rudari, R., Ferraris, L., Brugioni, M., Castelli, F. 2018. Quantification of Flood risk mitigation benefits: a building-scale damage assessment through the RASOR platform. *J Environ Manag* 207:92–104.
- Arseni, M., Rosu, A., Calmuc, M., Calmuc, V.A., Iticescu, C., Georgescu, L.P. 2020. Development of flood risk and hazard maps for the lower course of the Siret River. Romania. *Sustain.* 12 (16), 6588. <https://doi.org/10.3390/su12166588>.
- Ashu, R. E.A., Dewald, V.N. 2022. Building national and local capacity for disaster risk management in Cameroon. *Disaster Prev. Manag.* 29, pp. 457 – 470.
- Baggio, C., Bernardini, A., Colozza, R., Coppari, S., Corazza, L., Della Bella, M., Di Pasquale, G., Dolce, M., Goretti, A., Martinelli, A., Orsini, G., Papa, F., Zuccaro, G. 2007. Field manual for post-earthquake damage and safety assessment and short term countermeasures, *JRC Scientific and Technical Reports, EUR 22868 EN-2007*: Pinto A, Taucer F (eds). Translation from Italian: Goretti A, Rota M.
- Baker, J. W., Bradley, B. A. & Stafford, P. J. 2021. Seismic Hazard and Risk Analysis. *Cambridge University Press*, Cambridge, England.
- Balica, S., Douben, N. & Wright, N. 2009. Flood vulnerability indices at varying spatial scales. *Water Science and Technology* 60(10), 2571-2580.
- Barkham, R., Brown, K., Parpa, C., Breen, C., Carver, S., Hooton, C. 2014. Resilient Cities: A Grosvenor Research Report. *Grosvenor*.

- Barros, V.R., Field, C.B., Dokke, D.J., Mastrandrea, M.D., Mach, K.J., Bilir, T.E., Girma, B. 2014. Climate change 2014: Impacts, adaptation, and vulnerability. Part B: Regional aspects. *Contribution of Working Group II to the fifth assessment report of the Intergovernmental Panel on Climate Change*. Cambridge: Cambridge University Press .
- Bazzurro, P., Cornell, C., Menun, C. & Motahari, M. 2004. Guidelines for seismic assessment of damaged buildings. *13th World Conference on Earthquake Engineering, Vancouver, BC, Canada, Paper 1708*.
- Bellos, V. 2012. Ways for flood hazard mapping in urbanised environments : A short literature review. *Water Util. J.* 25–31.
- Bernardini, A., Lagomarsino, S., Mannella, A., Martinelli, A., Milano, L., Parodi, S. 2010. Forecasting seismic damage scenarios of residential buildings from rough inventories: a case-study in the Abruzzi Region (Italy). *Proc. IMech E Part O: J. Risk and Reliability*, 224: 279-296.
- Bertelli, S., Rossetto, T. & Ioannou, I. 2018. Derivation of empirical fragility functions from the 2009 Aquila earthquake, *16th European conference on earthquake engineering, Thessaloniki*, pp 1–12.
- Bevington, J., Eguchi, R., Huyck, C., Crowley, H., Dell’Acqua, F., Iannelli, G., Jordan, C., Morley, J., Wieland, M., Parolai, S., Pittore, M., Porter, K., Saito, K., Sarabandi, P., Wright, A., Wyss, M. 2012. Exposure Data Development for the Global Earthquake Model: Inventory Data Capture Tools. In: *Proceedings of the 15th World Conference on Earthquake Engineering, Lisbon*.
- Boisvert, R. 1992. “Indirect Economic Consequences of a Catastrophic Earthquake,” *Direct and Indirect Economic Losses from Lifeline Damage, under FEMA Contract EMW-90-3598, Development Technologies Inc., Chapter 7*.
- BORIS, 2022a. Deliverable 4.1: Guidelines for cross-border risk assessment: Shared framework for single and multirisk assessment at cross-border sites. Available at <http://www.borisproject.eu/wp-content/uploads/2022/06/BORIS-Deliverable-D4.1.pdf>
- BORIS, 2022b. Deliverable D5.1: Seismic risk, flood risk and multi-risk assessment at pilot cross-border sites. Available at <http://www.borisproject.eu/wp-content/uploads/2022/06/BORIS-Deliverable-D5.1.pdf>
- Borzi, B., Faravelli, M. & Di Meo, A. 2021. Application of the SP-BELA methodology to RC residential buildings in Italy to produce seismic risk maps for the national risk assessment. *Bulletin of Earthquake Engineering*, 19, 3185–3208, <https://doi.org/10.1007/s10518-020-00953-6>.
- Borzi, B., Pinho, R. & Crowley, H. 2008. Simplified pushover-based vulnerability analysis for large scale assessment of RC buildings. *Engineering Structures*, 30 (3) (2008), pp. 804–820.
- Braga, F., Dolce, M. & Liberatore, D. 1982. A statistical study on damaged buildings and an ensuing review of the MSK-76 scale. *Proceedings of the Seventh European Conference on Earthquake Engineering, (Athens)*, 431–450., s.n.
- Bruneau, M., Chang, S., Eguchi, R., Lee, G., O’Rourke, T., Reinhorn, A., Shinozuka, M., Tierney, K., Wallace, W., Winterfeldt, D. 2003. A Framework to Quantitatively Assess and Enhance the Seismic Resilience of Communities. *Earthquake Spectra - EARTHQ SPECTRA*. 19. 10.1193/1.1623497.
- Brunkard, J., Namulanda, G., Ratard, R. 2008. Hurricane Katrina deaths, Louisiana, 2005. *Disaster Med Public Health Prep*. 2008 Dec;2(4):215-23. doi: 10.1097/DMP.0b013e31818aaf55. PMID: 18756175.

- Brzev, S., C. Scawthorn, A.W. Charleson, L. Allen, M. Greene, K. Jaiswal, and V. Silva. 2013. GEM building taxonomy version 2.0. *GEM Technical Report 2013-02 V1.0.0*. Pavia, Italy: GEM Foundation.
- Bustillos Ardaya, A., Evers, M., Ribbe, L. 2019. Participatory approaches for disaster risk governance? Exploring participatory mechanisms and mapping to close the communication gap between population living in flood risk areas and authorities in Nova Friburgo Municipality, RJ, Brazil. *Land Use Policy*, Volume 88, 2019, 104103, ISSN 0264-8377, <https://doi.org/10.1016/j.landusepol.2019.104103>.
- Cacace, F., Zuccaro, G., D. G. D. & Perelli, F. 2018. Building Inventory at National scale by evaluation of seismic vulnerability classes distribution based on Census data analysis: BINC procedure. *International Journal of Disaster Risk Reduction*, 28, pp. 384-393.
- Cardona, O. 1986. Estudios de vulnerabilidad y evaluación del riesgo sísmico: Planificación física y urbana en áreas propensas. *Boletín Técnico de la Asociación Colombiana de Ingeniería Sísmica*, 33(2), 32-65.
- Cardona, O. & Carreño, M. 2011. Updating the Indicators of Disaster Risk and Risk Management for the Americas. *IDRiM (2011) 1(1) ISSN: 2185-8322*.
- Cardona, O.D., Ordaz, M., Reinoso, E., Yamín, L.E., Barbat, A.H. 2012. CAPRA—Comprehensive approach to probabilistic risk assessment: International initiative for risk management effectiveness. *Proceedings of the 15th world conference on earthquake engineering*, 24–28 September 2012, Lisbon, Portugal.
- Cariam. 2006. Plans de prévention des risques naturels prévisibles (ppr). *Cahier de recommandations sur le contenu des ppr. Tech. rep., Ministère de l'Écologie et du Développement Durable (in French)*.
- Carnelli, F. & Frigerio, I. 2016. A socio-spatial vulnerability assessment for disaster management: Insights from the 2012 Emilia earthquake (Italy). *Sociologia Urbana E Rurale* 111: 22-44.
- Carpignano, A., Golia, E., Di Mauro, C., Bouchon, S., Nordvik, J.-P. 2009. A methodological approach for the definition of multi-risk maps at regional level: first application. *Journal of Risk Research*, 12, 513–534.
- Casajus Valles, A., Marin Ferrer, M., Poljanšek, K. & Clark, I. 2020. Science for Disaster Risk Management 2020: acting today, protecting tomorrow. *EUR 30183 EN, Publications Office of the European Union, Luxembourg, 2020, ISBN 978-92-76-18181-1, doi:10.2760/438998, JRC114026*.
- Chaudhuri, G., Clarke, K. 2013. The SLEUTH Land Use Change Model: A Review. *Environ. 625 Resour. Res.* 1, 88–105.
- Chang, K.-T., Chiang, S.-H. & Hsu, M.-L. 2007. Modeling typhoon- and earthquake-induced landslides in a mountainous watershed using logistic regression. *Geomorphology* 89: 335{347.
- Chang, L., Lin, C. & M.-D. 2008. Application of geographic weighted regression to establish flood-damage functions reflecting spatial variation. *Water SA [online]* 34(2) (2008) 209–216.
- Chang, S. 2000. “Transportation Performance, Disaster Vulnerability and Long-Term Effects of Earthquakes,” *Second Euro Conference on Global Change and Catastrophe Risk Management, Luxemburg, Austria, July 6-9*.
- Chang, S., Pasion, C., Tatebe, K. & Ahmad, R. 2008. *Linking lifeline infrastructure performance and community disaster resilience: models and multi-stakeholder processes. Technical Report MCEER-08-0004*.

- Chaudhuri, G. & Clarke, K. 2013. The SLEUTH land use change model: A review. *Environ. Resour. Res.* 1, 88–105.
- Chen, W., Cutter, S., Emrich, C. & Shi, P. 2013. Measuring social vulnerability to natural hazards in the Yangtze River Delta region, China. *International Journal of Disaster Risk Science* 4(4): 169–181.
- Chiesa, C., Laben, C. & Cicone, R. 2003. An Asia Pacific natural hazards and vulnerabilities atlas. *30th international symposium on remote sensing of environment*.
- Choine, M.N., O'Connor, A., Gehl, P., D'Ayala, D., Garcia-Fernández, M., Jiménez, M., Gavin, K., Van Gelder, P., Salceda, T., Power, R. 2015. A multihazard risk assessment methodology accounting for cascading hazard events. *12th International Conference on Applications of Statistics and Probability in Civil Engineering, ICASP12, Vancouver, Canada*.
- Coburn, A., Spence, R. & Pomonis, A. 1992. Factors determining human casualty levels in earthquakes: mortality prediction in building collapse. *Proceedings of the 10th world conference on earthquake engineering*, pp 5989–5994.
- Cohen, S., Brakenridge, G.R., A., Kettner, Bates, B., Nelson, J., McDonald, R., Huang, Y., Munasinghe, D., Zhang, J. 2018. Estimating Floodwater Depths from Flood Inundation Maps and Topography. *Journal of the American Water Resources Association*, 54 (4), 847–858.
- Cremen, G., Galasso, C. & McCloskey, J. 2021. Modelling and quantifying tomorrow's risks from natural hazards. *Science of the Total Environment*, Volume 817(4):152552; 10.1016/j.scitotenv.2021.152552.
- Cremen, G., Galasso, C. & McCloskey, J. 2022 . A simulation-based framework for earthquake risk-informed and people-centered decision making on future urban planning. *Earth's Future*, 10, e2021EF002388. <https://doi.org/10.1029/2021EF002388>.
- Crowley, H., Despotaki, V., Rodrigues, D., Silva, V., Toma-Danila, D., Riga, E., Karatzetou, A., Fotopoulou, S., Zugic, Z., Sousa, L., Ozcebe, S., Gamba, P. 2020a. Exposure model for European seismic risk assessment. *Earthquake Spectra*; DOI: 10.1177/8755293020919429.
- Crowley, H., V. Despotaki, D. Rodrigues, V. Silva, C. Costa, D. Toma-Danila, E. Riga, A. Karatzetou, et al. 2020b. European exposure model data repository (v0.9). *Zenodo*. <https://doi.org/10.5281/zenodo.4402820>. Accessed 12 Dec 2021.
- Crowley, H., Ozcebe, S., Baker, H., Foulser-Piggott, R., Spence, R. 2014. D7. 2 State of the knowledge of building inventory data in Europe, *NERA Deliverable, 7, v3*.
- Crowley, H., M. Colombi, V. Silva, N. Ahmad, M. Fardis, G. Tsionis, A. Papailia, F. Taucer, et al. 2011. D3.1 Fragility functions for common RC building types in Europe. *SYNER-G Deliverable 3.1*. <http://www.vce.at/SYNER-G/files/dissemination/deliverables.html>.
- Cutter, S., Boruff, B. & Shirley, W. 2003. Social vulnerability to environmental hazards. *Social Science Quarterly* 84(2):242–261.
- Cutter, S. L., Mitchell, J. & Scott, M. 2000. Revealing the Vulnerability of People and Places: A Case Study of Georgetown County, South Carolina. *Annals of the Association of American Geographers* 90(4):713–37.
- da Porto, F., Donà, M., Rosti, A., Lagomarsino, S., Cattari, S., Borzi, B., Onida, M., De Gregorio, D., Perelli, F.L., Del Gaudio, C., Ricci, P. & Speranza, E. 2021. Comparative analysis of the fragility curves for Italian residential masonry and RC buildings. *Bull Earthquake Eng* 19, 3209–3252. <https://doi.org/10.1007/s10518-021-01120-1>

- Dabbeek, J., & V. Silva. 2019. Modelling the residential building stock in the Middle East for multi-hazard risk assessment. *Natural Hazards* 100: 781–810.
- De Groeve, T., Poljansek, K. & Ehrlich, D. 2013. Recording Disaster Losses: Recommendation for a European approach, *EUR 26111, ENPublications Office of the European Union, Luxembourg, JRC83743*.
- De Pippo, T., Donadio, C., Pennetta, M., Petrosino, C., Terizzi, F., Valente, A. 2008. Coastal hazard assessment and mapping in northern. *Geomorphology* 97(3-4), 451-466.
- De Risi, R., Jalayer, F., De Paola, F., Iervolino, I., Giugni, M., Topa, M.E., Mbuya, E., Kyessi, A., Manfredi, G., Gasparini, P. 2013. Flood risk assessment for informal settlements. *Nat. Hazards* 69 (1) (2013) 1003–1032.
- de Ruiter, M. C., De Bruijn, J. A., Englhardt, J., Daniell, J. E., de Moel, H., Ward, P. J. 2021. The asynergies of structural disaster risk reduction measures: Comparing floods and earthquakes. *Earth's Future*, 9(1), e2020EF001531. <https://doi.org/10.1029/2020EF001531>.
- DeKay, M. L. & McClelland, G. H. 1993. Predicting loss of life in cases of dam failure and flash flood. *Risk Anal.*, 13, 193–205.
- Del Gaudio, C., De Martino, G., Di Ludovico, M., Manfredi, G., Prota, A., Ricci, P., Verderame, G.M. 2019. Empirical fragility curves for masonry buildings after the 2009 L'Aquila, Italy, earthquake. *Bull Earthq Eng* 17(11):6301–6330.
- Del Gaudio, C., Di Ludovico, M., Polese, M., Manfredi, G., Prota, A., Ricci, P., Verderame, G. 2020. Seismic fragility for Italian RC buildings based on damage data of the last 50 years. *Bulletin of earthquake engineering*, pp. 18 (5), pp 2023-2059, DOI 10.1007/s10518-0.
- Delmonaco, G., Margottini, C. & Spizzichino, D. 2006a. Report on New Methodology for Multi-Risk Assessment and the Harmonisation of Different Natural Risk Maps. *Deliverable 3.1, ARMONIA*.
- Delmonaco, G., Margottini, C. & Spizzichino, D. 2006b. ARMONIA Methodology for Multi-Risk Assessment and the Harmonisation of Different Natural Risk Maps. *Deliverable 3.1.1, ARMONIA*.
- DEMA. 2013. The Danish Emergency Management Agency (2013), *National Risk Profile (NRP)*.
- Dessler, A. 2021. Introduction to Modern Climate Change, *Cambridge: Cambridge University Press*.
- Di Ludovico, M., De Martino, G., Prota, A., Manfredi, G., Dolce, M. 2021. Damage Assessment in Italy, and Experiences After Recent Earthquakes on Reparability and Repair Costs. Akkar, S., Ilki, A., Goksu, C., Erdik, M. (eds) *Advances in Assessment and Modeling of Earthquake Loss. Springer Tracts in Civil Engineering* . Springer, Cham. [https://doi.org/10.1007/978-3-030-68813-4\\_4](https://doi.org/10.1007/978-3-030-68813-4_4).
- Di Pasquale, G., Orsini, G. & Romeo, R. W. 2005. New developments in seismic risk assessment in Italy. *Bulletin of Earthquake Engineering*, 101–128. doi: 10.1007/s10518-005-0202-1.
- Dilley, M., Chen, U. R. D., Lerner-Lam, A. & Arnold, M. 2005. Natural disaster hotspots: a global risk analysis. In: *Disaster Risk Management Series*, 5, The World Bank.
- Dolce, M., Prota, A., Borzi, B., da Porto, F., Lagomarsino, S., Magenes, G., Moroni, C., Penna, A., Polese, M., Speranza, E., Verderame, G. M., Zuccaro, G. 2021. Seismic risk assessment of residential buildings in Italy. *Bulletin of Earthquake Engineering*, 19, 2999–3032, <https://doi.org/10.1007/s10518-020-01009-5>.



- Dong, Y. & Frangopol, D. 2017. Probabilistic life-cycle cost-benefit analysis of portfolios of buildings under flood hazard. *Eng. Struct.* 142 (2017) 290–299.
- Dottori, F., Figueiredo, R., Martina, M., Molinari, D., Scorzini, A.R. 2016. INSYDE: a synthetic, probabilistic flood damage model based on explicit cost analysis. *Nat. Hazards Earth Syst. Sci. Discuss.* 2016. 1–23, <https://doi.org/10.5194/nhess-2016-163>.
- EERI (Earthquake Engineering Research Institute). 2000. World housing encyclopedia. Oakland, CA: EERI. <https://www.worldhousing.net/>. Accessed 12 Dec 2021.
- El Morjani, Z., Ebner, S., Boos, J., Abdel Ghaffar, E., Musani, A. 2007. Modelling the spatial distribution of five natural hazards in the context of the WHO/EMRO Atlas of Disaster Risk as a step towards threduction of the health impact related to disasters. *Int J Health Geogr* 6:1–28.
- Enke, D., Tirasirichai, C. & Luna, R. 2008. "Estimation of Earthquake Loss due to Highway Damage in the St. Louis Metropolitan Area: Part II - Indirect Loss.". ASCE Natural Hazards Review, Vol. 9, No. 1: 12-19.
- ESRI. 2017. ArcGIS for Desktop – Focal Statistics. *ESRI*: <http://desktop.arcgis.com/en/arcmap/10.3/tools/spatial-analyst-toolbox/focal-statistics.htm>.
- European Commission. 2011. Risk Assessment and Mapping Guidelines for Disaster Management. *European Commission staff working paper, European Union*.
- Fatemi, F., Ardalan, A., Aguirre, B., Mansouri, N., Mohammadfam, I. 2017. Social vulnerability indicators in disasters: Findings from a systematic review. *International Journal of Disaster Risk Reduction* 22: 219–227.
- Fekete, A. 2010. *Assessment of Social Vulnerability to River-Floods in Germany*.
- FEMA. 2003. Federal Emergency Management Agency. Multi-hazard loss estimation methodology earthquake model. *HAZUS-MH MR3 Technical Manual*.
- FEMA. 2009. Multi-hazard Loss Estimation Methodology – Flood Model HAZUS MH MR4. Technical Manual, *Department of Homeland Security, Federal Emergency Management Agency, Mitigation Division, Washington, DC, 2009*.
- FEMA. 2013. Federal Emergency Management Agency. Multi-hazard loss estimation methodology earthquake model,HAZUS-MH MR3 Technical Manual.
- FEMA. 2015. HAZUS MH 2.1, Technical Manual, Multi-Hazard Loss Assessment Methodology. *Federal Emergency Management Agency, Washington, D.C., USA*.
- FEMA. 2022. Hazus 5.1, Hazus Flood Technical Manual. *Federal Emergency Management Agency, Washington, D.C*.
- Fire and Disaster Management. 2022. "平成23年（2011年）東北地方太平洋沖地震（東日本大震災）について（第162報）（令和4年3月8日）
- Flanagan, B. E., Gregory, E. W., Hallisey, E. J., Heitgerd, J. L., Lewis, B. 2011. A Social Vulnerability Index for Disaster Management. *Journal of Homeland Security and Emergency Management: Vol. 8: Iss. 1, Article 3. DOI: 10.2202/1547-7355.1792*.
- Fleming, K., Parolai, S., Garcia-Aristizabal, A., S., Tyagunov, Vorogushyn, S., Kreibich, H., Mahlke, H. 2016. Harmonising and comparing single-type natural hazard risk estimations. *Annals of Geophysics* 59(2), So216.
- Foerster E, Krien Y, Dandoulaki M, Priest S, Tapsell S, Delmonaco G, Margottini C, Bonadonna C. 2009. Methodologies to assess vulnerability of structural systems. *Del. 1.1.1., ENSURE*, <http://eea.eionet.europa.eu/Public/irc/eionet->

[circle/airclimate/library?l=/public/2010\\_citiesproject/interchange/project\\_deliverables/ensure\\_del111pdf/\\_EN\\_1.0\\_&a=d](https://circle.airclimate/library?l=/public/2010_citiesproject/interchange/project_deliverables/ensure_del111pdf/_EN_1.0_&a=d), access 24 March 2011

Frigerio, I., Ventura, S., Strigaro, D., Mattavelli, M., De amicis, M., Mugnano, S., Boffi, M. 2016. A GIS-based approach to identify the spatial variability of social vulnerability to seismic hazard in Italy. *Applied Geography*. 74. 12 - 22. [10.1016/j.apgeog.2016.06.014](https://doi.org/10.1016/j.apgeog.2016.06.014).

Frigerio, I., Carnelli, F., Cabinio, M. & De Amicis, M. 2018. Spatiotemporal Pattern of Social Vulnerability in Italy. *Int J Disaster Risk Sci* (2018) 9:249–262. <https://doi.org/10.1007/s13753-018-0168-7>.

Galasso, C., Pregnolato, M. & Parisi, F. 2021. A model taxonomy for flood fragility and vulnerability assessment. *International Journal of Disaster Risk Reduction* 53 (2021) 101985.

Gamba, P., Jaiswal, K., Crowley, H. & Huyck, C. 2012. The GED4GEM project: development of a global exposure database for the Global Earthquake Model initiative. *Proceedings of the 15th World Conference on Earthquake Engineering, Lisbon*.

Garcia-Aristizabal, A., Di Ruocco, A. & Marzocchi, W. 2013. Naples test case. *European Commission project MATRIX, Project No.265138, D7.3*.

Gentile, R. & Galasso, C. 2020. Hysteretic energy-based state-dependent fragility for groundmotion sequences. *arthq.Eng. Struct. Dyn.* 50 (4), 1187–1203.

Ghosh, J. & Padgett, J. 2010. Aging considerations in the development of time-dependent seismic fragility curves. *Journal of Structural Engineering* 136(12), 1497.

Gill, J. & Malamud, B. 2014. Reviewing and visualising the interactions of natural hazards. *Reviews of Geophysics* 52, 680.

Gill, J. & Malamud, B. 2016. Hazard Interactions and interaction networks (cascades) within multi-hazard methodologies. *Earth System Dynamics* 7, 659.

Greco, S., Ishizaka, A., Tasiou, M. & Torrisi, G. 2019. On the Methodological Framework of Composite Indices: A Review of the Issues of Weighting, Aggregation, and Robustness. *Soc Indic Res* 141, 61–94 (2019). <https://doi.org/10.1007/s11205-017-1832-9>

Greensfelder, R. 1974. *California Department of Conservation, Division of Mines and Geology Map Sheet 23*.

GRS, 2018. National Disaster Risk Assessment, Version 2.0. *Government of the Republic of Slovenia (in Slovenian)*.

Grünthal, G. 1998. European Macroseismic Scale. *Chaiers du Centre Européen de Géodynamique et de Séismologie*, vol. 15 Luxembourg.

Grünthal, G., Thieken, A. H, Schwarz, J., Radtke, K. S., Smolka, A., Merz, B. 2006. Comparative risk assessments for the city of Cologne—storms, floods, earthquakes. *Natural Hazards*, 38(1), 21-44.

Guha-Sapir, D., Below, R. & Hoyois, P. H. 2016. EM-DAT: The CRED/OFDA International Disaster Database. [www.emdat.be](http://www.emdat.be). *Université Catholique de Louvain, Brussels, Belgium*.

Guillard-Goncalves, C., Cutter, S., Emrich, C. & Ze^zere, J. 2014. Application of Social Vulnerability Index (SoVI) and delineation of natural risk zones in Greater Lisbon, Portugal. *Journal of Risk Research* 18(5): 651–674.

Gutenberg, B. & Richter, C. F. 1944. *Frequency of earthquakes in California*.

- Hamideh, S., Sen, P. & Fischer, E. 2022. Wildfire impacts on education and healthcare: Paradise, California, after the Camp Fire. *Nat Hazards* 111, 353–387 (2022). <https://doi.org/10.1007/s11069-021-05057-1>
- Hewitt, K. & Burton, I. 1971. *Hazardousness of a place: a regional ecology of damaging events*. Toronto Press, Toronto and Buffalo.
- Huizinga, H. 2007. Flood Damage Functions for EU Member States. HKV Consultants, Contract No. 382442-F1SC awarded by the European Commission – *Joint Research Centre*.
- Huizinga, H., de Moel, H. & Szewczyk, W. 2017. Global Flood Depth-Damage Functions - Methodology and the Database with Guidelines. *Joint Research Centre*, 2017, <https://doi.org/10.2760/16510>. EUR 28552 EN.
- ICPR, 2002. (International Commission for the Protection of the Rhine) Non structural flood plain management – Measures and their effectiveness. *ICPR, Koblenz, Germany*, 2002.
- Iervolino, I., Giorgio, M. & Chioccarelli, E. 2015a. Age- and state-dependent seismic reliability of structures. *12th International Conference on Applications of Statistics and Probability in Civil Engineering. ICASP12, Vancouver, Canada*.
- Iervolino, I., Giorgio, M. & Polidoro, B. 2015b. Reliability of structures to earthquake clusters. *Bulletin of Earthquake Engineering* 13, 983-1002.
- Inter American Development Bank. 2010. Indicators for disaster risks management: program for Latin America and Caribbean.
- IPCC, 2014. Climate Change 2014: Impacts, adaptation, and vulnerability. Part A: Global and sectoral aspects – contribution of Working Group II to the Fifth Assessment Report of the Intergovernmental Panel on Climate Change. C.B., V.R. Barros, D.J. Dokken, K.J. Mach, M.D. Mastrandrea, T.E. Bilir, M. Chatterjee, K.L. Ebi, Y.O. Estrada, R.C. Genova, B. Girma, E.S. Kissel, A.N. Levy, S. MacCracken, P.R. Mastrandrea, and L.L. White: Cambridge University Press, Cambridge, United Kingdom and New York, NY, USA, pp. 1-32.
- ISO, 2009. ISO 31000:2009(en): Risk management—Principles and guidelines. <https://www.iso.org/obp/ui/#iso:std:iso:31000>.
- ISTAT, 2001. *Italian National Institute of Statistics (2001) 14° Censimento della popolazione*, Roma, 2001
- ISTAT, 2011. *Italian National Institute of Statistics (2011) 15° Censimento della popolazione*. Roma, 2011.
- ISTAT, 2016. *BES 2016 - Il benessere equo e sostenibile in Italia*, ISTAT.
- Jaiswal, K.S., & D.J. Wald. 2008. Creating a global building inventory for earthquake loss assessment and risk management. U.S. Geological Survey Open-File Report 2008-1160. Washington, DC: U.S. Department of the Interior, U.S. Geological Survey.
- Jesinghaus, J. 1997. In Moldan, B. And Billharz, S. (Eds). Sustainability Indicators. Report on the project on Indicators of Sustainable Development, John Wiley and Sons, Chichester.
- Jonkman, S., Bořkarjova, M., Kok, M. & Bernardini, P. 2008. Integrated hydrodynamic and economic modelling of flood damage in The Netherlands. *Ecol. Econ.* 66 (1) (2008) 77-90.
- JRC, E. C. 2015. Guidance for Recording and Sharing Disaster Damage and Loss Data. Towards the development of operational indicators to translate the Sendai Framework into action. EU expert working group on disaster damage and loss data.
- Juntunen, L. 2005. Addressing Social Vulnerability to Hazards. *Disaster Safety Review* 4(2):3–10.

- Kappes, M., Keiler, M. & Glade, T. 2010. From single- to multi-hazard risk analyses: a concept addressing emerging challenges. *Mountain risks: bringing science to society*. CERG Editions, Strasbourg, France, p.351.
- Kappes, S., Keiler, M., Von Elverfeldt, K. & Glade, T. 2012. Challenges of analysing multi-hazard risk: a review. *Natural Hazards* 64(2), 1925-1958.
- Kappos, A., Pitilakis, K. & Stylianidis, K. 1995. *Cost-Benefit Analysis for the Seismic Rehabilitation of Buildings in Thessaloniki, Based on a Hybrid Method of Vulnerability Assessment*.
- Kappos, A., Stylianidis, K. & Pitilakis, K. 1998. Development of Seismic Risk Scenarios Based on a Hybrid Method of Vulnerability Assessment. *Natural Hazards*, Vol. 17, No. 2, pp. 177-192.
- Karababa, F. & Pomonis, A. 2010. Damage data analysis and vulnerability estimation following the August 14, 2003 Lefkada Island, Greece, Earthquake. *Bulletin of Earthquake Engineering*, pp. 9. 1015-1046. 10.1007/s10518-010-9231-5.
- Karababa, F. & Pomonis, A. 2010. Damage data analysis and vulnerability estimation following the August 14, 2003 Lefkada Island, Greece, earthquake. *Bull Earthq Eng* 9:1015–1046.
- Karaman, H., Şahin, M. & A.S., E. 2008. Earthquake Loss Assessment Features of Maeviz-Istanbul (Hazturk). *Journal of Earthquake Engineering* 12(S2):175–186.
- Kelman, I. 2017. Urban design caused the Hurricane Harvey disaster Dezeen. <https://www.dezeen.com/2017/09/01/urban-design-caused-hurricane-harvey-disaster-houston-flooding-ilan-kelman-opinion/>
- Kelman, I. & Spence, R. 2003. A limit analysis of unreinforced masonry failing under floodwater pressures. *Masonry Int.* 16 (2) (2003) 51–61.
- Khazai, B., Vangelsten, B., Franchin, P., Daniell, J., Cavalieri, F., Plapp-Kunz, T., Iervolino, I., Esposito, S. 2012. A new approach to modeling post-earthquake shelter demand: integrating social vulnerability in systemic seismic vulnerability analysis. *Proceedings of the 15th world conference on earthquake engineering*.
- Kramer, S. 1996. *Geotechnical earthquake engineering*.
- Kreibich, H., Piroth, K., Seifert, I., Maiwald, H., Kunert, U., Schwarz, J., Merz, B., Thieken, H. 2009. Is flow velocity a significant parameter in flood damage modelling?. *Nat. Hazards Earth Syst. Sci.* 9 (5) (2009) 1679–1692.
- Kunz, M. & Hurni, L. 2008. Hazard maps in Switzerland: state-of-the-art and potential improvements. *Proceedings of the 6th ICA Mountain Cartography Workshop, Lenk, Switzerland*.
- Lacasse, S., Eidsvig, U., Nadim, F., Høeg, K., Blikra, L. 2008. Event tree analysis of Aknes rock slide hazard. *IV Geohazards Quebec, 4th Canadian Conf. on Geohazards*, pp. 551–557.
- Lagomarsino, S., Cattari, S. & Ottonelli, D. 2021. The heuristic vulnerability model: fragility curves for masonry buildings. *Bulletin of Earthquake Engineering*, pp. <https://doi.org/10.1007/s10518-021-01063-7>.
- Lagomarsino, S. & Giovinazzi, S. 2006. Macro seismic and mechanical models for the vulnerability and damage assessment of current buildings. *Bulletin of Earthquake Engineering volume 4*, pages 415–443.
- Lee, C.-T., Huang, C.-C., Lee, J.-F., Pan, K.-L., Lin, M.-L., Dong, J.-J. 2008. Statistical approach to earthquake-induced landslide susceptibility. *Engineering Geology* 100: 43/58.

- Lee, K. & Rosowsky, D. 2006. Fragility analysis of woodframe buildings considering combined snow and earthquake loading. *Structural Safety* 28(3), 289-303.
- Liu, Z., Nadim, F., Garcia-Aristizabal, A., Mignan, A., Fleming, K., Luna, B. 2015. A three-level framework for multi-risk assessment. *Georisk: Assessment and Management of Risk for Engineered Systems and Geohazards* 9(2), 59-74.
- Loat, R. 2010. Risk management of natural hazards in Switzerland. Tech. rep. Federal Office for the Environment FOEN.
- Lucantoni, A., Bosi, V., Bramerini, F., De Marco, R., Lo Presti, T., Naso, G., Sabetta, F. 2001. Il rischio sismico in Italia. *Ingegneria Sismica*, 1, 5-35.
- Luino, F. 2005. Sequence of instability processes triggered by heavy rainfall in the northern Italy. *Geomorphology* 66(1-4), 13-39.
- Maiti, S. 2007. *Defining a Flood Risk Assessment Procedure using Community Based Approach with Integration of Remote Sensing and GIS - Based on the 2003 Orissa Flood*. Thesis IIRS-India & ITC - the Netherlands.
- Marchesini, I., Salvati, P., Rossi, M., Donnini, M., Sterlacchini, S. 2021. Data-driven flood hazard zonation of Italy. *Journal of Environmental Management* 294 (2021) 112986.
- Marchezini V., Trajber R., Olivato D., Muñoz V.A., de Oliveira Pereira F., Oliveira Luz A.E. 2017. Participatory Early Warning Systems: Youth, Citizen Science, and Intergenerational Dialogues on Disaster Risk Reduction in Brazil. *International Journal of Disaster Risk Science*, 8 (4), pp. 390 - 401, Cited 45 times. DOI: 10.1007/s13753-017-0150-9
- Marin Ferrer, M., Vernaccini, L. & Poljansek, K. 2017. INFORM Index for Risk Management: Concept and Methodology, Version 2017. *EUR 28655 EN. Luxembourg (Luxembourg). Publications Office of the European Union; 2017. JRC106949.*
- Marzocchi, W., Mastellone, M. & Di Ruocco, A. 2009. Principles of Multi-Risk Assessment: Interactions Amongst Natural and Man-Induced Risks. *European Commission*. <http://cordis.europa.eu/documents/documentlibrary/106097581EN6.pdf>.
- Marzocchi, W., Sandri, L., Gasparini, P., Newhall, C., Boschi, E. 2004. Quantifying probabilities of volcanic events: the example of volcanic hazard at Mount Vesuvius. *Journal of Geophysical Research* 109, B11201.
- Marzocchi, W., Sandri, L. & Selva, J. 2008. BET\_EF: a probabilistic tool for long- and short-term eruption forecasting. *Bulletin of Volcanology* 70, 623.
- Marzocchi, W., Sandri, L. & Selva, J. 2010. BET\_VH: a probabilistic tool for long-term volcanic hazard assessment. *Bulletin of Volcanology* 72, 717.
- Mazziotta, M. & Pareto, A. 2013. Methods for Constructing Composite Indices: One for All or All for One?. *Rivista Italiana di Economia Demografia e Statistica*, Volume LXVII n. 2 Aprile-Giugno 2013.
- Mazziotta, M. & Pareto, A. 2015. On a generalized non-compensatory composite index for measuring socio-economic phenomena. *Social Indicators Research* 127(3): 983–1003.
- Mazzoni, S., Castori, G., Galasso, C., Calvi, P., Dreyer, R., Fischer, E., Fulco, A., Sorrentino, L., Wilson, J., Penna, A., Magenes, G. 2018. 2016–2017 Central Italy earthquake sequence: Seismic retrofit policy and effectiveness. *Earthquake Spectra* 34(4): 1671–1691.
- McCarthy, J., Canziani, O., Leary, N. & Dokken, D. 2001. Climate change 2001: impacts, adaptation and vulnerability. *Cambridge, UK: Cambridge University Press*.
- Medvedev, S. 1977. Seismic Intensity Scale M.S.K.-76. *Publ. Inst. Geophys. Pol. Acad. Sc., A-6 (117)*.

- Merz, B., Kreibich, H., Thieken, A. & Schmidtke, R. 2004. Estimation uncertainty of direct monetary flood damage to buildings. *Nat. Hazards Earth Syst. Sci.* 4 (1) 153-163.
- Mesta, C., Cremen, G. & Galasso, C. 2022. Urban growth modelling and social vulnerability assessment for a hazardous Kathmandu Valley. *Scientific Reports*. 12. 10.1038/s41598-022-09347-x.
- Mignan, A., Wiemer, S. & Giardini, D. 2014. The quantification of low-probability-high-consequences events: Part 1, a generic multi-risk approach. *Natural Hazards* 73(3), 1999-2022.
- Mimura, N., Yasuhara, K., Kawagoe, S., Yokoki, H., Kazama, S. 2011. Damage from the Great East Japan Earthquake and Tsunami-a quick report. *Mitigation and adaptation strategies for global change*, 16(7), 803-818. <https://doi.org/10.1007/s11027-011-9297-7>.
- Molina Palacios, S., Lang, D. & Lindholm, C. 2010. *SELENA: an open-source tool for seismic risk and loss assessment using a logic tree computation procedure*. *Comput Geosci* 36(2010):257–269.
- Molinari, D., Ballio, D. & Menoni, S. 2013 . Modelling the benefits of flood emergency management measures in reducing damages: a case study on Sondrio, Italy. *Nat. Hazards Earth Syst. Sci.*, 13, 1913–1927, 2013. <https://doi.org/10.5194/nhess-13-1913-2013>.
- Mori, F., Mendicelli, A., Moscatelli, M., Romagnoli, G., Peronace, E., Naso, G. 2020. A new Vs30 map for Italy based on the seismic microzonation dataset. *Engineering Geology*, Volume 275, ISSN 0013-7952, <https://doi.org/10.1016/j.enggeo.2020.105745>.
- Morrow, B. 1999. Identifying and Mapping Community Vulnerability. *Disasters* 23(1)1–18.
- Mouroux, P., E. Bertrand, M. Bour, B. Le Brun, S. Depinois, and P. Masure. 2004. The European RISK-UE project: An advanced approach to earthquake risk scenarios. In Proceedings of the 13th World Conference on Earthquake Engineering, 1–6 August 2004, Vancouver, Canada, paper no. 3329.
- Nardo, M., Saisana, M., Saltelli, A. & Tarantola, S. 2005. Tools for Composite Indicators Building. *Report number: JRC31473* Affiliation: *European Commission, Joint Research Centre (JRC)*.
- Nardo, M., Saisana, M., Saltelli, A., Tarantola, S., Hoffmann, A., Giovannini, E. 2008. Handbook on Constructing Composite Indicators: Methodology and User Guide. *Paris (France): OECD publishing; 2008. JRC47008*.
- Nascimento, N., Baptista, M., Silva, A., Lea Machado, M., Costa de Lima, Goncalves, J.M., Silva, A., Dias, R., Machado, E. 2006. *Flood-damage curves: methodological development for the Brazilian context*. *Water Pract. Technol.* 1 (1) (2006).
- Neri, M., Aspinall, W., Bertagnini, A., Baxter, P.J., Zuccaro, G., Andronico, D., Barsotti, S., D Cole, P., Ongaro, T.E., Hincks, T., Macedonio, G., Papale, Rosi, M., Santacroce, R., Woo, G. 2008. Developing an event tree for probabilistic hazard and risk assessment at Vesuvius. *Journal of Volcanology and Geothermal Research* 178(3), 397-415.
- Newhall, C. & Hoblitt, R. 2002. Constructing event trees for volcanic crises. A method for multi-hazard mapping in poorly known volcanic areas: an example from Kanlaon (Philippines). *Bulletin of Volcanology* 64, 3.
- Nguyen, H. & Akerkar, R. 2020. Modelling, Measuring, and Visualising Community Resilience: A Systematic Review. *Sustainability*. 12. 7896. 10.3390/su12197896.
- NIBS, N. I. o. B. S. 2004. *HAZUS-MH: users's manual and technical manuals*.

- NR&M. 2002. *Guidance on the Assessment of Tangible Flood Damages*, Department of Natural Resources and Mines, Queensland Government, Queensland, Australia, 2002.
- NTC. 2018. Norme Tecniche per le costruzioni. Decreto Ministeriale 17 Gennaio 2018. Supplemento Ordinario n. 8 alla Gazzetta Ufficiale n. 42 del 20 febbraio 2018.
- Odeh Engineers, I. 2001. Statewide hazard risk and vulnerability assessment for the state of Rhode Island Tech. rep., NOAA Coastal Services Center, [http://www.csc.noaa.gov/rihazard/pdfs/rhdisl\\_hazard\\_report.pdf](http://www.csc.noaa.gov/rihazard/pdfs/rhdisl_hazard_report.pdf), access 09 March 2010.
- OECD. 2018. *National Risk Assessments: A Cross Country Perspective*. Paris: OECD Publishing, <https://doi.org/10.1787/9789264287532-en>.
- Oliveri, E. & Santoro, M. 2000. *Estimation of urban structural flood damages: the case study of Palermo*. Urban Water J. 2 (2000) 223–234.
- Oliver-Smith, A. 1999. What is a disaster? Anthropological perspectives on a persistent question. *New York: Routledge*.
- OPCM 3519/06. Ordinanza del Presidente del Consiglio dei Ministri del 26 Aprile 2006. Gazzetta Ufficiale n. 108 del 11 maggio 2006.
- OPCM 3274/03. Ordinanza del Presidente del Consiglio dei Ministri del 20 Marzo 2003. Gazzetta Ufficiale n. 105 del 8 maggio 2003 - S.o. n.72.
- Pagani, M., Garcia-Pelaez, J., Gee, R., Johnson, K., Poggi, V., Styron, R., Weatherill, G., Simionato, M., Viganò, D., Danciu, L., Monelli, D. 2018. *Global Earthquake Model (GEM) Seismic Hazard Map (version 2018.1 - December 2018)*. DOI: 10.13117/GEM-GLOBAL-SEISMIC-HAZARD-MAP-2018-1.
- Papadopoulos, A., Bazzurro, P. & Marzocchi, W. 2020. Exploring probabilistic seismic risk assessment accounting for seismicity clustering and damage accumulation: part I. Hazard analysis. *Earthq. Spectra* 37 (2), 803–826 page 8755293020957338.
- Papathoma, M., Dominey-Howes, D., Zong, Y. & Smith, D. 2003. Assessing tsunami vulnerability, an example from Herakleio, Crete. *Natural Hazards and Earth System Sciences* 3, 377-389.
- Peacock, W., Morrow, B. & Gladwin, H. 1997. Hurricane Andrew and the Reshaping of Miami: Ethnicity, Gender, and the Socio-Political Ecology of Disasters. *Gainesville, Fla.: University Press of Florida*.
- Perles Roselló, M. & Cantarero Prados, F. 2010. Problems and challenges in analyzing multiple territorial risks: methodological proposals for multi-hazard mapping. *Boletín de la Asociación de Geógrafos Españoles*, 52, 399–404.
- Peter, B., Cohen, S., Lucey, R., Munasinghe, D., Raney, A., Brakenridge, R. 2022. Google Earth Engine Implementation of the Floodwater Depth Estimation Tool (FwDET-GEE) for Rapid and Large Scale Flood Analysis. *IEEE GEOSCIENCE AND REMOTE SENSING LETTERS*, VOL. 19, 2022.
- Petitta, M., Calmanti, S. & Cucchi, M. 2016. The extreme climate index: a novel and multi-hazard index for extreme weather events. *Geophysical Research Abstracts* 18, EGU2016—13861, EGU General Assembly 2016.
- Petrone, C., Rossetto, T., Goda, K. & Eames, I. 2016. Tsunami fragility curves of a RC structure through different analytical methods. *1st International Conference on Natural Hazards & Infrastructure (ICONHIC)*. Chania, Greece.
- Pitilakis, K., Crowley, H. & Kaynia, A. 2014. *SYNER-G: Typology Definition and Fragility Functions for Physical Elements at Seismic Risk: Buildings, Lifelines, Transportation*

*Networks and Critical Facilities*. SYNER-G: Typology Definition and Fragility Functions for Physical Elements at Seismic Risk.

Ploegeer, S.K., Sawada, M., Elsabbagh, A., Saatcioglu, M., Nastev, M., Rosetti, E. 2016. Urban RAT: New Tool for Virtual and Site-Specific Mobile Rapid Data Collection for Seismic Risk Assessment. *Journal of Computing in Civil Engineering* 30(2):04015006.

Polese, M., Di Ludovico, M., Prota, A. & Manfredi, G. 2012. Damage-dependent vulnerability curves for existing buildings. *Earthquake Engineering & Structural Dynamics* 42(6), 853–870.

Polese, M., Di Ludovico, M., Tocchi, G. & Prota, A. 2021. *The use of an integrated approach for building inventory and effects on risk estimations at the territorial scale*. Athens, 8th International Conference on Computational Methods in Structural Dynamics and Earthquake Engineering Methods in Structural Dynamics and Earthquake Engineering, January 2021, doi:10.7712/120121.8714.18981.

Polese, M., Gaetani d'Aragona, M. & Prota, A. 2019. Simplified approach for building inventory and seismic damage assessment at the territorial scale: an application for a town in southern Italy. *Soil dynamics and earthquake engineering*, 121, 405-420, DOI 10.1016/j.soildyn.2019.03.028.

Polese, M., Marcolini, M., Zuccaro, G. & F., C. 2015. Mechanism based assessment of damage-dependent fragility curves for rc building classes. *Bulletin of Earthquake Engineering* 13(5), 1323–1345.

Polese, M., Verderame, G.M., Mariniello, C., Iervolino, I., Manfredi, G. 2008. Vulnerability analysis for gravity load designed RC buildings in Naples–Italy. *Journal of Earthquake Engineering*, 12(S2) (2008), pp. 234-245.

Poljanšek, K., Casajus Valles, A., Marin Ferrer, M., De Jager, A., Dottori, F., Galbusera, L., Garcia Puerta, B., Giannopoulos, G., Girgin, S., Hernandez Ceballos, M., Iurlaro, G., Karlos, V., Krausmann, E., Larcher, M., Lequarre, A., Theocharidou, M., Montero Prieto, M., Naumann, G., Necci, A., Salamon, P., Sangiorgi, M., Sousa, M., Trueba Alonso, C., Tsionis, G., Vogt, J., Wood, M. 2019. Recommendations for National Risk Assessment for Disaster Risk Management in EU , EUR 29557 EN. *Publications Office of the European Union, Luxembourg, 2019, ISBN 978-92-79-98366-5 (online), doi:10.2760/084707 (online), JRC114650*.

Preedy, V. & Watson, R. 2010. Handbook of Disease Burdens and Quality of Life Measures. Springer, New York, NY. [https://doi.org/10.1007/978-0-387-78665-0\\_5051](https://doi.org/10.1007/978-0-387-78665-0_5051).

Renschler, C., Frazier, A., Arendt, L., Cimellaro, G., Reinhorn, A., Bruneau, M. 2010. Developing the 'PEOPLES' resilience framework for defining and measuring disaster resilience at the community scale. 10.13140/RG.2.1.1563.4323.

Ritchie, H., Rosado, P. & Roser, M. 2022. "Natural Disasters". *Published online at OurWorldInData.org*. Retrieved from: '<https://ourworldindata.org/natural-disasters>'.

Rodolico, F. 1965. Le pietre delle città d'Italia. Firenze: Le Monnier .

Rofiat, B. M., S., N., Ismail, A. & Waheed, B. 2021. Flood hazard mapping methods: A review. *Journal of Hydrology* 603 (2021) 126846.

Roopnarine, R., Eudoxie, G., Wuddivira, M.N., Saunders, S., Lewis, S., Spencer, R., Jeffers, C., Haynes-Bobb, T., Roberts, C. 2021. Capacity building in participatory approaches for hydro-climatic Disaster Risk Management in the Caribbean, International Journal of Disaster Risk Reduction, Volume 66, 2021, 102592, ISSN 2212-4209, <https://doi.org/10.1016/j.ijdr.2021.102592>.



- Rosenkoetter, M.M., Covan, E.K., Cobb, B.K., Bunting, S., Weinrich, M. 2007. Perceptions of older adults regarding evacuation in the event of a natural disaster. *Public Health Nurs.* 24 (2007) 160–168.
- Rossetto, T. & Elnashai, A. 2003. Derivation of vulnerability functions for European-type RC structures based on observational data. *Engineering Structures*, Volume Volume 25, Issue 10, 2003, pp. Pages 1241-1263, ISSN 0141-0296, [https://doi.org/10.1016/S0141-0296\(03\)00060-9](https://doi.org/10.1016/S0141-0296(03)00060-9).
- Rossetto, T. & Elnashai, A. 2005. A new analytical procedure for the derivation of displacement-based vulnerability curves for populations of RC structures. *Engineering structures*, 27(3) (2005), pp. 397-409.
- Rossetto, T. & Ioannou, I. 2018. Chapter 4 - Empirical Fragility and Vulnerability Assessment: Not Just a Regression. In: *Risk Modeling for Hazards and Disasters*. Gero Michel, Elsevier, 2018, Pages 79-103, ISBN 9780128040713, <https://doi.org/10.1016/B978-0-12-804071-3.00004-5>.
- Rosti, A., Rota, M. & Penna, A. 2021a. Empirical fragility curves for Italian URM buildings. *Bulletin of Earthquake Engineering*, DOI: 10.1007/s10518-020-00845-9.
- Rosti, A., Del Gaudio, C., Rota, M., Ricci, P., Di Ludovico, M., Penna, A., Verderame, G.M. 2021b. Empirical fragility curves for Italian residential RC buildings. *Bulletin of Earthquake Engineering*, <https://doi.org/10.1007/s10518-020-00971-4>.G.
- Rosti, A., Rota, M. & Penna, A. 2018. Damage classification and derivation of damage probability matrices from L'Aquila (2009) post-earthquake survey data. *Bull Earthq Eng* 16:3687–3720. <https://doi.org/10.1007/s10518-018-0352-6>.
- Rota, M., Penna, A. & Magenes, G. 2010. A methodology for deriving analytical fragility curves for masonry buildings based on stochastic nonlinear analyses. *Engineering Structures*, 32(5), pp. 1312-1323.
- Rota, M., Penna, A. & Strobbia, C. 2008. Processing Italian damage data to derive typological fragility curves. *Soil Dyn Earthq Eng* 28(10):933–947.
- Saito, K., Spence, R., Going, C. & Markus, M. 2004. Using high-resolution satellite images for post-earthquake buildings damage assessment: a study following the 26.1.01 Gujarat earthquake. *Earthquake Spectra*; 20(1):145-70.
- Salmoiraghi, F. 1982. *Materiali naturali da costruzione*. Milano: 1982.
- Sampson, C., Smith, A., Bates, P., Neal, J., Alfieri, L., Freer, J. 2015. A high-resolution global flood hazard model. *Water Resources Research*. 51. 10.1002/2015WR016954.
- Sanchez-Silva, M., Klutke, G. & Rosowsky, D. 2011. Life-Cycle Performance of Structures Subject to Multiple Deterioration Mechanisms. *Structural Safety* 33(3), 206–217.
- Saretta, Y., Sbrogiò, L. & M.R., V. 2021. Seismic response of masonry buildings in historical centres struck by the 2016 Central Italy earthquake. Calibration of a vulnerability model for strengthened conditions. *Construction and Building Materials*, Volume 299, 2021, 123911, ISSN 0950-0618, <https://doi.org/10.1016/j.conbuildmat.2021.123911>.
- Schmidtlein, T. & King, P. 1995. Risk factors for death in the 27 March 1994 Georgia and Alabama tornados. *Disasters* 19 (1995) 170–177.
- Schwarz, J. & Maiwald, H. 2012. *Empirical vulnerability assessment and damage for description natural hazards following the principles of modern microseism scales*, 15th World Conference on Earthquake Engineering, 24-28 September 2012, Lisbon, Portugal, 2012.

- Scorzini, A. & Frank, E., 2015. *Flood damage curves: new insights from the 2010 flood in Veneto, Italy*. *J. Flood Risk Manag.* (2015) 1–12, <https://doi.org/10.1111/jfr3.12163>.
- Seifert, I., Kreibich, H., Merz, B. & Thieken, A. 2010. *Application and validation of FLEMOcs – a flood loss estimation model for the commercial sector*. *Hydrol. Sci. J.* 55 (2010) 1315–1324.
- Selva, J. 2013. Long-Term Multi-Risk Assessment: Statistical Treatment of Interaction among Risks. *Natural Hazards* 67(2), 701-722.
- Selva, J., Marzocchi, W., Papale, P. & Sandri, L. 2012. Operational Eruption Forecasting at High-Risk Volcanoes: The Case of Campi Flegrei, Naples. *Journal of Applied Volcanology, Society and Volcanoes*, 1, 5.
- Shi, P., Shuai, J., Chen, W. & Lu, L. 2010. Study on the risk assessment and risk transfer mode of large scale disasters. *The 3rd International Disaster and Risk Conference IDRC, Davos, Switzerland*.
- Silva, M. & Pereira, S. 2014. Assessment of Physical Vulnerability and Potential Losses of Buildings due to Shallow Slides. *Natural Hazards* 72(2), 1029-1050.
- Silva, V., Yepes-Estrada, C., Dabbeek, J., Martins, L., Brzev, S. 2018. GED4ALL - Global Exposure Database for Multi-Hazard Risk Analysis—Multi-Hazard Exposure Taxonomy. *GEM Technical Report 2018-01. GEM Foundation, Pavia, Italy*.
- Silva, V., Brzev, S., Yepes-Estrada, C., Dabbeek, J., Crowley, H. 2022. A Building Classification System for Multi-hazard Risk Assessment. *International Journal of Disaster Risk Science*. 13. [10.1007/s13753-022-00400-x](https://doi.org/10.1007/s13753-022-00400-x).
- Silvestro, F., Rebora, N., Rossi, L., Dolia, D., Gabellani, S., Pignone, F., Trasforini, E., Rudari, R., De Angeli, S., Masciulli, C. 2016. What if the 25 October 2011 event that struck Cinque Terre (Liguria) had happened in Genoa, Italy? Flooding scenarios, hazard mapping and damage estimation. *Nat. Hazards Earth Syst. Sci.*, 16, 1737–1753, <https://doi.org/10.5194/nhess-16-1737-2016>.
- Simon, C., Belyakov, A. & Feichtinger, G. 2012. Minimizing the dependency ratio in a population with below-replacement fertility through immigration. *Theoretical Population Biology, Volume 82, Issue 3, 2012, Pages 158-169, ISSN 0040-5809*, <https://doi.org/10.1016/j.tpb.2012.06.009>.
- Singhal, A. & Kiremidjian, A. S. 1996. Method for Probabilistic Evaluation of Seismic Structural Damage. *Journal of Structural Engineering, Vol. 122, Issue 12 (December 1996)*, [https://doi.org/10.1061/\(ASCE\)0733-9445\(1996\)122:12\(1459\)](https://doi.org/10.1061/(ASCE)0733-9445(1996)122:12(1459)).
- Smith, D. 1994. *Flood damage estimation - a review of urban stage damage curves and loss functions*. *WaterSA* 20 (3) (1994) 231–238.
- Sohrabizadeh, S., Tourani, S. & Khankeh, H. 2014. The gender analysis tools applied in natural disasters management: a systematic literature review. *PLOS Currents Disasters*. 2014 Mar 18 . Edition 1. [doi: 10.1371/currents.dis.5e98b6ce04a3f5f314a8462f60970aef](https://doi.org/10.1371/currents.dis.5e98b6ce04a3f5f314a8462f60970aef).
- Solangaarachchi, D., Griffin, A. & Doherty, M. 2012. Social vulnerability in the context of bushfire risk at the urban-bush interface in Sydney: A case study of the Blue Mountains and Kuring-gai local council areas. *Natural hazards* 64(2): 1873–1898.
- Soltani, M., Abu-Abaileh, A. & Scott Rowe, B. 2021. Statistical approach to modeling reduced shear capacity of corrosion-damaged reinforced concrete beams. *Pract. Period. Struct. Des. Constr.* 26 (2), 04020073.

- Spence, R., Coburn, A. & Pomonis, A. 1992. *Correlation of ground motion with building damage: the definition of a new damage-based seismic intensity scale*. Proceedings of 10th world conference on earthquake engineering, Balkema, Rotterdam.
- Spence, R., Foulser-Piggott, R., Pomonis, A., Crowley, H., Gue'guen, P., Masi, A., Chiauuzzi, L., Zuccaro, G., Cacace, F., Zulfikar, C., Markus, M., Schaefer, D., Sousa, M.L., Kappos, A. 2012. The European building stock inventory: creating and validating a uniform database for earthquake risk modeling and validating a uniform database for earthquake risk modeling risk modeling. *The 15th world conference on earthquake engineering, Sept 2012, Lisbon, Portugal*.
- Spence, R., So, E. & Scawthorn, C. 2011. Human casualties in earthquakes: progress in modelling and mitigation. 29. *Springer, Berlin. Ed, Vol. 29. Springer, Berlin*.
- Stec, S., Jendro'ska, J. 2019. The Escazú Agreement and the Regional Approach to Rio Principle 10: Process, Innovation, and Shortcomings, *Journal of Environmental Law, Volume 31, Issue 3, November 2019, Pages 533–545, <https://doi.org/10.1093/jel/eqz027>*
- Stewart, J., Zimmaro, P., Lanzo, G. & Mazzoni, S. 2018. Reconnaissance of 2016 Central Italy earthquake sequence. *Earthquake Spectra* 34(4): 1547–1555.
- Stucchi, M., Akinci, A., Faccioli, E., Gasperini, P., Malagnini, L., Meletti, C., Montaldo, V., Valensise, G. 2004. *Mappa di Pericolosità sismica del territorio Nazionale [http://zonesismiche.mi.ingv.it/documenti/rapporto\\_conclusivo.pdf](http://zonesismiche.mi.ingv.it/documenti/rapporto_conclusivo.pdf) (in italian)*.
- Stucchi, M., Meletti, C., Montaldo, V., Crowley, H., Calvi, G.M., Boschi, E. 2011. *Seismic hazard assessment (2003-2009) for the Italian building code*. Bull Seism Soc of Am 101:1885–1911.
- Tarvainen, T. J. J. G. S. 2006. Spatial Pattern of Hazards and Hazard Interactions in Europe. *Natural and Technological Hazards and Risks Affecting the Spatial Development of European Regions. Schmidt-Thomé, P. (Ed.), Geological Survey of Finland, Special Paper 42, 83*.
- Tate, E., Muñoz, C. & Suchan, J. 2014. Uncertainty and Sensitivity Analysis of the HAZUS-MH Flood Model. *Natural Hazards Review*. 16. 04014030. 10.1061/(ASCE)NH.1527-6996.0000167.
- Taubenböck, H., Esch, T. & Roth, A. 2006. An urban classification approach based on an object-oriented analysis of high resolution satellite imagery for a spatial structuring within urban areas. *Proceedings of the 1st EARSeL workshop of the SIG urban remote sensing, Berlin*.
- Thierry, P., Stieltjes, L., Kouokam, E., Nguya, P., Salley, P. M. 2008. Multi-hazard risk mapping and assessment on an active volcano: the GRINP project at Mount Cameroon. *Natural Hazards* 45: 429/456.
- Tocchi, G., Polese, M., Di Ludovico, M. & Prota, A. 2022a. Regional based exposure models to account for local building typologies. *Bulletin of Earthquake Engineering* 20 (11), January 2022.
- Tocchi, G., Polese, M. & Prota, A. 2022b. Improving building inventory with a machine learning approach: application in southern Italy. *Turin, Italy, XIX ANIDIS Conference, Seismic Engineering in Italy, September 2022*.
- Toombes, L. & Chanson, H. 2011. *Numerical Limitations of Hydraulic Models*. 34th IAHR World Congress - Balance and Uncertainty 33rd Hydrology & Water Resources Symposium 10th Hydraulics Conference. Brisbane, Australia, pp. 2322–2329.
- Tyagunov, S., Heneka, P., Stempniewski, L., Zschau, J., Ruck, B., Kottmeier, C. 2005, In Proceedings of the 1st ARMONIA conference. Barcelona, Spain.

- U.S., D. o. T. 2006. *June 1, 2006. Catastrophic Hurricane Evacuation Plan Evaluation: A Report to Congress.*
- UNDRO. 1980. Natural disasters and vulnerability analysis : report of Expert Group Meeting, 9-12 July 1979. *Office of the United Nations Disaster Relief Coordinator.*
- UNDRR. 2016. <https://www.unisdr.org/we/inform/publications/51748>.
- UNDRR. The TEN Essentials for Making Cities Resilient.  
<https://www.unisdr.org/campaign/resilientcities/toolkit/article/the-ten-essentials-for-making-citiesresilient.html>
- UNDRR. 2009. *Terminology on Disaster Risk Reduction.* [Online] Available at: (<http://www.unisdr.org/we/inform/terminology>)
- UNDRR. 2015. (*United Nations International Strategy for Disaster Reduction*). *Sendai framework for disaster risk reduction 2015–2030.* Geneva: UNISDR.
- UNDRR. 2015. *Global Assessment Report.* United Nations Office for Disaster Risk Reduction. ISBN/ISSN/DOI.
- UNDRR. 2018. United Nations Office for Disaster Risk Reduction: 2018 annual report.
- UNDP (United Nations Development Programme). 2010. Human Development Report 2010: The Real Wealth of Nations: Pathways to Human Development. New York.
- United Nations Development Programme. 2020. *The Next Frontier: Human Development and the Anthropocene.* (2020), *Human Development Report 2020.*
- USACE. 1985. *Business Depth–Damage Analysis Procedures, US Army Corps of Engineers, Engineering Institute for Water Resources, Alexandria, VA, 1985. Research Rep.85-R-5.*
- Van Westen, C. J., Quan Luna, B. & Vargas Franco, R. D. 2010. Development of training materials on the use of geo – information for multi – hazard risk assessment in a mountainous environment. *J.-P. Malet, T. Glade and N. Casagli (eds), Mountain Risks: Bringing Science to Society : Proceedings of the Mountain Risks International Conference, 24–26 November 2010, Firenze, Italy. CERIG, Strasbourg. ISBN 2-95183317-1-5. pp. 469–475.*
- Velásquez, C.A., Cardona, O.D., Mora, M.G., Yamin, L. E., Carreno Tibaduiza, M.L., Barbat, A. H. 2014. Hybrid loss exceedance curve (HLEC) for disaster risk assessment. *Natural Hazards. Doi: 72.10.1007/s11069-013-1017-z.*
- Wachinger, G., Renn, O., Begg, C. & Kuhlicke, C. 2013. The Risk Perception Paradox—Implications for Governance and Communication of Natural Hazards. *Risk Analysis, Vol. 33, No. 6, 2013.*
- Wald, D. J., Worden, C. B., Quitoriano, V. & Pankow, K. L. 2006. *ShakeMap® Manual, technical manual, users guide, and software guide, available at <http://pubs.usgs.gov/tm/2005/12A01/pdf/508TM12-A1.pdf>, 156 pp.*
- Wang, J., Huang, D. & Yang, Z. 2012. *Deterministic seismic hazard map for Taiwan developed using an in-house Excel-based program.*
- Wang, Y., Hong, H., Chen, W., Li, S., Pamučar, D., Gigović, L., Drobnjak, S., Bui, D.T., Duan, H. 2019. A hybrid GIS multi-criteria decision-making method for flood susceptibility mapping at Shangyou. *China. Remote Sens. 11 (1), 62. <https://doi.org/10.3390/rs11010062>.*
- Weatherill, G. A., Kotha, S. R., Cotton, F., Danciu, L. 2020. Innocations in ground motion characterization for the 2020 European seismic hazard model (ESHM2020). 7th World Conference on Earthquake Engineering, Sendai, Japan, September 2020.

- Westen, C. & Greiving, S. 2017. Environmental Hazards Methodologies for Risk Assessment and Management. In: *Environmental hazards Methodologies for Risk Assessment and Management. International Water Institute (IWA) publishing* Editors: N.R. Dalezios.
- Whitman, R. V., Reed, J. W. & Hong, S. T. 1973. Earthquake damage probability matrices, *Proceedings of the Fifth World Conference on Earthquake Engineering (Rome)*, 2531–2540.
- Wieland, M., Pittore, M., Parolai, S., Zschau, J., Moldobekov, B., Begaliev, U. 2012. Estimating building inventory for rapid seismic vulnerability assessment: Towards an integrated approach based on multi-source imaging. *Soil Dynamics and Earthquake Engineering* 36:70–83.
- Wisner, B., Blaikie, P., Cannon, T. & Davis, I. 1994. At Risk: Natural Hazards, People's Vulnerability, and Disasters. *Routledge, London*.
- Wisner, B., Blaikie, P., Cannon, T. & Davis, I. 2004. At Risk: Natural Hazards, People's Vulnerability and Disasters. *London: Routledge*.
- WMO. 1999. Technical document 955, World Meteorological Organisation, [http://www.planat.ch/ressources/planat\\_product\\_en\\_198.pdf](http://www.planat.ch/ressources/planat_product_en_198.pdf), access 05 May 2010.
- Woessner, J., Laurentiu, D., Giardini, D., Crowley, H., Cotton, F., Grünthal, G., Valensise, G., Arvidsson, R., Basili, R., Demircioglu, M.B., Hiemer, S., Meletti, C., Musson, R.W., Rovida, A.N., Sesetyan, K., Stucchi, M., Consortium, the SHARE. 2015. The 2013 European seismic hazard model: key components and results. *Bulletin of Earthquake Engineering*, 13(12), 3553-3596.
- Wood, N., Burton, C. & Cutter, S. 2010. Community variations in social vulnerability to Cascadia-related tsunamis in the US Pacific Northwest. *Natural Hazards* 52(2): 369–389.
- Xu, L., Meng, X. & Xu, X. 2014. Natural Hazard Chain Research in China: A Review. *Natural Hazards* 70(2), 1631-1659.
- Yamaguchi, N. & Yamazaki, F. 2000. Fragility curves for buildings in Japan based on damage surveys after the 1995 Kobe earthquake.
- Yepes-Estrada, C., Silva, V., Valcárcel, J., Acevedo, A.B., Tarque, N., Hube, M., Coronel, D.G., Santa-Maria, H. 2017. Modeling the Residential Building Inventory in South America for Seismic Risk Assessment. *Earthquake Spectra* 33(1), p. 299–322. doi: 10.1193/101915EQS155DP.
- Yoon, D. 2012. Assessment of social vulnerability to natural disasters: A comparative study. *Natural Hazards* 63(2): 823–843.
- Zamanian, S., Hur, J. & Shafieezadeh, A. 2020. A high-fidelity computational investigation of buried concrete sewer pipes exposed to truckloads and corrosion deterioration. *Eng. Struct.* 221, 111043.
- Zschau, J. 2017. Where are we with multihazards, multirisks assessment capacities?. [drmkc.jrc.ec.europa.eu](http://drmkc.jrc.ec.europa.eu).
- Zuccaro, G., Cacace, F., Spence, R. & Baxter, P. 2008. Impact of explosive eruption scenarios at Vesuvius. *Journal of Volcanology and Geothermal Research* 178: 416{453.
- Zuccaro, G., Della Bella, M. & Papa, F. 1999. *Caratterizzazione tipologico strutturale a scala nazionale*. Torino, Atti 9° Convegno Nazionale ANIDIS, L'ingegneria Sismica in Italia.
- Zuccaro, G., Dolce, M., De Gregorio, D., Speranza, E., Moroni, C. 2015. La scheda CARTIS per la caratterizzazione tipologico- strutturale dei comparti urbani costituiti da edifici ordinari. Valutazione dell'esposizione in analisi di rischio sismico. *Proceedings of GNGTS*.

Zuccaro, G. & Leone, M. 2011. Volcanic crisis management and mitigation strategies: a multi-risk framework case study. *Earthzine*, 4.

Zuccaro, G., Perelli, F., De Gregorio, D. & Cacace, F. 2020. Empirical vulnerability curves for Italian masonry buildings: evolution of vulnerability model from the DPM to curves as a function of acceleration. *Bull Earthq Eng*. <https://doi.org/10.1007/s10518-020-00954-5>.

Zuconi, M., Di Ludovico, M. & Sorrentino, L. 2022. Census-based typological usability fragility curves for Italian unreinforced masonry buildings. *Bulletin of Earthquake Engineering*. [10.1007/s10518-022-01361-8](https://doi.org/10.1007/s10518-022-01361-8).

Zuconi, M., Sorrentino, L. & Ferlito, R. 2017. Principal component analysis for a seismic usability model of unreinforced masonry buildings. *Soil Dyn Earthq Eng* 96:64–75. <https://doi.org/10.1016/j.soildyn.2017.02.014>.